

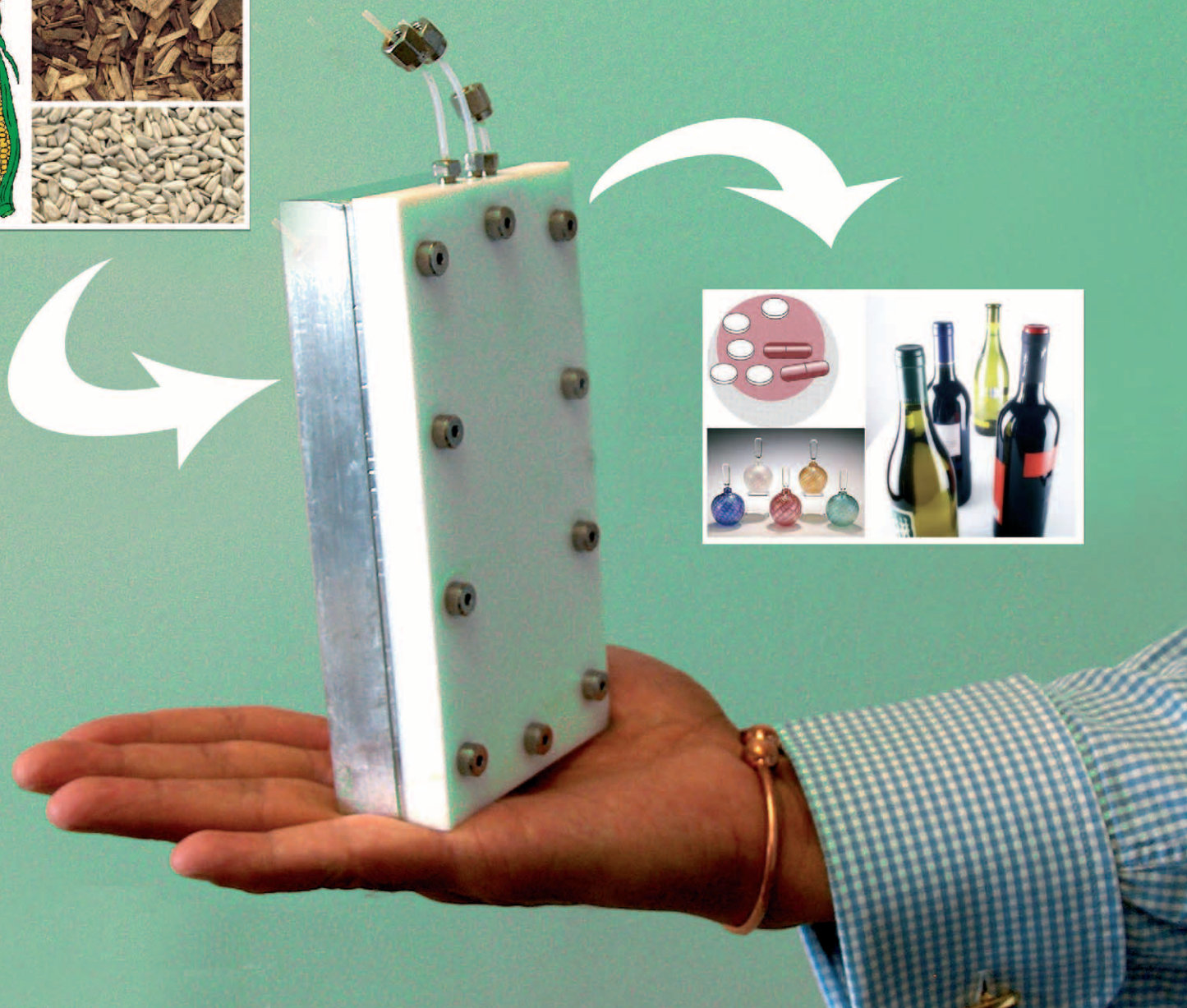
Green Chemistry

Cutting-edge research for a greener sustainable future

www.rsc.org/greenchem

Volume 8 | Number 1 | January 2006 | Pages 1–112

Downloaded on 06 November 2010
Published on 23 December 2006 on http://pubs.rsc.org | doi:10.1039/B517442M



ISSN 1463-9262

RSC Publishing

Jachuck *et al.*
Process intensification using a
continuous reactor

Gupta *et al.*
Construction of polycyclic ring
systems

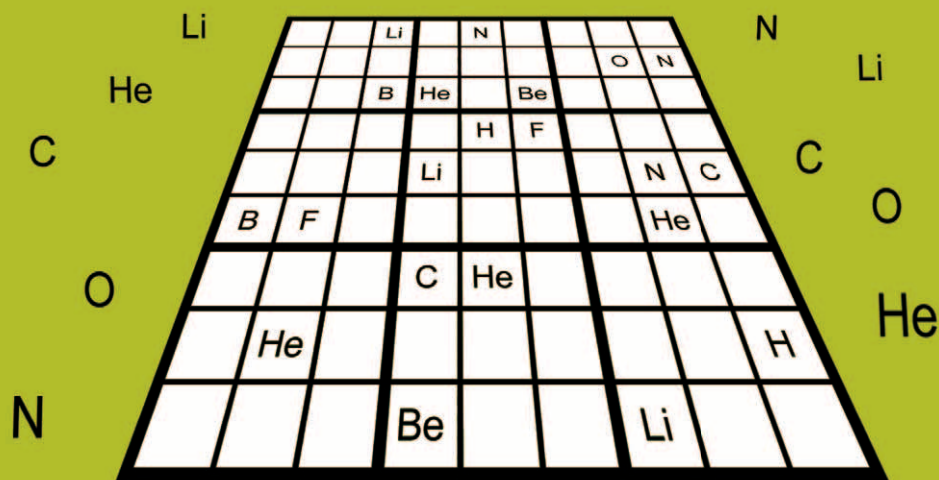
Raveendran *et al.*
Synthesis of Au and Ag alloy
nanoparticles

Aplander *et al.*
Pinner-cyclization of hydroxynitriles
in water



1463-9262 (2006) 8:1;1-D

Numerical Alchemy ?

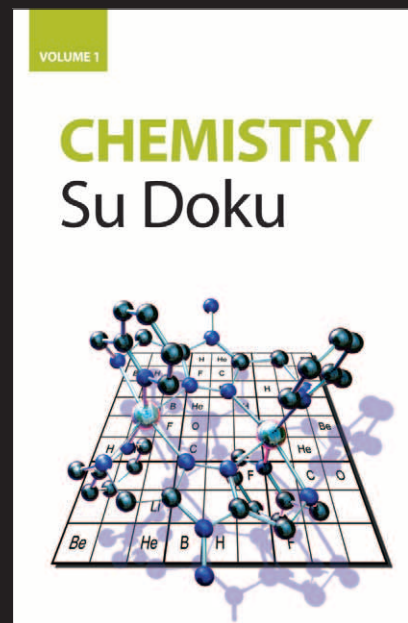


Chemistry Su Doku

- Specially developed to incorporate chemical symbols instead of numbers
- The perfect gift for a chemist
- Go online buy your copy today!

Try our other puzzle book
Chemistry Crosswords Vol.1

Softcover | 0 85404 693 3 | 2005 | 116 pages | £7.95



Green Chemistry

Cutting-edge research for a greener sustainable future

www.rsc.org/greenchem

RSC Publishing is a not-for-profit publisher and a division of the Royal Society of Chemistry. Any surplus made is used to support charitable activities aimed at advancing the chemical sciences. Full details are available from www.rsc.org

IN THIS ISSUE

ISSN 1463-9262 CODEN GRCHFJ 8(1) 1-112 (2006)



Cover

An isothermal reactor has been developed for continuous processing under microwave irradiation. The system has the potential for high-value throughput at a low cost and offers tremendous benefits to green chemistry. Image reproduced by permission of Roshan Jachuck from *Green Chem.*, 2006, **8**(1), 29.

CHEMICAL TECHNOLOGY

T1

Chemical Technology highlights the latest applications and technological aspects of research across the chemical sciences.

Chemical Technology

January 2006/Volume 3/Issue 1

www.rsc.org/chemicaltechnology

EDITORIALS

11

Happy New Year from *Green Chemistry*

Sarah Ruthven, Editor of *Green Chemistry*, reflects on the past year and looks to the future and the exciting developments in RSC Publishing.



EDITORIAL STAFF

Editor

Sarah Ruthven

News writer

Markus Hölscher

Publishing assistant

Emma Hacking

Team leader, serials production

Stephen Wilkes

Administration coordinator

Sonya Spring

Editorial secretaries

Lynne Braybrook, Jill Segev, Julie Thompson

Publisher

Adrian Kybett

Green Chemistry (print: ISSN 1463-9262; electronic: ISSN 1463-9270) is published 12 times a year by the Royal Society of Chemistry, Thomas Graham House, Science Park, Milton Road, Cambridge, UK CB4 0WF.

All orders, with cheques made payable to the Royal Society of Chemistry, should be sent to RSC Distribution Services, c/o Portland Customer Services, Commerce Way, Colchester, Essex, UK CO2 8HP. Tel +44 (0) 1206 226050; E-mail sales@rscdistribution.org

2006 Annual (print + electronic) subscription price: £859; US\$1571. 2006 Annual (electronic) subscription price: £773; US\$1414. Customers in Canada will be subject to a surcharge to cover GST. Customers in the EU subscribing to the electronic version only will be charged VAT.

If you take an institutional subscription to any RSC journal you are entitled to free, site-wide web access to that journal. You can arrange access via Internet Protocol (IP) address at www.rsc.org/ip. Customers should make payments by cheque in sterling payable on a UK clearing bank or in US dollars payable on a US clearing bank. Periodicals postage paid at Rahway, NJ, USA and at additional mailing offices. Airfreight and mailing in the USA by Mercury Airfreight International Ltd., 365 Blair Road, Avenel, NJ 07001, USA.

US Postmaster: send address changes to Green Chemistry, c/o Mercury Airfreight International Ltd., 365 Blair Road, Avenel, NJ 07001. All despatches outside the UK by Consolidated Airfreight.

PRINTED IN THE UK

Advertisement sales: Tel +44 (0) 1223 432243; Fax +44 (0) 1223 426017; E-mail advertising@rsc.org

Green Chemistry

Cutting-edge research for a greener sustainable future

www.rsc.org/greenchem

Green Chemistry focuses on cutting-edge research that attempts to reduce the environmental impact of the chemical enterprise by developing a technology base that is inherently non-toxic to living things and the environment.

EDITORIAL BOARD

Chair

Professor Colin Raston,
Department of Chemistry
University of Western Australia
Perth, Australia
E-mail clraston@chem.uwa.edu.au

Scientific editor

Professor Walter Leitner,
RWTH-Aachen, Germany
E-mail leitner@itmc.rwth-aachen.de

Members

Professor Joan Brennecke,
University of Notre Dame, USA
Professor Steve Howdle, University
of Nottingham, UK

Dr Janet Scott, Centre for Green
Chemistry, Monash University,
Australia

Dr A Michael Warhurst,
University of Massachusetts,
USA
E-mail michael-warhurst@uml.edu

Professor Tom Welton,
Imperial College, UK
E-mail t.welton@ic.ac.uk

Professor Roshan Jachuck,
Clarkson University, USA
E-mail rjachuck@clarkson.edu

Dr Paul Anastas, Green Chemistry
Institute, USA
E-mail p_anastas@acs.org

Professor Buxing Han, Chinese
Academy of Sciences
E-mail hanbx@iccas.ac.cn

Associate editors

Professor C. J. Li, McGill
University, Canada
E-mail cj.li@mcgill.ca

Professor Kyoko Nozaki
Kyoto University, Japan
E-mail nozaki@chembio-tu-tokyo.ac.jp

INTERNATIONAL ADVISORY EDITORIAL BOARD

James Clark, York, UK
Avelino Corma, Universidad
Politécnica de Valencia, Spain
Mark Harmer, DuPont Central
R&D, USA
Herbert Hugl, Lanxess Fine
Chemicals, Germany
Makato Misono, Kogakuin
University, Japan
Robin D. Rogers, Centre for Green
Manufacturing, USA

Kenneth Seddon, Queen's
University, Belfast, UK
Roger Sheldon, Delft University of
Technology, The Netherlands
Gary Sheldrake, Queen's
University, Belfast, UK
Pietro Tundo, Università ca
Foscari di Venezia, Italy
Tracy Williamson, Environmental
Protection Agency, USA

INFORMATION FOR AUTHORS

Full details of how to submit material for publication in Green Chemistry are given in the Instructions for Authors (available from <http://www.rsc.org/authors>). Submissions should be sent via ReSource: <http://www.rsc.org/resource>.

Authors may reproduce/republish portions of their published contribution without seeking permission from the RSC, provided that any such republication is accompanied by an acknowledgement in the form: (Original citation) – Reproduced by permission of the Royal Society of Chemistry.

© The Royal Society of Chemistry 2006. Apart from fair dealing for the purposes of research or private study for non-commercial purposes, or criticism or review, as permitted under the Copyright, Designs and Patents Act 1988 and the Copyright and Related Rights Regulations 2003, this publication may only be reproduced, stored or transmitted, in any form or by any means, with the prior permission in writing of the Publishers or in the case of reprographic reproduction in accordance with the terms of

licences issued by the Copyright Licensing Agency in the UK. US copyright law is applicable to users in the USA.

The Royal Society of Chemistry takes reasonable care in the preparation of this publication but does not accept liability for the consequences of any errors or omissions.

Ⓢ The paper used in this publication meets the requirements of ANSI/NISO Z39.48-1992 (Permanence of Paper).

Royal Society of Chemistry: Registered Charity No. 207890

EDITORIALS

13

All solutions have a solvent

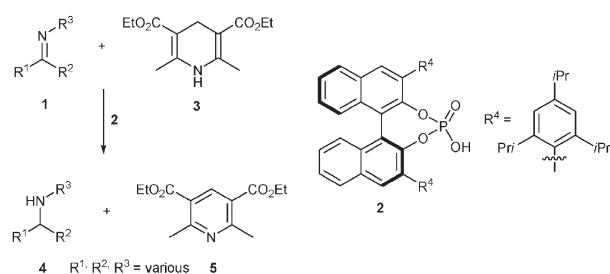
Tom Welton

HIGHLIGHT

14

Highlights

Markus Hölscher reviews some of the recent literature in green chemistry.



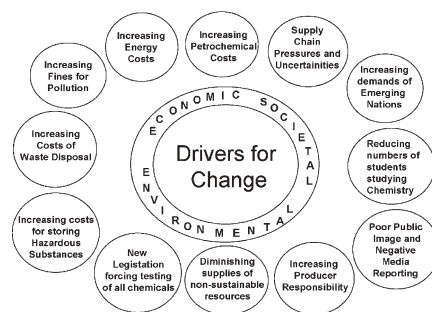
FEATURE ARTICLE

17

Green chemistry: today (and tomorrow)


James H. Clark

The drivers for green chemistry are more powerful than ever. The volume of research and examples of industrial application are increasing. We now need to do more research on green and sustainable product design to meet legislative and societal requirements.



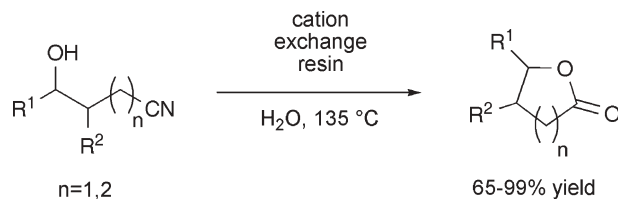
COMMUNICATIONS

22

 **A green and facile route to γ - and δ -lactones via efficient Pinner-cyclization of hydroxynitriles in water**

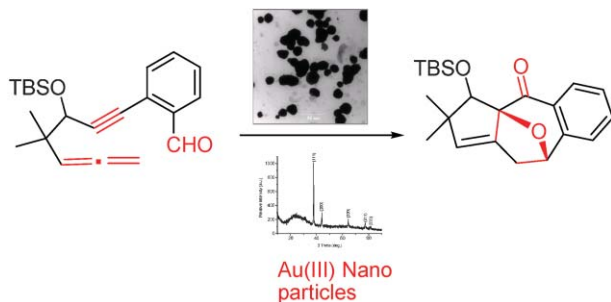
Karolina Aplander, Olle Hidestål, Kambiz Katebzadeh and Ulf M. Lindström*

The Pinner cyclization of hydroxynitriles and subsequent hydrolysis of the cyclic imidate is an attractive route to γ - and δ -lactones but limited in scope due to the harsh conditions usually required. Herein we employ a recyclable acidic resin in water to obtain lactones in high purity after simple filtration.



COMMUNICATIONS

25



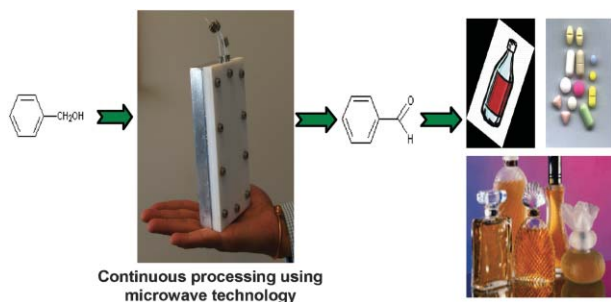
Gold nanoparticle-catalysed [3 + 2]dipolar cycloaddition of 1,6-allenylbenzaldehydes: construction of polycyclic ring systems

Arun Kumar Gupta, Chul Yun Rhim, Chang Ho Oh,*
R. S. Mane and Sung-Hwan Han*

We have isolated spherical-shaped monodispersed 12–14 nm range gold nanoparticles, when *o*-1,6-allenylbenzaldehyde underwent a novel mode of tandem cycloaddition and cyclization using AuCl₃ precatalyst. This cyclization can be found in the construction of many polycyclic natural product skeletons.

PAPERS

29



Process intensification: oxidation of benzyl alcohol using a continuous isothermal reactor under microwave irradiation

R. J. J. Jachuck,* D. K. Selvaraj and R. S. Varma

The performance of a compact microwave reactor capable of continuous rather than batch mode of operation under isothermal conditions has been described.

34

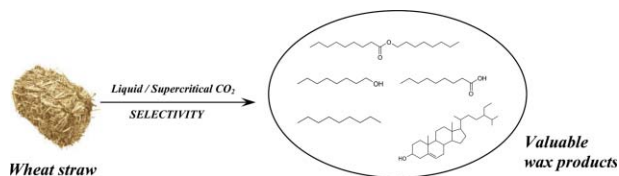


A simple and “green” method for the synthesis of Au, Ag, and Au–Ag alloy nanoparticles

Poovathinthodiyil Raveendran,* Jie Fu and Scott L. Wallen*

Au, Ag, and Au–Ag alloy nanoparticles are synthesized in aqueous medium using glucose as the reducing agent and starch as the protecting agent.

39



The fractionation of valuable wax products from wheat straw using CO₂

Fabien E. I. Deswarte, James H. Clark,*
Jeffrey J. E. Hardy and Paul M. Rose

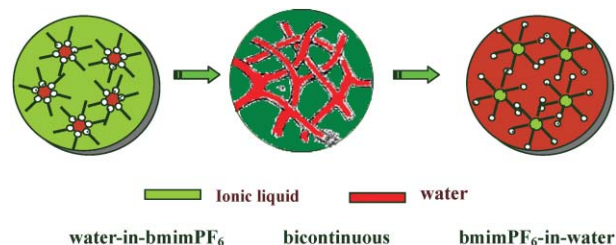
Liquid and supercritical CO₂ have been used for the first time to achieve direct extraction of valuable wax products from agro-residue wheat straw, including cosmetic, nutraceutical and semiochemical products.

43

A cyclic voltammetric technique for the detection of micro-regions of bmimPF₆/Tween 20/H₂O microemulsions and their performance characterization by UV-Vis spectroscopy

Yan'an Gao, Na Li, Liqiang Zheng,* Xueyan Zhao, Shaohua Zhang, Buxing Han,* Wanguo Hou and Ganzuo Li

The ionic liquid bmimPF₆, Tween 20 and water can form a microemulsion. Three types of micro-regions were identified by cyclic voltammetry: W/IL, bicontinuous and IL/W. These microemulsions can solubilize salts and biochemical species.

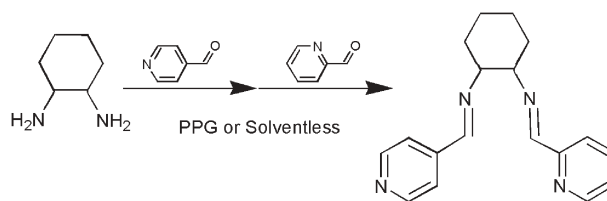


50

Benign approaches for the synthesis of bis-imine Schiff bases

Tania R. van den Ancker,* Gareth W. V. Cave and Colin L. Raston

Bis-imine Schiff bases are readily accessible in high yield, typically >95%, under solvent-free conditions or in poly(propyleneglycol) (PPG) as a recyclable reaction medium, with negligible waste.

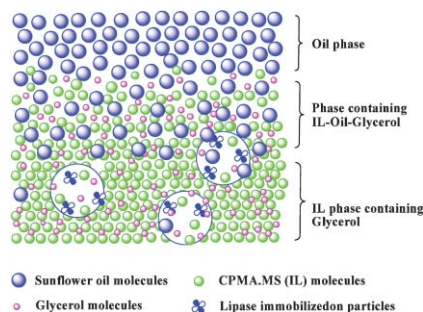


54

Lipase-catalyzed glycerolysis of fats and oils in ionic liquids: a further study on the reaction system

Zheng Guo and Xuebing Xu*

Mass transfer limitation and occurring partial phase separation were found to have a profound effect on the lower initial rate and the occurrence of the induction period for *Candida antarctica* lipase B-catalyzed glycerolysis of sunflower oil in a tetraammonium-based ionic liquid.

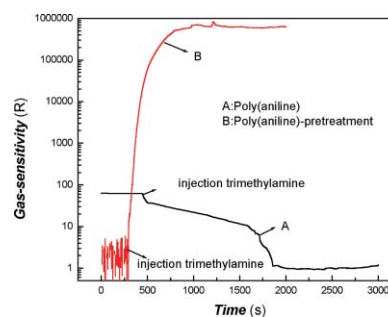


63

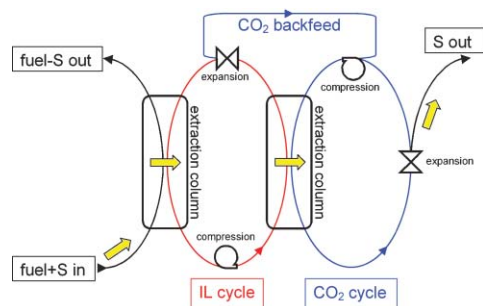
Unusual electrical response of a poly(aniline) composite film on exposure to a basic atmosphere and its application to sensors

Xingfa Ma,* Guang Li,* Mang Wang, Ru Bai, Feng Yang and Hongzheng Chen

An unusual electrical response of a poly(aniline) composite film on exposure to a basic atmosphere is reported. Based on this feature, it is possible to develop a novel kind of gas-sensor with high sensitivity and rapid response which can be easily recovered with N₂.



70

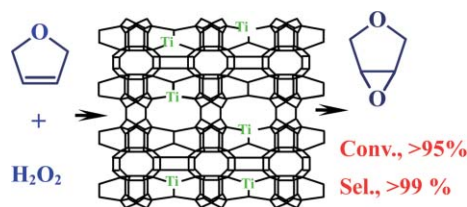


Distribution of sulfur-containing aromatics between [hmim][Tf₂N] and supercritical CO₂: a case study for deep desulfurization of oil refinery streams by extraction with ionic liquids

Josef Planeta, Pavel Karásek and Michal Roth*

We report partition data of several sulfur compounds between [hmim][Tf₂N] and supercritical CO₂ for feasibility assessment of their reextraction from ionic liquids following the deep desulfurization of oil refinery streams.

78

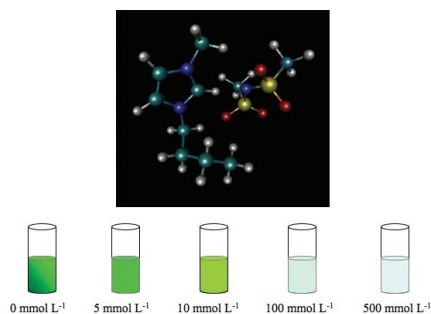


Highly efficient and clean synthesis of 3,4-epoxytetrahydrofuran over a novel titanosilicate catalyst, Ti-MWW

Haihong Wu, Lingling Wang, Haijiao Zhang, Yueming Liu, Peng Wu* and Mingyuan He

The Ti-MWW/H₂O₂ system is extremely effective for the selective epoxidation of 2,5-dihydrofuran to 3,4-epoxytetrahydrofuran.

82

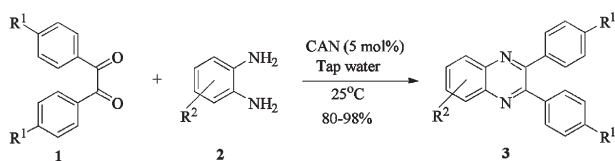


Assessing the factors responsible for ionic liquid toxicity to aquatic organisms *via* quantitative structure–property relationship modeling

David J. Couling, Randall J. Bernot, Kathryn M. Docherty, JaNeille K. Dixon and Edward J. Maginn*

Quantitative structure–property relationship modeling is used to determine the factors that govern the toxicity of a range of different ionic liquids to aquatic organisms.

91



Cerium (IV) ammonium nitrate (CAN) as a catalyst in tap water: A simple, proficient and green approach for the synthesis of quinoxalines

Shivaji V. More, M. N. V. Sastry and Ching-Fa Yao*

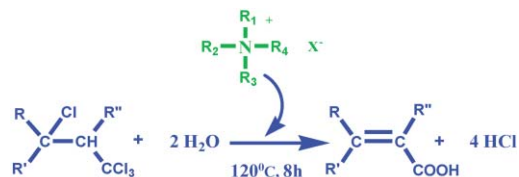
Various biologically important quinoxaline derivatives have been efficiently synthesized in excellent yields using catalytic amounts of cerium (IV) ammonium nitrate in water.

96

Novel quaternary ammonium ionic liquids and their use as dual solvent-catalysts in the hydrolytic reaction

Jiayang Weng, Congmin Wang, Haoran Li* and Yong Wang

Novel quaternary ammonium ionic liquids are used as acidic catalysts for the synthesis of cinnamic acid. The need for inorganic acid catalysts and volatile organic solvents are avoided.



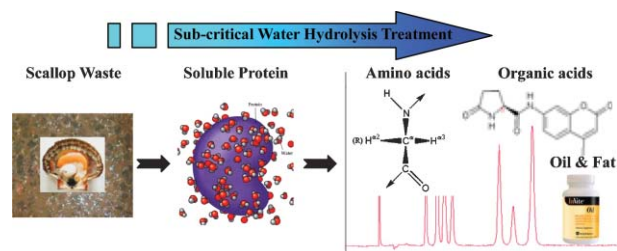
1. Novel, cheap and easily prepared ionic liquids
2. High conversion and selectivity
3. Ionic liquids could be easily reused

100

Conversion of scallop viscera wastes to valuable compounds using sub-critical water

Omid Tavakoli and Hiroyuki Yoshida*

Sub-critical water hydrolysis was used as a green and environmentally benign conversion technology to achieve zero emission approach. Here it is shown that this method is effective in the production of valuable compounds such as amino acids, organic acids, fatty acids, oil and other organic materials from scallop wastes.

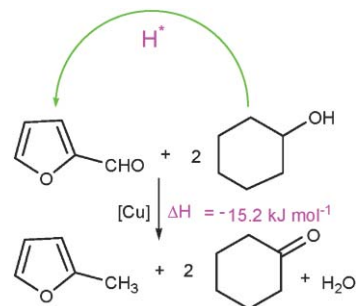


107

An environmentally benign process for the efficient synthesis of cyclohexanone and 2-methylfuran

Hong-Yan Zheng, Yu-Lei Zhu,* Zong-Qing Bai, Long Huang, Hong-Wei Xiang and Yong-Wang Li

A new route involving the coupling of cyclohexanol dehydrogenation and furfural hydrogenation has been developed for the synthesis of cyclohexanone and 2-methylfuran from a green and atom economic perspective. It is found that hydrogen and heat energy are utilized with high efficiency in this process.



AUTHOR INDEX

- Aplander, Karolina, 22
 Bai, Ru, 63
 Bai, Zong-Qing, 107
 Bernot, Randall J., 82
 Cave, Gareth W. V., 50
 Chen, Hongzheng, 63
 Clark, James H., 17, 39
 Couling, David J., 82
 Deswarte, Fabien E. I., 39
 Dixon, JaNeille K., 82
 Docherty, Kathryn M., 82
 Fu, Jie, 34
 Gao, Yan'an, 43
 Guo, Zheng, 54
 Gupta, Arun Kumar, 25
 Han, Buxing, 43
 Han, Sung-Hwan, 25
- Hardy, Jeffrey J. E., 39
 He, Mingyuan, 78
 Hidestål, Olle, 22
 Hou, Wanguo, 43
 Huang, Long, 107
 Jachuck, R. J. J., 29
 Karásek, Pavel, 70
 Katebzadeh, Kambiz, 22
 Li, Ganzuo, 43
 Li, Guang, 63
 Li, Haoran, 96
 Li, Na, 43
 Li, Yong-Wang, 107
 Lindström, Ulf M., 22
 Liu, Yueming, 78
 Ma, Xingfa, 63
 Maginn, Edward J., 42
- Mane, R. S., 25
 More, Shivaji V., 91
 Oh, Chang Ho, 25
 Planeta, Josef, 70
 Raston, Colin L., 50
 Raveendran, Poovathinthodiyil, 34
 Rhim, Chul Yun, 25
 Rose, Paul M., 39
 Roth, Michal, 70
 Sastry, M. N. V., 91
 Selvaraj, D. K., 29
 Tavakoli, Omid, 100
 van den Ancker, Tania R., 50
 Varma, R. S., 29
 Wallen, Scott L., 34
 Wang, Congmin, 96
- Wang, Lingling, 78
 Wang, Mang, 63
 Wang, Yong, 96
 Weng, Jianyang, 96
 Wu, Haihong, 78
 Wu, Peng, 78
 Xiang, Hong-Wei, 107
 Xu, Xuebing, 54
 Yang, Feng, 63
 Yao, Ching-Fa, 91
 Yoshida, Hiroyuki, 100
 Zhang, Haijiao, 78
 Zhang, Shaohua, 43
 Zhao, Xueyan, 43
 Zheng, Hong-Yan, 107
 Zheng, Liqiang, 43
 Zhu, Yu-Lei, 107

FREE E-MAIL ALERTS AND RSS FEEDS


Contents lists in advance of publication are available on the web *via* www.rsc.org/greenchem - or take advantage of our free e-mail alerting service (www.rsc.org/ej_alert) to receive notification each time a new list becomes available.

RSS Try our RSS feeds for up-to-the-minute news of the latest research. By setting up RSS feeds, preferably using feed reader software, you can be alerted to the latest Advance Articles published on the RSC web site. Visit www.rsc.org/publishing/technology/rss.asp for details.

ADVANCE ARTICLES AND ELECTRONIC JOURNAL

Free site-wide access to Advance Articles and the electronic form of this journal is provided with a full-rate institutional subscription. See www.rsc.org/ejs for more information.

* Indicates the author for correspondence: see article for details.

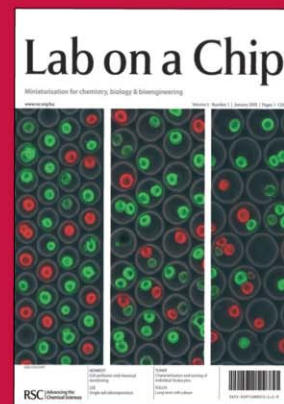
 Electronic supplementary information (ESI) is available *via* the online article (see <http://www.rsc.org/esi> for general information about ESI).

Lab on a Chip

Miniaturisation for chemistry, biology and bioengineering

Publishing the latest key developments, novel applications and fundamental research at the micro- and nano-scale

- Fast times to publication – typically 90 days
- Impact factor: 5.047
- Indexed in MEDLINE



RSC Publishing

www.rsc.org/loc

Happy New Year from *Green Chemistry*

DOI: 10.1039/b517158j

Welcome to the New Year and issue 1 2006 of *Green Chemistry*. In this Editorial I reflect on the past year and look to the future and the exciting developments in RSC Publishing.

Rapid technological advances at the Royal Society of Chemistry

2005 has seen RSC Publishing invest significantly in technological developments across all of its products. First there was the introduction of the new website in the summer which included a contemporary, fresh look and an enhanced structure for improved and intuitive navigation between relevant, associated content (Fig. 1). The improvements to the technological infrastructure have made the site more flexible and efficient, and better equip the RSC to deliver enhanced publishing products and services for its customers in the future. The new look was just the start and towards the end of the year we were

pleased to provide further enhancements in the form of RSS feeds and 'forward linking' facilities, increasing the functionality of the electronic journal. Each of these developments is explained briefly below, to show how they can help your research.

RSS, or 'really simple syndication', is the latest way to keep up with the research published by the RSC. The new service provides subscribers with alerts as soon as an Advance Article is published in their journal of choice. Journal readers simply need to go to the journal homepage, click on the RSS link, and follow the step-by-step instructions to register for these enhanced alerts. RSS feeds include both the graphical abstract and text from a journal's contents page—*i.e.* they deliver access to new

research straight to a reader's PC, as soon as it is published. Many feed reader software packages also have the added benefit of remembering what has been read previously, which in turn makes tracking and managing journal browsing more efficient.

'Forward linking', the reverse of reference linking, enables readers to link from any RSC published paper to the articles in which it is cited. In essence, it allows researchers to easily track the progression of a concept or discovery, since its original publication. With one click of a button (on the 'search for citing articles' link) a list of citing articles included in Cross-Ref is presented, complete with DOI links. At a time when research is becoming increasingly interdisciplinary in nature and the amount of published works continues to grow, it is hoped that the new technology, developed in conjunction with Cross-Ref, will significantly reduce the time spent by researchers searching for information.

These developments demonstrate the investment in publishing products and services over the past year and 2006 will see us enhancing our products further, with improvements to the HTML functionality of all journals and ReSource (the author and referee web interface) already underway.

The 2004 impact factors, released by ISI[®] in June 2005, showed an impressive average increase of over 10% for RSC journals (Fig. 2). The impact factor for *Green Chemistry* increased significantly from 2.8 to 3.5—an increase of 25%, reflecting the wider acceptability of the subject material and providing justification for our recent efforts to improve the quality of published material. We would like to thank our referees for their help in achieving this impact factor through their continued rigorous reviewing of *Green Chemistry* manuscripts. Calculated annually, ISI[®] impact factors provide an indication of the quality of a

Fig. 1 The new *Green Chemistry* website.

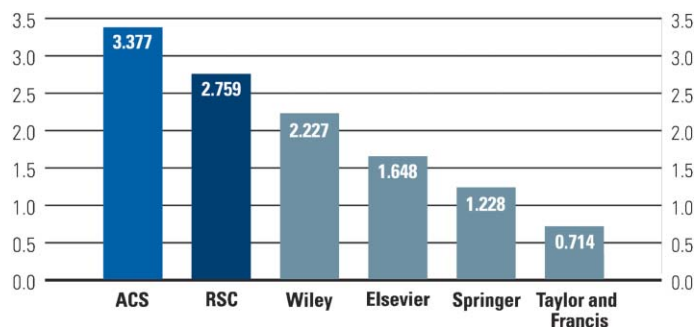


Fig. 2 Median impact factor in seven ISI core chemistry categories.

journal—they take into account the number of citations in a given year for all the citeable documents published within a journal in the preceding two years. It is worth noting that alongside the ACS publications, journals from RSC Publishing have the highest median impact factor among publishers in the chemical

sciences. This encouraging statistic demonstrates the recognition and status that researchers place in society published work.

Chemical biology content published in this journal is highlighted in the *Chemical Biology Virtual Journal*. The portal, which was launched in 2002 in recognition of the significant amount of

chemical biology material published across RSC journals, enables interested readers to readily access relevant items. All chemical biology articles and related papers published in RSC journals are drawn together online every two weeks, with a selection of the primary literature free to access for a month.

As well as an impressive portfolio of prestigious journals, the RSC has a significant collection of book titles. The first titles in three new series: *RSC Biomolecular Sciences*; *RSC Nanoscience & Nanotechnology Series*; and *Issues in Toxicology* were published in 2005, with further titles due during 2006. Future growth in the books publishing programme is planned, which reflects the increasingly interdisciplinary nature of the chemical sciences.

Sarah Ruthven

Editor

All solutions have a solvent

DOI: 10.1039/b514869n

For some time now papers have been being submitted to Green Chemistry where reactions have been variously described as 'solventless' or 'solvent-free' in spite of the fact that the reaction mixture is clearly a homogeneous solution. This appears to be particularly the case where one of the neoteric solvents, such as an ionic liquid or supercritical fluid, is being used and a claim to greenness is being made.

Although there are many environmentally damaging volatile organic liquids that can, and do, get used as solvents, this is not the definition of what a solvent is. Therefore, eliminating their use by using an environmentally benign alternative does not lead to solvent-free conditions.

Leaving to one side the issue of solid solutions; a solution is a liquid mixture in which the solute(s) is(are) uniformly distributed within the solvent. Whenever there is a solution present there must be a solvent present. The solvent is the major component of the solution and it is usually a liquid under

the conditions described when pure. Of course, in more complex systems, it is possible to have a mixture of liquids acting as the solvent.

One source of confusion seems to be when the solvent has more than one function. For instance, it is often the case that one of the starting materials for a reaction is a liquid that can dissolve all of the other components. In these cases it is often unnecessary to add another liquid to act as the solvent. However, this is not a solvent-free process; it is a process where one of the components is acting both as a reagent and a solvent.

In my own subject area of ionic liquids many examples are coming to the fore where the ionic liquid is acting as a catalyst for a reaction. Again, some care is needed here. If the ionic liquid is a minor component of the reaction solution, it is a catalyst that happens to be a liquid and the major component (whatever that is) is the solvent; if it is the major component it is acting as both the catalyst and the solvent. However, in this circumstance, further care is needed.

Whenever changing solvent leads to a faster reaction the new solvent can be viewed as being a catalyst. After all, the reaction has been accelerated and the solvent has not been permanently changed by the process. However, this is usually regarded as a solvent effect rather than catalysis. In this case a good rule of thumb is that if a specific chemical interaction can be identified between the solvent and the solute that is giving rise to the acceleration of the reaction then it can be described as catalysis, whereas if it is a generalised polarity effect then the term should not be used.

So when can a reaction be described as solvent-free? Obviously, a dry solid phase reaction is solvent-free, also a reaction where there is a liquid present, but it is not acting as a solvent (*i.e.* nothing is dissolved in it) is also solvent-free, but that is the extent of the list. If there is a solution present there is a solvent present.

Tom Welton, Imperial College of Science, Technology and Medicine, London

Highlights

DOI: 10.1039/b516605p

Markus Hölscher reviews some of the recent literature in green chemistry

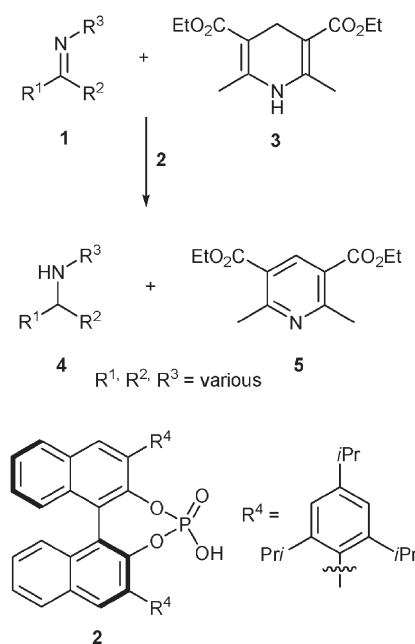
Sugar catalysts for the production of biodiesel

The transformation of diesel from vegetable oil suffers from the lack of an ecologically friendly catalyst. In its present form the process for the esterification of higher fatty acids uses H_2SO_4 , which is both highly energy consumptive and chemically wasteful. Other materials such as Nafion or sulfonated carbonized naphthalene are either very expensive and have low activity or they are too soft and leach out during the liquid-phase reactions, leading also to a significant loss of activity. A collaboration of researchers from Tokyo, Yokohama and Ibaraki (Toda, Takagaki, Okamura, Kondo, Hayashi, Domen and Hara) recently investigated the possibility of carbonizing D-glucose at low temperatures, followed by sulfonation to generate an alternative catalyst for biodiesel production.¹ The material obtained consists of sheets of amorphous carbon with hydroxyl and carboxyl and also SO_3H groups in high density. As anticipated the solid is an appropriate catalyst for the esterification of the vegetable-oil constituents oleic acid and stearic acid, as was deduced from the high activity (more than half of the activity of liquid sulfuric acid) outperforming many other known solid catalysts for this reaction. Neither did the catalyst lose its activity nor was a leaching of SO_3H detectable in repeated reactions at temperatures between 80 and 180 °C. Apart from the production of biodiesel the material might have potential for other acid catalyzed reactions that await a more sustainable process than the ones in use currently.

Asymmetric transfer hydrogenation of imines with brønsted acids

Knowledge about asymmetric transfer hydrogenations of ketimines is scarce, although the resulting products are chiral amines, which are industrially relevant

building blocks. As the interest in organocatalytic reactions with chiral acids is growing, it was obvious to envision the use of chiral phosphoric acids in such reactions. List and coworkers from the Max-Planck-Institute of Coal Reserach, Mülheim, have very recently demonstrated the high potential of this approach.²



A ketimine (**1**) is protonated by the acid catalyst (**2**), while the hydrogen centres are transferred from a Hantzsch ester (**3**) generating the desired chiral amine (**4**) and the corresponding pyridine (**5**). In a catalyst screening for evaluating the most promising catalyst structure it was found that modifications of **2** at the 3,3'-positions of the binaphthol core using the 2,4,6-*iso*-propylphenyl rest yielded a catalyst capable of generating high *ee* values. However, the conversion of a test substrate remained disappointingly low. Interestingly simple tuning of the reaction conditions improved the result significantly generating a catalyst system useful for the transfer hydrogenation of a large variety of ketimines with *ee* values up to 93% and yields of up to 98%.

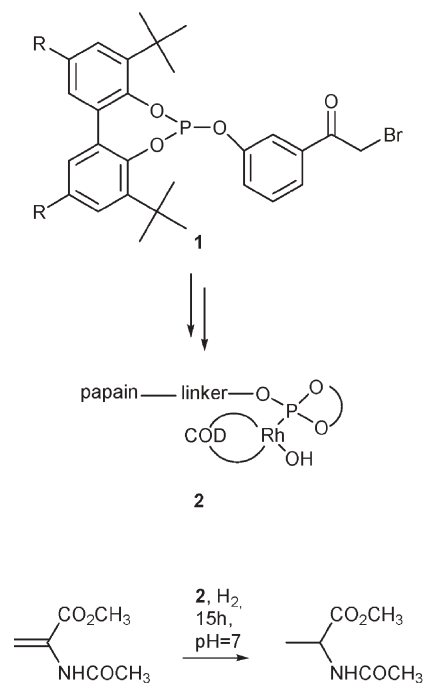
Boehmite nanofibers as hosts for Rhodium nanoparticles—hydrogenation of arenes under mild conditions

Nanoparticles attract increasing attention for applications in catalysis. Mild hydrogenations of arenes are one of the fields in which these nanoparticles can be applied successfully. Though many different methods for the synthesis of nanoparticles have been developed, often these techniques suffer from difficult synthetic procedures, while generating nanoparticles of low stability and low activity. Park *et al.* from Pohang university, Korea, recently reported about the incorporation of Rhodium nanoparticles in a boehmite matrix, yielding stable, easy recyclable and highly active catalysts for the hydrogenation of various arenes.³ The simple synthesis consists of the mixing of RhCl_3 hydrate with 2-butanol and $\text{Al}(\text{O-}i\text{-sec-Bu})_3$ with subsequent trapping of the material in boehmite by gelation with water. According to TEM images the boehmite nanofiber structure is maintained with Rh-nanoparticles residing inside the pores. The inner surface of the material amounts to *ca.* 600 $\text{m}^2 \text{g}^{-1}$ as calculated from BET adsorption measurements. The material was tested as a catalyst for the hydrogenation of a variety of arenes (benzene, anisole, toluene, phenol, ethyl benzoate, 1-phenylethanol, xylenes, cresols, naphthalene, to name a few) with yields of 100%, while operating either in solvents or solventless. Under a pressure of 1 atm of H_2 in many cases the reactions did not require any heating and yielded the desired hydrogenated products in reaction times typically varying between 0.5 and 5 h.

Homogeneous catalysis meets biocatalysis—Papain modified Rh-phosphites as hydrogenation catalysts

Asymmetric catalysis is considered as one of the key technologies for atom

economic and highly selective transformations which by appropriate tuning (right choice of the environmentally benign solvents and reaction engineering) generally offers the possibility for the creation of sustainable chemical processes. However, due to practical considerations (*e.g.* time-to-market pressure) asymmetric catalysis has not evolved yet as the method of choice for industry. In an attempt to generate novel alternatives for the traditional homogeneous catalysts de Vries *et al.* have recently added an interesting example to the combined bio-metal-catalytic approach.⁴ They reasoned that a transition metal bound to an easily synthesizable, however achiral ligand, which in turn is anchored to readily available enzymes (which are chiral inherently) might yield an active and selective catalyst for asymmetric transformations.



In a first set of experiments they have synthesized phosphite **1**, which can be coupled to the enzyme papain, which has a highly nucleophilic SH-group usable for covalent binding of the phosphite. Additionally catalysts of this type have to be hydrolytically stable, a feature which is provided by the presence of bulky groups near the phosphorous centre. The resulting compound—a hybrid of a phosphorous ligand and an enzyme—is reacted with an appropriate Rhodium complex yielding the desired

metallo-enzyme **2**. As anticipated **2** is an active catalyst for the hydrogenation of 2-acetamidoacrylate yielding the corresponding alanine derivative with 100% conversion of the reactant and 100% product selectivity. However, no enantioselectivity was observed at all, which might be a result of the chiral environment of the enzyme being too far away from the catalytically active metal centre. Though disappointing at a first glance the approach is highly desirable due to the readily available starting materials.

Kenneth G. Hancock Memorial Student Award in Green Chemistry

Outstanding examples of studies or research by undergraduate and graduate students that address the scope and objectives of green chemistry can be honored by the Kenneth G. Hancock Memorial Student Award in Green Chemistry by the Green Chemistry Institute of the American Chemical Society. The prize is awarded annually and includes not only a one-time cash award of \$1000 but also participation in the prestigious Presidential Green Chemistry Challenge Awards Ceremony in Washington, DC. The deadline for applications is February 1, 2006. Details can be found under <http://chemistry.org/greenchemistryinstitute>, but naturally the prize focuses on alternative synthetic pathways for green chemistry, use of alternative reaction conditions and the design of alternative chemicals of less toxicity than of compounds currently in use.

Green Chemistry Institute Sabbatical/Fellow Program

Sabbaticals or fellowships for professionals active in sustainable chemistry can be supported by the Green Chemistry Institute of the American Chemical Society. Applicants must provide a project proposal in an area relevant to green chemistry and support is granted for assistant, associate and full professors. Also junior and senior level professionals from industry and government can apply. The duration of the the fellowship is one academic year and the deadline for the 2006

applications is February 1. See <http://chemistry.org/greenchemistryinstitute> for more detailed information on the program.

Green chemistry—it's in the books

Green chemistry is everywhere but no one writes about it?! Provocative but wrong. Having grown aware of the important consequences man-made chemical production brings to the planet, chemists from around the world have not only started making chemical processes sustainable many years ago (at least in some parts of the world), they have also considered the importance of bringing the ideas and fundamentals of sustainable chemical production into classrooms, management offices and—last not least—into the minds of the ones that take political decisions. Admittedly the process did not start from science alone, it needed the help of the growing public concern, but here it is: Knowledge about green chemical technology, renewable resources, waste management, sustainable consumption, supercritical fluids and future challenges (and many many more relevant topics) is brought together by the many books and articles that have been written by distinguished experts in the fields. The world-wide-web helps a lot here. Under www.chemsoc.org/pdf/gen/Books.pdf there is a list citing titles, authors, publishers and ISBN numbers of many interesting books about the field.

Institute for Green Oxidation Chemistry

The Institute for Green Oxidation Chemistry is located at Carnegie Mellon University, Pittsburgh, USA. Three major areas were defined by the institute which need substantial modifications to improve on the development of sustainable technologies. Firstly, renewable energy technologies with a high emphasis on solar technologies should be at the core for the production of electricity in an industrial society. The institute aims to develop technologies for converting solar energy into chemical energy and then back to electrical energy. Secondly, chemical feedstocks should stem from renewable

sources and thirdly, the institute carries out research to minimize the production of pollutants accompanying chemical processes. Learn more about the institute at <http://www.chem.cmu.edu/groups/Collins>.

References

- 1 M. Toda, A. Takagaki, M. Okamura, J. N. Kondo, S. Hayashi, K. Domen and M. Hara, *Nature*, 2005, **438**, 178.
- 2 S. Hoffmann, A. M. Seayad and B. List, *Angew. Chem.*, 2005, **17**, 7590–7593.
- 3 I. S. Park, M. S. Kwon, N. Kim, J. S. Lee, K. Y. Kang and J. Park, *Chem. Commun.*, 2005, 5667–5669.
- 4 L. Panella, J. Broos, J. Jin, M. W. Fraaije, D. B. Janssen, M. Jeronimus-Stratingh, B. L. Feringa, A. J. Minnaard and J. G. de Vries, *Chem. Commun.*, 2005, 5656–5658.



Don't waste anymore time searching for that elusive piece of vital chemical information.

Let us do it for you at the Library and Information Centre of the RSC.

We provide:

- Chemical enquiry helpdesk
- Remote access chemical information resources
- Expert chemical information specialist staff

So tap into the foremost source of chemical knowledge in Europe and send your enquiries to

library@rsc.org

RSCPublishing

www.rsc.org/library

16050519

Green chemistry: today (and tomorrow)

James H. Clark

First published as an Advance Article on the web 2nd December 2005

DOI: 10.1039/b516637n

It is more than 7 years since I wrote my opening article for the first issue of *Green Chemistry*—“Green chemistry: challenges and opportunities”.¹ In this update article I will present a personal view of how the area has changed—mostly for the better—and what we need to do now. I will consider how the key drivers for major changes in the way that we practise chemistry have strengthened, how the range of relevant research has broadened, how the case studies from industry have increased and, perhaps most importantly, how our appreciation of what green chemistry should mean has matured. I will also be looking ahead at the immediate and longer-term challenges and opportunities as I now see them—in research and in industrial application and also in education and promotion.

Drivers for change

In the 1999 article¹ I used the “Costs of Waste” to help provide detail on why waste was becoming increasingly expensive to industry—waste disposal, fines for pollution, loss in efficiency and costs of raw materials.

These costs are even more important today and remain important drivers for change. However, we are now entering an age where legislation is likely to become as important a driver for change as process economics. When put alongside the social pressures resulting from the poor image the public have of chemical manufacturing and their largely irrational fear of “chemicals” we can now see how the three cornerstones of sustainable development—economic, environmental and social benefit, each provide the drivers of change that should help to push the application of green chemistry forward (Fig. 1).

What is also interesting is how these drivers now cover the three key stages of the life cycle of a chemical product—resources, manufacture and product use and fate (Fig. 2)

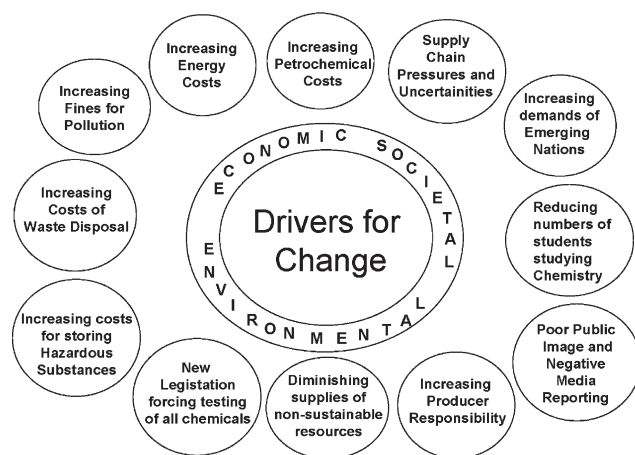


Fig. 1 Drivers for change.

which seems very appropriate given the essential need to see green chemistry cut across product lifecycles and help achieve true sustainability. Each stage in the lifecycle of a chemical product is resource consuming and waste generating and we cannot change one without affecting the other but for every problem there is a potential solution and with it an opportunity for commercial advantage (Fig. 2).

The costs of petrochemicals—the building blocks of over 90% of today’s organic chemical manufacturing have been increasing at a dramatic rate—both due to rapidly escalating oil prices and to massive market distortions due to the extraordinary growth in manufacturing industry in Asia. A good example of this is phenol, the price of which tripled in 2004 (exceeding €1 kg⁻¹ at one point). This will force industry to reconsider its traditional feedstocks (looking more carefully at alternative sustainable sources based on biomass) and the efficiency of resource utilisation.

The costs of the disposal of hazardous substances, typically coming from the use of hazardous process auxiliaries (organic solvents, stoichiometric reagents, work-up acids and bases, *etc.*) and the fines for pollution climb at above the rate of inflation in many countries, while penal taxation makes the storage of large quantities of dangerous chemicals very expensive.

The new European chemicals legislation REACH—the Registration, Evaluation and Authorisation of Chemicals—is probably going to become the most important chemicals legislation we have ever seen.²

At the time of writing, the final details of the legislation are yet to be finalised and considerable pressure from the chemical industry and national governments (within and without the EU) has resulted in some significant amendments which some regard as a dilution of its power. Nonetheless, REACH will force the testing of an unprecedented number of chemicals and, apart from the added costs, REACH will undoubtedly result in a significant number of chemical applications becoming very expensive or even prohibited. While this has largely been seen as a threat to European chemical manufacturers by industry, I believe that it can also be seen as an opportunity. By being forced to test chemicals, employ more benign substitutes where necessary and build up detailed

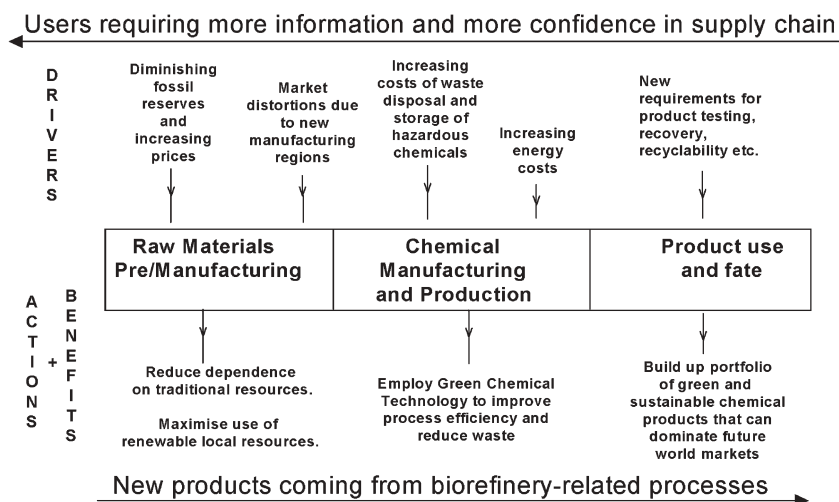


Fig. 2 Challenges and opportunities through the chemical product lifecycle.

information about toxicology and environmental impact, European manufacturers will be able to claim an unmatched level of 'green credentials' for their products which should give them an edge in world markets where consumers are becoming increasingly concerned about chemicals. It was interesting to hear recently from a European Trades Union representative that some countries outside of Europe are viewing REACH as protectionist and threatening to their industries rather than it giving them a cost advantage in the European market.³ Alongside REACH, the EU is also introducing more product or sector related chemicals legislation such as the Restriction on Hazardous Substances (RoHS), which will prohibit or severely restrict the use of the most dangerous chemicals in electronic and electrical equipment. This has already resulted in some companies advertising RoHS compliant products ahead of the legislation and thus attempting to secure a market lead based on greener products. I believe that other regions in the world will follow the EU trend and impose ever more challenging and restrictive chemicals legislation encouraged by public and media pressure to match that in other regions. In the USA for example, new legislation will more carefully control the chemical substances used in items handled by children.

As the economic opportunities for greener products becomes more apparent so should this process of product greening accelerate and in an ideal situation, iterative innovation to improve the environmental performance of chemical products will become continuous and embedded in industry's philosophy. Now is the time as the drivers come into effect to ensure that this process is indeed sustainable by never losing sight of the lifecycle of any chemical product.

Progress in research into green and sustainable chemistry

The last 6 years has seen a significant growth in the volume and scope of green chemistry related research. This has been driven by numerous national and, to a lesser extent, trans-national initiatives to fund the area and by the growing appreciation of the value of green chemistry at all stages in the

lifecycle from "cradle to grave" (Fig. 3). It is pleasing to see that sustainable chemistry will feature in "Framework 7"—the new EU research funding programme that will come into effect in 2006.

While the bulk of the research effort continues to be in the manufacturing box (with catalysis, alternative solvents and new routes continuing to dominate) reports of research at all stages in the lifecycle are emerging and with this journal seeing publications in many areas (Fig. 4).

I am, however, concerned that while renewable resource-based research is gaining momentum largely driven by the White Biotechnology revolution,⁴ the research effort going into the design of new greener and more sustainable chemical products will be insufficient to meet the demand that will result from legislation such as REACH. Our own efforts to engage the producers and retailers as well as the users of products containing chemicals in the green chemistry networks project, "Green Chemistry and the Consumer", has made us aware of the very small amount of relevant research reported in the mainstream chemistry journals.⁵

The move from our well-established petrochemical based organics chemical industry to one based on renewable resources^{6,7} is beginning to open the door to numerous opportunities for exciting new chemistry research including benign extraction of valuable chemicals from biomass (e.g. using supercritical fluids),⁸ adding value to nature's most abundant polymers (starch, cellulose, chitin, etc) and the bulk conversion of biomass to new "bio-platform molecules"

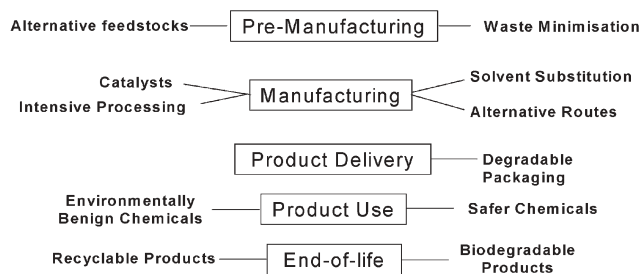


Fig. 3 Green chemistry applied from the cradle to the grave.

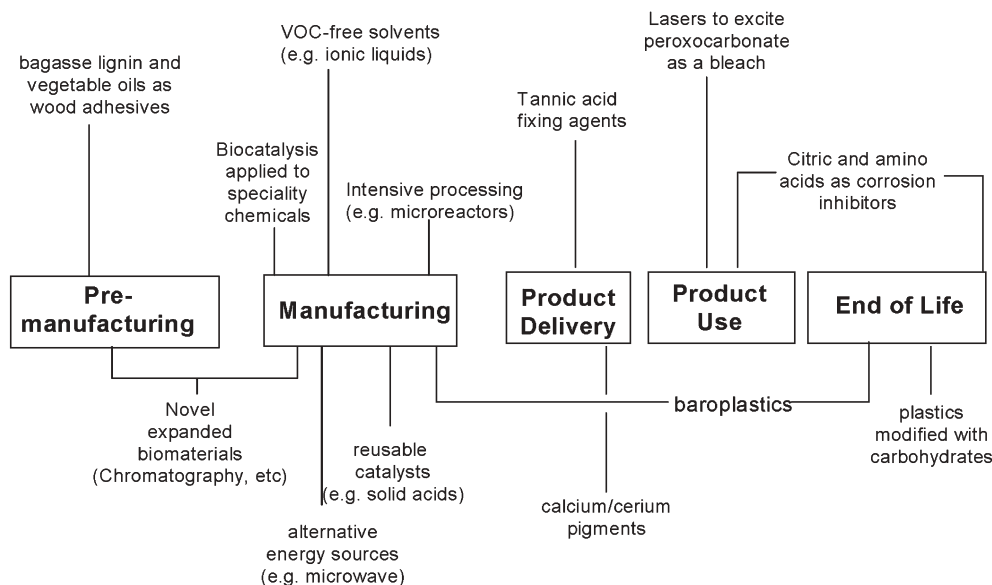


Fig. 4 Some examples of recent progress in green chemistry R&D.

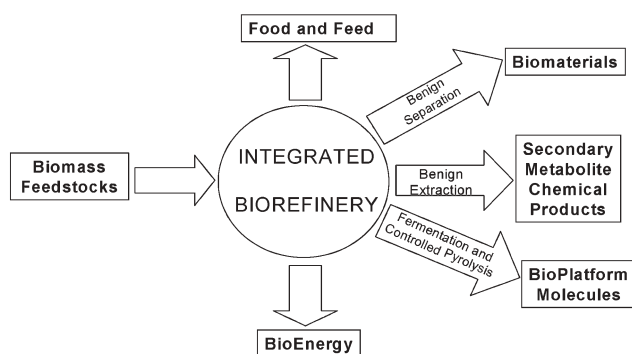


Fig. 5 Green chemistry and the biorefinery.

(Fig. 5). We recently reported methodology for physically expanding starch for example, to a very high surface area porous solid suitable for use in applications including as a catalyst support,⁹ as a stationary phase for chromatographic separation¹⁰ and in novel composite materials.¹¹ Cellulose can also be expanded into a high surface area, mesoporous solid. Most recently we have found that controlled carbonisation of starch materials can lead to entirely new forms of carbon that we have nicknamed “starbons”¹² (Fig. 6).

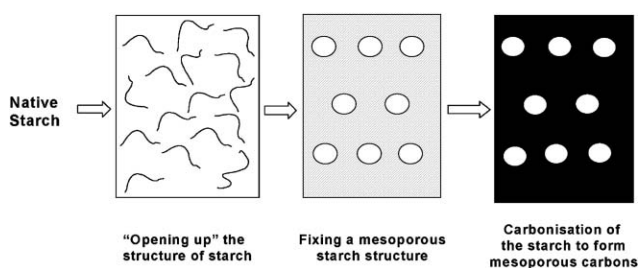


Fig. 6 Schematic illustrations of the synthesis of mesoporous carbons “starbons”.

It seems such a ‘waste’ that these diversely abundant and renewable materials currently have such low value uses. Nature’s other large volume polymers cellulose¹³ and chitin¹⁴ also offer great potential for better exploitation.

Bioplatform molecules are the beginning of a new and vital challenge for organic chemists.¹⁵ Can we build on them as we have done over the last 70 years with the now well-established petro-platform molecules such as ethene and benzene (Fig. 7)? With the rapid growth in biotechnology we can expect to see both more candidates for new platform molecules and more selective bioprocesses for making platform molecules. We need a substantial growth in research activity on the conversion of these platform molecules to valuable products and including the effective use of the dilute ‘broths’ containing these molecules. The processing of these sustainable product mixtures needs careful control—we cannot afford to apply old, dirty, chemical methods and we must ensure that the overall environmental impact of the process from biomass to

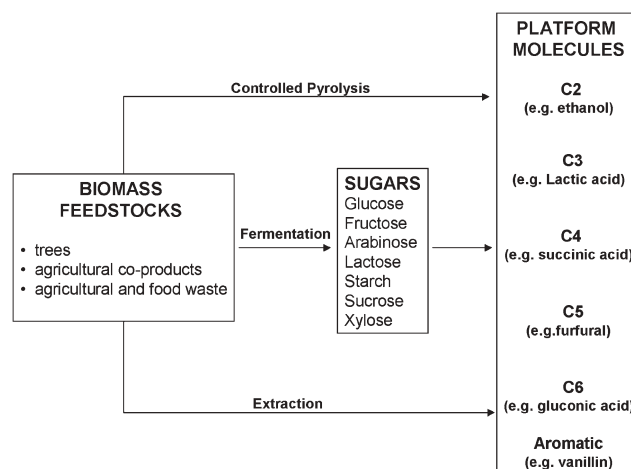


Fig. 7 Bioplatform molecules.

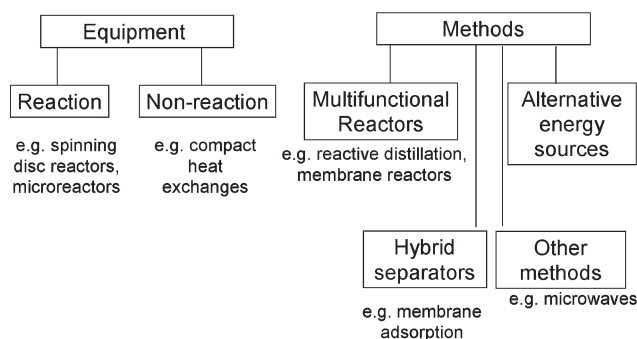


Fig. 8 Process intensification.

final product is kept low. The green processes involved are likely to be a mix of green chemical and biochemical (e.g. enzymatic) methods. I suggest that we need to carefully monitor this rapidly evolving technology for example through the use of “acceptability criteria”. These might, for example, state that there should be no more than three steps from the biomass to the final product and that each step should have a maximum E factor of 1 or 2 or similar green chemistry metric evaluation.

The green chemistry process research on novel catalysts, benign (non-VOC) solvents, *etc* is now being strengthened and moved closer to industrial application through the innovative contributions from chemical and process engineers, notably in the context of process intensification—scale out, not up (Fig. 8)!

The growth in industrial utilisation of new, greener technologies in recent years is encouraging though it still only represents a tiny fraction of the total volume of chemical manufacturing worldwide. Interesting case studies are now available at all stages in the lifecycle (Fig. 9) and this journal regularly publishes good examples of research that should guarantee a pipeline of green chemistry processes that will make their way through to industrial applications. Highly publicised and sought after awards and prizes, notably the US

Presidential Green Chemistry Awards play an important role in promoting good case studies and more should be encouraged especially with a product focus. Legislation is placing a new emphasis on chemical products that needs a strong response from industry and research. This should also include research grant programmes which focus on green product design and which encourage collaboration throughout the supply chain including a greater involvement from the user community. The importance and complexity of chemicals in cars and electronic equipment is now recognised in new legislation which affects the chemical inputs at manufacture (e.g. RoHS) and the fate of chemicals at end-of-life (e.g. end-of-life vehicle directives, WEEE). We should quickly extend this to other consumer goods—the thousands of different products in a modern department store represent an enormous contribution of chemicals to society and also an enormous challenge to meet new legislation and societal requirements to remove the more hazardous substances. This will force the search for substitutes for substances of concern, which in turn will reveal many gaps in the suitable chemicals that are available. How do we replace the more hazardous brominated flame retardants, surface primers, volatile organic solvents and plasticizers, which are so prevalent in the products of modern society? The challenges and opportunities ahead for green chemistry are greater than ever!

The last 7 years have also seen a very welcome growth in the number of green chemistry centres, initiatives and networks across the world. I have been delighted to see major local activities start in countries and regions in Europe, Asia and the Americas. In many cases local activities have started with a very appropriate blend of education and research, reflecting the trend in the more established networks such as the GCN¹⁶ and the GCI.¹⁷ Education at all levels is vital to the future of green chemistry but while we see examples of good practice now in many countries and at school as well as tertiary level, the teaching of green chemistry at universities is still more the exception than the norm. We must ensure that the principles and practice of green chemistry are embedded in every

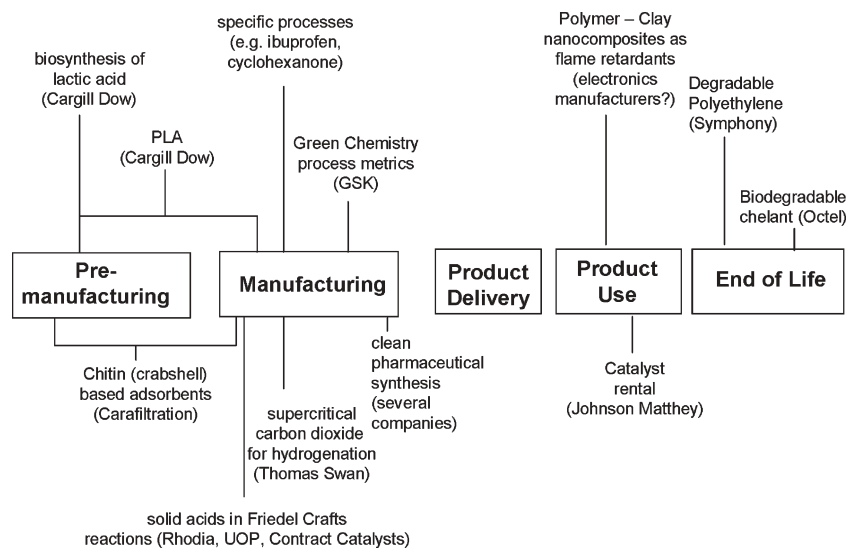


Fig. 9 Examples of green chemistry in practice.

chemical sciences degree course so that future generations of chemical scientists are at the heart of a sustainable 21st century society.

References

- 1 J. H. Clark, *Green Chem.*, 1999, **1**, 1.
- 2 <http://europa.eu.int/comm/environment/chemical/reach.htm>.
- 3 <http://www-european-voice.com/downloads/WithinREACHConferenceReport.pdf>.
- 4 *Industrial Biotechnology and Sustainable Chemistry*, Royal Belgian Academy Council of Applied Science, Brussels, January 2004.
- 5 *Green Chemistry and the Consumer*, <http://www.york.ac.uk/inst.greenchemic/gcc/GC&Chome.htm>.
- 6 *Sustainable Development in Practice*, ed. A. Azapagic, S. Podan and R. Clift, Wiley, Chichester, 2004.
- 7 *Renewable Bioresources*, ed. C. V. Stevens and R. G. Verte, Wiley, Chichester, 2004.
- 8 F. E. I. Deswarte, J. H. Clark, J. J. E. Hardy and P. M. Rose, *Green Chem.*, 2006, **8**, DOI: 10.1039/b514978a.
- 9 J. H. Clark, S. Doi, K. Milkowski and D. J. Macquarrie, *Chem. Commun.*, 2002, 2632.
- 10 V. Budarin, J. H. Clark, F. E. I. Deswarte, J. J. E. Hardy, A. J. Hunt and F. M. Kerton, *Chem. Commun.*, 2005, 2869.
- 11 K. Milkowski, J. H. Clark and S. Doi, *Green Chem.*, 2004, **6**, 189.
- 12 *UK Pat. Application*, GB 0510471.6, 2005.
- 13 J. H. Clark, J. J. E. Hardy, K. Milkowski, F. M. Kerton, A. J. Hunt and F. E. I. Deswarte, *PCT Int. Pat. Application*, 2005, WO 2005.011836.
- 14 J. J. E. Hardy, S. Hubert, D. J. Macquarrie and A. J. Wilson, *Green Chem.*, 2004, **6**, 53.
- 15 Top value added chemicals from biomass: http://www.eere.energy.gov/biomass/products_rd.html.
- 16 <http://www.chemsoc.org/gcn>.
- 17 <http://www.chemistry.org/portal/a/c/s/1/acdisplay.html?DOC=greenchemistryinstitute>.

ReSource

Lighting your way through the publication process

A website designed to provide user-friendly, rapid access to an extensive range of online services for authors and referees.

ReSource enables authors to:

- Submit manuscripts electronically
- Track their manuscript through the peer review and publication process
- Collect their free PDF reprints
- View the history of articles previously submitted

ReSource enables referees to:

- Download and report on articles
- Monitor outcome of articles previously reviewed
- Check and update their research profile

Register today!

RSC Publishing

www.rsc.org/resource

02030508

A green and facile route to γ - and δ -lactones *via* efficient Pinner-cyclization of hydroxynitriles in water†

Karolina Aplander, Olle Hidestål, Kambiz Katebzadeh and Ulf M. Lindström*

Received 26th September 2005, Accepted 16th November 2005

First published as an Advance Article on the web 23rd November 2005

DOI: 10.1039/b513656c

In the presence of a recyclable cationic exchange resin hydroxynitriles smoothly undergo a Pinner cyclization/hydrolysis two-step reaction in pure water to give lactones in good to excellent yields.

Lactones are frequently occurring structural subunits in many biologically active natural products, for example natural flavors and pheromones. Functionalized chiral lactones have found extensive use as building blocks for the stereoselective preparation of alkaloids, antibiotics, pheromones and flavor components.¹ It is therefore of importance to develop simple and reliable methods of preparing lactones, and a variety of methods have indeed been introduced, the most common being cyclization of hydroxyacids or haloacids.² On the other hand, hydroxynitriles should be highly useful as precursors of lactones because of the ease with which various nitriles can be prepared, for example by cyanide ion nucleophilic substitution at electrophilic carbons. Nevertheless, this approach towards lactones has been severely hampered by the harsh conditions usually required. A recent attempt to convert hydroxynitriles into lactones *via* mild, enzymatic hydrolysis of the cyano group was of limited value for synthetic purposes.³ Thus, a useful method for the direct conversion of hydroxynitriles into lactones is a desirable yet unfulfilled goal. Also, because of environmental concerns and increased restrictions on the use of hazardous organic solvents it has recently become of significant interest to develop reactions in water, which is a cheap, safe and non-toxic solvent.⁴ If, in addition, aqueous reactions can be efficiently mediated by heterogeneous catalysts that can be recycled and reused many times, the result will be nearly ideal processes in terms of both greenness and simplicity. Herein we present the direct, high-yielding conversion of hydroxynitriles into lactones using water as solvent and a cationic exchange resin as a recyclable, heterogeneous catalyst.

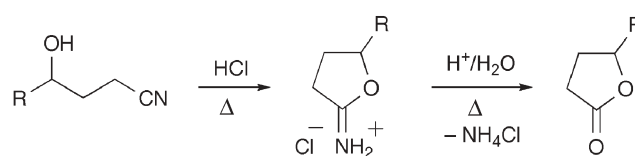
In an ongoing synthetic project we needed to convert a γ -hydroxynitrile into the corresponding lactone. The few reported experiments that exist on this transformation are two-step procedures.⁵ First, cyclization of the starting hydroxynitrile is achieved by an intramolecular Pinner reaction to give a cyclic imidate (Scheme 1). This step has been shown to require strong acid catalysis in organic media (*e.g.* HCl/EtOH or HCl/ether),^{5d,e} except in highly favorable cases where aqueous basic,^{5a} or even neutral^{5b} conditions have been used. The second step, hydrolysis of

the cyclic imidate into the lactone, typically involves highly acidic aqueous conditions at elevated temperatures.^{5a,b,d,e}

Not surprisingly, the harsh conditions caused severe problems with side reactions in our synthetic study and it was necessary for us to develop an alternative method. Recently, Mizuno and co-workers reported an efficient procedure for the hydration of nitriles to amides in water using an alumina-supported ruthenium catalyst ($\text{Ru}(\text{OH})_x/\text{Al}_2\text{O}_3$).⁶ The reaction was proposed to proceed *via* coordination of the nitrile to the ruthenium metal. The activated nitrile then undergoes facilitated hydrolysis. We reasoned that if a hydroxynitrile was used, an intramolecular attack of the hydroxyl group could take place to form a cyclic imidate rather than an open chain amide. In a first attempt we heated hydroxynitrile **1a** at 125 °C in water in the presence of $\text{Ru}(\text{OH})_x/\text{Al}_2\text{O}_3$ (5% Ru). This led to complete conversion of starting material, but only after 27 h, and three products were detected. These were identified as the expected cyclic imidate **2a** and, gratifyingly, lactone **3a** in a 3 : 2 ratio, along with minor amounts of the amide corresponding to the hydrolysis product of nitrile **1a** (Table 1, entry 1).

The formation of significant amounts of lactone was encouraging at this stage. The presence of amide in the product mixture was not surprising in view of the work by Mizuno and co-workers described above. However, according to their mechanistic proposal, the hydroxide that is added to the cyano group does not originate from the surrounding water but from $\text{Ru}(\text{OH})_x$ *via* an intramolecular transfer. We therefore decided to test the use of RuCl_3 a reagent which, although inferior to $\text{Ru}(\text{OH})_x/\text{Al}_2\text{O}_3$, also converted nitriles to amides but presumably *via* a different mechanism where the hydroxide must be delivered from a source external to the $\text{RuCl}_3\text{-CN}$ complex. Indeed, heating **1a** with RuCl_3 (5%) in water in a sealed tube at 135 °C for 42 h yielded no detectable amide, but cleanly converted starting material into lactone **3a** and cyclic imidate **2a** in a 9 : 1 ratio (entry 2). No other products were observed.

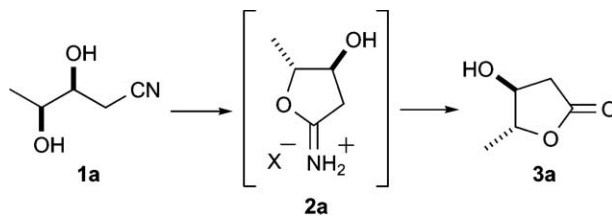
With hopes of reducing reaction time, we decided to add a Brønsted acid as co-catalyst. An initial attempt using acetic acid as additive had no significant effect on the rate of the reaction



Scheme 1 The two-step Pinner-cyclization/hydrolysis reaction sequence has been of limited use in the preparation of lactones due to the harsh conditions usually required.

Organic Chemistry, Lund University, P. O. Box 124, SE-221 00 Lund, Sweden. E-mail: ulf.lindstrom@organic.lu.se; Fax: +46 46 2228209; Tel: +46 46 2228211

† Electronic supplementary information (ESI) available: General experimental details and procedures for the preparation of **1e** and **3e**. ¹³C-NMR spectra for all lactones. See DOI: 10.1039/b513656c

Table 1 Optimization of conditions for the cyclization of hydroxynitrile **1a** into lactone **3a**


Entry	Catalyst ^a	X ⁻	Time/h	T/°C	3a : 2a
1	Ru(OH) _x	OH ⁻	27	125	2 : 3 ^b
2	RuCl ₃	OH ⁻	42	135	9 : 1
3	RuCl ₃ /acetic acid (100%)	AcO ⁻	42	130	7 : 3
4	RuCl ₃ /Dowex 50 × 8 (H ⁺)	RSO ₃ ⁻	6	135	1 : 0
5	Dowex 50 × 8 (H ⁺)	RSO ₃ ⁻	1	135	1 : 0
6	—	OH ⁻	6	135	1 : 3

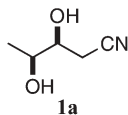
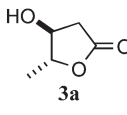
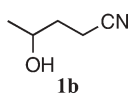
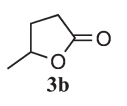
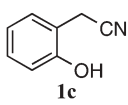
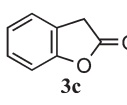
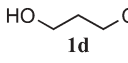
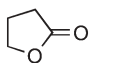
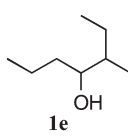
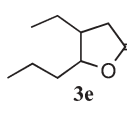
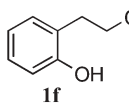
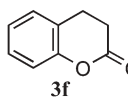
^a 5% Ru was used in entries 1–4. ^b Also contained minor amounts of amide corresponding to the hydrolysis product of **1a**.

(entry 3). On the other hand, a remarkable improvement was found when we ran the reaction in the presence of a solid-supported acid catalyst. Heating **1a** with RuCl₃ (5%) in water with acidic Dowex 50 W × 8–200 (1.7 meq mL⁻¹) cation exchange resin at 135 °C afforded lactone **3a** exclusively in only 6 h (entry 4).⁷ At this point we became interested in deducing the roles played by the metal and the acid catalyst in mediating lactonization, and to initiate such a study we ran the reaction without RuCl₃. Surprisingly, the reaction proceeded efficiently also in the absence of metal! In addition, we were able to reduce the reaction time drastically to just one hour (entry 5). No other products were detected and the lactone was obtained in spectroscopic purity (¹H-, ¹³C-NMR) after filtration and removal of the solvent under reduced pressure. When we ran the reaction in neat water, *without catalyst*, we found to our further surprise that significant amounts of the lactone was formed after 6 h reaction at 135 °C. No starting material was observed and the imidate was the major product (**3a/2a** 1 : 3, entry 6). From this result we draw the conclusion that the resin plays an important part in accelerating the hydrolysis of the intermediate imidate. A plausible mechanistic rationale is that the charged cyclic imidate becomes localized at the ionic surface of the catalyst, where hydrolysis to lactone should be facilitated because of the highly acidic environment.

The high purity of the crude product can in part be explained by efficient removal of the stoichiometric ammonium ion byproduct from the reaction mixture through salt formation with the sulfonic acid groups of the catalyst resin, which also accounts for the need for more than a stoichiometric amount of catalyst. Unfortunately, attempts at running the reaction at lower temperature were not successful. At temperatures below 100 °C the reaction became extremely sluggish. On the other hand, higher temperatures than 140 °C led to thermal decomposition of the resin.

After having established that the use of a cationic exchange resin in water efficiently promotes the projected Pinner cyclization/hydrolysis reaction sequence, we proceeded to investigate the scope of this method by applying it to other hydroxynitriles. As can be seen in Table 2, various γ -hydroxynitriles (**1a–1f**) cyclize to the corresponding γ -lactones (**3a–3e**) in good to excellent yields (65–99%) under the described conditions (entries 1–5). Gratifyingly, we

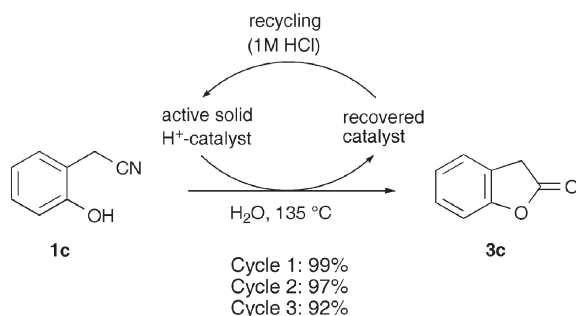
Table 2 Cyclization of hydroxynitriles **1a–1f** into lactones **3a–3f** using acidic cation exchange resin in water at 135 °C^a

Entry	Hydroxynitrile	Lactone	Time/h	Yield (%) ^b
1			1	96
2			6	95 ^c
3			6	>99
4			30	83 ^c
5 ^d			1	65
6			47	79

^a For a typical experimental procedure, see ref. 8. ^b Yields refer to crude products of >95% purity by NMR, except for **3a** which was purified by flash chromatography. ^c Work-up by extraction with diethyl ether. Quantitative recovery of unreacted imidate from the water phase. ^d Performed with a mixture of diastereomers. Diastereomeric ratio retained in the product.

were also able to apply this method to the preparation of a δ -lactone. Cyclization of δ -hydroxynitrile **1f** under the described conditions gave dihydrocoumarin, **3f**, thus suggesting an efficient entry to the attractive coumarin derivatives. A considerably longer reaction time (47 h) was required, however, in order to get a good yield (79%, entry 6). In general, the procedure for isolating the products from the aqueous reaction mixture was limited to removal of the cation exchange resin by filtration and evaporation of the solvent.

Alternatively, in the cyclizations of **1b** and **1d**, where volatility was a potential problem, lactones **3b** and **3d** were extracted from the filtrate with diethyl ether (entries 2 and 4). In these cases, the lactones and the water-soluble unreacted imidate intermediates were efficiently separated into the organic and the aqueous phases, respectively, and the material was quantitatively recovered by concentration of the phases. Either work-up procedure led to >95% pure lactones (¹H-, ¹³C-NMR) thus obviating the need for costly and time-consuming chromatography for most synthetic purposes.



Scheme 2 Recovery of the cation exchange resin for recycling and use in subsequent cyclization/hydrolysis reactions.

Finally, in order to verify that the solid catalyst could be recycled, we recovered the resin from the cyclization of **1c**, reactivated it by treatment with a small amount of 1 M HCl and used it in subsequent cyclizations. The reaction was performed three times using the same resin and only a small decrease in the isolated yield of **3c** was observed (Scheme 2).

In conclusion we have developed a useful method of preparing synthetically attractive γ - and δ -lactones *via* the cyclization of γ - and δ -hydroxynitriles. In comparison with reported protocols for preparing lactones from hydroxynitriles, the method presented herein avoids the use of concentrated mineral acids in organic and aqueous–organic media and instead employs a heterogeneous catalyst that is easily removed from the product mixture, and which can be recycled and reused. No metals or other hazardous chemicals are employed and the reactions are run in pure water, which is the cheapest and most harmless solvent available. Finally, lactones of >95% purity were simply and conveniently obtained by filtration followed by concentration of the filtrate. This is in part due to relatively short reaction times, but also because ionic byproducts can associate strongly with the catalyst itself and efficiently be removed from the reaction mixture, thus greatly facilitating purification procedures. These synthetic as well as green advantages should make cyclization of hydroxynitriles a more attractive route to various lactones.

Acknowledgements

We thank the Swedish Research Council and the Crafoord Foundation for financial support.

References

- (a) C. García, T. Martín and V. S. Martín, *J. Org. Chem.*, 2001, **66**, 1420; (b) H. Takahata, Y. Uchida and T. Momose, *J. Org. Chem.*, 1994, **59**, 7201 and references therein.
- For a list of methods, see: M. B. Smith and J. March, *Advanced Organic Chemistry*, Wiley, New York, 5th edn, 2001, p. 1680.
- S. K. Taylor, N. H. Chmiel, L. J. Simons and J. R. Vyvyan, *J. Org. Chem.*, 1996, **61**, 9084.
- For recent reviews, see: (a) C. J. Li, *Chem. Rev.*, 2005, **105**, 3095; (b) U. M. Lindström, *Chem. Rev.*, 2002, **102**, 2751; (c) *Organic Synthesis in Water*, ed. P. A. Grieco, Blackie Academic & Professional, London, 1998; (d) C. J. Li and T. H. Chan, *Organic Reactions in Aqueous Media*, Wiley, New York, 1997. See also thematic issue: "Organic Reactions in Water", *Adv. Synth. Catal.*, 2002, **344**(3–4).
- For representative examples, see: (a) F. Fringuelli, O. Piermatti and F. Pizzo, *J. Chem. Educ.*, 2004, **81**, 874; (b) S. Darvesh, A. S. Grant, D. I. MaGee and Z. Valenta, *Can. J. Chem.*, 1991, **69**, 723; (c) M. J. Fisher, W. J. Hehre, S. D. Kahn and L. E. Overman, *J. Am. Chem. Soc.*, 1988, **110**, 4625; (d) R. Kwok and M. E. Wolff, *J. Org. Chem.*, 1963, **28**, 423; (e) D. H. R. Barton, J. M. Beaton, L. E. Geller and M. M. Pechet, *J. Am. Chem. Soc.*, 1960, **82**, 2640.
- K. Yamaguchi, M. Matsushita and N. Mizuno, *Angew. Chem., Int. Ed.*, 2004, **43**, 1576.
- The amount of dry resin used was 10 times the weight of the starting hydroxynitrile, which based on the exchange capacity of Dowex 50 W \times 8–200 (2.1 meq g⁻¹) corresponds to approximately 2 equivalents of acid.
- Representative procedure: 2-Coumaranone (**3c**). To a mixture of 2-hydroxyphenylacetonitrile, **1c** (18.8 mg, 0.14 mmol), in H₂O (1 mL) was added cationic exchange resin (190 mg, Dowex 50 W \times 8–200). The reaction mixture was stirred vigorously in a sealed tube at 135 °C for 6 h. After cooling to room temperature, the catalyst was filtered off and washed with ethanol. The filtrate was concentrated with gentle heating under reduced pressure to give 2-coumaranone, **3c**, in quantitative yield. Spectroscopic data were in accordance with commercially available material. Reactions with more volatile molecules can alternatively be worked up by a double extraction of the filtrate with diethyl ether, followed by drying of the combined organic phases over MgSO₄ and concentration at reduced pressure.

Gold nanoparticle-catalysed [3 + 2]dipolar cycloaddition of 1,6-allenylbenzaldehydes: construction of polycyclic ring systems

Arun Kumar Gupta,^a Chul Yun Rhim,^a Chang Ho Oh,^{*a} R. S. Mane^b and Sung-Hwan Han^{*b}

Received 24th August 2005, Accepted 15th November 2005

First published as an Advance Article on the web 24th November 2005

DOI: 10.1039/b512034a

We have isolated spherical-shaped monodispersed 12–14 nm range gold nanoparticles, when *o*-1,6-allenylbenzaldehyde underwent a novel mode of tandem cycloaddition and cyclization using AuCl₃ precatalyst. This cyclization can be found in the construction of many polycyclic natural product skeletons.

Recently it has been found that *anhydrous* AuCl₃ catalyzes the formation of C–C and C–O bonds, behaving as an effective Lewis-acid catalytic system;¹ such as selective cross cycloisomerization/dimerization of propargyl or alkynyl ketones, benzoannulation between *o*-alkynylbenzaldehydes and alkynes or cyclizations of alkynyl furan.^{1a} Due to the excellent alkynophilicity of gold; particular attention has been paid to the gold-based alkyne activation as an attractive strategy for developing new and efficient catalytic cyclizations. Yamamoto and co-workers recently reported a novel gold-catalyzed benzoannulation of *o*-alkynylbenzaldehydes with alkynes involving [4 + 2] cycloaddition of a Au-pyrylium intermediate with dienophiles such as alkynes and enol ethers.² They also reported that enals bearing a pendant alkyne group underwent [4 + 2] benzannulations intramolecularly.³ Recently we reported that enynes bearing an aldehyde group underwent unprecedented Rh-catalyzed cyclization which could involve [3 + 2] cycloaddition of a Rh-carbenoid dipolar carbonyl ylide intermediate.⁴ However, there were no reports on cycloaddition of such complexes to pendent allene group either inter or intramolecularly.

Unique reactivity of two orthogonal π -bonds present in allenyne have made them to be of great interest in the field of organometallics⁵ as well as for the construction of natural product⁶ frameworks. Very recently, Qilong and Hammond reported that the formation of [2 + 2] cycloaddition product **2** from molybdenum catalyzed reactions of 1,7-allenyne **1**, where the metal complex was used catalytically.⁷ A similar cycloaddition reaction under microwave irradiation was reported by Brummond and Chen,⁸ and their reports on a stoichiometric Pauson–Khand reaction (PKR) with a similar substrate **1** using the same catalyst, gave **3** and **4** as products (Scheme 1).⁹

We have also showed that allenyne **5** have different cyclization modes with different palladium catalysts. Cycloreduction occurred at the triple bond to give an alkenylpalladium species that underwent carbo-palladation to give six-membered cycles **6**, whereas rhodium catalyzed cyclizations of those allenyne **5** gave

five membered rings **7** chemoselectively. In the case of 1,6-allenyne **8**, these gave five membered ring cycles **9** upon cycloreduction, whereas six-membered ring systems **10** were obtained on arylative cyclization under palladium catalysis (Scheme 2).¹⁰

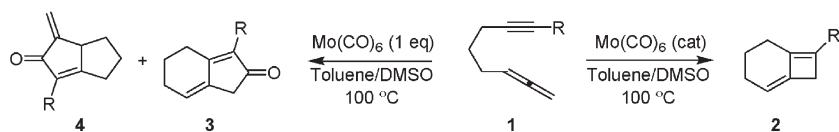
In continuation of our research interest in allenyne¹¹ and also in pursuit of previous investigations, a closer outlook prompted us to secure cycloisomerisation involving Huisen-type cycloaddition of Au-pyrylium intermediates with dipolarophiles.¹² Here we wish to report a highly economical as well as an environmentally benign methodology for intramolecular tandem [3 + 2] cycloaddition and cyclization of *o*-1,6-allenylbenzaldehydes under gold (III) chloride catalysis at room temperature. Also, the catalyst gold (III) chloride was recovered as monodispersed spherical nanoparticles and reused for the same reaction. At first, we have taken 3 mmol% gold (III) chloride and 1,6-allenylbenzaldehyde **12** (1 mmol) in a 10 mL test tube containing 2 mL of 1,2-dichloroethane. Here we have found that compound **12** underwent a novel mode of cycloaddition–cyclization,¹³ with the formation of gold spherical, monodispersed nanoparticles. The structure of product **13** was confirmed by IR, ¹H NMR, CMR, MS and HRMS.¹⁴ The gold nanoparticles' structure, surface properties and particle size were characterized by XRD, SEM and finally confirmed with TEM.

In our experiments, we could isolate the product **13** exclusively, which is similar to our Rh-catalyzed reactions of enynals. Au-catalysed reactions of allenyne might also occur *via* 1,3-dipolar cycloaddition to form the electron deficient Au-carbene species which subsequently underwent sequential fragmentation to give product **13** and to generate AuCl₃ for the next cycle (Scheme 3). The fused polycyclic products obtained from this study were very stable during silica gel chromatography and prolonged storage at room temperature. We studied this reaction in 1,2-dichloroethane with different gold catalysts. AuCl₃ with/without combining AgOTf catalyzed [3 + 2] cycloaddition,¹⁵ whereas a combination of AuCl₃ with PPh₃ did not catalyze any of these pathways (Table 1, entries 1–3). Triphenylphosphine might react with AuCl₃ to destroy its catalytic activity or Lewis acidity. Au (+1) also catalyzed [3 + 2] cycloisomerization but albeit in low yield (Table 1, entry 4). Among the reaction conditions we have tried, gold (III) chloride with 3 mmol% in 1,2-dichloroethane solution at room temperature is the best suitable condition for the present study (Table 1, entry 1).

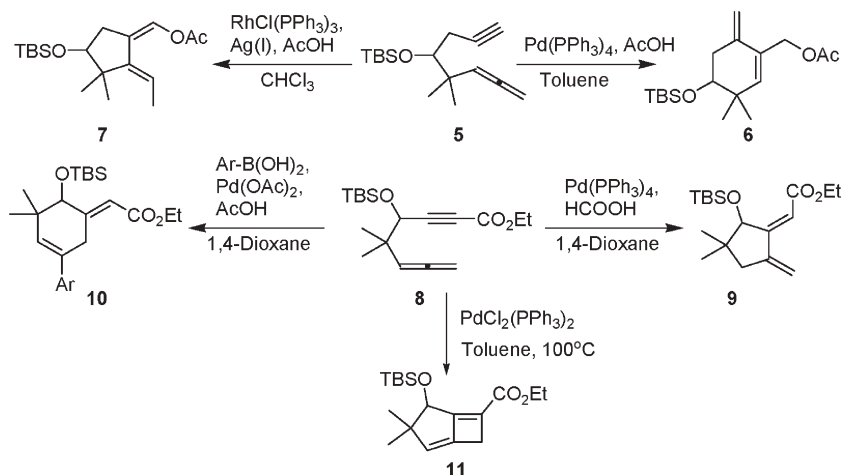
A plausible mechanism for the present metal catalyzed cycloaddition–cyclization reaction is AuCl₃-complexation of *o*-1,6-allenylbenzaldehyde which is expected to form a zwitterion as proposed by Yamamoto *et al.*¹⁶ This intermediate on successive tandem [3 + 2] cycloaddition with tethered allene will lead to the

^aGOS Lab, Department of Chemistry, Hanyang University, Seoul, 133 791, South Korea

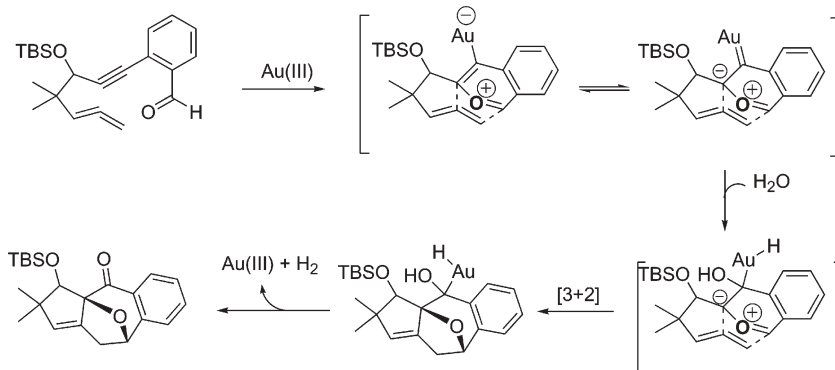
^bInorganic Nanomaterials Lab, Department of Chemistry, Hanyang University, Seoul, South Korea



Scheme 1



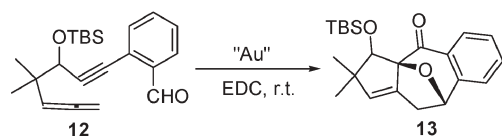
Scheme 2



Scheme 3

Table 1 Intramolecular [3 + 2] cyclization–cycloaddition under various reaction conditions

Entry	Reaction conditions	$T/^\circ\text{C}$, t/h	Yield (%)
1	AuCl_3	25, 8	69
2	$\text{AuCl}_3/\text{AgOTf}$	25, 8	43
3	$\text{AuCl}_3/\text{PPh}_3$	80, 10	Trace
4	AuCl	25, 24	23
5	AuBr_3	25, 36	46
6	AuCl_3 nanoparticles	25, 12	63
7.	AuCl_3 nanoparticles	25, 12	60



observed oxabicyclic product and addition of water can occur at any stage, regenerating Au (III) and molecular hydrogen (Scheme 3).

The gold nanoparticles formed were adsorbed onto a glass substrate of plate dimension $1 \times 1 \text{ cm}^2$ and characterized by X-ray diffraction (XRD) (Siemens D-5005 diffractometer) using graphite-monochromatized Cu $K\alpha$ radiation at 40 kV and 100 mA. Fig. 1a shows the X-ray diffraction pattern of gold nanoparticles recorded at room temperature. The location of planes corresponding to (111), (200), (220), (311) and (222) are in good agreement with the Joint Committee on Powder Diffraction Standards (JCPDS No. 040-784) reference diagrams for the corresponding bulk phases with lattice constant $a = 4.087 \text{ \AA}$. The satisfactory agreement among the ' d ' (interplanar spacing) values confirms the presence of gold nanoparticles. In the XRD pattern the presence of the (111) reflection as a dominant peak along with

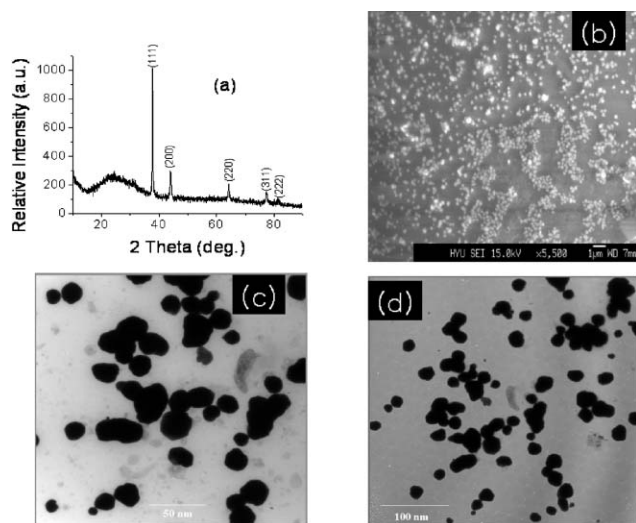


Fig. 1 (a) XRD profile of as-deposited gold nanoparticles onto a 1 × 1 cm² glass substrate, (b) SEM image, (c), (d), low and high magnified TEM images.

the presence of reflections from planes of other types, indicates the formation of nanocrystallites with a moderate degree preferred orientation. Nothing other than a broad hump (15–40°), a characteristic peak due to the glass substrate, was detected in XRD spectrum. This observation reveals that the gold nanoparticles preferentially grew in 3D rather than 1D or 2D. An intense peak (111) was used to calculate the grain size using Scherrer's formula with a correction factor of 0.94 due to the specific geometry of grains and non-conducting nature of the substrate.¹⁷ The 12.4 nm grain size was calculated for as-formed gold nanoparticles.

In the SEM image¹⁸ (Fig. 1b), good film substrate coverage of gold nanoparticles in the form of monodispersed spheres with considerable void spaces are clearly observed. The resolution limit of the SEM made it difficult for us to calculate the exact nanoparticle size, where we preferred to use transmission electron microscopy (TEM).¹⁹ Representative TEM images of gold nanoparticles for two different magnifications are shown in Fig. 1c and d, indicating a controlled growth of spherical gold nanoparticles. It can be seen in Fig. 1c that there exists a large number of gold nanoparticles with sphere-like surface morphology. Observation of the magnified image in Fig. 1d, shows that the gold nanoparticles are either isolated or in colony form. The average diameter of 12–14 nm was obtained which was found to be consistent with XRD data.

The recovered valuable gold catalyst, as 12–14 nm range spherical nanoparticles, was reused in the same reaction (Table 1, entries 6 and 7) as well as its applications in various fields.²⁰

In summary, Au-catalyzed [3 + 2] intramolecular tandem cycloaddition–cyclization of 1,6-allenylbenzaldehydes with the formation of nanoparticles was shown. Thus we have demonstrated a very simple, eco-friendly, and more economical methodology for the synthesis of fused polycyclic ring systems from the corresponding *o*-1,6-allenylbenzaldehydes. We are currently pursuing the application of this methodology to the generation of a large library of polycyclic ring systems, which will

be of interest to medicinal chemistry and in the construction of natural products.²¹

Acknowledgements

This work was supported by the Korean Science and Engineering Foundation (ABRL R14-2003-014-01001-0). AKG is thankful to the KOSEF for a Brain Pool fellowship.

References

- (a) A. S. K. Hashmi, L. Schwarz, J.-H. Choi and T. M. Frost, *Angew. Chem., Int. Ed.*, 2000, **39**, 2285–2287; (b) A. S. K. Hashmi, T. M. Frost and J. W. Bats, *J. Am. Chem. Soc.*, 2000, **122**, 11553–11554; (c) N. Asao, K. Takahashi, S. Lee, T. Kasahara and Y. Yamamoto, *J. Am. Chem. Soc.*, 2002, **124**, 12650–12651.
- (a) N. Asao, H. Aikawa and Y. Yamamoto, *J. Am. Chem. Soc.*, 2004, **126**, 7458–7459; (b) A. S. K. Hashmi, T. M. Frost and J. W. Bats, *J. Am. Chem. Soc.*, 2000, **122**, 11553–11554; (c) A. S. K. Hashmi, T. M. Frost and J. W. Bats, *Catal. Today*, 2002, **72**, 19–27; (d) J. W. Dankwardt, *Tetrahedron Lett.*, 2001, **42**, 5809–5812.
- N. Asao, K. Sato, Menggenbater and Y. Yamamoto, *J. Org. Chem.*, 2005, **70**, 3682–3685.
- S. Shin, A. K. Gupta, C. Y. Rim and C. H. Oh, *Chem. Commun.*, 2005, 4429–4431.
- (a) H. Urabe, T. Takeda, D. Hideura and F. Sato, *J. Am. Chem. Soc.*, 1997, **119**, 11295–112305; (b) C. Mukai, I. Nomura and S. Kitagaki, *J. Org. Chem.*, 2003, **68**, 1376–1385; (c) N. Cadran, K. Cariou, G. Hervé, C. Aubert, L. Fensterbank, M. Malacria and J. Marco-Contelles, *J. Am. Chem. Soc.*, 2004, **126**, 3408–3409; (d) A. Padwa, H. Lipka, S. H. Watterson and S. S. Murphree, *J. Org. Chem.*, 2003, **68**, 6238–6250; (e) K. Hiroi, T. Watanabe and A. Tsukui, *Chem. Pharm. Bull.*, 2000, **48**, 405–409.
- (a) K. M. Brummond and J. Lu, *J. Am. Chem. Soc.*, 1999, **121**, 5087–5088; (b) K. M. Brummond, J. Lu and J. Petersen, *J. Am. Chem. Soc.*, 2000, **122**, 4915–4920; (c) K. M. Brummond, D. P. Curan, B. Mitasev and S. Fischer, *J. Org. Chem.*, 2005, **70**, 1745–1753.
- S. Qilong and G. B. Hammond, *J. Am. Chem. Soc.*, 2002, **124**, 6534–6535.
- K. M. Brummond and D. Chen, *Org. Lett.*, 2005, **16**, 3473–3475.
- (a) K. M. Brummond, H. Chen and J. L. Kent, *J. Org. Chem.*, 1998, **63**, 6535–6526; (b) K. M. Brummond, A. D. Kerekes and H. Wan, *J. Org. Chem.*, 2002, **67**, 5156–5163.
- (a) K. M. Brummond, H. Chen, P. Sill and L. You, *J. Am. Chem. Soc.*, 2002, **124**, 15186–15187; (b) S. Shin and T. V. RajanBabu, *J. Am. Chem. Soc.*, 2001, **123**, 8416–8417; (c) T. Shibata, Y. Takesue, S. Kadowaki and K. Takagi, *Synlett*, 2003, 268–270; (d) C. H. Oh, S. H. Jung and C. Y. Rhim, *Tetrahedron Lett.*, 2001, **42**, 8669–8671; (e) C. H. Oh, S. H. Jung, D. I. Park and J. H. Choi, *Tetrahedron Lett.*, 2004, **45**, 2499–2501; (f) A. K. Gupta, C. Y. Rhim and C. H. Oh, *Tetrahedron Lett.*, 2005, **46**, 2247–2250.
- C. H. Oh, D. I. Park, S. H. Jung, V. R. Reddy, A. K. Gupta and Y. M. Kim, *Synlett*, 2005, **13**, 2092–2094.
- In fact, the Huisgen-type [3 + 2] cycloaddition transition states of carbonyl ylides and alkynes have been known for more than 30 years. (a) R. Huisgen, *Angew. Chem., Int. Ed. Engl.*, 1968, **7**, 321–323; (b) H. Hamberger and R. Huisgen, *J. Chem. Soc. D*, 1971, **19**, 1190.
- Typical experimental procedure: Into a 10 mL round bottomed flask was placed 1 mmol of 1,6-allenylbenzaldehyde and 3 mol% AuCl₃. To this, 1,2-dichloroethane (2 mL) was added through the glass syringe. The reaction mixture was first stirred for 10 min at 0 °C and then allowed to warm to room temperature. After completion of the reaction, the reaction mixture was decanted and the nanoparticles were thoroughly washed with 1–2 mL of 1,2-dichloroethane to be reused for the next time. The solvent thus decanted was evaporated and subjected to column chromatography to obtain pure compound **13**.
- Spectroscopic data of compound **13b**: (Colorless syrupy liquid, *R_f* = 0.55, 5% EtOAc–hexane). IR (neat): 2957, 2928, 2857, 1704, 1603, 1463, 1211, 1174, 1145, 1023, 971 cm⁻¹; ¹H NMR (CDCl₃): (8.02 (d, *J* = 8.0 Hz, 1 H), 7.50 (t, *J* = 6.4 Hz, 1 H), 7.37 (d, *J* = 8.0 Hz, 1 H), 7.19 (d, *J* = 8.0 Hz, 1H), 5.67 (s, 1 H), 5.50 (d, *J* = 6.8 Hz, 1 H), 4.03 (s, 1 H), 2.95 (dd, *J* = 9.2, 6.8 Hz, 1 H), 2.23 (d, *J* = 16.4 Hz, 1 H), 1.26 (s, 3 H), 1.17 (s, 3 H), 0.8 (s, 12 H), 0.05 (s, 3 H), –0.04 (s, 3 H); ¹³C NMR

- (CDCl₃): (190.25, 147.13, 138.15, 137.15, 133.23, 130.99, 127.87, 127.25, 122.87, 98.91, 86.48, 77.32, 55.18, 32.633, 28.22, 22.65, 18.02, -4.71, -5.51; MS (*m/z*): 370, 355, 313, 295, 269, 221, 195, 155, 105, 75; HRMS: exact mass calculated for: C₂₂H₃₀O₃Si (M⁺): 370.1964; found: 370.1960.
- 15 (a) T. Yao, X. Zhang and R. C. Larock, *J. Am. Chem. Soc.*, 2004, **126**, 11164–11165; (b) R.-V. Nguyen, X.-Q. Yao, D. S. Bohle and C.-J. Li, *Org. Lett.*, 2005, **7**, 673–675; (c) X.-Q. Yao and C.-J. Li, *J. Am. Chem. Soc.*, 2004, **126**, 6884–6885.
- 16 (a) B. F. Straub, *Chem. Commun.*, 2004, 1726–1728; (b) N. Asao, K. Takahashi, S. Lee, T. Kasahara and Y. Yamamoto, *J. Am. Chem. Soc.*, 2002, **124**, 12650–12651.
- 17 R. S. Mane and Sung-Hwan Han, *Electrochem. Commun.*, 2005, **7**, 205–207.
- 18 For the SEM analysis, the gold nanoparticle film was coated with a 10 nm platinum layer using a Polaron scanning electron microscopy (SEM) sputter coating unit E-2500, before taking the image.
- 19 Samples for TEM investigations were prepared by putting an aliquot of dichloromethane solution of gold nanoparticles onto an amorphous carbon substrate supported on a copper grid. The excess liquid was then wicked away with tissue, and the grid was allowed to dry at room temperature.
- 20 M. Christne and D. Astruc, *Chem. Rev.*, 2004, **104**, 293–346.
- 21 Natural products: (a) M. George, H. Rodgers, Z. Yong, T. Xinrong, F. T. Lee, F. Jing and D. Sam, *J. Org. Chem.*, 1996, **61**, 8169–8185; (b) K. A. Ghosh, C. Mukhopadhyay and U. R. Ghatak, *J. Chem. Soc., Perkin Trans. 1*, 1994, **3**, 327–332; (c) T. Ohta, E. Yuichi, K. Rikako and N. Shigeo, *Heterocycles*, 1994, **38**, 55; (d) M. F. MacKay, B. G. I. Martin and P. R. Phyland, *Acta Crystallogr., Sect. C*, 1997, **C53**, 1497; (e) T. L. Matthew, B. G. John, B. S. Jeffrey, D. K. Gary, L. Robert, L. O. Daniel, L. J. Deann and H. K. Terrence, *US Pat.*, 151792, 2004; (f) M. Hideaki and N. Mitsutaka, *Tetrahedron Lett.*, 2002, **43**, 2913–2917; (g) G. Saha, S. R. Supti and S. Ghosh, *Tetrahedron*, 1990, **46**, 8229–8236; (h) D. Soumitra, B. Gopa and U. R. Ghatak, *J. Chem. Soc., Perkin Trans. 1*, 1990, **5**, 1453–1458; (i) H. Shinichi, K. Toshimi and H. Yoshiyuki, *Phytochemistry*, 1985, **24**, 1545–1551; (j) H. Hong, N. Neamati, H. E. Winslow, J. L. Christensen, A. Orr, Y. Pommier and G. W. Milne, *Antiviral Chem. Chemother.*, 1998, **9**, 461.

chemistryworld

A "must-read" guide to current chemical science!



Chemistry World provides an international perspective on the chemical and related sciences by publishing scientific articles of general interest. It keeps readers up-to-date on economic, political and social factors and their effect on the scientific community.

16080521

RSC Publishing

www.chemistryworld.org

Process intensification: oxidation of benzyl alcohol using a continuous isothermal reactor under microwave irradiation

R. J. J. Jachuck,^{*a} D. K. Selvaraj^a and R. S. Varma^b

Received 8th September 2005, Accepted 25th October 2005

First published as an Advance Article on the web 14th November 2005

DOI: 10.1039/b512732g

In the past two decades, several investigations have been carried out using microwave radiation for performing chemical transformations. These transformations have been largely performed in conventional batch reactors with limited mixing and heat transfer capabilities. The reactions were performed under adiabatic conditions where the enhancements in the reaction rate reported in these publications may be due to the rapid increase in the reaction temperature during the course of the reaction. The concept of process intensification has been used to develop a narrow channel reactor that is capable of carrying out reactions under isothermal conditions while being exposed to microwave irradiation. Oxidation of benzyl alcohol to benzaldehyde has been carried out using the above-mentioned isothermal micro reactor. Results and the findings of this investigation are discussed in this paper.

Introduction

Chemical reactions under microwave radiation have been studied with great interest since the sixties.^{1,2} Significant momentum in this field was generated after it was shown in 1986^{3,4} that the rate of organic chemical synthesis of chemicals was much faster under microwave irradiation as compared to conventional methods. Since then, numerous researchers have studied and proved that various types of reactions experienced huge rate enhancements under the influence of a microwave field.^{5–11} There have been few instances where microwave enhanced reactions were carried out in continuous reactors.^{12,13} Virtually none of the reactions reported in published literature were carried out in a continuous isothermal reactor and hence there has been considerable debate over the true rate enhancement mechanism of microwave fields, as rapid increase in reaction temperature could result in significant rate enhancement.

Benzaldehyde is one of the most industrially useful members of the aromatic aldehyde family. It is used as a raw material for a large number of products in organic synthesis, including perfumery, beverage and pharmaceutical industries.¹⁴ Microwave oxidation of benzyl alcohol into benzaldehyde using clayfen was studied by Varma and Dahiya¹⁵ and it was found that microwaves did play an influential role in increasing the rate of the reaction.

As part of this investigation, it was intended to design, fabricate and study the performance of a micro reactor capable of operating isothermally under a microwave field. The aim of the study was to investigate the oxidation of benzyl alcohol and obtain experimental data to prove conclusively that the

rate enhancement observed by Varma and Dahiya was due to a true microwave influence, such as rotational movement of the bonds, and not just a temperature effect.

Experimental facility

Experiments were carried out using a 900 Watts Westpointe microwave operating at 2.45 GHz with an internal volume of 0.9 m³. The test facility shown in Fig. 1 consisted of the isothermal micro reactor, which was placed inside the microwave unit and was connected to inlet–outlet ports of the heat transfer side and reactant–product ports of the reaction side.

The reactor was designed and developed by the PICT group at Clarkson University. Fig. 2 shows that the micro reactor consisted of two main sections: an aluminium section and a Poly Tetra Fluoro Ethylene (PTFE) section, used for the heat transfer side and the reaction side respectively. The overall heat transfer coefficient of the reactor, U , was found to be about 2.5 kW m⁻² K⁻¹. The heat generated due to the exposure to a microwave (MW) environment on the reaction side was rapidly absorbed by the heat transfer fluid (H₂O) on the heat transfer side. The materials used in the construction were carefully selected in order to allow near 100% transparency to microwave in the reaction zone and 0%

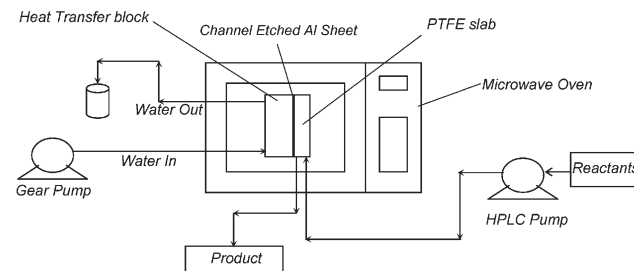


Fig. 1 Schematic of the experimental setup.

^aProcess Intensification and Clean Technology (PICT) Group, Department of Chemical and Biomolecular Engineering, Clarkson University, Potsdam, NY – 13699, USA. E-mail: rjachuck@clarkson.edu
^bNational Risk Management Research Laboratory, US Environmental Protection Agency, 26 West MLK Drive, MS 443, Cincinnati, OH – 45268, USA

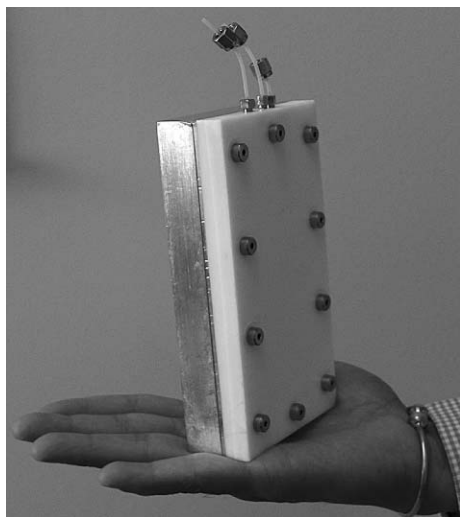
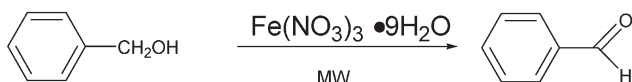


Fig. 2 Isothermal continuous narrow channel reactor.

transparency on the heat transfer side. The reactor had a volume of $2.7 \times 10^{-7} \text{ m}^3$ in the reaction zone and $6 \times 10^{-6} \text{ m}^3$ in the heat transfer zone.

The following is the chemical reaction studied under the influence of microwave irradiation:



The reactant was prepared at room temperature by dissolving solid $\text{Fe}(\text{NO}_3)_3 \cdot 9\text{H}_2\text{O}$ (98+% ACS Reagent) in the benzyl alcohol solution (99+% ACS Reagent). The mixture was stirred thoroughly and filtered using a Fisherbrand[®] filter paper. Experiments were performed using the continuous isothermal reactor under the influence of microwave irradiation for a range of residence times (3–17 s) corresponding to different flow rates ($1\text{--}5 \text{ ml min}^{-1}$) and different microwave intensities (0 W to 39 W). The feed was pumped through the reactor using an HPLC pump (Model: LKB Bromma 2150) and the heat transfer fluid (water) was circulated through the heat transfer zone of the reactor at 120 ml min^{-1} by using a peristaltic pump (Model: Cole Parmer Instrument Co. 7520-01).

In order to benchmark the performance of the narrow channel reactor under the influence of microwaves, several batch experiments were also carried out without exposure to the microwaves. Limited tests were carried out using a PTFE capillary reactor under microwave irradiation to investigate the rate of reaction under adiabatic conditions. These experiments were carried out under non-isothermal conditions by passing the reactants continuously through the narrow channel PTFE tubing for similar residence times as in the isothermal continuous narrow channel reactor.

The inlet and the outlet temperatures of both the reaction and the heat transfer fluid were monitored continuously using a PICO temperature recorder. All the thermocouples were of K type with an error of $\pm 0.3 \text{ }^\circ\text{C}$. Analyses of the results were performed in a Mattson Galaxy Series FTIR-5000. Fig. 3 shows the distinct peaks of benzyl alcohol, in the region of

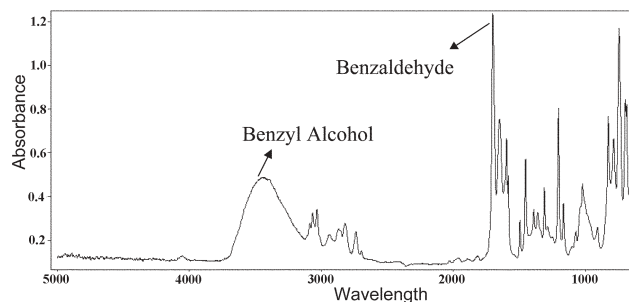


Fig. 3 FTIR Graph showing the peaks of benzyl alcohol and benzaldehyde.

$3100\text{--}3600 \text{ cm}^{-1}$ and benzaldehyde in the region of $1670\text{--}1720 \text{ cm}^{-1}$. Calibration was done using pure benzyl alcohol and benzaldehyde (99.5+% ACS Reagent) solutions. The peak height ratios obtained from the calibration data were used to find the conversion percentage to benzaldehyde from oxidation of benzyl alcohol. Benzyl alcohol and benzaldehyde peaks in the FTIR spectrum obtained from experimental samples were compared with the FTIR library from Mattson Instruments Inc. Peaks obtained from the samples matched accurately with the peaks of the library spectrum. The findings of the experimental investigations for the above conditions have been discussed in the following section.

Results and discussion

In this section, experimental results are presented and discussed critically in order to validate the initial aim of the investigation. Initially, tests were performed using a narrow channel reactor to ensure the following.

(1) Negligible temperature differential (ΔT) between the inlet and the outlet temperature of water (on the heat transfer side), when flowing through the heat transfer side without any reactant flow and the microwave turned off. This was essential in order to prove that any ΔT seen in the inlet and outlet water temperature was due to the heat generated by the reaction when the reactant is exposed to a microwave environment. As can be seen in Table 1, $\Delta T = 0.2 \text{ }^\circ\text{C}$, which is well within the experimental error range.

(2) Under the influence of microwaves, with no reactant in the reaction zone, the ΔT in water stream (heat transfer side) remained negligible. This was important to prove that the microwave did not penetrate the heat transfer side but only penetrated the reaction side, as can be clearly seen in Table 1.

(3) The heat generated on the reaction side when the reactor system was exposed to microwave was completely absorbed by the water flowing on the heat transfer side. This test was essential in order to prove that during the course of the reaction there was negligible rise in the reaction temperature ($<0.3 \text{ }^\circ\text{C}$), ensuring the system was operating under isothermal conditions. As seen in Table 1, when the reaction was operated with both the reactant and the heat transfer fluid flow in their respective chambers coupled with microwave irradiation, a ΔT of $0.2 \text{ }^\circ\text{C}$ at the reaction zone and a ΔT of $3.2 \text{ }^\circ\text{C}$ at the heat transfer zone were measured. This clearly showed that the heat generated by the microwave irradiation and the heat of

Table 1 Isothermal behavior of the narrow channel reactor

Condition	Water inlet (T_1)/°C	Water outlet (T_2)/°C	$(T_1 - T_2)$; ΔT	Reactant inlet (t_1)/°C	Product outlet (t_2)/°C	$(t_1 - t_2)$; Δt	Conclusion
Microwave off No reactant flow	21.9	22.1	0.2	—	—	—	Negligible temperature rise due to friction
Microwave on No reactant flow	22.7	23.0	0.3	—	—	—	Effective microwave shielding of the cooling compartment
Microwave on Reactant flow	22.7	25.9	3.2	21.7	21.9	0.2	Water absorbing heat. Reaction under isothermal conditions.

reaction was absorbed by the heat transfer fluid, thus providing isothermal characteristics to the reactor.

This set of experiments clearly proves and validates our claims that the reactor fabricated is, indeed, an isothermal one suitable for operation under the effect of microwave irradiation.

Influence of residence time

Having performed the initial experiments to establish the capability of the reactor for characterizing isothermal reactions, tests were carried out to study the influence of residence time on the conversion of benzyl alcohol to benzaldehyde under microwave irradiation. The residence time was varied by changing the flow rate from 1–5 ml min⁻¹. The length of the reactor was kept constant. Since all the experiments were carried out under laminar flow conditions as shown in Table 2, it may be assumed that the transport mechanism (mixing) was purely diffusive and hence the approach of studying the residence time effect by changing the flow rate is valid for the conditions experimentally studied. The conversion of benzyl alcohol for various residence times is shown in Fig. 4. Every experimental data point used in Fig. 4, 5, 6, 8 and 9 is an average of data sets based on three experiments under identical conditions and each product sample was analyzed at least three times. The average deviation of the repeat experimental runs was always less than 5%.

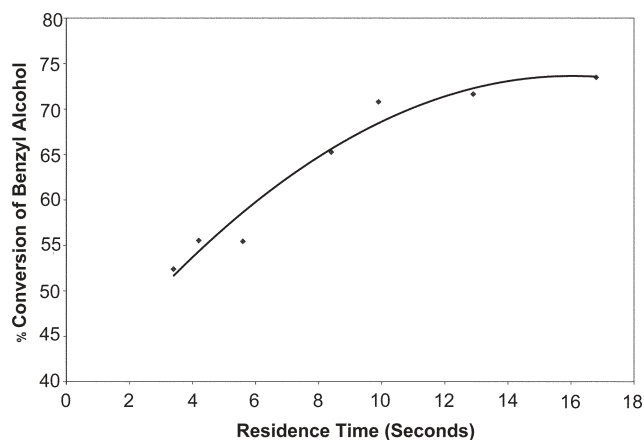
Comparison of adiabatic and isothermal conditions

Tests were also carried out to compare the conversion achieved under isothermal conditions with those under adiabatic conditions. This test was deemed essential in order to justify whether the rate enhancements predicted under microwave irradiation were purely temperature effect or whether it was a combined effect of temperature and bipolar movements. The adiabatic tests were carried out in a 57 cm long, 1/16" OD, and

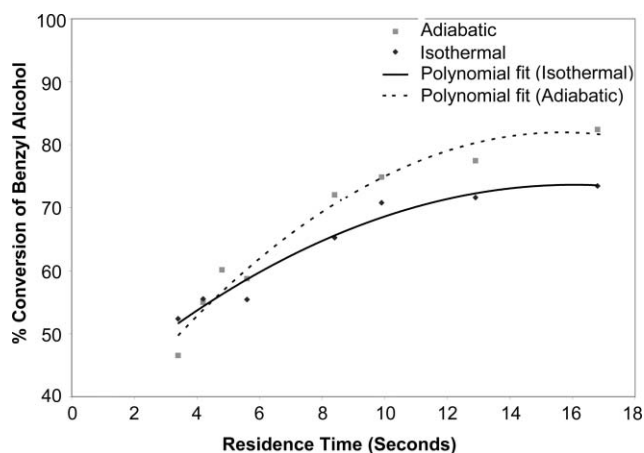
Table 2 Reynolds number (Re) and residence times for experimental flow rates

Flow rate/ml min ⁻¹	Residence time/s	$Re = D_h V_m \rho / \mu$
1	17	3.14
1.3	13	4.09
1.7	10	5.35
2	8.4	6.29
3	5.6	9.44
4	4.2	12.58
5	3.4	15.73

D_h = hydraulic diameter, m; V_m = velocity, m s⁻¹; ρ = density, kg m⁻³; μ = viscosity, kg m⁻¹ s⁻¹.

**Fig. 4** Conversion of benzyl alcohol as a function of residence time under isothermal conditions.

1/32" ID PTFE capillary tube. It can be clearly seen in Fig. 5 that the conversion achieved under adiabatic conditions was higher than the conversion achieved under isothermal conditions, especially for higher residence times. For lower residence times, the conversion was similar for both adiabatic and isothermal conditions. Higher conversions were experienced under adiabatic conditions because the reaction was performed at approximately 10 °C higher temperature. A temperature difference of 10 degrees was recorded for the adiabatic tests as compared to a ΔT of 0.2 °C for isothermal experiments. Conversions for shorter residence times were similar for both isothermal and adiabatic runs because the temperature rise was

**Fig. 5** Comparison under adiabatic and isothermal conditions.

very small for shorter residence times during the adiabatic tests.

Influence of microwave intensity

Experiments were also carried out to study the effect of the influence of the microwave intensity on the conversion of benzyl alcohol. This was done by changing the in-built power settings in the control panel of the microwave oven. Table 3 illustrates that the intensity of the microwave played a very important role in the conversion of benzyl alcohol to benzaldehyde. The actual power consumed by the reactants was calculated experimentally using the equation, $Q = mC_p\Delta T$, where m = mass flow rate, kg s^{-1} and C_p = specific heat, $\text{J kg}^{-1} \text{ }^\circ\text{C}^{-1}$. Fig. 6 shows a graphical representation of the change in conversion with changes in the microwave intensities. These studies were carried out for a reaction residence time of 17 seconds.

Table 3 Effect of microwave intensity on conversion of benzyl alcohol

Residence time/s	Microwave intensity (%)	Conversion (%)	Power/W
17	100	75.39	38.7
17	80	71.56	37.2
17	60	59.33	28.3
17	40	47.82	22.0
17	20	30.50	17.0
17	0	8.37	0

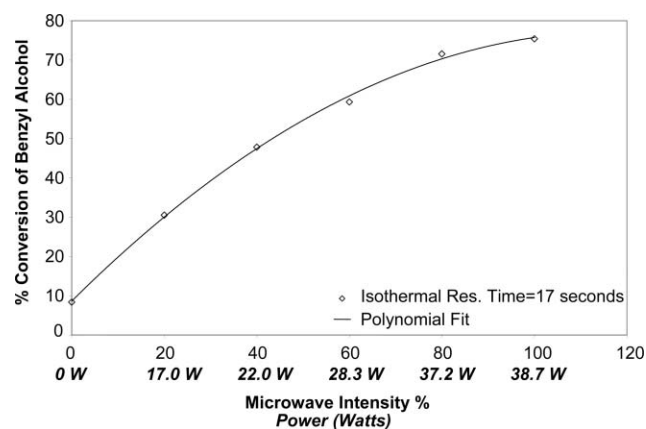


Fig. 6 Influence of microwave intensity on benzyl alcohol conversion under isothermal conditions.

Table 4 Comparison with batch reactor results

Conditions	Residence time	Conversion (%)
Batch mixing at room temperature (21 °C)	18 hours	~30
Batch mixing at 50 °C	6 hours	~40
MW assisted isothermal continuous reaction using iron (III) nitrate	17 seconds	75
MW assisted adiabatic continuous reaction using iron (III) nitrate	75 seconds	96
MW assisted batch reaction using clayfen ¹⁵	15 seconds	92

Comparison with batch experimental results

Experiments were also carried out to see the effectiveness of microwave radiation when compared to the traditional batch methods. Table 4 shows the various conditions and the conversion data. It can be seen that the conversion of benzyl alcohol to benzaldehyde was much faster under the influence of microwave irradiation than the traditional batch methods. Varma and Dahiya¹⁵ achieved 92% conversion in 15 seconds in a batch system. But the volume of the reactants that was used with a different catalyst, clayfen, was miniscule (about 0.175 ml). In this study, 96% conversion was achieved under adiabatic conditions for a residence time of 75 seconds (flow rate of 4 ml min⁻¹: 5 ml benzyl alcohol converted in 75 seconds). Fig. 7 shows a graphical representation of the time required to convert 100 ml of benzyl alcohol to benzaldehyde. It can be seen that using a continuous microwave reactor, a significant saving in processing time can be achieved.

Reaction kinetics

Calculations were performed to determine the rate of the reaction of the oxidation of benzyl alcohol into benzaldehyde for both isothermal and adiabatic conditions under the influence of microwave irradiation. Using the integrated rate law method, it was found that the reaction was second order with respect to benzyl alcohol for both cases. It can be seen from Fig. 8 and 9 that plots of $1/[\text{benzyl alcohol}]$ vs. time resulted in a linear fit.

The rate constant, k , for the continuous isothermal oxidation of benzyl alcohol under the effect of microwave irradiation was determined to be $0.0176 \text{ l mol}^{-1} \text{ s}^{-1}$. The rate law for the isothermal reaction was found to be $-r_A = 0.0176[A]^2$, where A = benzyl alcohol. Similarly, the rate constant for the same reaction under adiabatic conditions was found to be $0.029 \text{ l mol}^{-1} \text{ s}^{-1}$. The rate law was found to be $-r_A = 0.029[A]^2$ for adiabatic oxidation of benzyl alcohol under the influence of microwave irradiation.

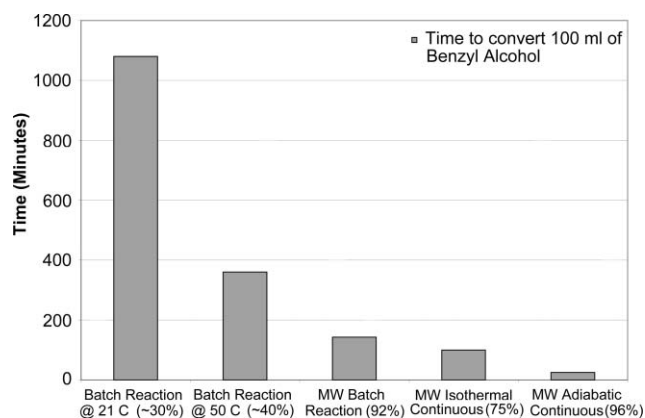


Fig. 7 Equivalent time to convert 100 ml of benzyl alcohol using different methods.

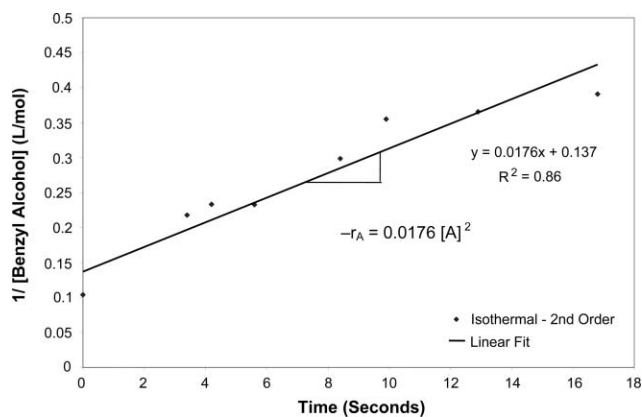


Fig. 8 Determination of the order of reaction under isothermal conditions.

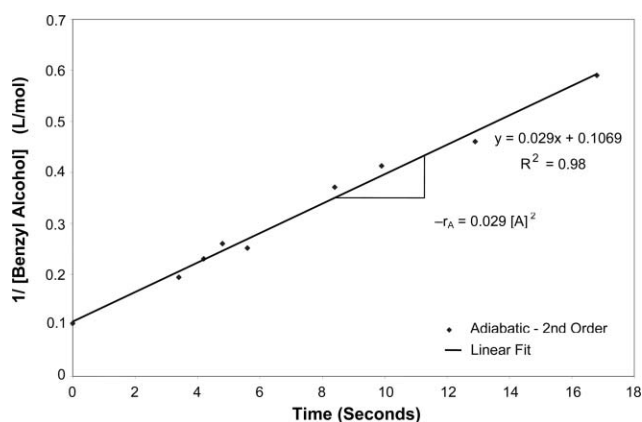


Fig. 9 Determination of the order of reaction under adiabatic conditions.

Conclusions

A compact continuous flow reactor based on narrow channel configuration was investigated to understand the influence of microwave irradiation of benzyl alcohol oxidation under isothermal conditions. The influences of microwave intensity and residence time were studied and it was seen that microwave truly does have a positive influence on the reaction rate. Having isolated the temperature effect, it was found that the microwave does invigorate the molecules to achieve higher reaction rate.

The findings of this research have wide ranging implications in not just promoting the concept of green technology, but also addressing the potential commercial opportunity for using a microwave environment for producing chemical feedstock. This reactor in its current form is particularly suitable for high

value, low throughput problems seeking high yield, selectivity and conversion. There are several reactions reported in literature which result in products with high selectivity^{5–11} and sometimes unique structures¹² when microwave radiation is used to initiate the reaction. These reactions, we believe, can be carried out continuously in an isothermal narrow channel reactor.

Acknowledgements

The authors would like to acknowledge the contributions made by the members of the PICT lab at Clarkson University and New York State Office of Science, Technology and Academic Research (NYSTAR) for the financial support for this work.

References

- 1 N. F. Brockmeier, *Chemical Reactions Induced in a Microwave Discharge*, PhD Dissertation, Massachusetts Institute of Technology, 1966.
- 2 W. W. Cooper IV, *The Oxidation of Hydrogen Chloride in a Microwave Discharge*, PhD Dissertation, Massachusetts Institute of Technology, 1966.
- 3 R. Gedye, F. Smith, K. Westaway, H. Ali, L. Baldisera, L. Laberge and J. Rousell, The use of microwave ovens for rapid organic synthesis, *Tetrahedron Lett.*, 1986, **27**, 3, 279–282.
- 4 R. J. Giguere, T. L. Bray, S. M. Duncan and G. Majetich, Application of commercial microwave ovens to organic synthesis, *Tetrahedron Lett.*, 1986, **27**, 41, 4945–4948.
- 5 B. L. Hayes, *Microwave Synthesis: Chemistry at the Speed of Light*, CEM Publishing, Matthews, NC, USA, 2002.
- 6 R. S. Varma, *Advances in Green Chemistry: Chemical Syntheses using Microwave Irradiation*, Kavitha Printers, Bangalore, India, 2002.
- 7 Evalueserve, Special Report; Developments in Microwave Chemistry, *Chem. World*, 2005, **2(4)**.
- 8 C. O. Kappe, Synthetic methods: Controlled microwave heating in modern organic synthesis, *Angew. Chem., Int. Ed.*, 2004, **43**, 46, 6250–6284.
- 9 M. Nüchter, B. Ondruschka, W. Bonrath and A. Gum, Microwave assisted synthesis—a critical technology overview, *Green Chem.*, 2004, **6**, 3, 128–141.
- 10 M. Nuechter, U. Mueller, B. Ondruschka, A. Tied and W. Lautenschlaeger, Microwave-assisted chemical reactions, *Chem. Eng. Technol.*, 2003, **26**, 12, 1207–1216.
- 11 A. Fini and A. Breccia, Chemistry by microwaves, *Pure Appl. Chem.*, 1999, **71**, 4, 573–579.
- 12 R. Rodriguez-Clemente and J. Gomez-Morales, Microwave precipitation of CaCO₃ from homogeneous solutions, *J. Cryst. Growth*, 1996, **169**, 2, 339–346.
- 13 P. He, S. J. Haswell and P. D. I. Fletcher, Microwave-assisted Suzuki reactions in a continuous flow capillary reactor, *Appl. Catal., A: Gen.*, 2004, **274**, 111–114.
- 14 J. A. B. Satrio and L. K. Doraiswamy, Production of benzaldehyde: a case study in a possible industrial application of phase-transfer catalysis, *Chem. Eng. J.*, 2001, **82**, 1–3, 43–56.
- 15 R. S. Varma and R. Dahiya, Microwave-assisted oxidation of alcohols under solvent-free conditions using clayfen, *Tetrahedron Lett.*, 1997, **38**, 12, 2043–2044.

A simple and “green” method for the synthesis of Au, Ag, and Au–Ag alloy nanoparticles

Poovathinthodiyil Raveendran,^{*ab} Jie Fu^a and Scott L. Wallen^{*a}

Received 5th September 2005, Accepted 15th November 2005

First published as an Advance Article on the web 30th November 2005

DOI: 10.1039/b512540e

Integration of “green chemistry” principles into nanotechnology is one of the key issues in nanoscience research today. In this work, we report an environmentally benign method for the preparation of Au, Ag, and Au–Ag nanoparticles in water, using glucose as the reducing agent and starch as the protecting agent. The alloy nanoparticles prepared in this way appears to be homogeneous and their sizes are well within the quantum size domain (<10 nm), where they are more amenable to size-dependent changes in electronic properties.

1. Introduction

Metal and alloy nanoparticles in the quantum-size domain have attracted much attention over the last decade with the possibilities of size dependent tuning of their electrical, optical and catalytic properties as well as the potential technological revolutions in the quantum-size domain.^{1–17} Alloy nanoparticles have received special attention due to the possibility of tuning the optical and electronic (and thus catalytic) properties over a broad range by simply varying the alloy composition. One of the key issues in the synthesis of alloy nanoparticles is the atomic scale phase separation resulting in core–shell nanoparticles.^{18–23} While there are several methods reported for the synthesis of metal and alloy nanoparticles, only some of these methods result in the formation of alloy nanoparticles below 10 nm size range, where their properties exhibit considerable size-dependent variations. With significant growth in the rather cross-disciplinary nanoscience research involving chemists, physicists, biologists and engineers, researchers have begun concerned about the need for developing more environmentally friendly and sustainable methods for the synthesis of nanomaterials. There is a current drive to integrate all the “green chemistry” approaches to design environmentally benign materials and processes.^{24–25} Such an approach will also be of advantage for the integration of metal and alloy quantum dots into biologically relevant systems. Recently, we had suggested an environmentally friendly method for the synthesis and stabilization of metal nanoparticles by suitable choice of materials and solvents.²⁶ It was shown that by gently heating an aqueous solution of silver nitrate, soluble starch and glucose, one can synthesize “starched” silver nanoparticles in the 1–8 nm size range. While glucose serves as an environmentally benign reducing agent for the metal ions, starch provides stable surface passivation or protection to prevent the aggregation of these

particles. Apart from being environmentally benign, there is a key advantage in using glucose as the reducing agent. It is a mild reagent (requires heat or a base catalyst for activation) and thereby it is possible to control the kinetics of the reduction process by varying the temperature or the pH of the solution. In the present work, we demonstrate the synthesis of starch-protected silver (Ag), gold (Au) and Ag–Au alloy nanoparticles.

2. Results and discussion

The intra- and inter-molecular associations of the starch molecules facilitated by the extensive networks of hydrogen bonds provide nanoscopic solution domains for the growth of nanoparticles. The starch hydroxyl groups also help to passivate the surfaces of these particles, in the absence of which they will aggregate as a result of high surface energies. The production of such “starched” silver particles is very simple.²⁶ By gentle heating of an aqueous silver nitrate solution containing soluble starch and D-glucose, we had obtained relatively mono-disperse silver nanoparticles. We extended this method for the production of silver nanoparticles by incorporating microwave heating. Aqueous starch dispersions containing Ag⁺ ions are prepared by adding 10 μ l of a 0.1 M solution of AgNO₃ (Sigma) and 25 μ l of a 0.1 M solution of D-glucose (Fluka) to about 2 ml of 0.20%w aqueous solution of soluble starch (Sigma). This was then treated in a microwave oven for 60 s for the reduction of metal ions. In this case, the reduction takes place under boiling conditions.

The advantage of using microwave radiation is that it provides uniform heating around the nanoparticles and can assist the digestive ripening of such particles without aggregation. The transmission electron microscope (TEM) image of the silver nanoparticles synthesized using this method is presented in Fig. 1. The corresponding UV-Visible absorption spectrum ($\lambda_{\text{max}} = 418$ nm) and a histogram describing the dispersity in size distribution of the particles are also shown.

It is seen that the size dispersity is close to that observed in our previous experiments²⁶ in the absence of microwave radiation. The non-aggregation of the particles even in the

^aDepartment of Chemistry and NSF STC for Environmentally Responsible Solvents and Processes, The University of North Carolina, Chapel Hill, North Carolina -27599-3290, USA.
E-mail: wallen@email.unc.edu

^bNational Institute for Advanced Industrial Science and Technology, 4-2-1, Nigatake, Miyagino-ku Sendai, 983-8551, Japan.
E-mail: ravi@ni.aist.go.jp

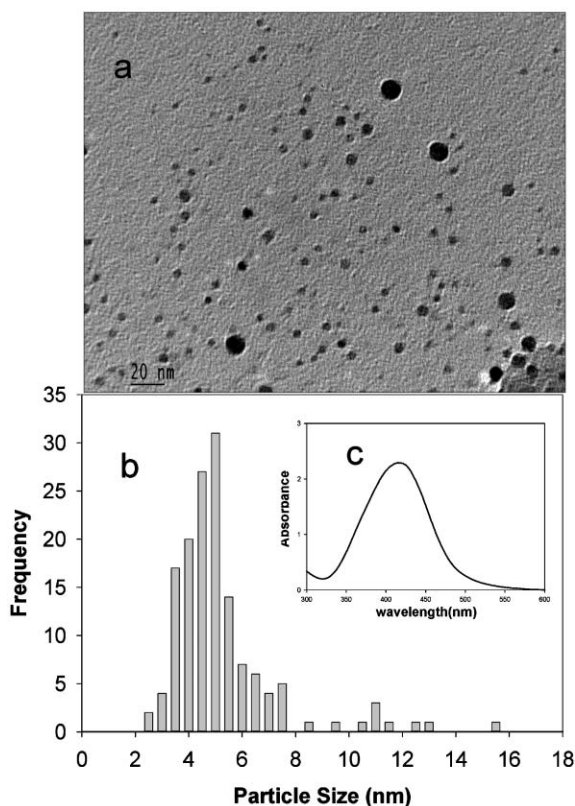


Fig. 1 (a) Typical TEM image of the “starched” silver nanoparticles synthesized in microwave radiation (average particles size = 5.9 nm, δ = 2.0 nm); (b) particle size distribution; (c) UV-Visible absorption spectrum.

presence of microwave heating further confirms that the “starched” silver nanoparticles prepared thus are quite stable. Since the synthesis utilizes only non-toxic materials and solvent, it is thought viable to readily integrate these particles into a variety of systems, especially those that are relevant to biological and biomedical applications.

While mild heating is sufficient for the glucose reduction of silver ions, the reduction of the Au^{3+} ions of AuCl_4^- takes place only in the presence of a base such as NaOH. We used chlorauric acid ($\text{HAuCl}_4 \cdot 3\text{H}_2\text{O}$), soluble starch and anhydrous D-glucose as purchased. Gold nanoparticles are prepared by adding 40 μl of a 0.1 M solution of HAuCl_4 and 60 μl of a 0.1 M solution of D-glucose to about 2 ml of 0.20%w aqueous solution of soluble starch followed by 15 μl 1M solution of NaOH. The solution remained colorless for the initial 30 min, following which it turned red slowly, indicating the formation of gold nanoparticles. The base facilitates the opening of the glucose ring by the abstraction of the α -proton of the sugar ring oxygen and the metal ions oxidize glucose to gluconic acid. The process is similar to the classical reaction of glucose with Tollen’s reagent. The time evolution of the absorption spectra showing the growth of Au nanoparticles is shown in Fig. 2.

We monitored the growth of the gold nanoparticles at varying times (and the changing solution pH) using both the UV-Visible absorption spectroscopy and the TEM images of the dispersions sampled on TEM grids at each time. The

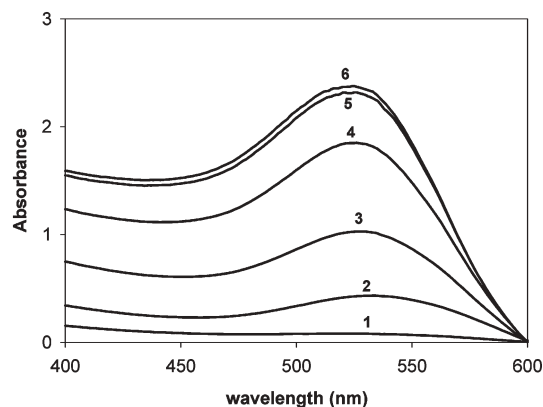


Fig. 2 Time evolution of the surface plasmon absorption band indicating the continuous formation of the gold nanoparticles. The time intervals are: (1) 40 min; (2) 43 min; (3) 44 min; (4) 45 min; (5) 47 min; (6) 50 min.

intensity of the surface plasmon absorption increased with time indicating continued reduction of the metal ions. We did not observe any notable shift in the λ_{max} with time indicating the size selectivity of the Au nanoparticles. The TEM images and the particle size distribution histograms corresponding to different reaction times are shown in Fig. 3.

The histograms clearly reveal an increase in the particle sizes with increasing time. The observed pattern indicates slow growth of Au nanoparticles in the starch solution template to the size limit of the template parameters. An analysis of the time evolution of the particle size distribution further suggests a clear size selectivity of the reaction and the preferred particle sizes seem to be around 6–10 nm.

Nanoparticles of bimetallic alloys are also of interest since it is possible to tune the optical and electronic properties as a function of the alloy composition and various approaches have been reported previously for the synthesis of Au–Ag alloy nanoparticles.^{18–23} We employed the sugar–starch combination scheme²⁶ for the synthesis of Au–Ag alloy nanoparticles by the co-reduction of the silver and gold ions using glucose in the presence of alkali. Alloy nanoparticles with various Au/Ag mole ratios (0 : 1, 0.25 : 0.75, 0.5 : 0.5, 0.75 : 0.25, and 1 : 0) are prepared by using pre-determined initial mole ratios of the gold and silver ions in the solution. The resulting nanoparticle dispersions exhibited different colors based on the initial compositions, indicating the formation of Au–Ag alloy nanoparticles (Fig. 4). While the dispersions containing pure silver and gold particles exhibited light yellow and purple colors respectively, the intermediate compositions resulted in colors that are varying between yellow and red as can be seen from the digital photographs in Fig. 4. The corresponding UV-Visible absorption spectra are also given in Fig. 4.

Some of the previous reports on alloy synthesis revealed a phase separation at the atomic scale leading to the formation of core–shell particles.^{27–30} However, several groups have reported the synthesis of homogeneous Au–Ag alloy nanoparticles.^{21–23,31–34} In order to examine whether the nanoparticles synthesized using the current methodology are alloys as against the core–shell particles, we have carried out the UV-Visible absorption spectroscopic studies. It is well known that

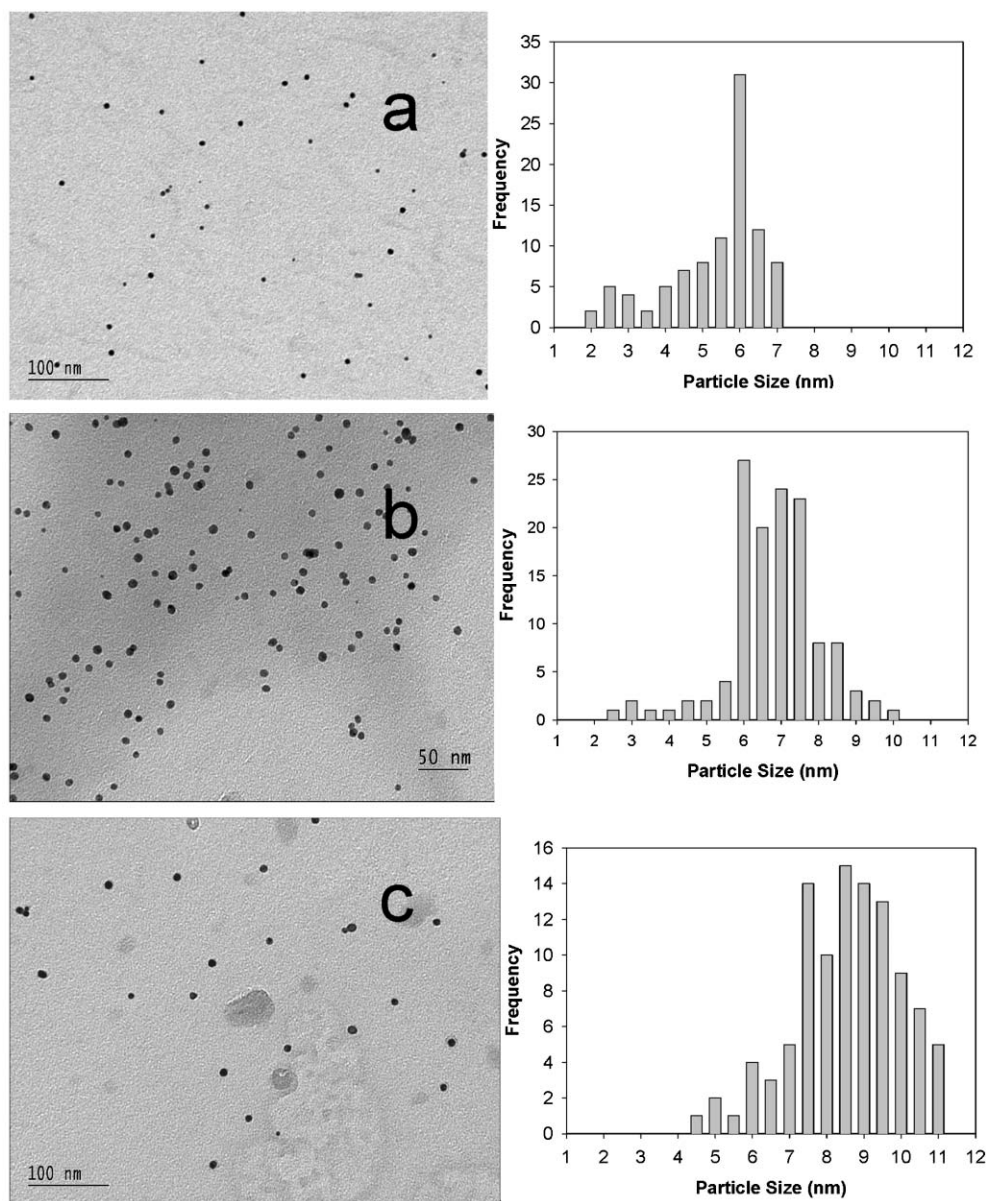


Fig. 3 TEM images and the time evolution of the size distribution of the “starched” gold nanoparticles. The average particle sizes are: (a) 5.6 nm, $\sigma = 1.37$ nm, 40 min, pH = 10.17; (b) 6.70 nm, $\sigma = 1.24$ nm, 43 min, pH = 9.84; (c) 8.80 nm, $\sigma = 1.39$ nm, 49 min, pH = 9.44.

the surface plasmon bands are characteristic for the metal and alloy nanoparticles.^{21–23,35–36} The core-shell nanoparticles will give rise to two surface plasmon absorption bands and the individual band intensities should depend on the initial composition of the metal ions. A similar situation will arise from a dispersion containing separate gold and silver nanoparticles instead of the homogeneous alloy particles.²³

It is seen from Fig. 4 that only a single absorption band is obtained for each composition with the absorption maxima varying between those for pure gold and silver nanoparticle dispersions, supporting that only homogeneous alloy particles are formed. It is also expected that in an ideal alloy system the surface plasmon absorption maximum should be linearly related to the alloy compositions. The plot of the absorption maximum *versus* the initial Au/Ag mole fractions is presented in Fig. 5.

It is observed that there is a linear relationship between the λ_{\max} values and the Au-mole ratio supporting that the particles are homogeneous alloys of Au and Ag. Thus, this approach is suitable for the synthesis of alloy nanoparticles.

In summary we have shown that it is possible to prepare starch stabilized aqueous dispersions of Au, Ag and Au–Ag alloy nanoparticles after being reduced from the corresponding metal ions by glucose. The metal and alloy nanoparticles prepared thus are highly stable and do not show any signs of aggregation even after storage for several months. Since the reagents used in the synthetic procedure are entirely non-toxic, the method can be readily integrated with biological applications. Since starch can easily form gel with water, we presume that it will help to synthesize nanogels for a wide range of biomedical applications. These aqueous nanofluids can also find several applications in heat transfer devices.

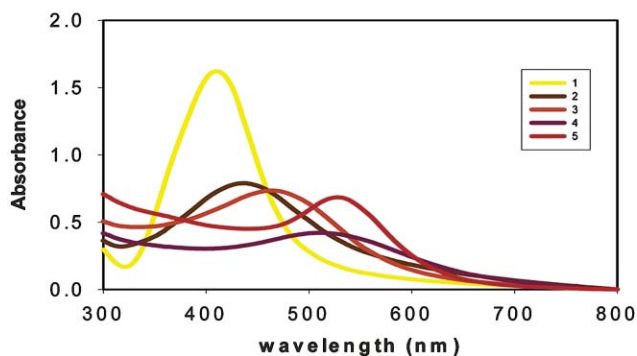


Fig. 4 Photographs of the aqueous dispersions of starch stabilized Au, Ag and the various Au–Ag alloy compositions. The Au/Ag mole ratios are: (1) 0 : 1; (2) 0.25 : 0.75; (3) 0.5 : 0.5; (4) 0.75 : 0.25; (5) 1 : 0. The corresponding surface-plasmon absorption bands are also shown.

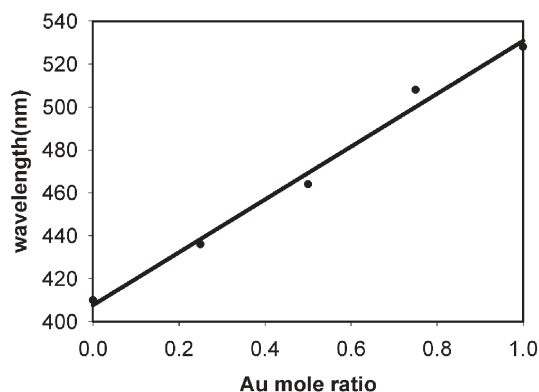


Fig. 5 Plot of the plasmon absorption maximum (λ_{\max}) against the Au mole ratio for the various alloy compositions.

3. Experimental

1. Synthesis of silver nanoparticles

Aqueous starch dispersions containing Ag^+ ions are prepared by adding 10 μl of a 0.1 M solution of AgNO_3 (Sigma) and 25 μl of a 0.1 M solution of D-glucose (Fluka) to about 2 ml of 0.20%w aqueous solution of soluble starch (Sigma). This was then treated in a microwave oven for 60 s for the reduction of metal ions. In this case, the reduction takes place under hot conditions.

2. Synthesis of gold nanoparticles

We used chlorauric acid ($\text{HAuCl}_4 \cdot 3\text{H}_2\text{O}$), soluble starch and anhydrous D-glucose as purchased. Gold nanoparticles are prepared by adding 40 μl of a 0.1 M solution of HAuCl_4 and 60 μl of a 0.1 M solution of D-glucose to about 2 ml of 0.20%w aqueous solution of soluble starch followed by 15 μl 1 M solution of NaOH. The solution remained colorless for the initial 30 min, following which it turned red slowly, indicating the formation of gold nanoparticles.

3. Synthesis of alloy nanoparticles

Alloy nanoparticles with various Au/Ag mole ratios (0 : 1, 0.25 : 0.75, 0.5 : 0.5, 0.75 : 0.25, and 1 : 0) are prepared using the same procedure for the gold nanoparticles, using pre-determined initial mole ratios of the gold and silver ions in the solution.

Acknowledgements

We acknowledge partial financial support from the STC Program of the National Science Foundation under Agreement No. CHE-9876674. PR also thanks JSPS for a fellowship.

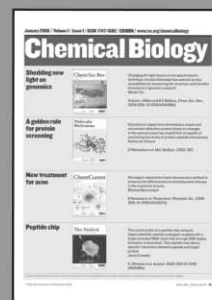
References

- J. A. Creighton and D. G. Eadon, *J. Chem. Soc., Faraday Trans.*, 1991, **87**, 3881.
- M. Brust, M. Walker, D. Bethell, D. J. Schiffrin and R. Whyman, *J. Chem. Soc., Chem. Commun.*, 1994, **7**, 801.
- T. S. Ahmadi, Z. L. Wang, T. C. Green, A. Henglein and M. A. El-Sayed, *Science*, 1996, **272**, 1924.
- J. Belloni, *Curr. Opin. Colloid Interface Sci.*, 1996, **1**, 1996.
- A. Ullman, *Chem. Rev.*, 1996, **96**, 1533.
- S. Link and M. A. El-Sayed, *J. Phys. Chem. B*, 1999, **103**, 8410.
- C. N. R. Rao, G. U. Kulkarni, P. J. Thomas and P. P. Edwards, *Chem. Eur. J.*, 2002, **8**, 28.
- R. Wang, J. Yang, Z. Zheng, M. D. Carducci, J. Jiao and S. Seraphin, *Angew. Chem., Int. Ed.*, 2001, **40**, 549.
- C. T. Campbell, S. C. Parker and D. E. Starr, *Science*, 2002, **298**, 811.
- S.-J. Park, T. A. Taton and C. A. Mirkin, *Science*, 2002, **295**, 1503.
- Y. Sun and Y. Xia, *Science*, 2002, **298**, 2176.
- M. Valden, X. Lai and D. W. Goodman, *Science*, 1998, **281**, 1647.
- K. Esumi, A. Suzuki, A. Yamahira and K. Torigoe, *Langmuir*, 2000, **16**, 2604.
- R. G. Ispasoiu, L. Balogh, O. P. Varnavski, D. A. Tomalia and T. Goodson, *J. Am. Chem. Soc.*, 2000, **122**, 11005.
- M. Zhao, L. Sun and R. M. Crooks, *J. Am. Chem. Soc.*, 1998, **120**, 4877.
- R. S. Ingram, M. J. Hostetler and R. W. Murray, *J. Am. Chem. Soc.*, 1997, **119**, 9175.
- N. R. Jana and X. Peng, *J. Am. Chem. Soc.*, 2003, **125**, 14280.
- G. C. Papavassiliou, *J. Phys. F: Metal Phys.*, 1976, **6**, L103.
- B. K. Teo, K. Keating and Y. H. Kao, *J. Am. Chem. Soc.*, 1987, **109**, 3494.
- N. Toshima, T. Yonezawa and K. Kushihashi, *J. Chem. Soc., Faraday Trans.*, 1993, **89**, 2537.
- S. Link, Z. L. Wang and M. A. El-Sayed, *J. Phys. Chem. B*, 1999, **103**, 3529.
- Y. H. Chen and C. S. Yeh, *Chem. Commun.*, 2001, 371.
- M. P. Mallin and C. J. Murphy, *Nano Lett.*, 2002, **2**, 1235.
- P. T. Anastas and J. C. Warner, *Green Chemistry: Theory and Practice*, Oxford University Press Inc., New York, 1998.
- A. S. Matlack, *Introduction to Green Chemistry*, Marcel Decker Inc., New York, 2001.

- 26 P. Raveendran, J. Fu and S. L. Wallen, *J. Am. Chem. Soc.*, 2003, **125**, 13940.
- 27 C. S. Ah, S. D. Hong and D. J. Jang, *J. Phys. Chem. B*, 2001, **105**, 7871.
- 28 K. Mallik, M. Mandal, N. Pradhan and T. Pal, *Nano Lett.*, 2001, **1**, 319.
- 29 S. Mandal, P. R. Selvakannan, R. Pasricha and M. Sastry, *J. Am. Chem. Soc.*, 2003, **125**, 8440.
- 30 L. Lu, H. Wang, Y. Zhou, S. Xi, H. Zhang, J. Hu and B. Zhao, *Chem. Commun.*, 2002, 144.
- 31 L. M. Liz-Marzan and A. Philipse, *J. Phys. Chem.*, 1995, **99**, 15120.
- 32 N. Kometani, M. Tsubonishi, M. Fujita, K. Asami and Y. Yonezawa, *Langmuir*, 2001, **17**, 578.
- 33 D. Chen, *J. Mater. Chem.*, 2002, **12**, 1557.
- 34 I. Lee, S. Han and K. Kim, *Chem. Commun.*, 2001, 1782.
- 35 J. Sinzig, U. Radtke, M. Quinten and U. Kreibitz, *Z. Phys. D*, 1993, **26**, 242.
- 36 M. Moskovitz, I. Srnova-Sloufova and B. Vlckova, *J. Chem. Phys.*, 2002, **116**, 10435.

Chemical Biology

An exciting news supplement providing a snapshot of the latest developments in chemical biology



Free online and in print issues of selected RSC journals!*

Research Highlights – newsworthy articles and significant scientific advances

Essential Elements – latest developments from RSC publications

Free links to the full research paper from every online article during month of publication

*A separately issued print subscription is also available

30110533

RSC Publishing

www.rsc.org/chemicalbiology

The fractionation of valuable wax products from wheat straw using CO₂

Fabien E. I. Deswarte,^a James H. Clark,^{*a} Jeffrey J. E. Hardy^a and Paul M. Rose^b

Received 21st October 2005, Accepted 2nd November 2005

First published as an Advance Article on the web 24th November 2005

DOI: 10.1039/b514978a

Liquid and supercritical CO₂ have been used for the first time to achieve direct isolation of valuable wax products from wheat straw (J. H. Clark, F. E. I. Deswarte and J. J. E. Hardy, *PCT Pat. Appl.*, PCT/GB 0502337.9, 2005).¹

Introduction

A biorefinery is a factory that processes crops to produce various refined specialised products in a similar way to which a petroleum refinery processes oil to make specialised chemical products.² The ideal biorefinery of the future should be capable of taking low value local feedstocks, such as agricultural co-products, extracting the high value components and subsequently transforming the residues into 'platform molecules' or bioproducts, biofuel, and bioenergy.³ It is vital to the environmental sustainability of the biorefinery that low environmental impact technologies are used throughout the processing. We must learn from what are now considered to be unacceptable aspects of petrochemical production and avoid hazardous and environmentally harmful process auxiliaries such as toxic reagents and volatile organic solvents.⁴

A particularly good example of an abundant and low value bio-feedstock in many countries is wheat straw. In the UK for example, 10 million tonnes of wheat straw are produced annually of which 4 million tonnes have no commercial market. The isolation, characterisation and use of the major components of wheat straw (cellulose, hemicellulose and lignin) has been extensively studied but little work has been done on the secondary metabolites.^{5–7}

Wheat straw, like many other plants, is known to contain a significant quantity of wax (*ca.* 1% by weight);⁸ wax is normally made up of a mixture of primarily long chain fatty acids and fatty alcohols, sterols and alkanes. Natural waxes have a wide range of industrial uses in cosmetics, personal care products, polishes and coatings with a world market of tens of thousands of tonnes.

Plant waxes are traditionally extracted by volatile organic solvents including hexane, chloroform, dichloromethane and benzene.⁹ Apart from the environmental and toxicological problems of using such solvents, the extraction is unselective co-extracting a large number of unwanted compounds such as pigments, polar lipids, and free sugars.¹⁰ Alternative low environmental impact, efficient and non-toxic extraction methods are therefore highly desirable. Here we report for

the first time, the selective extraction/fractionation of waxes from agro-residue wheat straw by liquid and supercritical CO₂.

Experimental

Isolation of wheat straw waxes by organic solvents

Ground consort variety wheat straw (30 g) was Soxhlet extracted with 900 cm³ of solvent for 5 h. The recovered extracts were filtered, concentrated to dryness by rotary evaporation, then kept under vacuum in a desiccator overnight before weighing (crude yield). Crude extracts were then eluted over silica gel in a column with a 85:15 v:v mixture of hexane/diethylether to give the wax fraction (wax yield). The experiment was repeated with yields within $\pm 6\%$ of the original.

Variation in crude and pure wax yields with wheat varieties, botanical components and age (hexane Soxhlet extraction)

The above experiment was repeated using Sabre, Maris Widgeon, IMP, Xi19, Wallace and Squarehead's Master wheat varieties grown under controlled field conditions. Similarly, we also studied the effect of the botanical component by separating the wheat straw into leaves, node and internodes (Consort variety) before carrying out extractions and separations on each component as described above. Crude and pure wax yields were reproducible between experiments on the same variety to $\pm 6\%$. Finally, year to year variations were investigated by carrying out extractions of Sabre wheat straw harvested in 2003 and 2005 in North Yorkshire, UK.

Isolation of wheat straw waxes using supercritical carbon dioxide and with a modifier

Ground wheat straw (*ca.* 200 g of Sabre variety with a water content of 9.7 w/w%) was exhaustively extracted by supercritical carbon dioxide at different pressures and temperatures with a constant supercritical fluid extraction (SFE) flow rate of 5 kg h⁻¹ for 420 min. The crude extracts (wax and water) were dried by evaporation and then left under vacuum in a desiccator overnight before weighing. The effect of a modifier (5–10 v:v% ethanol and acetone) was also tested under the same conditions.

Results and discussion

We now report the first example of the selective extraction of valuable wax products from wheat straw utilising CO₂ as

^aCentre for Clean Technology, Department of Chemistry, University of York, Heslington, York, UK YO10 5DD. E-mail: jhe1@york.ac.uk; Fax: +44 (0)1904 432705; Tel: +44 (0)1904 432559

^bBotanix Ltd, Hop Pocket Lane, Paddock Wood, Kent, UK TN12 6DQ. E-mail: paul.rose@botanix.co.uk; Fax: +44 (0) 1892 836987; Tel: +44 (0) 1892 833415

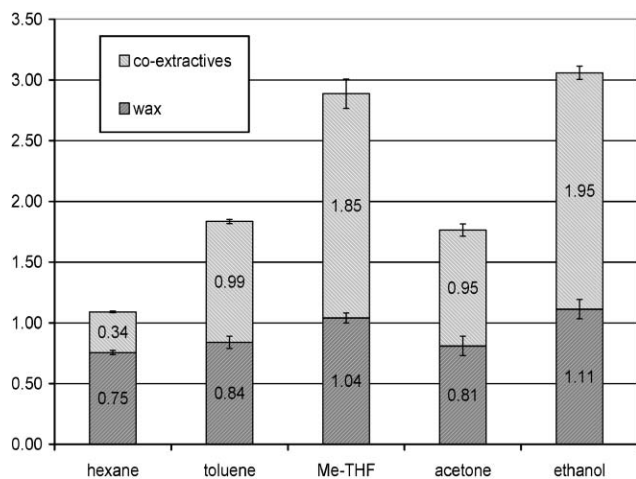


Fig. 1 Purified wheat straw wax as a percentage of total wax extract from Soxhlet extraction with hexane, toluene, methyl-tetrahydrofuran (THF), acetone and ethanol. DM : dry matter.

solvent. The products isolable from wheat straw were determined by Soxhlet extraction, with organic solvents of various polarities, in order to set a comparison basis for the CO₂ study. Fig. 1 shows the selectivity achieved using hexane, toluene, methyltetrahydrofuran (methyl-THF), acetone and ethanol. Crude yields varied between 1.1 and 3.1% (EtOH extract) depending on the solvent used.

In the most part, the organic solvents provided a complete but unselective extraction of wheat straw wax (<50% of wax present in total extract); hexane proved to be the most selective solvent giving a 70% weight yield of wax compared to total extract.

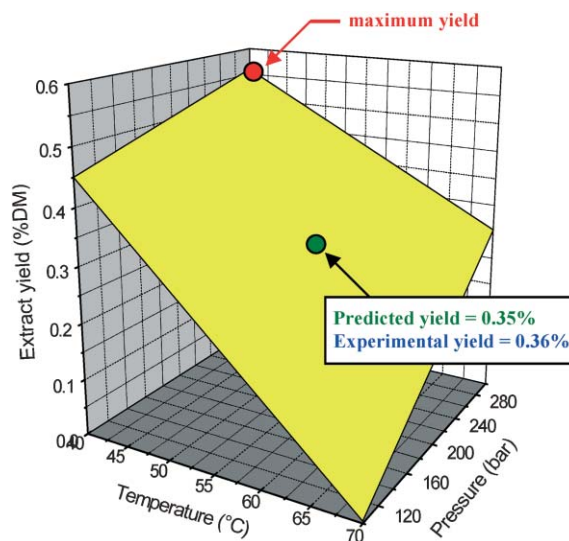


Fig. 2 1st order factorial design to optimise extraction of pure waxes from wheat straw (DM: dry matter).

We also studied the effect of changing the variety of the wheat (see Experimental) on the crude and wax yields using hexane as a solvent. Similarly, great variations in wax recoveries were observed through different varieties (from 0.5 up to 1.0% of dry matter for Sabre) highlighting the potential of increasing wax yield through breeding. In addition, it was demonstrated that wax yields were greatly dependant on the botanical component (experimental) with the leaves showing the highest yield (up to 1.6%) and the internodes the lowest (*ca.* 0.4%), consistent with previous observations.¹¹ However no appreciable difference in the crude yield was observed from

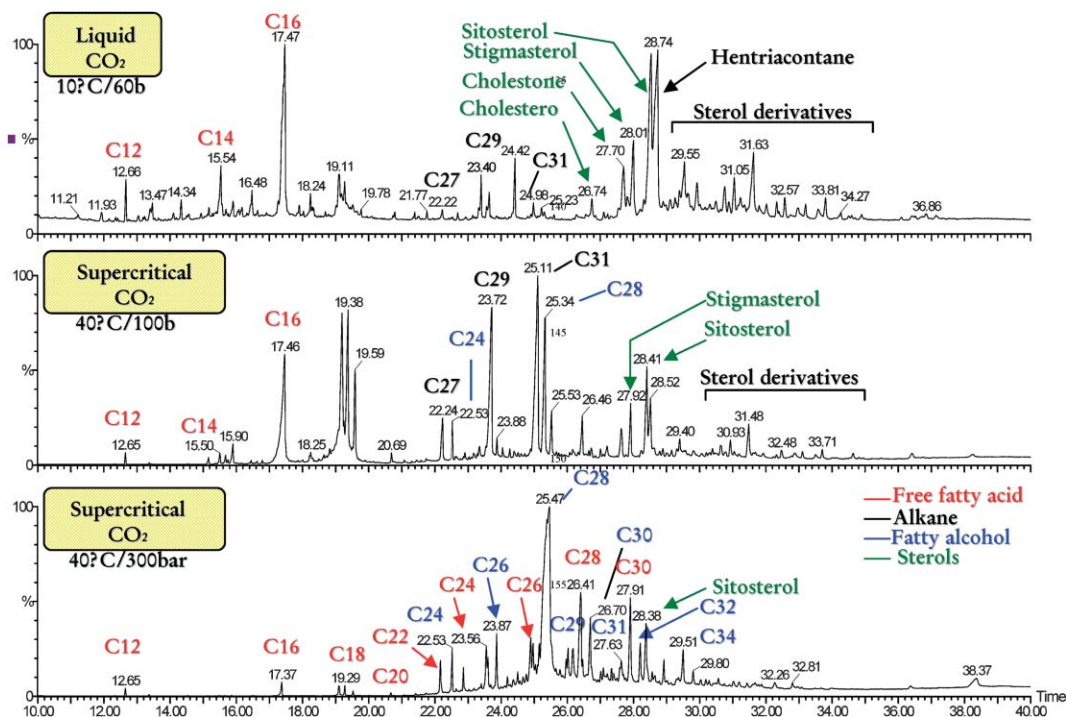


Fig. 3 HT-GC/MS chromatograms of fractionated waxes obtained using CO₂. Capillary column (DB17-HT, 30m) temperature programmed from 50 °C (1 min) to 350 °C (20 min) at 10 °C min⁻¹. The identity of major compounds is shown on the chromatograms.

the same variety in different years ($1.26 \pm 0.04\%$ for 2003 compared to $1.31 \pm 0.01\%$ for 2005; see experimental).

Supercritical and liquid CO_2 have been shown to be excellent solvents for waxes from several material sources including cosmetic products and sheeps wool.^{12–13} The properties of CO_2 mean that it is a tuneable system and when the system pressure is released it leaves a product with no solvent residue which is desirable in many product end-use industries such as cosmetics. Here CO_2 was used as solvent under different conditions of temperature and pressure. The flow rate (5 kg h^{-1}) and particle size range (0.5–5 mm) were kept constant throughout the study. Unlike all the organic solvents tested in this study the extraction proved to be completely selective to the desired waxes over a range of conditions.

Experimental design (2^2 full factorial)¹⁴ was applied to determine the optimal temperature and pressure conditions for a maximum yield of the desired waxes (minimum temperature 40°C and maximum pressure 300 bar corresponding to the maximum CO_2 density and therefore solvent strength; Fig. 2). An experiment under parameters at the centre of the matrix ($55^\circ\text{C}/200\text{ bar}$) was conducted to estimate the experimental error and minimise the risk of missing a non-linear relationship in the middle of the domain. This gave a wax yield (0.36%) in agreement with the predicted value (0.35%). In addition, a dynamic study was carried out to determine the optimum extraction time for a maximum wax yield. It was determined that 99.9% of the total extractable wax could be recovered after *ca.* 100 min while 99.0% could be isolated after less than 70 min.

Water is also extracted by the supercritical CO_2 in quantities between 3.4–6.3% by weight (dependent on the CO_2 pressure and temperature) and unlike the wax products, reaches a maximum at the highest temperature and pressure used ($70^\circ\text{C}/300\text{ bar}$).

The use of a modifier (ethanol and acetone in the range 5–10 v/v%) was also tested. This led to an unselective extraction similar to that obtained using the organic solvents and with total (crude) yields varying with the temperature and pressure.

Most significantly, we have demonstrated that by adjusting the supercritical/liquid CO_2 conditions, the waxes can be fractionated into more valuable products. For example, at relatively low pressures, the extract contains a high proportion of alkanes (useful as insect semiochemicals) whereas at higher pressures the extracts contain a high proportion of fatty alcohols (used as cholesterol reducing agents). The waxes and wax fractions were characterised by high temperature GC and GCMS, examples of which are shown in Fig. 3.

As mixtures of compounds, waxes are often characterised by their melting points; this physical measurement is a useful indicator for application value in areas such as cosmetics. The thermograms of different wax fractions obtained under different CO_2 conditions, as measured by Differential Scanning Calorimetry (DSC), complemented the GC/GCMS data in terms of peak complexity and softening temperatures. Thus, while a hexane extract showed multiple peaks ranging from 37–65 $^\circ\text{C}$, the CO_2 -extracts showed peaks over narrower temperature ranges. With CO_2 at 40°C and 100 bar, a single, albeit broad, peak was observed at $<60^\circ\text{C}$ whereas higher temperature peaks were observed for wax fractions obtained at

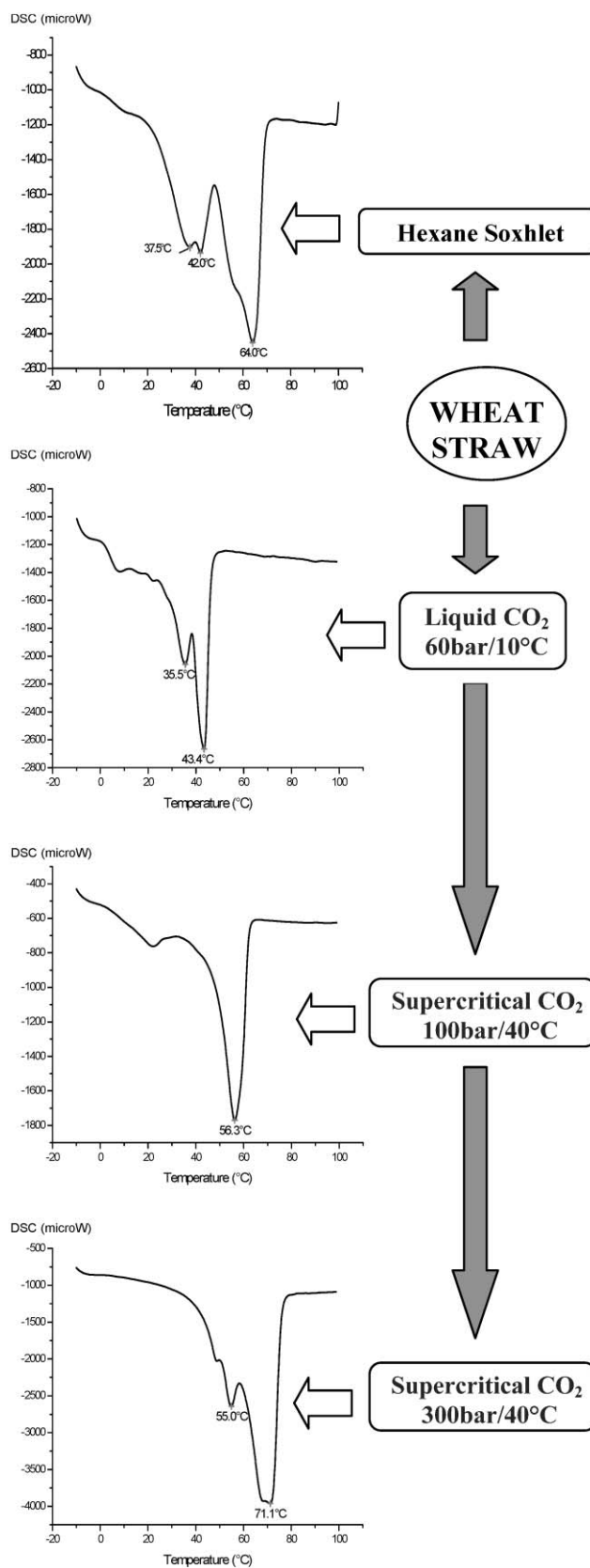


Fig. 4 DSCs for some fractionated waxes obtained using hexane and carbon dioxide.

higher pressures. Interestingly, the DSC for the wax extract using liquid CO₂ showed two peaks both at much lower temperatures than the DSCs for the wax extracts using hexane and supercritical CO₂. Examples of these thermograms are shown in Fig. 4.

Conclusions

Greater utilisation of natural, renewable resources is vital for an economically viable and environmentally sound society. We have demonstrated a low environmental impact technology for the direct production of valuable consumer products from low or zero value wheat co-products, a sustainable and widely available resource. As part of a successful industrial collaboration with Botanix Ltd, we have scaled up the extractions to >75 kg and the products obtained are being tested in the preparation of formulations, which will be carried out in extended collaboration with industry. Not all the botanical components of the crop are equally valuable so wheat straw may be selectively harvested/chopped. This would have the added advantage of reduced transportation and storage costs. A single-pass multi-component harvesting technology that simultaneously and selectively harvests grain and the desired plant component has been developed in the USA to facilitate this.¹¹ In addition, waxes and/or high-value wax fractions could be further enhanced through wheat selection programmes. Finally, an extension to Green Chemistry methodology to include simple and low environmental impact chemical modifications of the wax products so as to improve properties and add value is also planned.

It has to be noted that the same methodology could be applied to other crops or any other process by-products and

wastes as the first step of a single integrated facility, commonly named the biorefinery.

Acknowledgements

We thank the University of York and CSL for supporting this project, Botanix Ltd for the use of their pilot plant, and other members of the York Green Chemistry Group for their intellectual input.

References

- 1 J. H. Clark, F. E. I. Deswarte and J. J. E. Hardy, *PCT Pat. Appl.*, PCT/GB 0502337.9, 2005.
- 2 E. Audsley and J. E. Annetts, *Agric. Syst.*, 2003, **76**, 39–59.
- 3 *Renewable Bioresources*, ed. C. V. Stevens and R. Verhé, Wiley, Chichester, 2004.
- 4 *Handbook of Green Chemistry and Technology*, ed. J. H. Clark and D. J. Macquarrie, Blackwell, Oxford, 2002.
- 5 R. C. Sun, J. M. Lawther and W. B. Banks, *Carbohydr. Polym.*, 1996, **29**, 325–331.
- 6 R. Sun, J. M. Lawther and W. B. Banks, *Ind. Crops Prod.*, 1996, **5**, 291–300.
- 7 X. F. Sun, R. C. Sun, P. Fawler and M. S. Baird, *Carbohydr. Polym.*, 2004, **55**, 379–391.
- 8 *Waxes: Chemistry, Molecular Biology and Functions*, ed. R. J. Hamilton, The Oily Press, Dundee, 1995.
- 9 A. P. Tulloch, Chemistry of Waxes of Higher Plant, in *Chemistry and Biochemistry of Natural Waxes*, Elsevier, Amsterdam, 1976.
- 10 W. W. Christie, *Lipid Analysis*, The Oily Press, Bridgwater, 3rd edn, 2003.
- 11 D. N. Thompson, P. G. Shaw and J. A. Lacey, *Appl. Biochem. Biotech.*, 2003, **105–108**, 205–218.
- 12 J. Li, *Chemom. Intell. Lab. Syst.*, 1999, **45**, 385–395.
- 13 R. Alzaga, E. Pascual, P. Erra and J. M. Bayona, *Anal. Chim. Acta*, 1999, **381**, 39–48.
- 14 M. Kane, J. R. Dean and S. M. Hitchen, *Anal. Chim. Acta*, 1993, **271**, 83–90.

A cyclic voltammetric technique for the detection of micro-regions of bmimPF₆/Tween 20/H₂O microemulsions and their performance characterization by UV-Vis spectroscopy

Yan'an Gao,^{ab} Na Li,^a Liqiang Zheng,^{*a} Xueyan Zhao,^a Shaohua Zhang,^a Buxing Han,^{*b} Wanguo Hou^a and Ganzuo Li^a

Received 2nd August 2005, Accepted 28th October 2005

First published as an Advance Article on the web 16th November 2005

DOI: 10.1039/b510902g

As green solvents, ionic liquids (ILs) can be substitutes for traditional organic solvents, and form useful microemulsions with water. Microemulsions consisting of the IL, 1-butyl-3-methylimidazolium hexafluorophosphate (bmimPF₆), the non-ionic surfactant Tween 20 and water were formed at 30.0 °C, and the phase behavior of the ternary system was investigated. Three regions of the microemulsions: water-in-bmimPF₆ (W/IL), bicontinuous, and bmimPF₆-in-water (IL/W) were identified by cyclic voltammetry using potassium ferrocyanide K₄Fe(CN)₆ as an electroactive probe. The polarity of the microemulsion environment was investigated by UV-Visible spectroscopy using methyl orange as a probe. Use of the ionic compound K₃Fe(CN)₆ in UV-Visible measurements revealed that the bmimPF₆/Tween 20/H₂O microemulsions could solubilize salt species into the microemulsion droplets. Moreover, the solubilization of riboflavin in the microemulsions was also shown by UV-Visible spectra. These results show that these IL-based microemulsions have potential in the production of metal nanomaterials, in biological extractions or as solvents for enzymatic reactions.

Introduction

Ionic liquids (ILs) are receiving much attention as a class of solvents, because of their special physical and chemical properties, such as low volatility, non-flammability and high thermal stability.^{1–5} They are also regarded as environmentally benign solvents for chemical reactions, separations, electrochemical applications and, more recently, for syntheses of biopolymers, molecular self-assembly and interfacial syntheses.^{1,6,7} As potential substitutes for traditional organic solvents, they afford significant environmental benefits and can contribute to green chemistry techniques.

The structure of microemulsions is a field of much current interest.^{8–11} In order to study ionic liquid microemulsions, it is necessary to investigate the microemulsion structure and structural transitions. Although conductivity is frequently used to investigate structure and structural changes in microemulsions on the basis of percolation theory, the microstructure of the ionic liquid microemulsions cannot be differentiated through traditional conductivity measurements because ionic liquids are essentially molten salts. Several measurements of the diffusion coefficients of micelles or microemulsions have been performed using Fourier transform pulsed-gradient spin-echo NMR^{12–15} and dynamic light scattering,^{16–18} which provide sensitive tests of structural models of micelles or microemulsions. Also, electrochemical cyclic voltammetry has been successfully used to obtain

information about the microstructure of micelles or microemulsions.^{10,19–35} Changes in the microstructure were identified by using electrochemical probes such as ferrocene or its derivatives, ferricyanide, or methyl viologen. This detection was actually accomplished by determining diffusion coefficients of the probes which made it possible to investigate different microenvironments, in that the electrochemical reversibility of the probes was affected by the structure of the microemulsions and appeared to reflect the ease of mobility across interphases.¹⁰ Chokshi and Shah^{28,29} concluded that the diffusion coefficients probed by electrochemical probes and cyclic voltammetric measurements could also be considered self-diffusion coefficients in microemulsion systems.

As is well known, solubilization of a solute and chemical reactivity are dependent on the micropolarity of dispersed droplets in reverse microemulsions. The local environment within a microemulsion droplet may be characterized by UV-Vis measurements with solvatochromic probes. The solvatochromic probes selected should be anchored to the polar core of the aggregates, to satisfy the procedural requirement of being soluble in the local environment media. Furthermore, this probe must be sensitive to the polarity of its environment and reflect the polarity through a shift of absorption maximum. Methyl orange has been successfully used to detect the microenvironment in ammonium carboxylate perfluoro polyether (PFPE) surfactant reverse microemulsions in CO₂,³⁶ and TX-100 reverse micelles in cyclohexane.³⁷ Recently, our group showed that a water domain exists in Dynol-604-based water-in-CO₂ microemulsions.³⁸ A low polarity environment in fluorosurfactant F-53B based water-in-CO₂ microemulsions has also been found.³⁹

^aKey Laboratory of Colloid and Interface Chemistry (Shandong University), Ministry of Education, Jinan 250100, China

^bCenter for Molecular Science, Institute of Chemistry, Chinese Academy of Sciences, Beijing 100080, China

UV-Vis measurements are frequently used to characterize the solubilization of metal salts or biochemical compounds. Aqueous acidified $K_2Cr_2O_7$ has been found to be completely soluble in water-in- CO_2 microemulsion by UV-Vis spectroscopy.³⁶ Han and co-workers employed UV-Vis spectroscopy to monitor the extraction of trypsin solubilized in AOT/decane/water reverse micelles into compressed CO_2 .⁴⁰

Recently, microemulsions have been used in the preparation and processing of various materials.^{41–46} In the production of metal or semiconductor nanomaterials, water-in-oil microemulsions act as aqueous micro-reactors to dissolve metal salts. One major limitation to the broader use of ILs is their inability to dissolve a number of chemicals including some hydrophilic substances. In order to extend IL-based microemulsions to the field of nanomaterials, it is necessary to investigate the solubilization of metal salts in ionic liquid microemulsions. Similarly, the solubilization of biological molecules in microemulsions is essential to biological applications such as enzyme-catalyzed reactions and extraction. To overcome these limitations, microemulsions consisting of 1-butyl-3-methylimidazolium hexafluorophosphate (bmimPF₆), water and TX-100 have been prepared in which water is dispersed in a continuous ionic liquid phase,⁴⁷ thus allowing hydrophilic substances to be solubilized in the microscopic water droplets. In this work, microemulsions consisting of bmimPF₆, the non-ionic surfactant Tween 20 and water were formed at 30.0 °C, and the phase behavior of the system was investigated. Cyclic voltammetry provided direct insight into the microstructure and structural changes of our ionic liquid microemulsions, and methyl orange was also used to probe the polarity environment of the ionic liquid microemulsions by UV-Vis spectroscopy. The ionic complex $K_3Fe(CN)_6$ and riboflavin were chosen as the test salt and biological molecule, respectively. The experimental results showed that water domains with the approximate properties of bulk water exist in the microemulsions, thus allowing solubilization of ionic and biological compounds.

Experimental

Materials

The non-ionic surfactant Tween 20 and biochemical reagent riboflavin were purchased from Sigma and used as received. Potassium ferrocyanide, $K_4Fe(CN)_6$, used as an electrochemical probe, was purchased from Shanghai Experimental Reagent Co., Ltd. Potassium ferricyanide $K_3Fe(CN)_6$ was obtained from Fisher. Methyl orange was supplied by Beijing Chemical Reagent Co. The ionic liquid bmimPF₆ used in our experiments was synthesized according to the method reported previously.⁴⁸ Water used was deionized and doubly distilled.

Apparatus and procedure

For cyclic voltammetry, an electrochemical analyzer, CHI832A (CH Instruments, Austin, TX) was used. The electrochemical measurements were conducted using a three-electrode configuration, which consisted of a glassy carbon working electrode, a Ag/AgCl reference electrode, and a platinum flake counter-electrode. The spacing between adjacent electrodes was set at

2.0 cm. All potentials quoted are with respect to the Ag/AgCl reference. Before each measurement, the working electrode was polished using 0.05 μm aluminum oxide slurries and then washed carefully with distilled water. After polishing, the electrode was ultrasonicated in distilled water for about 5 min immediately before use. The working electrode areas were determined using cyclic voltammetry experiments on a reversible system (4 mM $K_3Fe(CN)_6$ in 1 M KCl), by use of the diffusion coefficient $D = 6.3 \times 10^{-10} m^2 s^{-1}$.²⁰ The electrode area was $4.15 \times 10^{-6} m^2$. The potential was scanned between 0.5 and $-0.5 V$, and the sweep rate range was 20–100 $mV s^{-1}$. The experiments were carried out under a nitrogen atmosphere to avoid the effect of oxygen. All experiments were carried out at 30 ± 0.5 °C.

The UV-Vis spectra were performed on a computer-controlled UV-Vis spectrometer (TU-1201, Beijing Instrument Company). The path length of the quartz cell used in this experiment was 1 cm. Appropriate amounts of substances were uniformly mixed in advance and then added to the quartz cell. The experiment was carried out at 30.0 °C.

Results and discussion

The electrochemical behavior of the $K_4Fe(CN)_6$ probe in the ionic liquid microemulsion

In cyclic voltammetry, the peak current i_p for a redox-active reversible system is given by the Randles–Sevcik equation:²⁸

$$i_p = \frac{0.447F^{3/2}An^{3/2}D^{1/2}Cv^{1/2}}{R^{1/2}T^{1/2}} \quad (1)$$

where n is the number of electrons involved in oxidation or reduction, A is the area of the working electrode, D is the diffusion coefficient of the electroactive probe, C is the concentration of electroactive probe in the solution, v is the sweep rate, F is the Faraday constant, R is the gas constant, and T is the absolute temperature.

It follows from eqn (1) that i_p will increase linearly with $v^{1/2}$ for a given electrode and a constant electroactive probe concentration. Diffusion coefficients can be obtained from a linear regression of the slope of i_p versus $v^{1/2}$ using the known surface area of the electrode. With microemulsion systems involving an electrochemical probe completely solubilized in the microemulsion, the diffusion coefficient D in eqn (1) corresponds to the microemulsion diffusion coefficient, since the probe diffuses with the microemulsion droplets.¹⁹ The cyclic voltammetry experiments were carried out at various scan rates in microemulsion environments in order to verify the diffusion-controlled nature of the process. Electrochemical charge transfer must be diffusion-controlled in order to study the microstructure of microemulsions by cyclic voltammetry.²⁸ Fig. 1 shows typical plots of i_p versus $v^{1/2}$ for 3 microemulsion systems, and the plots are straight lines passing through the origin. This fact indicates that the electron transport for the $[Fe(CN)_6]^{3-}/[Fe(CN)_6]^{4-}$ electrode reactions in the microemulsion medium is diffusion-controlled.^{19,23,24} Similar results were observed for all the other microemulsion systems we made. Thus, potassium ferricyanide, $K_4Fe(CN)_6$, is a suitable

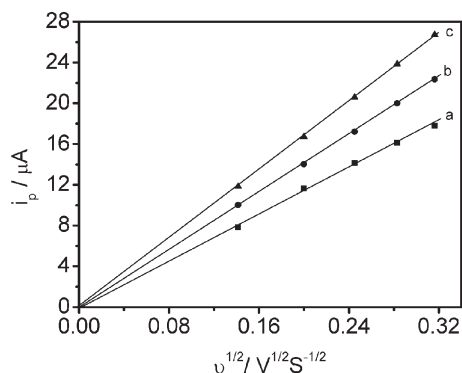


Fig. 1 Scan rate dependence of peak current in ionic liquid microemulsions: (a) 66.9% Tween 20 + 11.8% bmimPF₆ + 21.3% H₂O; (b) 54.1% Tween 20 + 9.6% bmimPF₆ + 36.3% H₂O; (c) 46.7% Tween 20 + 8.2% bmimPF₆ + 45.1% H₂O. 0.037 g K₄Fe(CN)₆ was added as electroactive probe for all systems.

electrochemical probe to study the microstructures and structural transitions of these microemulsions.

Phase behavior of the Tween 20/bmimPF₆/H₂O three-component system

The test microemulsions consisted of hydrophobic ionic liquid bmimPF₆, surfactant Tween 20 and water. In preparation of the microemulsions, each component was added by weight and the solution mechanically stirred until clear and homogeneous. The aqueous solution of probe was freshly made and used immediately. The phase behavior of the Tween 20/bmimPF₆/water three-component microemulsions at 30.0 °C is shown in Fig. 2. The phase diagram was constructed by titration with water as follows. Firstly, the required masses of Tween 20 and bmimPF₆ were mixed. For each titration, the bmimPF₆-to-Tween 20 weight ratio (*I*) was fixed. The phase boundaries were determined by observing the transition from turbidity to transparency or from transparency to turbidity. In Fig. 2, the region marked “single phase” was transparent and the region marked “two phases” was turbid. By repeating the experiment for other *I* values, the phase diagram was established.

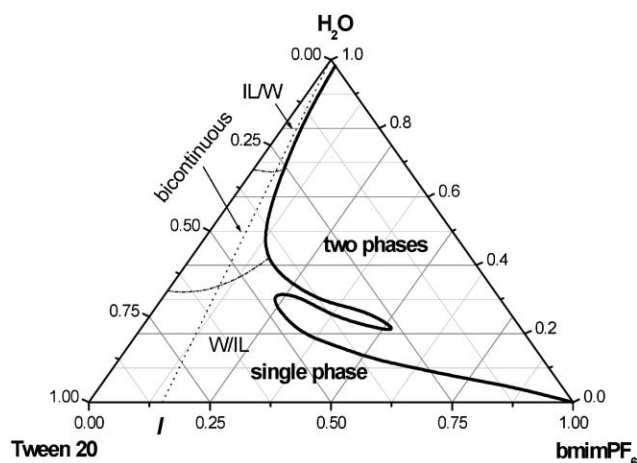


Fig. 2 Phase diagram of the Tween 20/bmimPF₆/H₂O three-component system at 30.0 °C.

The diffusion behavior of the probe in the microemulsion

Test microemulsions were prepared using the ratios indicated by the dashed line in the phase diagram (Fig. 2): bmimPF₆-to-Tween 20 weight ratios, *I* = 0.05, 0.11, 0.18, 0.25 and 0.33 were chosen. This range of compositions corresponds to a relatively low IL content and a wide range of water content. The compositions of the microemulsion were changed by adding water. All results are, therefore, reported as a function of water content. The content of each component in the solutions is derived from precise weight measurements. No phase separation was found in any of the microemulsions investigated after storage at room temperature for two months. It is obvious from Fig. 2 that the compositions of the microemulsions changed in a systematic fashion to span the range of possible structures from microdroplets to bicontinuous structures, because a single microemulsion region can always be observed along the dashed line from relatively high bmimPF₆ content to relatively high water content. The single phase region is suitable for studying the microstructure and structural transition of the microemulsions.^{10,19,20} The electroactive probe concentration had little effect on the diffusion coefficients *D*, since the shape and size of the microemulsions were not disturbed by the presence of the electroactive probe over a large concentration range.³³ This is confirmed by the fact that the electron transport of [Fe(CN)₆]³⁻/[Fe(CN)₆]⁴⁻ electrode reactions was diffusion-controlled. Therefore, our experiments were carried out with a fixed initial K₄Fe(CN)₆ quantity and the concentration of the probe changed by the addition of water.

As an example, the changes in the diffusion coefficient of the probe, estimated from the Randles–Sevcik equation with *I* = 0.18 as a function of added water in microemulsions, are illustrated in Fig. 3. It can be seen that the diffusion coefficients of K₄Fe(CN)₆ increase with increasing water content in the whole single phase microemulsion region. When the water content was less than about 34%, the diffusion coefficients increased gradually, because at low water content, a water-in-bmimPF₆ microemulsion formed. K₄Fe(CN)₆ is expected to probe the water environment preferentially due to

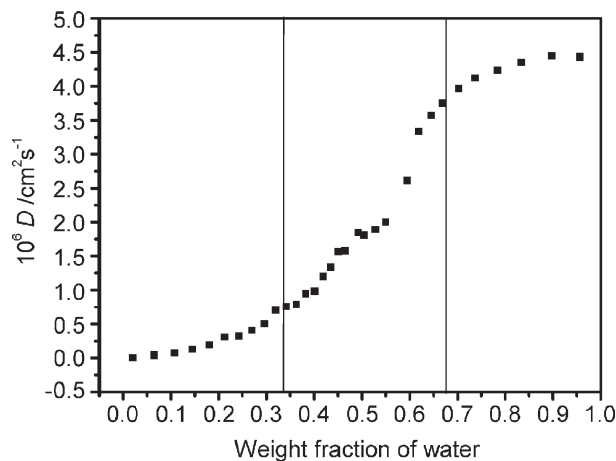


Fig. 3 The diffusion coefficient of K₄Fe(CN)₆ as a function of water content with bmimPF₆-to-TX100 weight ratio *I* = 0.18 and initial K₄Fe(CN)₆ quantity = 0.037 g.

its limited solubility in bmimPF₆. Therefore, the diffusion coefficient of K₄Fe(CN)₆ should correspond to the diffusion coefficient of water-in-bmimPF₆ microemulsion droplets. Thus the value of the diffusion coefficient of the probe is relatively small.

Lindman *et al.*⁴⁹ also discovered that molecules confined in a closed domain will give rise to low self-diffusion coefficients. The diffusion coefficients increase with the increasing water content, but as long as the diffusion of probe is confined in microemulsion droplets, the curve increases gently. Therefore, the gradual change indicates that the microenvironment of the microemulsions is unchanged. A similar trend was also observed for this microemulsion system when the water content was above 67%. In the latter case, the ionic liquid microdroplets were dispersed in a continuous water medium. The diffusion coefficient of the probe may correspond to the continuous water medium and show high mobility, and thus a high diffusion coefficient. The gradual increase of the diffusion coefficients derives from the fact that the aqueous microenvironment is not sensitive to water content in continuous water phase microemulsions. However, a relatively dramatic change in probe diffusion coefficients with water content is observed when the water content is in the range 34–67%, which indicates that the environment of the microemulsions is different from the droplet structure of the microemulsions. According to the principle of distinguishing sub-regions in microemulsions using apparent diffusion coefficients,^{19,20,49} these results suggest that when the water content is 34–67%, a bicontinuous microstructure, in which water and immiscible bmimPF₆ are both local continuous phases, is formed. Lindman *et al.*⁴⁹ stated that molecules in the continuous medium will be characterized by rapid diffusion. Thus a continuous structure is expected to give a higher self-diffusion coefficient than a droplet structure.²⁵ Therefore, we can recognize the structure and structural transition of the microemulsions by comparison of the diffusion coefficients of the electrochemical probe, and deduce the existence of three types of microstructure of IL microemulsions including W/IL, bicontinuous and IL/W, differentiated by different *I* values. The structural transition points at different *I* values are listed in Table 1, and the differentiated microemulsion domains are shown in Fig. 2.

Microenvironment of the ionic liquid microemulsions

Methyl orange is a sensitive solvatochromic probe of aqueous and microemulsion environments. As the water content in microemulsions increases, the visible absorption maximum

Table 1 Structural transition points for water/bmimPF₆/Tween 20 microemulsions at different *I* values. *I* = bmimPF₆-to-Tween 20 weight ratio

<i>I</i>	W/IL → bicontinuous Water (wt%)	Bicontinuous → IL/W Water (wt%)
0.05	32.1	67.4
0.11	32.5	67.5
0.18	33.7	67.1
0.25	36.0	67.4
0.33	40.2	Two phases

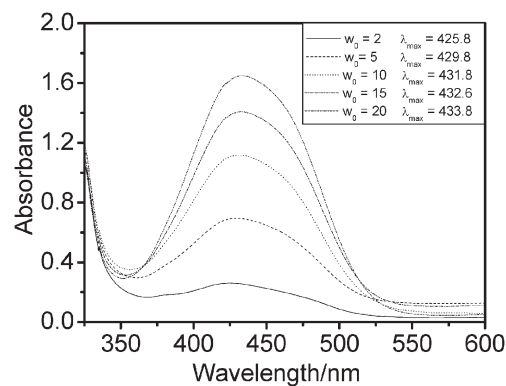


Fig. 4 Absorbance of methyl orange in the ionic liquid microemulsion at *I* = 4.00 as a function of added aqueous methyl orange solution at 30.0 °C.

λ_{max} of methyl orange shifts to longer wavelengths (red shift), indicating greater polarity.³⁹ Fig. 4 shows the UV-Vis absorbance spectra of different amounts of 9.6×10^{-5} M aqueous methyl orange solution added to the microemulsion. As expected, the absorption maximum λ_{max} of methyl orange increases. The λ_{max} of methyl orange in the microemulsions is in the range 425.8–433.8 nm, while the λ_{max} of methyl orange is 464 nm in pure water and 417 nm in ethanol. These results suggest that the polarity of the environment of the solubilized methyl orange is intermediate between that of bulk water and ethanol; that is, the polarity of the water domains in water-in-bmimPF₆ reverse microemulsions is lower than that of bulk water, which has also been observed for other reverse microemulsions.⁵⁰

The solubilities of salt and biochemical species

The use of conventional water-in-oil reverse microemulsions as micro-reactors is well established. Several different processes have been investigated including enzymatic reactions^{51–54} and synthesis of metallic and semiconductor nanomaterials.^{41–46} One of the interests in this study is to investigate the possibility of dissolution of ionic metal compounds and biochemical reagents in ionic liquid microemulsions. These compounds can only dissolve if the solvating properties of the medium approach those of pure water. K₃Fe(CN)₆ was chosen mainly due to the fact that K₃Fe(CN)₆ is insoluble in bmimPF₆ and Tween 20, even after prolonged ultrasonication of the mixture. However, after adding water, the microemulsion system takes on a distinct yellow-green color, indicating that K₃Fe(CN)₆ is solubilized in micro-aqueous regions. The UV-Vis spectra (Fig. 5) reveal that the spectroscopic features are similar to those in conventional aqueous solution. The effect of different concentrations of K₃Fe(CN)₆ in water-in-bmimPF₆ reverse microemulsions on the absorption spectra was also studied. A series of aqueous K₃Fe(CN)₆/Tween 20/bmimPF₆ microemulsions were prepared with a fixed bmimPF₆-to-Tween 20 weight ratio, *I* = 4.00, and a fixed water content (ratio of water to surfactant, *W*₀ = 10), but with different K₃Fe(CN)₆ concentrations. As shown in Fig. 6, the observed absorbance of K₃Fe(CN)₆ at the maximum wavelength increases linearly with K₃Fe(CN)₆ concentration. The result is in good agreement

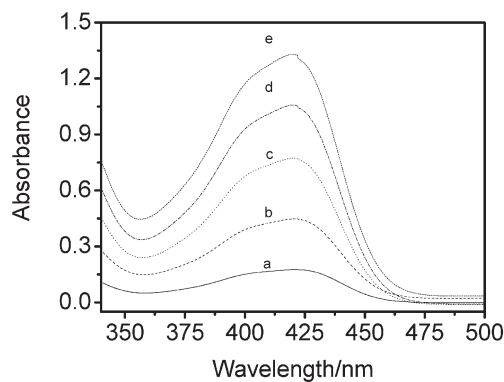


Fig. 5 Absorption spectra of $\text{K}_3\text{Fe}(\text{CN})_6$ in water-in-bmimPF₆ reverse microemulsions at 30.0 °C. a: 0.17 mM; b: 0.40 mM; c: 0.72 mM; d: 1.00 mM; e: 1.22 mM.

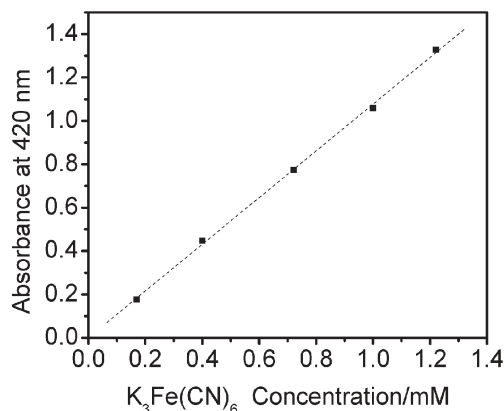


Fig. 6 The maximum absorbance intensity of aqueous $\text{K}_3\text{Fe}(\text{CN})_6$ solution in ionic liquid microemulsions with different $\text{K}_3\text{Fe}(\text{CN})_6$ concentrations.

with the Lambert–Beer plot.⁵⁵ Thus, UV-Vis spectroscopy confirms the solubilization of $\text{K}_3\text{Fe}(\text{CN})_6$ in the ionic liquid microemulsions. Considering that $\text{K}_3\text{Fe}(\text{CN})_6$ is a highly ionic compound and requires a strong aqueous environment to dissolve,⁵⁶ it is likely that the microemulsion system will dissolve other metal ions.

In biochemistry, a number of intractable questions focus on the separation of biological molecules. The use of microemulsion droplets to extract biological molecules and support biological reactions has been investigated.^{52–54} We investigated the solubilization of biochemical reagents in the bmimPF₆/Tween 20/water IL microemulsion. Riboflavin, a yellow-orange compound, was used as a molecular spectroscopic probe. Riboflavin does not dissolve in pure bmimPF₆, however, if water-in-IL reverse microemulsions are present, the solvent takes on a yellow-orange transparent phase, indicating that the microemulsion droplets can dissolve riboflavin.

A saturated aqueous riboflavin solution (about 3×10^{-4} M at 30.0 °C) was used to adjust the ratio of water to surfactant, W_0 . Fig. 7 shows the UV-Vis spectra for riboflavin in microemulsions with different W_0 at $I = 4.00$. Over the wavelength range from 320 to 550 nm, there are two absorbance peaks at 363 ± 2 and 445 ± 1 nm, while the

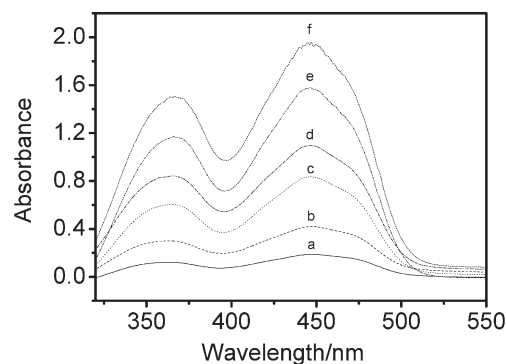


Fig. 7 Absorption spectra of riboflavin in water-in-IL microemulsions at $I = 4.00$ with different W_0 values at 30.0 °C. a: $W_0 = 2$; b: $W_0 = 5$; c: $W_0 = 8$; d: $W_0 = 10$; e: $W_0 = 16$ and f: $W_0 = 20$.

UV-Vis spectrum of riboflavin in pure water has λ_{max} at 373 ± 2 and 444 ± 2 nm.⁵⁶ The aqueous environment in the ionic liquid microemulsions is not exactly the same as in bulk water. The riboflavin absorbance increased with the addition of saturated riboflavin solution, but the plot of maximum absorbance values *versus* riboflavin concentration was not linear (Fig. 8). The maximum absorbances are distinctly lower (relative to the dashed line) for the microemulsions with low water content, such as $W_0 = 2$ and 5. The reason is that the solubilized water in these microemulsion systems exhibits behavior markedly different from that of bulk water, and the bulk water content is too small to dissolve riboflavin in a microemulsion with a small W_0 value. It is likely that in these samples a portion of the riboflavin was still in the solid particle form, dispersed in these microemulsion droplets. Even so, this class of novel microemulsions has the potential to dissolve biological molecules.

Conclusion

In summary, microemulsions consisting of bmimPF₆, the surfactant Tween 20 and water were prepared and the phase behavior of the ternary system was investigated. The water-in-bmimPF₆ (W/IL), bicontinuous, and bmimPF₆-in-water (IL/W) micro-regions of the ionic liquid microemulsions were successfully identified by a simple cyclic voltammetry method

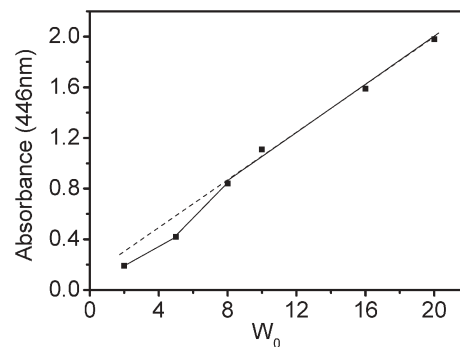


Fig. 8 The maximum absorbance intensity of aqueous riboflavin solution in IL microemulsions with different W_0 values (the components of the samples are the same as those in Fig. 7).

using potassium ferrocyanide $K_4Fe(CN)_6$ as the electroactive probe. The UV-Vis absorption spectra of methyl orange indicated that the polarity of the water domains in water-in-bmimPF₆ reverse microemulsions was lower than that of bulk water. The experimental results revealed that the water domains were sufficiently well formed to support the solubility of ionic species in the water-in-bmimPF₆ microemulsions, and spectroscopic data indicated that the ionic species was in aqueous solution. We have also demonstrated that a biological molecule, riboflavin, may be solubilized in the ionic liquid microemulsion droplets. These results are essential to the use of water-in-bmimPF₆ microemulsions as solvent systems in the preparation and processing of semiconductors and nanomaterials, in enzyme-catalyzed reactions and in extraction applications.

Acknowledgements

The authors are grateful to the National Natural Science Foundation of China (20133030, 50472069) and the Ministry of Science and Technology for financial support (2003CCA02900). They would also like to thank Dr Pamela Holt, Shandong University, for helpful discussions in the preparation of the manuscript.

References

- 1 T. Welton, Room-temperature ionic liquids. solvents for synthesis and catalysis, *Chem. Rev.*, 1999, **99**, 2071–2084.
- 2 S. G. Kazarian, B. J. Briscoe and T. Welton, Combining ionic liquids and supercritical fluids: in situ ATR-IR study of CO₂ dissolved in two ionic liquids at high pressures, *Chem. Commun.*, 2000, 2047–2048.
- 3 H. X. Gao, J. C. Li, B. X. Han, W. N. Chen, J. L. Zhang, R. Zhang and D. D. Yan, Microemulsions with ionic liquid polar domains, *Phys. Chem. Chem. Phys.*, 2004, **6**, 2914–2916.
- 4 J. L. Anderson, J. Ding, T. Welton and D. W. Armstrong, Characterizing ionic liquids on the basis of multiple solvation interactions, *J. Am. Chem. Soc.*, 2002, **124**, 14247–14254.
- 5 J. L. Anderson, V. Pino, E. C. Hagberg, V. V. Sheares and D. W. Armstrong, Surfactant solvation effects and micelle formation in ionic liquids, *Chem. Commun.*, 2003, 2444–2445.
- 6 B. P. Binks, A. K. F. Dyab and P. D. I. Fletcher, Novel emulsions of ionic liquids stabilised solely by silica nanoparticles, *Chem. Commun.*, 2003, 2540–2541.
- 7 T. Nakashima and N. Kimizukua, Interfacial synthesis of hollow TiO₂ microspheres in ionic liquids, *J. Am. Chem. Soc.*, 2003, **125**, 6386–6387.
- 8 P. G. de Gennes and C. Taupin, Microemulsions and the flexibility of oil/water interfaces, *J. Phys. Chem.*, 1982, **86**, 2294–2304.
- 9 E. W. Kaler, K. E. Bennett, H. T. Davies and L. E. Scriven, Toward understanding microemulsion microstructure: A small-angle X-ray scattering study, *J. Chem. Phys.*, 1983, **79**, 5673–5684.
- 10 R. A. Mackay, S. A. Myers, L. Bodalbhai and A. Brajter-Toth, Microemulsion structure and its effect on electrochemical reactions, *Anal. Chem.*, 1990, **62**, 1084–1090.
- 11 A. Ceglie, K. P. Das and B. Lindman, Microemulsion structure in four-component systems for different surfactants, *Colloids Surf.*, 1987, **28**, 29–40.
- 12 C. H. Chew, L. M. Gan, L. H. Ong and K. Zhang, Bicontinuous structures of polymerized microemulsions: ¹H NMR self-diffusion and conductivity studies, *Langmuir*, 1997, **13**, 2917–2921.
- 13 A. Spornath, A. Yagmur, A. Aserin, R. E. Hoffman and N. Garti, Self-diffusion nuclear magnetic resonance, microstructure transitions, and solubilization capacity of phytosterols and cholesterol in Winsor IV food-grade microemulsions, *J. Agric. Food Chem.*, 2003, **51**, 2359–2364.
- 14 H. Kataoka, T. Eguchi, H. Masui, K. Miyakubo, H. Nakayama and N. Nakamura, Scaling relation between electrical conductivity percolation and water diffusion coefficient in sodium bis(2-ethylhexyl) sulfosuccinate-based microemulsion, *J. Phys. Chem. B*, 2003, **107**, 12542–12548.
- 15 E. Johannessen, H. Walderhaug and B. Balinov, Aqueous microemulsions of a fluorinated surfactant and oil studied by PFG-NMR: transformation from threadlike to spherical micelles, *Langmuir*, 2004, **20**, 336–341.
- 16 C. A. T. Laia, P. Lopez-Cornejo, S. M. B. Costa, J. d'Oliveira and J. M. G. Martinho, Dynamic light scattering study of AOT microemulsions with nonaqueous polar additives in an oil continuous phase, *Langmuir*, 1998, **14**, 3531–3537.
- 17 C. A. T. Laia, W. Brown, M. Almgren and S. M. B. Costa, Light scattering study of water-in-oil AOT microemulsions with poly(oxy)ethylene, *Langmuir*, 2000, **16**, 465–470.
- 18 M. M. Velazquez, M. Valero and F. Ortega, Light scattering and electrical conductivity studies of the aerosol OT toluene water-in-oil microemulsions, *J. Phys. Chem. B*, 2001, **105**, 10163–10168.
- 19 C. Mo, 1.5-Order differential electroanalysis on Triton X-100 microemulsion, *Langmuir*, 2002, **18**, 4047–4053.
- 20 C. Mo, M. H. Zhong and Q. Zhong, Investigation of structure and structural transition in microemulsion systems of sodium dodecyl sulfonate + n-heptane + n-butanol + water by cyclic voltammetric and electrical conductivity measurements, *J. Electroanal. Chem.*, 2000, **493**, 100–107.
- 21 J. F. Rusling, C. N. Shi and T. F. Kumosinski, Diffusion of micelle-bound molecules to electrodes in solutions of ionic surfactants, *Anal. Chem.*, 1988, **60**, 1260–1267.
- 22 B. Geetha and A. B. Mandal, Self-diffusion studies on ω-methoxy polyethylene glycol macromonomer micelles by using cyclic voltammetric and fourier transform pulsed gradient spin-echo nuclear magnetic resonance techniques, *Langmuir*, 1995, **11**, 1464–1467.
- 23 A. B. Mandal, Self-diffusion studies on various micelles using ferrocene as electrochemical probe, *Langmuir*, 1993, **9**, 1932–1933.
- 24 A. B. Mandal and B. U. Nair, Cyclic voltammetric technique for the determination of the critical micelle concentration of surfactants, self-diffusion coefficient of micelles, and partition coefficient of an electrochemical probe, *J. Phys. Chem.*, 1991, **95**, 9008–9013.
- 25 S. A. Myers, R. A. Mackay and A. Brajter-Toth, Solution microstructure and electrochemical reactivity. Effect of probe partitioning on electrochemical formal potentials in microheterogeneous solutions, *Anal. Chem.*, 1993, **65**, 3447–3453.
- 26 C. Mo, The structural conversion in microemulsion systems of C₁₂H₂₅SO₃Na–C₄H₉OH–C₇H₁₆–H₂O, *Chin. Chem. Lett.*, 2000, **11**, 271–274.
- 27 A. B. Mandal, B. U. Nair and D. Ramaswamy, Determination of the critical micelle concentration of surfactants and the partition coefficient of an electrochemical probe by using cyclic voltammetry, *Langmuir*, 1988, **4**, 736–739.
- 28 K. Chokshi, S. Qutubuddin and A. Hussam, Electrochemical investigation of microemulsions, *J. Colloid Interface Sci.*, 1989, **129**, 315–326.
- 29 D. M. Shah, K. M. Davies and A. Hussam, Electrochemical investigation of amphiphilic cobalt(III) complexes and ferrocene derivatives in sodium dodecyl sulfate microemulsions, *Langmuir*, 1997, **13**, 4729–4736.
- 30 X. L. Zu and J. F. Rusling, Amphiphilic ferrocene alcohols as electroactive probes in micellar solutions and microemulsions, *Langmuir*, 1997, **13**, 3693–3699.
- 31 J. Santhanalakshmi and G. Vijayalakshmi, Microstructure and diffusion properties of dodecane ionic microemulsions containing cobalt(III) ion as the electrochemical probe, *Langmuir*, 1997, **13**, 3915–3920.
- 32 J. F. Rusling and G. N. Kamau, Electrocatalytic reactions in organized assemblies. Part II. Electrocatalytic reduction of allyl chloride by tris(2,2'-bipyridyl)cobalt(II) in micelles of dodecylsulfate, *J. Electroanal. Chem.*, 1985, **187**, 355–359.
- 33 D. M. Shah, K. M. Davies and A. Hussam, Electrochemical investigation of amphiphilic cobalt(III) complexes and ferrocene derivatives in sodium dodecyl sulfate microemulsions, *Langmuir*, 1997, **13**, 4729–4736.

- 34 G. Gounili, J. M. Bobbitt and J. F. Rusling, Electron transfer between amphiphilic ferrocenes and electrodes in a bicontinuous microemulsion, *Langmuir*, 1996, **11**, 2800–2805.
- 35 R. A. Mackay, S. A. Myers, L. Bodalbhai and A. Brajter-Toth, Microemulsion structure and its effect on electrochemical reactions, *Anal. Chem.*, 1990, **62**, 1084–1090.
- 36 M. J. Clarke, K. L. Harrison, K. P. Johnston and S. M. Howdle, Water in supercritical carbon dioxide microemulsions: spectroscopic investigation of a new environment for aqueous inorganic chemistry, *J. Am. Chem. Soc.*, 1997, **119**, 6399–6406.
- 37 D. M. Zhu and Z. A. Schelly, Investigation of the microenvironment in Triton X-100 reverse micelles in cyclohexane, using methyl orange as a probe, *Langmuir*, 1992, **8**, 48–50.
- 38 J. Liu, B. Han, G. Li, X. Zhang, J. He and Z. Liu, Investigation of nonionic surfactant Dynol-604 based reverse microemulsions formed in supercritical carbon dioxide, *Langmuir*, 2001, **17**, 8040–8043.
- 39 Y. N. Gao, W. Z. Wu, B. X. Han, G. Z. Li, J. W. Chen and W. G. Hou, Water-in-CO₂ microemulsions with a simple fluorosurfactant, *Fluid Phase Equilib.*, 2004, **226**, 301–305.
- 40 J. Chen, J. Zhang, D. Liu, Z. Liu, B. Han and G. Yang, Investigation on the precipitation, microenvironment and recovery of protein in CO₂-expanded reverse micellar solution, *Colloids Surf., B*, 2004, **33**, 33–37.
- 41 H. N. Ghosh and S. Adhikari, Trap state emission from TiO₂ nanoparticles in microemulsion solutions, *Langmuir*, 2001, **17**, 4129–4130.
- 42 M. Summers, J. Eastoe and S. Davis, Formation of BaSO₄ nanoparticles in microemulsions with polymerized surfactant shells, *Langmuir*, 2002, **18**, 5023–5026.
- 43 Z. L. Yin, Y. Sakamoto, J. L. Yu, S. X. Sun, O. Terasaki and R. R. Xu, Microemulsion-based synthesis of titanium phosphate nanotubes via amine extraction system, *J. Am. Chem. Soc.*, 2004, **126**, 8882–8883.
- 44 R. B. Khomane, A. Manna, A. B. Mandale and B. D. Kulkarni, Synthesis and characterization of dodecanethiol-capped cadmium sulfide nanoparticles in a Winsor II microemulsion of diethyl ether/AOT/water, *Langmuir*, 2002, **18**, 8237–8240.
- 45 S. Modes and P. Lianos, Luminescence probe study of the conditions affecting colloidal semiconductor growth in reverse micelles and water-in-oil microemulsions, *J. Phys. Chem.*, 1989, **93**, 5854–5859.
- 46 J. L. Zhang, M. Xiao, Z. M. Liu, B. X. Han, T. Jiang, J. He and G. Y. Yang, Preparation of ZnS/CdS composite nanoparticles by coprecipitation from reverse micelles using CO₂ as antisolvent, *J. Colloid Interface Sci.*, 2004, **273**, 160–164.
- 47 Y. A. Gao, S. B. Han, B. X. Han, G. Z. Li, D. Shen, Z. H. Li, J. M. Du, W. G. Hou and G. Y. Zhang, TX-100/water/1-butyl-3-methylimidazolium hexafluorophosphate microemulsions, *Langmuir*, 2005, **21**, 5681–5684.
- 48 J. Dupont, C. S. Consorti, P. A. Z. Suarez and R. F. Souza, Preparation of 1-butyl-3-methylimidazolium-based room temperature ionic liquids, *Org. Synth.*, 1999, **79**, 236–240.
- 49 P. Guering and B. Lindman, Droplet and bicontinuous structures in microemulsions from multicomponent self-diffusion measurements, *Langmuir*, 1985, **1**, 464–468.
- 50 M. B. Lay, C. J. Drummond, P. J. Thistlethwaite and F. Grieser, ET(30) as a probe for the interfacial microenvironment of water-in-oil microemulsions, *J. Colloid Interface Sci.*, 1989, **128**, 602–604.
- 51 Y. L. Khmelnsky, A. V. Hock, C. Veeger and A. J. W. G. Visser, Detergentless microemulsions as media for enzymatic reactions: spectroscopic and ultracentrifugation studies, *J. Phys. Chem.*, 1989, **93**, 872–878.
- 52 P. Plucinsk and W. Nistsch, Kinetics of interfacial phenylalanine solubilization in a liquid/liquid microemulsion system, *J. Phys. Chem.*, 1993, **97**, 8983–8998.
- 53 D. K. Lavallee, E. Huggins and S. Lee, Kinetics and mechanism of the hydrolysis of chlorophyll a in ternary solvent microemulsion media, *Inorg. Chem.*, 1982, **21**, 1552–1553.
- 54 M. Varshney, T. E. Morey, D. O. Shah, J. A. Flint, B. M. Moudgil, C. N. Seubert and D. M. Dennis, Pluronic microemulsions as nanoreservoirs for extraction of bupivacaine from normal saline, *J. Am. Chem. Soc.*, 2004, **126**, 5108–5112.
- 55 M. J. Meziani and Y. P. Sun, Spectrophotometry study of aqueous salt solution in carbon dioxide microemulsions, *Langmuir*, 2002, **18**, 3787–3791.
- 56 B. H. Hutton, J. M. Perera, F. Grieser and G. W. Stevens, AOT reverse microemulsions in scCO₂ – a further investigation, *Colloids Surf., A*, 2001, **189**, 177–181.

Benign approaches for the synthesis of bis-imine Schiff bases

Tania R. van den Ancker,^{*a} Gareth W. V. Cave^b and Colin L. Raston^c

Received 22nd September 2005, Accepted 28th October 2005

First published as an Advance Article on the web 17th November 2005

DOI: 10.1039/b513289d

Pure bis-imine Schiff bases are readily accessible in high yield, typically >95%, when aliphatic diamine/aldehyde condensation reactions are carried out under solvent-free conditions or in poly(propyleneglycol) (PPG) as a recyclable reaction medium, with negligible waste.

Introduction

Schiff base compounds are widely studied and used, attracting much attention in both organic synthesis and metal ion complexation.^{1,2} The traditional syntheses of such compounds are still commonplace alongside modern synthetic protocols.² Typically, the synthesis employs the use of a high boiling point volatile organic solvent such as toluene, followed by extensive recrystallisation and/or chromatography. In embracing the principles of green chemistry,³ herein we report two general approaches to the synthesis of Schiff base imines, (i) the use of solvent-free or the so-called solventless conditions, and (ii) the use of an alternative and recyclable reaction medium, poly(propyleneglycol) (PPG). The high yields and overall low waste generation of these approaches give them attractive green chemistry metrics, along with remarkable versatility.

Solvent-free reaction protocols used in the synthesis of condensation reactions such as aldol and Michael reactions are fast becoming the best synthetic approaches.^{3,4} New reactors designed specifically for such processes, both in the research laboratory and in industrial process intensification, has led to a realisation of the synthetic potential of solvent-free protocols that afford near quantitative yields with little or no waste.⁵ Such reactors also deal with heat transfer for highly exothermic reactions.

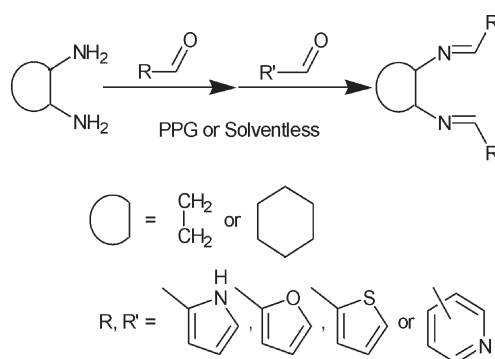
Ionic liquids, which have negligible vapour pressure, have become commonplace in research laboratories as viable alternative reaction media to volatile organic solvents.^{6,7} Despite claims that these expensive reaction media can be readily recycled, the process can seldom repeated in the same ionic liquid more than a dozen times before the overall efficiency starts to decline.⁷ Moreover, there are concerns about the toxicity of ionic liquids.⁷

Results and discussion

We have previously reported a facile “green” synthesis of resorcinol[4]arene and pyrogallol[4]arene utilising a solvent-free approach and the use of PPG as an alternative reaction medium.⁸ The fact that PPG can be readily prepared from biomass, and is extensively utilised in both the food and pharmaceutical industries, led us to explore its potential as an inexpensive and toxicologically tested reaction medium for other condensation reactions. To date there have been few studies on the use of PPG as a reaction medium,⁹ in contrast to the more hydrophilic poly(ethyleneglycol) (PEG).¹⁰

Herein, two benign, simple and versatile routes to bis-imine Schiff bases in good yield have been demonstrated. The study investigates the synthesis and characterisation of thirteen bis-imine products (two of which are previously unpublished) by (i) a solvent-free method and (ii) using PPG as a benign reaction medium.

An overview of the synthetic details is summarised in Scheme 1. Typically in the solvent-free preparation of 1–13 (each entry number for Table 1 corresponds to the number of the compound), the bis-imine Schiff base product is formed in near-quantitative yield by low intensity grinding of the diamine with two molar equivalents of the aldehyde using a pestle and mortar over a period of *ca.* 10 min, associated with constant agitation of the mixture. During the reaction a eutectic melt forms followed by formation of the product as a white or coloured solid. As the product solidifies from the reaction mixture, care needs to be taken to prevent it coating small quantities of the starting materials.



Scheme 1 Synthetic route to 1,2-bis-imines.

^aDepartment of Biological and Physical Sciences, University of Southern Queensland, Toowoomba, QLD 4350, Australia.

E-mail: ancker@usq.edu.au; Fax: +61 7 4631 1530; Tel: +61 7 4631 2363

^bSchool of Biomedical and Natural Sciences, Nottingham Trent University, Nottingham, NS11 8NS, UK.

E-mail: gareth.cave@ntu.ac.uk; Fax: +44 (0)115 848 6636;

Tel: +44 (0)115 848 3242

^cSchool of Biomedical, Biomolecular and Chemical Sciences, University of Western Australia, Crawley, WA 6009, Australia.

E-mail: claston@chem.uwa.edu.au; Fax: +61 8 9380 1005;

Tel: +61 8 9380 3045

Analysis of the bulk product by ^1H and ^{13}C NMR show only the pure products (typically >90%) and the unreacted starting materials. Potential limitations in the solvent-free method may be overcome using ultra high intensity grinding in a ball mill – we predict that the implementation of a spinning disk/cylinder reactor will also lead to improved conversion without additional purification steps.

The second method implemented in this study utilises PPG as a benign alternative solvent system and is designed to circumvent additional purification steps. Typically, the diamine and two molar equivalents of the aldehyde were heated in a minimal volume of PPG and stirred until the reaction was complete, as determined by TLC. The pure product precipitates out of the reaction medium on cooling and can be collected by vacuum filtration. PPG with $M_n = 425, 725, 1000$ and 2000 all yielded the pure product in similar yield; however, PPG with $M_n = 425$ was chosen due to its lower viscosity and subsequent ease of filtration. Traces of PPG can be removed from the product by washing with water. Any unreacted starting materials can be reclaimed from the bulk product by filtration of the pure product from PPG and subsequent removal of the starting materials from the PPG by vacuum distillation.

Mass spectrometry of the PPG following filtration of the pure product shows that a trace quantity of the product remains in the PPG (typically <3% by NMR). This can be removed by the addition of water, leading to the precipitation of the product from the PPG and water. The water is then removed from the PPG under vacuum before recycling.

In a batch process the PPG was recycled without removing the trace quantities of product, leading to a saturated PPG sample (typically containing ~5% product). In this study, the PPG was recycled five times as a batch process for representative samples. The PPG can be recycled in this way without any noticeable drop in overall yield. Typically, the reclaimed PPG reaction medium turned from a colourless solution to a transparent brown solution following the cycle. This decolourisation is attributed to the thermal degradation of the product and PPG over time. Analysis of the recycled PPG by MS and NMR techniques showed only PPG and product.

In quantitatively exploring this benign approach to the synthesis of Schiff base imines, two racemic aliphatic diamines, ethylene-1,2-diamine and cyclohexane-1,2-diamine, were treated with a variety of aromatic aldehydes, including heterocycles, the results of which are summarised in Table 1.

Cyclohexane-1,2-diamine was treated with equimolar quantities of 2-pyridine carboxaldehyde and 4-pyridine carboxaldehyde using both the solvent-free and PPG methods. In the solvent-free approach, 2- and 4-pyridine carboxaldehyde were added to the amine at the same time, and the mixture agitated (*ca.* 10 min). In the PPG reaction, the amine was added to PPG at 60°C and stirred (*ca.* 2 min), 4-pyridine carboxaldehyde was added, and the stirring continued (*ca.* 2 min). 2-Pyridine carboxaldehyde was then added and the resulting mixture stirred overnight. Analysis of the crude reaction mixtures by NMR and MS showed a statistical (1 : 2 : 1) distribution of the three bis-imines.

Table 1 Bis-imine products isolated

	Amine	R	R'	Yield (%) ^a	
				Grinding	PPG
1				95	98
2				>99	95
3				95	95
4				98	>99
5				90	>99
6				91	>99
7				85	95
8				91	97
9				98	99
10				>99	>99
11				98	>99
12				90	89
13				90	90

^a Isolated yields.

Crystals of **7**, **8** and **13** were isolated from the bulk PPG reactions and analysed by single crystal X-ray diffraction. The molecular structures of **7**, **8** and **13** are shown in Fig. 1. All the products in this study are racemic, and the molecular structures in Fig. 1 are those of an isolated single crystal and do not represent the bulk material. They nevertheless reveal

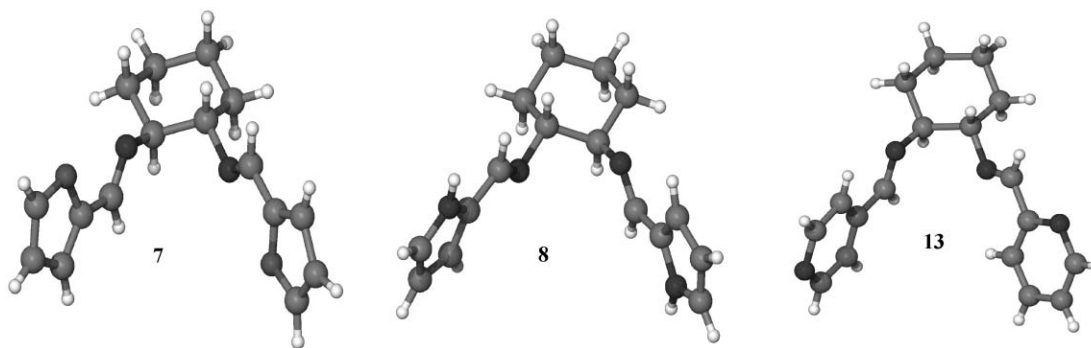


Fig. 1 Molecular structures of (a) *N,N'*-bis(furan-2-ylmethylene)cyclohexane-1,2-bis-imine, **7**; (b) *N,N'*-bis(1*H*-pyrrol-2-ylmethylene)cyclohexane-1,2-bis-imine, **8**; (c) *N*-(pyridin-2-ylmethylene)-*N'*-(pyridin-4-ylmethylene)cyclohexane-1,2-bis-imine, **13**.

the relative orientation of the heteroatoms of the aromatic rings and imine N-centres.

Conclusions

We have demonstrated that solvent-free conditions and the use of PPG as an alternative reaction media, are suitable methods for the synthesis of Schiff base bis-imines. During this feasibility study, we restricted the starting materials to inexpensive racemic amines; future experiments will look towards synthesising novel chiral analogues and their metal ion binding properties. We are currently investigating modern spinning disk/cylinder and micro-reactor technologies as potential process intensification techniques for downstream implementation of this new methodology.

Experimental

Synthesis

General experimental procedures:

Method 1: In a typical solventless experiment the aldehyde was added to the amine and the mixture agitated (*ca.* 1 min), affording an oil (ranging from cream to dark brown in colour). On further grinding (*ca.* 5 min) the solid bis-imine product was formed. If required, analytically pure product can be obtained by recrystallisation (from methanol or PPG).

Method 2: In a typical PPG experiment the amine was added to the PPG and stirred (*ca.* 2 min). The aldehyde was subsequently added and heated to between 60 and 90 °C (1 to 24 h). The reaction was cooled and the solid collected and washed with water. The precipitation of the product from the PPG can be facilitated by the addition of water to the reaction mixture. (In general the pure product crystallised out from the mother liquor as colourless crystals suitable for structural elucidation using single crystal diffraction data.) Any water in the PPG medium can be removed under vacuum at 100 °C, and the PPG recycled over 5 times with no reduction in the yield.

Compounds **1–13** were prepared from the appropriate aldehyde and diamine using the above procedures. The analyses (mp, NMR and/or MS) of compounds **1–11** were consistent with literature values.¹¹

Compound **12**: yellow crystalline solid, yield 90%. δ_{H} (250 MHz, CDCl_3) 8.71 (d, 2H), 8.52 (dd, 2H), 8.20 (s, 2H), 7.93 (ddd, 2H), 7.23 (d, 2H), 3.42 (m, 2H), 1.85 (br, 8H).

Crystallographic data

N,N'-Bis(furan-2-ylmethylene)cyclohexane-1,2-bis-imine, **7**, $\text{C}_{16}\text{H}_{18}\text{N}_2\text{O}_2$. Crystals suitable for structural analysis were grown from PPG. A colourless prism ($0.33 \times 0.29 \times 0.10 \text{ mm}^3$) was mounted with oil on a thin quartz fibre. The molecular structure was largely unexceptional with an absence of both directional H-bonding and π -stacking of the aromatics. Monoclinic, space group $P2_1/n$, $a = 9.4647(2)$, $b = 9.9534(2)$, $c = 15.7079(4) \text{ \AA}$, $\beta = 98.5090(10)^\circ$, $V = 1463.49(6) \text{ \AA}^3$, $D_c = 1.227 \text{ g cm}^{-3}$ for $Z = 4$. Least-squares refinement based on 11417 reflections with $I_{\text{net}} > 4\sigma(I_{\text{net}})$ (out of 3316 unique reflections) led to final value of $R_1 = 0.0467$.

N,N'-Bis(1*H*-pyrrol-2-ylmethylene)cyclohexane-1,2-bis-imine, **8**, $\text{C}_{16}\text{H}_{20}\text{N}_4$. Crystals suitable for structural analysis were grown from PPG. A colourless prism ($0.31 \times 0.15 \times 0.14 \text{ mm}^3$) was mounted with oil on a thin quartz fibre. Monoclinic, space group $C2/c$, $a = 18.5478(4)$, $b = 8.9189(2)$, $c = 9.2148(2) \text{ \AA}$, $\beta = 101.3880(10)^\circ$, $V = 1494.36(6) \text{ \AA}^3$, $D_c = 1.193 \text{ g cm}^{-3}$ for $Z = 4$. Least-squares refinement based on 3200 reflections with $I_{\text{net}} > 4\sigma(I_{\text{net}})$ (out of 1807 unique reflections) led to final value of $R_1 = 0.0371$.

N-(Pyridin-2-ylmethylene)-*N'*-(pyridin-4-ylmethylene)cyclohexane-1,2-bis-imine, **13**, $\text{C}_{18}\text{H}_{20}\text{N}_4$. Crystals suitable for structural analysis were grown from PPG. A colourless plate ($0.34 \times 0.27 \times 0.10 \text{ mm}^3$) was mounted with oil on a thin quartz fibre. The molecular structure was largely unexceptional with an absence of both directional H-bonding and π -stacking of the aromatics. Monoclinic, space group $C2/c$, $a = 35.5824(14)$, $b = 5.7010(3)$, $c = 16.8318(9) \text{ \AA}$, $\beta = 112.752(2)^\circ$, $V = 3148.7(3) \text{ \AA}^3$, $D_c = 1.234 \text{ g cm}^{-3}$ for $Z = 8$. Least-squares refinement based on 11262 reflections with $I_{\text{net}} > 4\sigma(I_{\text{net}})$ (out of 3804 unique reflections) led to final value of $R_1 = 0.0665$.

The intensity data was collected at 150(2) K using a Enraf–Nonius KappaCCD diffractometer and Mo- $\text{K}\alpha$ radiation ($\lambda = 0.71073 \text{ \AA}$). The structures were solved by direct methods using SHELXS and refined using SHELXL software.¹² CCDC reference numbers 280847, 280848 and 280849 for **7**, **8** and

13 respectively. For crystallographic data in CIF or other electronic format see DOI: 10.1039/b513289d.

Acknowledgements

We thank the Australian Research Council, EPSRC, Nottingham Trent University and University of Southern Queensland for the support of this work. T. A. thanks the RSC Journals Grants for International Authors.

References

- 1 R. W. Layer, *Chem. Rev.*, 1963, **63**, 489; V. Alexander, *Chem. Rev.*, 1995, **95**, 273; F. Toda and M. Ochi, *Enantiomer*, 1996, **1**, 85; F. Toda and M. Imai, *J. Chem. Soc., Perkin Trans. 1*, 1994, 2673; T. Wagner-Jauregg, *Synthesis*, 1976, 349; N. S. Isaacs, *Chem. Soc. Rev.*, 1976, **5**, 181; J.-L. Renaud, C. Brueau and B. Demerseman, *Synlett*, 2003, 408; S. Roland and P. Mangeney, *Eur. J. Org. Chem.*, 2000, **4**, 611; D. P. Lydon, G. W. V. Cave and J. P. Rourke, *J. Mater. Chem.*, 1997, **7**, 403; G. W. V. Cave, D. P. Lydon and J. P. Rourke, *J. Organomet. Chem.*, 1998, **555**, 81; D. J. Saccomando, C. Black, G. W. V. Cave, D. P. Lydon and J. P. Rourke, *J. Organomet. Chem.*, 2000, **601**, 305.
- 2 W. H. Correa and J. L. Scott, *Molecules*, 2004, **9**, 513; J. Schmeyer, F. Toda, J. Boy and G. Kaupp, *J. Chem. Soc., Perkin Trans. 2*, 1998, 989; W. H. Correa, S. Papadopoulos, P. Radnidge, B. A. Roberts and J. L. Scott, *Green Chem.*, 2002, **4**, 245; K. Tanaka and R. Shiraishi, *Green Chem.*, 2000, **2**, 272.
- 3 P. T. Anastas and J. C. Warner, *Green Chemistry: Theory and Practice*, Oxford Science Publications, New York, 1998; P. Anastas and T. Williamson, *Green Chemistry, Frontiers in Benign Chemical Synthesis and Processes*, Oxford Science Publications, New York, 1998; K. Tanaka, *Solvent-free Organic Synthesis*, Wiley-VCH, Weinheim, 2003.
- 4 G. W. V. Cave and C. L. Raston, *J. Chem. Educ.*, 2005, **82**, 468; G. W. V. Cave and C. L. Raston, *Tetrahedron Lett.*, 2005, **46**, 2361; C. L. Raston and G. W. V. Cave, *Chem.—Eur. J.*, 2004, **10**, 279; G. W. V. Cave and C. L. Raston, *J. Supramol. Chem.*, 2002, **2**, 317; G. W. V. Cave and C. L. Raston, *Chem. Commun.*, 2000, 2199; G. W. V. Cave and C. L. Raston, *J. Chem. Soc., Perkin Trans. 1*, 2001, 3258; G. W. V. Cave, C. L. Raston and J. L. Scott, *Chem. Commun.*, 2001, 2159.
- 5 J. R. Burns and R. Jachuck, *Appl. Therm. Eng.*, 2001, **21**, 495; K.V.K. Boodhoo, W. A. E. Dunk, M. S. Jassim and R. Jachuck, *J. Appl. Polym. Sci.*, 2004, **91**, 2079.
- 6 R. D. Rogers and K. R. Seddon, *Science*, 2003, **302**, 792; J. D. Holbery and K. R. Seddon, *J. Chem. Soc., Dalton Trans.*, 1999, 2133; T. Welton, *Chem. Rev.*, 1999, **99**, 2701; J. L. Scott, D. R. MacFarlane, C. L. Raston and C. M. Teoh, *Green Chem.*, 2000, **2**, 123; R. Mestres, *Green Chem.*, 2004, **6**, 583; D. B. Zhao, Z. F. Fei, C. A. Ohlin, G. Laurenczy and P. J. Dyson, *Chem. Commun.*, 2004, 2500; R. Vijayaraghavan, M. Surianarayanan and D. R. MacFarlane, *Angew. Chem., Int. Ed.*, 2004, **43**, 5363; M. Antonietti, D. B. Kuang, B. Smarsly and Z. Yong, *Angew. Chem., Int. Ed.*, 2004, **43**, 4988.
- 7 P. Wasserscheid, R. van Hal and A. Bosmann, *Green Chem.*, 2002, **4**, 400; R. P. Swatloski, J. D. Holbrey and R. D. Rogers, *Green Chem.*, 2003, **5**, 361; F. Stock, J. Hoffmann, J. Ranke, R. Störmann, B. Ondruschka and B. Jastorff, *Green Chem.*, 2004, **6**, 286.
- 8 J. Antesberger, G. W. V. Cave, M. C. Ferrarelli, M. W. Heaven, C. L. Raston and J. L. Atwood, *Chem. Commun.*, 2005, 892; B. A. Roberts, G. W. V. Cave, C. L. Raston and J. L. Scott, *Green Chem.*, 2001, **3**, 280; G. W. V. Cave, M. C. Ferrarelli and J. L. Atwood, *Chem. Commun.*, 2005, 2787.
- 9 N. F. Leininger, R. Clonta, J. L. Gainer and D. J. Kirwan, *Chem. Eng. Commun.*, 2003, **190**, 431; G. W. V. Cave, M. J. Hardie, B. A. Roberts and C. L. Raston, *Eur. J. Org. Chem.*, 2001, 3227.
- 10 J. Chen, S. K. Spear, J. G. Huddleston and R. D. Rogers, *Green Chem.*, 2005, 64; C. B. Smith, C. L. Raston and A. N. Sobolev, *Green Chem.*, 2005, **7**, 650.
- 11 M. H. Fomesca, E. Eibler, M. Zabel and B. König, *Inorg. Chim. Acta*, 2003, **352**, 136; W. S. Emerson and T. M. Patrick, Jr., *J. Org. Chem.*, 1949, **14**, 790; J. Weber, *Inorg. Chem.*, 1967, **6**, 258; G. K. Patra and I. Goldberg, *Eur. J. Inorg. Chem.*, 2003, 969; C. R. Baar, M. C. Jennings and R. J. Puddephatt, *Organometallics*, 1999, **18**, 4373; D. H. Busch and J. C. Blair, *J. Am. Chem. Soc.*, 1956, **78**, 1137; W.-Y. Sun, B.-L. Fei, T. Okamura, W.-X. Tang and N. Ueyama, *Eur. J. Inorg. Chem.*, 2001, 1855; X.-M. Ouyang, B.-L. Fei, T. Okamura, H.-W. Bu, W.-Y. Sun, W.-X. Tang and N. Ueyama, *Eur. J. Inorg. Chem.*, 2003, 618.
- 12 G. M. Sheldrick, *SHELXS-97, Program for solution of crystal structures*, University of Göttingen, Germany, 1997; G. M. Sheldrick, *SHELXL-97, Program for refinement of crystal structures*, University of Göttingen, Germany, 1997.

Lipase-catalyzed glycerolysis of fats and oils in ionic liquids: a further study on the reaction system

Zheng Guo and Xuebing Xu*

Received 8th August 2005, Accepted 8th November 2005

First published as an Advance Article on the web 23rd November 2005

DOI: 10.1039/b511117j

Candida antarctica lipase B-catalyzed glycerolysis of sunflower oil in a tetraammonium-based ionic liquid (IL) was studied to elucidate its distinct characteristics and to evaluate the contributions of important parameters. Mass transfer limitations and occurring partial phase separation were found to have a profound effect on the lower initial rate and the occurrence of the induction period. The investigation on the rheological behavior of the IL and its mixture with substrates showed that the plot of the viscosity of pure IL against temperature was better fitted with the Vogel–Tammann–Fulcher (VTF) equation, and the viscosity of the mixture is strongly agitation-dependent. A comparable diffusion time constant of the oil molecule in the IL to that of the reaction shows that the glycerolysis in the IL is controlled both diffusionally and kinetically, as experimentally verified by agitation effect and enzyme loading study. Interestingly, increasing water activity resulted in a decreasing initial reaction rate and a prolonged induction period, which possibly resulted from an elevated solvation barrier and the phase separation at higher water content. Studies on thermodynamics of glycerolysis show that there is a bigger energy barrier for the IL system, about 1.5 times that of the solvent-free or 3 times that of the *tert*-butyl alcohol system. Kinetic studies also show that IL system has the biggest V_{\max} and K_m among the three tested systems, indicating, respectively, its high productivity, and low substrate affinity to enzyme due to mass transfer limitation.

Introduction

Increasing interests in ionic liquids (ILs) stem primarily from the progressive concerns for environmental problems.^{1–4} A contradictory challenge facing chemists is to establish efficient as well as environmentally benign processing technology comparing to current processing approaches. Ionic liquids appear to be a possible solution to this objective. As molten salts, ILs not only possess negligible volatile pressure but also act much like common solvents, dissolving both polar and nonpolar compounds and even performing much better than commonly used solvents in many cases.^{5–8} Most importantly, as a reaction medium for biocatalysis, ILs have other important advantages beyond green technology. The advantages include adjustable solubility properties, protective effect or increased stability for enzymes, positive effects on the specificity of enzymes or on the shift of reaction equilibrium, as well as recoverability and recyclability.^{9–11} A key feature of ILs is that their properties can be modified by altering the nature of the cations, anions and substituents. This makes ILs real engineered solvents, which could provide new opportunities for many biocatalytic processes and create novel possibilities which are impossible in traditional solvents. These have been well documented by a number of excellent reviews and books.^{12–15}

Lipase-catalyzed lipid modification constitutes an important aspect with industrial potentials in biocatalysis area.

Enzymatic lipid processing has been extensively studied employing common solvents or in solvent-free systems.^{16–18} Many enzymatic processes have exhibited comparable advantages to chemical methods and some of them have been even used in industrial production.^{19–21} However, few protocols with practical interests and industrial potentials have been reported so far by employing ILs as reaction media.^{22–25} In practice, there remain big challenges in this area, especially for enzymatic production of partial glycerides.^{26,27}

Recently, for the first time, we have demonstrated a novel protocol for monoglyceride production employing an amphiphilic tetraammonium-based ionic liquid as a reaction medium to create a compatible system for glycerol and oils.²⁸ This approach achieved higher conversion of triglycerides and higher yields of desired products. The universal validity of the method has also been verified by being applied to different commercial oils and fats. However, interesting observations such as lower initial reaction rate, occurrence of the induction period and bulky substrate-tolerating capacity of the IL remain to be explored. The unique properties of cocosalkyl pentaethoxymethyl ammonium methosulfate (CPMA·MS), the interactions between water and the IL molecule or substrates, and their contributions to mass transfer limitations await further elucidation. Thus, in this paper, we investigated the rheological behaviors of CPMA·MS and its mixtures with substrates as well as their effects on mass transfer and reaction performance. Effects of some important parameters were evaluated. The relationship of water content and water activity in the IL was examined and its influence on the reaction rate was also discussed. Kinetic and thermodynamic studies on the

BioCentrum-DTU, Technical University of Denmark, DK-2800 Kgs. Lyngby, Denmark. E-mail: xx@biocentrum.dtu.dk; Fax: +45 45884922; Tel: +45 45252773

glycerolysis of sunflower oil in the IL were conducted and compared with the reaction in solvent-free and *tert*-butyl alcohol systems.

Results and discussion

Characteristics of the glycerolysis in CPMA·MS and important factors

Fig. 1 depicts a typical time course of the glycerolysis of sunflower oil in CPMA·MS. As also demonstrated in the previous work,²⁸ the reaction shows a higher yield of monoglyceride, a temperature-dependent induction period, a jump after the induction period, and a longer equilibrium time resulting from the lower initial reaction rate. Besides the above concerns, many other questions regarding the glycerolysis of triglycerides in the IL need to be addressed, such as: is this a kinetically controlled enzymatic reaction or a mass-transfer-controlled one? Besides temperature, are there any other contributing factors to the unique behavior of the reaction, and if so, to what extent?

One of the crucial significances of the IL is that it can provide an environment where oil and glycerol can interact efficiently. In reality, this capacity is not without limitation and can be lost when too high a substrate concentration is applied. A partial phase separation occurs at higher substrate concentration as shown in the study. Therefore, it is important to understand what has happened in such a system. In order to examine the presence of external mass resistance, the effect of agitation speed on the reaction rate was investigated in the range of 100–800 rpm (Fig. 2). It was observed that the conversion of triglyceride increased with the agitation rate until after 600 rpm. This observation indicated the existence of the external mass transfer limitation, which probably resulted from partial phase separation and high viscosity of the IL (a detail discussion on the effect of the viscosity see the following section). Mass transfer between two phases directly relates to the interfacial area, which is dependent on the shear rates and the two-phase volume ratio.²⁹ An increase in speed of agitation

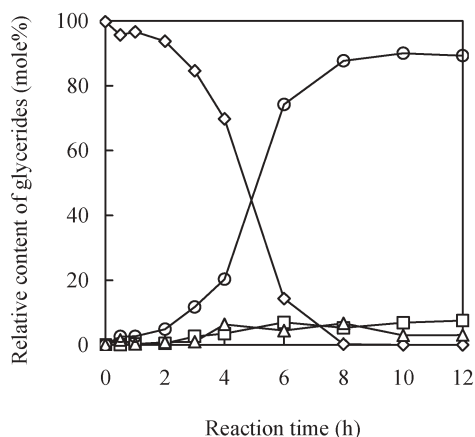


Fig. 1 Time course of the glycerolysis of sunflower oil in CPMA·MS. The reaction was conducted at 45 °C with magnetic agitation at 600 rpm. (◇), (△), (○) and (□) represent tri-, di-, mono- glycerides and fatty acid. The concentration of sunflower oil, glycerol and Novozym 435 is 0.188 mol L⁻¹, 0.94 mol L⁻¹ and 37.6 g L⁻¹, respectively.

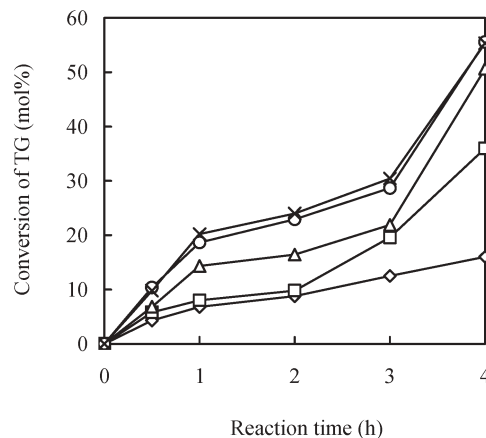


Fig. 2 Effect of agitation speeds. Reaction conditions: 50 °C, the concentration of substrates and enzyme is the same as in Fig. 1. (◇), (□), (△), (○) and (×) represent 100, 200, 400, 600 and 800 rpm, respectively.

will lead to the increasing dispersion of triglyceride into the IL phase and consequently a more efficient interaction with glycerol and the immobilized lipase, which resided in the IL phase. Overall, this will yield an increasing reaction rate. The result shows that a proper agitation rate in this reaction system is necessary to eliminate the external mass transfer limitation.

If no mass transfer limitations are present, the dependence of reaction rate upon the enzyme concentration should be linear; this is partially supported by performing the reaction at different enzyme loadings (Fig. 3A). The initial rate shows an approximately linear increase against the enzyme concentration at the range of 10.8 to 32 g L⁻¹. The increase slows down when enzyme loading is over 32 g L⁻¹ (Fig. 3B). At the same time the enzyme efficiency also obtains a relatively higher value at this lipase concentration. Thus from the commercial consideration, 30–40 g L⁻¹ should be a recommended enzyme dosage.

On the other hand, the linearity alone in Fig. 3 does not rule out the possibility of mass transfer limitations, especially internal diffusion, on the reaction rate. The presence of mass transfer limitations has received further support from the linear dependence of glycerolysis rates upon sunflower oil concentrations (Fig. 4). It is known that a mass-transfer-controlled reaction produces a linear rate dependency upon substrate concentrations. A very good linear correlation between the concentration of sunflower oil and reaction rate at the range of 0.19–0.5 mol L⁻¹ was observed. As discussed previously, CPMA·MS has a specific substrate-buffering capacity,²⁸ where the reaction will exhibit a different behavior beyond this capacity. At 0.55 mol L⁻¹ in this study, the volume of substrates is about twice the IL volume. Obviously, the reaction behavior at this concentration or higher significantly differs from a typical glycerolysis of triglyceride in CPMA·MS. Most likely this constitutes the leading cause for the decrease of reaction rate with the further increase of concentration of sunflower oil.

The glycerolysis of triglycerides is a two-step reversible reaction, in which excess glycerol could suppress the reversion of the first step and promote the further glycerolysis of the

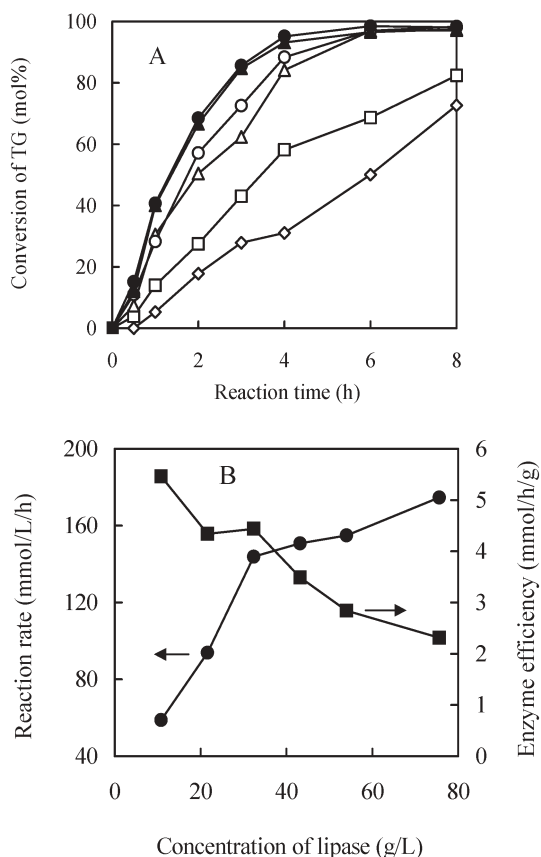


Fig. 3 Effects of enzyme loading on reaction rate (A) and enzyme efficiency (B). Reaction conditions: magnetic agitation, 300 rpm; 55 °C; concentration of sunflower oil, 0.432 and glycerol 2.16 mol L⁻¹; concentration of Novozym 435, 10.8 (◇), 21.6 (□), 32.4 (△), 43.2 (○), 54.0 (▲) and 75.6 (●) g L⁻¹.

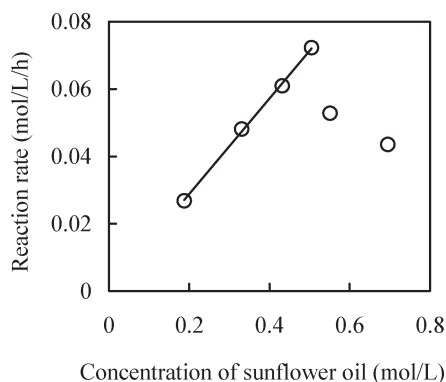


Fig. 4 Effect of the concentration of sunflower oil. Reaction conditions: IL, 2 mL; Novozym 435, 100 mg; Stirring rate, 600 rpm; 70 °C; and mole ratio of glycerol : sunflower oil, 5 : 1.

generated diglycerides, giving higher yield of MG. Fig. 5 reveals that there is no significant difference for the conversion of triglyceride from the stoichiometric ratio (2 : 1) to excess of glycerol. However the yield of the desired product increases with the glycerol excess, which we quantify as the glycerolysis degree (GD). To reflect the change of both conversion of triglycerides and MG yield, a new term, the glycerolysis degree, has been introduced in this study to indicate the

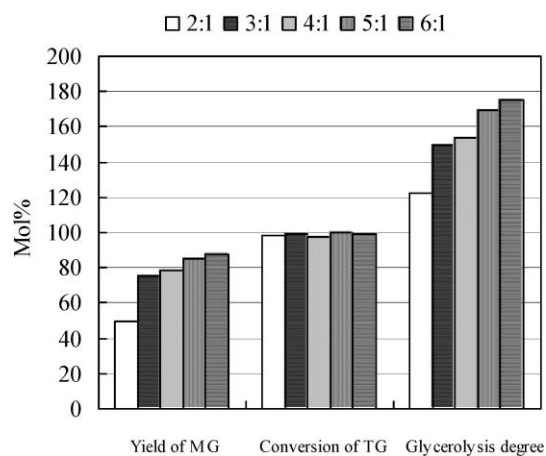


Fig. 5 Effect of glycerol dosage. Reaction conditions: 2 mL IL, 0.5 mmol sunflower oil, 50 °C, 500 rpm. The mole ratio of glycerol/sunflower oil varied from 2 to 6.

performance and progress of the reaction. Fig. 5 shows that glycerolysis degree is the conversion of TG plus half of the yield of MG when the yield of MG is lower, and a doubled value of MG yield when the yield of MG is higher. Glycerolysis degree is a combined index to synchronously denote the conversion of TG and yield of MG for the glycerolysis of triglycerides. The results also suggested that employing excess glycerol (more than 5 : 1) is still necessary to achieve a higher yield of MG even though the IL could induce the shift of equilibrium to the formation of monoglyceride by reducing the activity coefficients of partial glycerides.²⁸

Rheological behavior of CPMA·MS and its effects on mass transfer

CPMA·MS is a highly viscous ionic liquid with the melting point at 5–10 °C. The plot of the viscosity of CPMA·MS against temperature is shown in Fig. 6. Generally ILs have a viscosity essentially governed by van der Waals interaction and H-bonding, which is of two or more orders of magnitude greater than normal solvents. The massive occurrence of long alkyl chain and functional groups will significantly increase the viscosity of ILs.^{30–32} In CPMA·MS, there are a C₁₄ alkyl group and two polyethoxyl substituents, either of which could contribute to the increase of viscosity.³² However, the viscosity of the IL could be dramatically decreased by increasing temperature as indicated in Fig. 6A, which is important for its usage as a reaction medium. The change of viscosity of CPMA·MS seems well following Arrhenius model (eqn (1)), but is better described by the Vogel–Tammann–Fulcher (VTF) model^{33,34} (eqn (2)), though the difference is not so significant (Fig. 6B).

$$\ln \eta = \ln \eta_{\infty} + \frac{E_{\eta}}{RT} \quad (1)$$

$$\ln \frac{\eta}{\sqrt{T}} = \frac{k_{\eta}}{T - T_0} + \ln A_{\eta} \quad (2)$$

where T/K is the temperature; η and η_{∞} are the viscosity of fluid at T and infinite temperature; E_{η} is the activity energy for

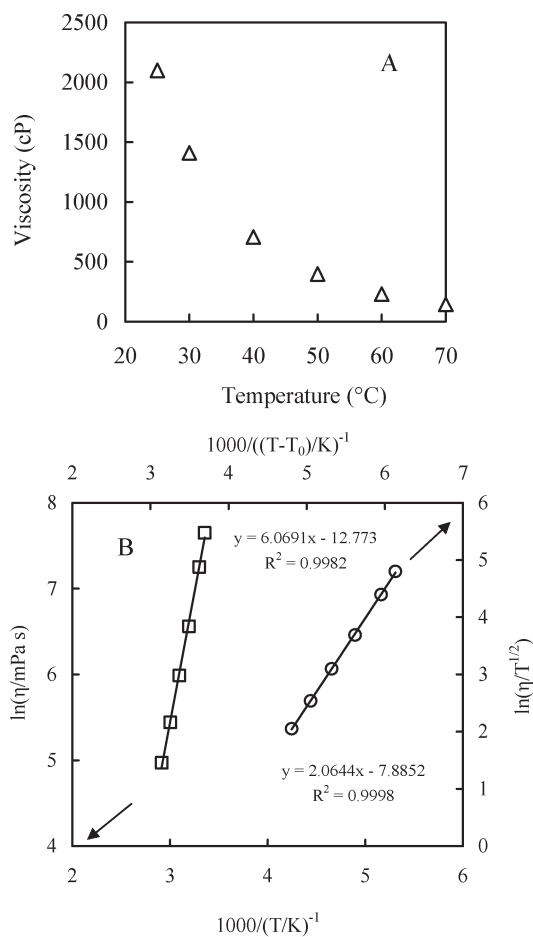


Fig. 6 Temperature dependency of the viscosity of CPMA·MS (A) and fitting plot of Arrhenius (□) and VFT (○) model (B).

viscous flow and R is gas constant. In eqn (2), k_η is a constant related with Arrhenius activity energy and A_η is another constant. T_0 is the ideal glass transition temperature of fluid, here fixed at $T_g - 50$ K. T_g was estimated from the assumption that the glass transition temperature is 2/3 of the melting temperature (here we use 5 °C as the melting point of CPMA·MS) of ILs.³⁵ The results show that CPMA·MS is not a typical Arrhenius fluid, which seems to be characteristic of many ILs.³³

Steady shear flow curves across a wide range of shear rates can provide important information regarding the ways in which the internal structure of the sample changes with the applied shear rate. The rheological behaviors of pure CPMA·MS and its mixtures with sunflower oil and glycerol have been shown in Fig. 7. Apparently the pure IL does not behave perfectly as a Newtonian liquid. The viscosity of CPMA·MS slightly increases with the increasing shear rate, in another word, exhibiting shear-thickening behavior.³⁴ On the other hand, the viscosity of the mixtures of the IL and substrates significantly decreases with increasing rates and shear time, in which the behaviors are somehow similar to a thixotropic liquid.³⁶ For a typical thixotropic liquid, the systems usually pack with loosely asymmetrical particles (network structure). There exists an equilibrium viscosity value at any valid shear rates and temperature. The time to

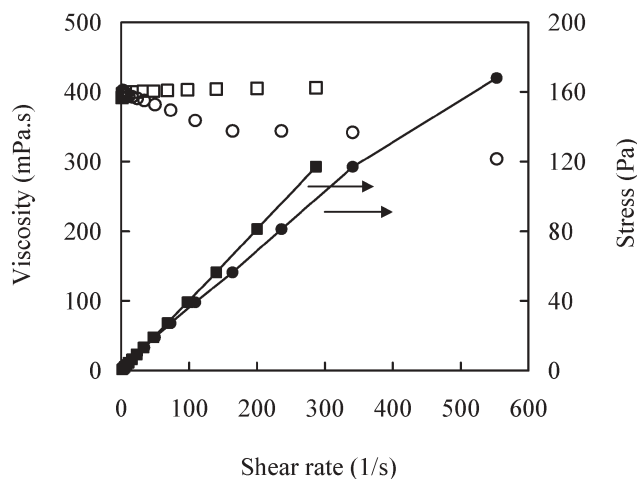


Fig. 7 Rheological behavior of the IL (□ and ■) and its mixture with substrates (○ and ●). The measurement is at 50 °C.

attain equilibrium strongly depends on shear rates. Such phenomena have been observed for the IL–sunflower oil–glycerol system in this study. In general, there are two contrary actions, breakdown and recovery of the network structure during shearing processes of a thixotropic liquid. Likewise, there also occur two opposite tendencies for the partially miscible IL–sunflower oil system, that is, the potential of oil molecules to disorganize the intrinsic compact structure of the system and the tendency to recover partial phase separation. Besides the shearing action, the hydrophobic interaction between fatty acid chains of oil and the alkyl group in CPMA·MS will promote the former process and help keep the dispersion state, which will lead to a dramatic decrease in the apparent viscosity of the mixtures. The repulsion action between the hydrophobic oil molecules and the hydrophilic group in the IL molecule and its ionic nature, on the other hand, will drive the system to recover its separated state, in which viscosity will be dominated by the IL with higher viscosity. The result suggests that vigorous agitation will not only eliminate external mass transfer limitation but also significantly reduce the viscosity of the reaction mixture, so as to facilitate the diffusion of substrates in the porous support particles of lipase.

Novozym 435 is a commercial enzyme in which *Candida antarctica* lipase B is immobilized on macroporous polyacrylate resin beads. There is no doubt that only the substrates being diffused into the particles and reacted with the lipase anchored there can result in the occurrence of reaction. Even though the external mass transfer limitation could be eliminated by agitation as mentioned above, the diffusion rate inside particles will be a decisive step for the reaction due to high viscosity of reaction medium. To address this question, it is useful to compare the two time constants for reaction (t_r) and diffusion (t_d), which are defined as follows, respectively:

$$t_r = c_0/r_{c,0} \quad (3)$$

$$t_d = D/(k_{SL})^2 \quad (4)$$

where $c_0/\text{mol L}^{-1}$ is the substrate concentration in bulk organic phase, $r_{c,0}$ the initial reaction rate, D the diffusivity of the substrate in solvent and $k_{\text{SL}}/\text{cm s}^{-1}$ the solute-liquid mass transfer coefficient in solvent. The mass transfer coefficient can be estimated by Sherwood number: $k_{\text{SL}} = 2 D/d$, where d is the diameter of the support particles.³⁷ Few studies regarding the diffusion of organic molecules in ILs have been published so far.³⁸ No available models could be applied to the present IL system. Therefore, we use Wilke–Chang correlation (eqn (5)), an empirical modification from the Einstein–Stokes equation) to estimate the diffusion of sunflower oil molecules in CPMA·MS.³⁷

$$D_{\text{AB}} = 7.4 \times 10^{-8} \frac{(\phi M_{\text{B}})^{1/2} T}{\eta_{\text{B}} V_{\text{A}}^{0.6}} \quad (5)$$

where $D_{\text{AB}}/\text{cm}^2 \text{ s}^{-1}$ is diffusion coefficient of solute A in solvent B, M_{B} molecular weight of solvent B, T/K temperature, η_{B} the viscosity of solvent B, $V_{\text{A}}/\text{cm}^3 \text{ mol}^{-1}$ the molar volume of solute A at its normal boiling temperature and ϕ association factor of solvent B, dimensionless. Because glycerol with much small molecule size is in excess and could be also fully dissolved in the IL, it is assumed that the mass transfer is mainly controlled by the diffusion of oil molecules. No literature value of ϕ is available so far. Considering the high degree of molecular association, 2.60, that occurs in CPMA·MS, the ϕ -value of water is used in the calculation.

It was observed that, at 50 °C and a concentration of oil of 0.188 mol L⁻¹, the initial reaction rate was $5.46 \times 10^{-6} \text{ mol L}^{-1} \text{ s}^{-1}$. Therefore, t_{r} should be $3.44 \times 10^4 \text{ s}$ according to eqn (3). The diffusion coefficient calculated by eqn (5) is $4.66 \times 10^{-8} \text{ cm}^2 \text{ s}^{-1}$ (sunflower oil is treated as trilinoleoyl glycerol). The diffusion time could be accordingly estimated as $1.756 \times 10^4 \text{ s}$ by eqn (4). At 35 °C, the calculated value of t_{d} is $4.51 \times 10^4 \text{ s}$. The same order of magnitude for t_{d} and t_{r} suggests that the effects of mass transfer on the glycerolysis of sunflower oil in CPMA·MS catalyzed by Novozym 435 should be seriously taken into account, especially when the reaction is performed at lower temperatures. In fact, the oil molecules might exist in clusters instead of singly; therefore the above calculation would only give a rough estimate and would not be an accurate description for the diffusion of oil molecules in the IL,³⁹ that is to say that the diffusion of oil in the IL may be slower than the above-calculated rates. This implies that mass transfer is a serious problem for the efficiency of the reaction.

Since the reaction in the IL is controlled by both mass transfer and intrinsic reaction kinetics and the viscosity of medium strongly depends on reaction temperature, it will be useful to have a quantitative evaluation on the contribution of mass transfer to the change of reaction rates. A similar data processing as above demonstrated that the glycerolysis of sunflower oil in *tert*-butyl alcohol is a kinetically controlled reaction (data not shown), so the effect of mass transfer in *tert*-butyl alcohol system could be neglected in the kinetic study. From 35 to 55 °C, the reaction rate increases by only 2.2 times for *tert*-butyl alcohol system, instead of 11.5 times for the reaction in the IL system. Assuming the glycerolysis in the two systems possesses similar kinetic behavior; this significant

difference should be mainly resulted from the marked decrease of the IL viscosity (from 1024 to 308 cP).

Water activity of the IL reaction system and its influence

The importance of hydration regarding enzyme activity in organic solvents and ionic liquids has been well-known.^{40,41} Enzyme activity, specificity, and hydrolytic activity are more or less dependent on the thermodynamic water activity (a_{w}).⁴⁰ Fig. 8 shows the changes of water activities of CPMA·MS and its mixtures with sunflower oil and glycerol as a function of water contents. A linear correlation of water activity and water content for pure IL was observed. It is notable that the water activity still remains at a lower level even when the water content is over 5%, which significantly differs from other types of ILs.⁴¹ This phenomenon could be ascribed to the occurrence of polyethoxyl moiety in CPMA·MS, which causes the IL to have a strong association with water molecules as well as to restrict their freedom. Within the range of water content up to 2%, the water activity of the mixtures of IL and substrates also shows a similar linear increase with the increasing water content. The evident deviation after the water content at 2% might arise from the partial separation. During the measurement of water activity, it was observed that the phase separation became faster when more water was added to the sample. This is probably because more association of water molecules with the IL molecules enhances the repulsion between the IL molecules and oil molecules. This consequently promotes phase separation.

The real interest of investigation in water activity lies in the acquirement of the effects of a_{w} on reaction performance. We conducted the glycerolysis of sunflower oil at varied a_{w} (Fig. 9A). Interestingly, inconsistent with normal observations, the initial rates, denoted by the conversion of TG, increase with the decrease of a_{w} . Similar observation for the transesterification in [bmim][PF₆] (1-butyl-3-methylimidazolium hexafluorophosphate) and hexane employing *Candida antarctica* lipase B was also reported.^{41,42} One possible explanation lies in a possible transport limitation of the hydrophobic substrate from the solvent medium through the water layer surrounding the enzyme at higher water activities. As also observed in

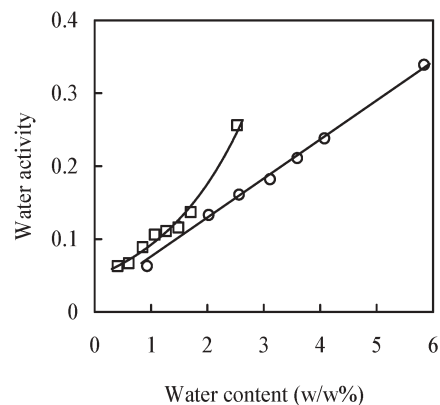


Fig. 8 A dependent relationship of the water activity of the IL (○) or its mixture with substrates (□) with the corresponding water content. The mixture consists of 1 mmol IL, 1 mmol sunflower oil, 5 mmol glycerol and variable water. All measurements are performed at 40 °C.

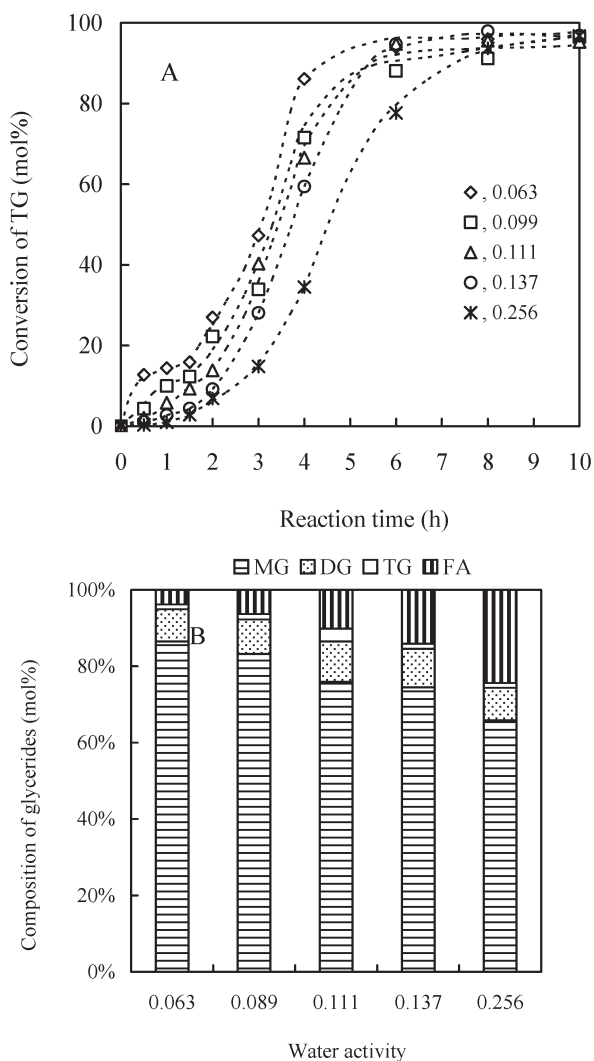


Fig. 9 Progress curves of the conversion of TG for the glycerolysis in the IL with different a_w (A); Effects of water activities on the composition of glycerides for the reaction in the IL at 10 h (B). The reaction system has the same components as in Fig. 8 other than 100 mg enzyme. The reaction is performed at 60 °C with magnetic stirring at 400 rpm.

experiments, phase separation was intensified with increase of water activity, which could result in stronger obstacle for oil molecules to diffuse into ILs. This has affected the length of induction periods, which becomes longer with the increase of a_w (Fig. 9A). With these considerations, we might propose a conceivable explanation for the occurrence of the induction period and a jumping increase after the induction period for the glycerolysis of triglyceride in this IL system as shown in Fig. 1. The mass transfer limitation and phase separation are likely the dominating reasons for the occurrence of the induction period. The steep increase of the reaction rate after the induction stage suggests that a critical phase transfer limitation point and a self-accelerating (self-affecting) phenomenon could have occurred. It is assumed that the yielded MG and DG promote phase homogenization, resulting in a significant diffusion enhancement and spectacular increase of rate.

Another negative effect of higher water activity for the glycerolysis in the IL is that more hydrolytic products were produced (Fig. 9B). This result indicated that even though the IL molecules had the capacity to reduce the number of free water molecules, a steady increase of hydrolytic products against the increasing water activity is unavoidable due to the competition between hydrolysis and glycerolysis.

Kinetic properties of the glycerolysis in IL system

Differing from typical lipases,⁴³ *Candida antarctica* lipase B does not display any interfacial activation and usually adopts an “open” conformation which makes the active site accessible to solvents.⁴⁴ It is well known that substrate specificity and catalytic efficiency depend upon the ability of the enzyme to utilize the free energy binding with the substrates.⁴⁵ This binding energy reflects the difference between binding energies of the substrate-enzyme and the substrate-solvent interactions.⁴⁶ Kinetic parameters for the description of enzyme behaviors, therefore, depend strongly on the solvent medium. In order to rationalize the lipase performance in the IL system and the effects of the IL, we have studied the kinetic behaviors of Novozym 435-catalyzed glycerolysis in the IL system and compared their performances with those in *tert*-butyl alcohol and solvent-free systems (Table 1).

The effect of temperature on the reaction activity of Novozym 435 in the IL system shows a spectacular increase of initial rates against temperature, yielding an enhanced activation energy estimated by Arrhenius equation. The E_a of the reaction in the IL system is about three times the value in *tert*-butyl alcohol and even considerably higher than the E_a for the solvent-free system. This striking difference is more likely to arise from the dramatic decrease of the IL viscosity with the increasing temperature and the resulting mass transfer enhancement, which has been proven to be one of the decisive factors for the glycerolysis in the IL as repeatedly mentioned above. The result also suggested that, in order to achieve an optimal reaction rate for the IL system, it is necessary to conduct the reaction at a higher temperature to overcome the elevated energy barrier.

To properly evaluate the selectivity of reaction systems, we studied the kinetic properties denoted by both conversion of TG and glycerolysis degree based on the Michaelis–Menten model (Table 1). The apparent value of K_m in the IL system is markedly bigger than those in *tert*-butyl alcohol and solvent-free systems, which shows a good agreement with the change of E_a . However, this does not consequently indicate any change of the affinity of lipase to substrates,²⁸ instead we believe that phase separation and mass transfer limitations cause the higher K_m in the solvent-free and IL systems. Interestingly the maximum reaction rate in the IL system is much higher than those in the other two systems even though the IL has the biggest K_m and a lower initial reaction rate. This indicates that the IL system has a higher productivity, which is consistent with our previous observation.²⁸ The reason is that the IL is better able to accommodate the resulting MG molecules (the IL molecule has more H-bonding sites) than *tert*-butyl alcohol, so is still able to shift the equilibrium at higher substrate concentration. It is noteworthy that, in

Table 1 Some kinetic properties of the glycerolysis of sunflower oil catalyzed by Novozym 435 in different systems

	$E_a/\text{kJ mol}^{-1}$	Denoted by conversion of TG		Denoted by GD		
		$V_{\text{max}}^C/\text{mol L}^{-1} \text{h}^{-1}$ (g enzyme) $^{-1}$	K_m^C/mM	$V_{\text{max}}^G/\text{mol L}^{-1} \text{h}^{-1}$ (g enzyme) $^{-1}$	K_m^G/mM	$V_{\text{max}}^G/V_{\text{max}}^C$
Solvent-free	^a 65.37	0.86	445	0.98	419	1.14
<i>tert</i> -Butyl alcohol	^b 33.20	1.14	147	1.83	124	1.60
Ionic liquid	^c 101.04	1.39	848	2.47	830	1.78

All kinetic assays were done at 60 °C with agitation speed 600 rpm and an excessive and constant concentration of glycerol. For the solvent-free, *tert*-butyl alcohol–IL system, the variation of concentration of sunflower oil is in the ranges of 0.32–0.76, 0.04–0.35 and 0.18–0.55 mol L⁻¹, respectively. E_a was measured at ^a 35–65 °C, ^b 25–55 °C and ^c 35–65 °C.

accordance with the change of GD values while the conversion of TG is close to 100%, the value of $V_{\text{max}}^G/V_{\text{max}}^C$ is approximately equal to the doubled yield percentage of MG (Table 1). This might imply the indexation value of GD for reaction selectivity. In the solvent-free system, the relative yield of MG is very low, though V_{max}^C is theoretically high (probably resulting from the high substrate concentration).

Conclusions

The primary motivation for this study is to explore the intrinsic reasons for the unique behavior of the glycerolysis of triglycerides in the IL system and to give a proper evaluation of the effects of the important parameters. It turns out that multiple factors result in the lower initial rate and the occurrence of induction period. Both the internal mass transfer limitation resulting from the high viscosity of the IL and the partial phase separation are found to play a crucial role. Therefore any measures to reduce the system viscosity or to eliminate the diffusion limitation such as by increasing temperature and improving mixing effect will significantly increase reaction rates and reduce the induction periods. Our observation also shows that the rheological behavior of CPMA·MS is slightly shear-thickening and could be more accurately described by VFT model, while the mixtures of the IL and substrate exhibit as a thixotropic liquid, suggesting that agitation not only facilitates diminishing the external mass transfer but also reduces the system viscosity to improve the internal mass transfer. The increase of water activity in the IL system leads to the decrease of reaction rate. Notably high K_m and V_{max} for the glycerolysis in the IL system indicate the special thermodynamic affinity property of the IL system and its higher productivity.

This work involves quantitative description of the mass transfer in the practical IL system with high viscosity. These efforts are believed to be useful for a better understanding of how the IL sustains a complicated reactive environment and produces such unique reaction behaviors. The study will provide a sound basis for reaction optimization and further screening of ILs.

Experimental

Materials

Novozym 435 (*Candida antarctica* lipase B immobilized on macroporous polyacrylate resin beads) was provided by Novozymes A/S (Bagsvaerd, Denmark). Glycerol (minimum

99%) was purchased from Sigma-Aldrich Co. (St. Louis, USA). Sunflower oil was obtained from Aarhus United (Aarhus, Denmark). Cocosalkyl pentaethoxymethyl ammonium methosulfate (CPMA·MS) was procured from Solvent Innovation GmbH (Köln, Germany) and of 98% minimum purity. Other chemicals and reagents were all of analytical grade and used as received.

Activity evaluation of glycerolysis and definition of glycerolysis degree

Different from hydrolytic activity of lipases, the definition of the glycerolysis activity of lipases is always a disputing topic, since glycerolysis can occur between TG and glycerol, between DG and glycerol, and between TG and MG. Nouredini and Harmeier⁴⁷ mentioned this problem and proposed a new definition of glycerolysis activity unit (GU) based on the consumption of both TG and glycerol. However, the method needs the accurate measurement of the consumption of glycerol, which is usually complicated. Theoretically the glycerolysis activity of lipases should include the formation of 1 mol DG and 1 mol MG from 1 mol TG as well as the formation of 2 mol MG from another 1 mol glycerol. This means that the glycerolysis activity can be expressed as the formation of DG (1 mol DG consumes 1 mol TG) and MG (3 mol MG consumes 2 mol glycerol), in which the amounts are obtained from the normalization of only glycerides and free fatty acids based on area percentages by TLC-FID analysis (All glycerides give similar response factors and the error is within $\pm 5\%$). The glycerolysis degree (GD), is calculated as follows:

$$\text{GD} = \frac{[\text{DG}] + \frac{2}{3}[\text{MG}]}{[\text{TG}] + \frac{[\text{MG}]}{3} + \frac{[\text{FA}]}{3} + \frac{2}{3}[\text{DG}]} [\text{TG}]_0 \quad (6)$$

where [TG], [DG], [MG] and [FA] represent the molar percentage of tri-, di- and mono-glycerides and free fatty acids, respectively. $[\text{TG}]_0$ is the initial concentration of triglycerides. In eqn (6), the numerator represents the glycerolysis activity in terms of equivalent consumption of TG, and the denominator is the sum of the molar fractions of TG being transformed into DG, MG and FA at reaction time t . Relative glycerolysis degree could be obtained without multiplying the initial concentration of triglycerides.

Parameter studies and kinetic measurement

Typical experimental procedure for glycerolysis of sunflower oil in IL: 2 mmol sunflower oil and 5 × 2 mmol glycerol were

mixed with 2 mL (2.2 g) cocosalkyl pentaethoxymethyl ammonium methosulfate (CPMA·MS) in a 25 mL jacketed vial by magnetic stirring. The reaction was initiated by the addition of 100 mg Novozym 435 and conducted at the desired temperature controlled by circulated water. The evolution of the reaction was monitored by sample withdrawal and TLC-FID analysis after dissolving the sample in chloroform-methanol (2 : 1 v/v) solution. All reactions were performed in duplicates. The developing solvents for TLC-FID consist of n-hexane, diethyl ether and acetic acid (35 : 35 : 1 v/v/v). The area percentage of glyceride and free fatty acid bands was used for the calculation of conversions of oil and yields of monoglycerides.⁴⁸

Important parameters influencing mass transfer and reaction, such as agitation rate, enzyme dosage, and substrate ratio, were investigated using the above experimental procedure with specific adjustment of parameters to meet the designed reactions.

The thermodynamic properties were acquired by investigating the plot of reaction rate against temperature and fitting the data to the Arrhenius equation, in which a 5-fold molar excess of glycerol to sunflower oil is applied to all reaction systems and the reaction rate indicates the molar conversion of TG.

Glycerolysis of sunflower oil is a two-substrate and two-step reaction. To simplify the kinetic model, an excess of glycerol was used for all systems and the change of its concentration during the measurement of reaction rate was neglected. Conversion of TG and glycerolysis degree were used to determine the maximum reaction rate and Michaelis–Menten constants.

Viscosity measurement and size assay of the immobilized particles

Absolute viscosity (η) of the pure IL and its mixture with substrates were measured with a Stresstech Rheometer (Rheologica Instruments AB, Lund, Sweden). Shear flow curves were obtained using a coaxial cylindrical geometry at shear rate ranging from 0 to 500 s⁻¹. The measuring temperature was controlled by circulated water with an accuracy of 0.1 K. For all measurements, a 5 min preshear with constant rate of 200 s⁻¹ was applied to the samples. The viscosities of the samples were first determined as a function of temperature during a heating cycle from 298 to 303 K. Afterwards the measurement was restarted after the solution was cooled to 298 K. All measurements were performed in duplicates.

The particle size distribution of Novozym 435 was measured by a Masterizer 2000 particle size analyzer (Malvern Instrument, UK). The dry Novozym 435 has a mean volume weighted diameter of 0.513 mm. A slight diameter expansion to constant was observed during the reaction and storage in solvent. The recovered Novozym 435 from reaction was washed with 70% ethanol and the diameter was measured to give a mean value of 0.572 mm, identical with those stored in 70% ethanol for overnight.

Water content adjustment and a_w measurement

The received CPMA·MS was first dried by vacuum of 1 mmHg at 50 °C for 8 h and its water content was measured with Karl

Fischer titration. Then a series of mixtures with substrates in specific water content were prepared by adding a certain amount of water. The resulting samples were preequilibrated for 24 h with magnetic stirring in a sealed vial before being subjected to a_w measurement. The water activity (a_w) of the IL with specific water content was measured with an Aqualab Water Activity Meter (Decagon Devices, Washington, DC) at the set temperature. The profiles of a_w for the IL and the mixture of the IL and substrates as a function of water content was accordingly established. The mixture of the IL and substrates with varied a_w was finally used for glycerolysis studies to examine the effects of a_w on the reaction.

Acknowledgements

We thank Nancy Kjøbæk (BioCentrum-DTU) for her kind assistance for the viscosity measurement. Financial supports from Danish Technological Research Council (STVF) and Center for Advanced Food Studies (LMC) are acknowledged.

References

- 1 J. M. DeSimone, *Science*, 2002, **297**, 799–803.
- 2 G. J. Lye, P. A. Dalby and J. M. Woodley, *Org. Process Res. Devel.*, 2002, **6**, 434–440.
- 3 M. M. Kirchhoff, *Environ. Sci. Technol.*, 2003, **37**, 5349–5353.
- 4 R. A. Sheldon, R. M. Lau, M. J. Sorgerdrager, F. van Rantwijk and K. R. Seddon, *Green Chem.*, 2002, **4**, 147–151.
- 5 J. F. Brennecke and E. J. Maginn, *AIChE J.*, 2001, **47**, 2384–2389.
- 6 J. S. Wilkes, *J. Mol. Catal. A: Chem.*, 2004, **214**, 11–17.
- 7 J. L. Anderson, J. Ding, T. Welton and D. W. Armstrong, *J. Am. Chem. Soc.*, 2002, **124**, 14247–14254.
- 8 J. Dupont, R. F. de Souza and P. A. Z. Suarez, *Chem. Rev.*, 2002, **102**, 3667–3692.
- 9 S. Park and R. J. Kazlauskas, *Curr. Opin. Biotechnol.*, 2003, **14**, 432–437.
- 10 T. Itoh, E. Akasaki, K. Kudo and S. Shirakami, *Chem. Lett.*, 2001, 262–263.
- 11 N. Jain, A. Kumar, S. Chauhan and S. M. S. Chauhan, *Tetrahedron*, 2005, **61**, 1015–1060.
- 12 U. Kragl, M. Eckstein and N. Kaftzik, *Curr. Opin. Biotechnol.*, 2002, **13**, 565–570.
- 13 *Ionic Liquids in Synthesis*, ed. P. Wasserscheid and T. Welton, Wiley-VCH, Weinheim, 2003.
- 14 *Ionic Liquids as Green Solvents*, ed. R. D. Rogers and K. R. Seddon, American Chemical Society, Washington, DC, 2002.
- 15 F. Van Rantwijk, R. M. Lau and R. A. Sheldon, *Trends Biotechnol.*, 2003, **21**, 131–138.
- 16 R. D. Schmid and R. Verger, *Angew. Chem., Int. Ed.*, 1998, **37**, 1608–1633.
- 17 Z. Guo, A. F. Vikbjerg and X. Xu, *Biotechnol. Adv.*, 2005, **23**, 203–259.
- 18 X. Xu, *Eur. J. Lipid Sci. Technol.*, 2000, **102**, 287–303.
- 19 V. M. Balcao and F. X. Malcata, *Biotechnol. Adv.*, 1998, **16**, 309–341.
- 20 T. Yamane, *J. Am. Oil Chem. Soc.*, 1987, **64**, 1657–1662.
- 21 M. T. Patel, R. Nagarajan and A. Kilara, *Chem. Eng. Commun.*, 1996, **152–153**, 365–404.
- 22 P. Lozano, T. de Diego, D. Carrié, M. Vaultier and J. L. Iborra, *Chem. Commun.*, 2002, 692–693.
- 23 M. T. Reetz, W. Wiesenhöfer, G. Franciò and W. Leitner, *Chem. Commun.*, 2002, 992–993.
- 24 R. M. Lau, F. van Rantwijk, K. R. Seddon and R. A. Sheldon, *Org. Lett.*, 2000, **26**, 4189–4191.
- 25 S. Park and R. J. Kazlauskas, *J. Org. Chem.*, 2001, **66**, 8395–8401.
- 26 J. C. Bellot, L. Choïnard, E. Castillo and A. Marty, *Enzyme Microb. Technol.*, 2001, **28**, 362–369.
- 27 U. T. Bornscheuer, *Enzyme Microb. Technol.*, 1995, **17**, 578–586.
- 28 Z. Guo and X. Xu, *Org. Biomol. Chem.*, 2005, **3**, 2615–2619.
- 29 G. D. Yadav and K. M. Devi, *Biochem. Eng. J.*, 2002, **10**, 93–101.

- 30 P. Bonhôte, A.-P. Dias, N. Papageorgiou, K. Kalyanasundaram and M. Grätzel, *Inorg. Chem.*, 1996, **35**, 1168–1178.
- 31 J. G. Huddleston, A. E. Visser, W. M. Reichert, H. D. Willauer, G. A. Broker and R. D. Rogers, *Green Chem.*, 2001, **3**, 156–164.
- 32 O. O. Okoturo and T. J. VanderNoot, *J. Electroanal. Chem.*, 2004, **568**, 167–181.
- 33 J. R. Sanders, E. D. Ward and C. L. Hussey, *J. Electrochem. Soc.*, 1986, **133**, 325–330.
- 34 A. Chagnes, A. Tougui, B. Carré, N. Ranganathan and D. Lemordant, *J. Solution Chem.*, 2004, **33**, 247–255.
- 35 F. W. Billmeyer, *textbook of polymer science*, John Wiley and Sons Inc., New York, 3rd edn, 1984.
- 36 M.-H. Oh, J.-H. So and S.-M. Yang, *J. Colloid Interface Sci.*, 1999, **216**, 320–328.
- 37 *Perry's Chemical Engineers' Handbook*, ed. R. H. Perry and D. W. Green, McGraw-Hill, New York, 6th edn, 1984, pp. 3–287.
- 38 H. A. Every, A. G. Bishop, D. R. MacFarlane, G. Örödd and M. Forsyth, *Phys. Chem. Chem. Phys.*, 2004, **6**, 1758–1765.
- 39 E. L. Cussler, *AIChE J.*, 1980, **26**, 43–51.
- 40 P. J. Halling, *Enzyme Microb. Technol.*, 1994, **16**, 178–206.
- 41 J. A. Berberich, J. L. Kaar and A. J. Russell, *Biotechnol. Prog.*, 2003, **19**, 1029–1032.
- 42 F. Chamouveau, D. Coulon, M. Girardin and M. Ghoul, *J. Mol. Catal. B*, 2001, **11**, 949–954.
- 43 M. Martinelle, M. Holmquist and K. Hult, *Biochim. Biophys. Acta*, 1995, **1258**, 272–276.
- 44 J. Uppenberg, M. T. Hansen, S. Patkar and T. A. Jones, *Structure*, 1994, **2**, 293–308.
- 45 C. R. Wescott and A. M. Klibanov, *J. Am. Chem. Soc.*, 1993, **115**, 1629–1631.
- 46 K. Ryu and J. S. Dordick, *Biochemistry*, 1992, **31**, 2588–2598.
- 47 H. Nouredini and S. E. Harmeier, *J. Am. Oil Chem. Soc.*, 1998, **75**, 1359–1365.
- 48 T. Tatara, T. Fujii, T. Kawase and M. Minagawa, *Lipids*, 1983, 732–736.

Chemical Science

An exciting news supplement providing a snapshot of the latest developments across the chemical sciences



Free online and in print issues of selected RSC journals!*

Research Highlights – newsworthy articles and significant scientific advances

Essential Elements – latest developments from RSC publications

Free access to the originals research paper from every online article

*A separately issued print subscription is also available

RSC Publishing

www.rsc.org/chemicalscience

Unusual electrical response of a poly(aniline) composite film on exposure to a basic atmosphere and its application to sensors

Xingfa Ma,^{*ac} Guang Li,^{*b} Mang Wang,^a Ru Bai,^a Feng Yang^a and Hongzheng Chen^a

Received 2nd August 2005, Accepted 4th November 2005

First published as an Advance Article on the web 24th November 2005

DOI: 10.1039/b511002e

An unusual electrical response of a poly(aniline) composite film on exposure to a basic atmosphere is reported in this paper. Based on this feature, it was possible to develop a novel kind of gas-sensor exhibiting high sensitivity, rapid response, good repeatability which can be easily recovered by purging with highly pure N₂. In order to study the gas-response mechanism of this unusual electrical response, comparative tests were carried out on the gas-sensing properties of N-type and P-type silicon with porosity under similar conditions. The electric field-induced surface photovoltage spectrum (FISPS) on the poly(aniline) composite film before and after pretreatment was also examined. The experimental results indicated that the transition from P-type to N-type of a poly(aniline) composite film may exist as a result of a doping effect.

Introduction

Gas-sensors are an important part of electronic nose systems to simulate olfaction and can have potential applications in many fields, such as environmental monitoring, foodstuff industry, chemical industry, medical diagnostic, explosives and neurotoxin detection for counter-terrorism, detection for insecticides and drugs, and so on.^{1,2}

Currently, many researchers expect to obtain sensors with high sensitivity, rapid response, reversibility at room temperature and convenient operation. All these rely on new, highly sensitive materials and good fabrication technology. So far, the materials in these areas have focused on the metal oxides semiconductors,^{3–7} single-wall carbon tubes (SWNTs), multi-wall carbon tubes (MWNTs),^{1,8–11} conductive polymers,^{12–19} metal organic compounds,^{20–23} and so on. Among these materials, conductive polymers are one kind of sensitive material that can be operated at or near room temperature.

Because of the mechanical flexibility, environmental stability and controllable conductivity with an acid/base (doping/undoping), poly(aniline) has attracted considerable attention as one of the typical conductive polymers, and has a lot of potential applications in many fields, such as lightweight battery electrodes, electromagnetic shielding devices, anti-corrosion coatings, and sensors.^{24–26}

At present, along with the preparation of nano-structure materials and nano-electrical devices, studies on controlling

the nano-structure and improving the properties of conductive polymers have become active. Template and non-template methods, nano-fiber seeding approaches, and so on, are applied for preparing conductive polymers with nano-structures.^{24–29} Some investigators pointed out that conductive polymers with nano-structures have potential applications for superb sensitive sensors, such as gas-sensors, due to the highly specific surface area and the excellent charge transmission. However, up to now, most of these researchers have focused on the preparation of materials and morphology characterization.^{27–29} Recently, Huang and co-workers investigated the sensing properties of sensors based on nanostructured poly(aniline) prepared using interface polymerization and interdigital gold electrodes to obtain good results.^{30–32} Therefore, these studies inspired us to develop some organic sensors with high sensitivity.

The literature has indicated that most sensors made of poly(aniline) are based on the reversible reaction of an acid/base, for instance, the conductivity of poly(aniline) increases with acid and decreases with base. However, in our experiments, we found an interesting and unusual phenomena. Based on this feature, a novel gas-sensor, having high sensitivity, rapid response and good repeatability which can be easily recovered by purging with highly pure N₂, in comparison with conventional poly(aniline) sensors, may be developed. Accordingly, this paper reports this abnormal behavior, discusses the sensitive mechanism, and also provides further evidence to support our previous reports.^{30–33}

Experimental

Materials

Aniline (A.R.) was freshly distilled under vacuum prior to use, ammonium peroxydisulfate (A.R.), hydrochloride (A.R.), toluene (A.R.), n-hexane (A.R.), alcohol (A.R.), N-type and P-type silicon with porosity, and so on, are commercially available. Deionized filtered water was used in all studies.

^aDepartment of Polymer Science and Engineering, State Key Lab of Silicon Materials, Zhejiang University, Hangzhou, 310027, P. R. China. E-mail: xingfazju@163.com; xingfamazju@yahoo.com.cn; Fax: +86-571-87951635; Tel: +86-571-87952557

^bDepartment of Biomedical Engineering, State Key Lab of Biosensors, Key Lab of Biomedical Engineering of Ministry of Education of China, Zhejiang University, Hangzhou, 310027, P. R. China. E-mail: guangli@cbeis.zju.edu.cn; Fax: +86-571-87951676; Tel: +86-13858068126

^cShandong Research Institute of Non-metallic Materials, Jinan, 250031, P. R. China

The interdigital electrodes are made of carbon paste, which are prepared with screen-printing technology, the gap and the length of electrode are 0.5 mm and 1 mm, respectively, the substrate of the electrode is a poly(propylene) plate with 0.5 mm thickness.

Preparation of sensing film

The coating mixture was prepared by adding equal mol aniline and ammonium peroxydisulfate in a hydrochloride solution. The gas-sensor was fabricated *via* the carbon electrode being immersed in the above mentioned mixture. The carbon electrode was taken out after 24 h of *in-situ* polymerization, and then was washed with deionized filtered water repeatedly, then dried at room temperature.

Pre-treatment of poly(aniline) film

The device was put into an airproof test box (about 2.5 L), and desorbed with high-purity N₂. A certain amount of trimethylamine or other base volatile solvent (about 0.2 mL) was injected into the test chamber with a syringe for deprotonation.

Gas-response characterization of sensor

The gas-response characterization of the sensor to vapors has been reported in ref. 33 and 34.

XRD characterization

X-ray diffraction patterns were recorded by a Rigaku D/max 2550 Pe diffractometer, equipped with a rotating anode X-ray generator, with Cu K α monochromatic radiation at 40 kV and 300 mA. The samples were the films deposited on a glass substrate by *in-situ* polymerization.

SPS and FISPS measurements

The SPS instrument was made by Jilin University (China). Monochromatic light was obtained by passing light from a 500 W xenon lamp (CHF XQ500W, Global xenon lamp power made in China) through a double-prism monochromator (Hilger and Watts, D 300, UK). The slit width of the entrance and exit is 1 mm. A lock-in amplifier (SR830-DSP, USA), synchronized with a light chopper (SR540, USA), was employed to amplify the photovoltage signal. The range of modulating frequency is from 20 to 70 Hz. The spectral resolution is 1 nm. The raw SPS data were normalized using the illuminometer (Zolix UOM-1S, China). The poly(aniline) casting film on the ITO glass was studied during the SPS and FISPS measurements, and the contact between samples and the indium tin oxide (ITO) electrode is not an ohmic contact since we carried out the measurement of the surface photovoltage. The construct of the photovoltaic cell is a sandwich structure (see Fig. 9 later, inset). It was ensured that the light penetrating depth was much less than the film layer thickness. The obvious absorption of the ITO electrode was observed at 400–950 nm. The potential of the irradiated electrode with respect to the back electrode denotes the signs of the applied electrical field.^{35,36}

Results and discussion

Electrical response behavior of protonation poly(aniline) film exposed to a basic atmosphere

The structure of the sensor in our experiments was reported in ref. 33.

It was well known that the conductivity of poly(aniline) strongly depends on the doping and de-doping of an acid/base. The conductivity of poly(aniline) increases with the acid added and decreases with the base added. In our experiments, we found an unusual phenomena in conjunction to the above-mentioned rule. Exposed to a basic atmosphere, the current flowing through the protonated poly(aniline) film decreased suddenly at the beginning and then increased significantly. At this time, this film could be easily desorbed with high-purity N₂ and be repeatedly utilized. This film was not only sensitive to an acid atmosphere (the current of film increasing), but also sensitive to a base (the current of film increasing as well). The essential difference was that the film exposed to an acid could not be desorbed with N₂, and had to be recovered in a basic atmosphere. This gave us the idea that the conductivity of the de-protonated poly(aniline) film increased with the quantity of absorbed base. Based on this feature, it was possible to develop a novel gas-sensor having a high sensitivity, rapid response, good repeatability and being easy to recover by purging with highly pure N₂. In this way, poly(aniline) could be used to develop two kinds of gas sensors for a basic atmosphere. One is based on the acid/base reversibility (the current of film increasing on exposure to an acid atmosphere and decreasing on exposure to a basic atmosphere). The other is based on the reversible process of polar vapor/N₂ (the current of film increasing on exposure to a basic atmosphere and decreasing on exposure to a N₂ atmosphere).³³

The conductivity dependence of the protonated poly(aniline) film on desorption with high-purity N₂ is shown in Fig. 1.

Fig. 1 shows that the conductivity of the protonated poly(aniline) film decreased slightly along with the desorption with high-purity N₂, which was mainly due to the absorption of a certain amount of gas in air. It took a few seconds to reach a steady baseline. Afterwards it became very difficult to further desorb with N₂ which results in the small decline.

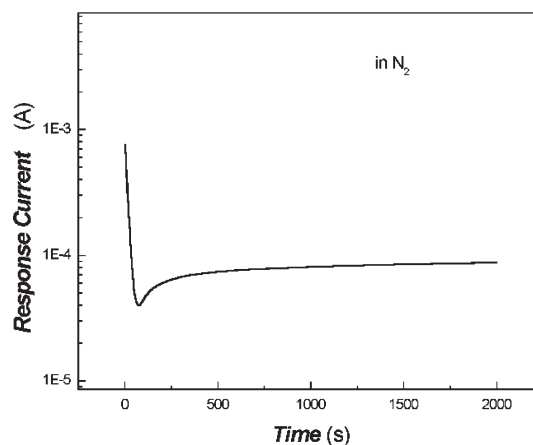


Fig. 1 Conductivity dependence of *in-situ* polymerized poly(aniline) film in an N₂ flow.

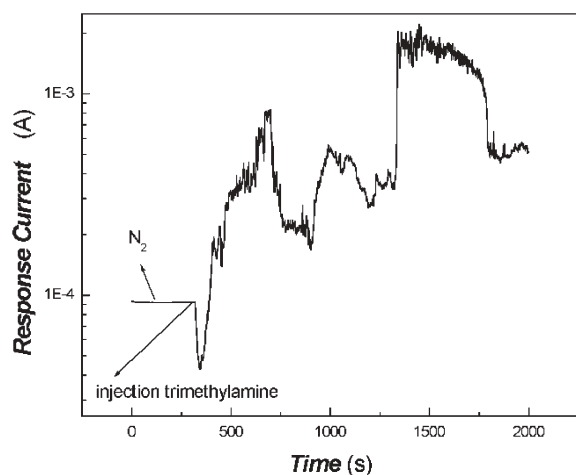


Fig. 2 Conductivity dependence of *in-situ* polymerized poly(aniline) film on exposure to trimethylamine (1.54×10^{-6} mol mL $^{-1}$).

When the protonated poly(aniline) film had obtained a steady current baseline and was exposed to a trimethylamine atmosphere, the conductivity dependence of the poly(aniline) film on the exposure time gave an interesting phenomenon, as shown in Fig. 2.

The current of the *in-situ* polymerized poly(aniline) composite film after desorption with N₂ remained constant at the beginning, then the current decreased sharply when the film was exposed to a trimethylamine atmosphere. Afterwards, the current increased rapidly along with the adsorption of trimethylamine, achieving a level of protonation of poly(aniline) with no desorption *via* N₂. This illustrates that the conductivity of poly(aniline) decreased along with an increasing extent of deprotonation. However, the increase of conductivity of poly(aniline) was very difficult to explain according to the usual reversible reaction of acids/bases and should be contributed to some other sensing mechanism.

The first exposure of poly(aniline) to a basic atmosphere acted as a pretreatment of the sensor in our research. In this way, the conductivity of poly(aniline) increases after the second, third, and fourth exposure to a basic atmosphere. The reversibility and repeatability were very good.

The comparative tests on gas-response between before and after pretreatment of poly(aniline) composite films to trimethylamine using the same sensor are shown in Fig. 3.

Fig. 3 shows that the sensitivity and response speed after pretreatment were much higher than that before pretreatment. For the same sensor, before pretreatment, it took about 1000 s to reach 1 order of magnitude change of gas-sensitivity, about 1600 s to reach 2 orders, but after pretreatment, its response was very quick. It took about 120 s to reach 4 orders of magnitude, and about 260 s to reach 5 orders. These phenomena showed that the mechanism of the sensor based on the reversible reaction of the acid/base of poly(aniline) is a protonation and de-protonation process, but the unusual electrical conductivity response of poly(aniline) pretreated in our studies should be attributed to the van der Waals interactions. The latter is very similar to that of the polymer system filled with carbon black.^{37–40} According to previous

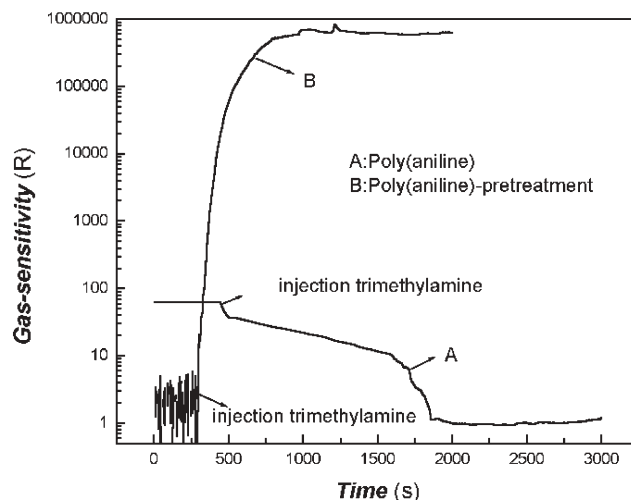


Fig. 3 Comparative tests on gas-response between before and after pretreatment of poly(aniline) composite films to trimethylamine (5.13×10^{-7} mol mL $^{-1}$).

literature, although the separation of amino acids had been carried out based on weak interactions of poly(aniline) with chromatographic technology,⁴¹ which acted as a stationary phase, some very similar amino acids can be identified. Therefore, it was meaningful to obtain a large measurable physical signal based on this weak interaction.

The sensing mechanisms mentioned above might be the result of grain boundary effects. It is well known that the poly(aniline) composite after deprotonation has a high resistance. When it absorbs chemical vapors, the potential barrier between intercrystallite boundaries is overcome. This leads to an increase of the film's conductivity. This mechanism can also be explained by the XRD results as shown in Fig. 4.

As shown in Fig. 4, the *in-situ* polymerized poly(aniline) film has a multi-crystal structure. This supports the sensing mechanism mentioned above.

On the other hand, poly(aniline) is an important electro-active material. When a voltage is applied, greater delocalization and polarization of the poly(aniline) will be induced,

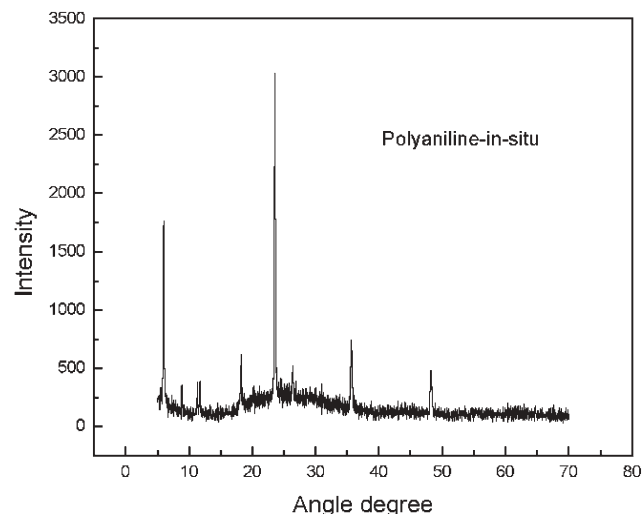


Fig. 4 XRD results of *in-situ* polymerized poly(aniline).

leading to the absorption ability of the poly(aniline) film to chemical vapors naturally increasing. Consequently, the response current of the poly(aniline) film increases. Of course, the real sensing mechanism still needs further investigation.

Effects of trimethylamine concentration on the gas-response of the sensor

The effects of trimethylamine concentration on the gas-response of the sensor to trimethylamine are shown in Fig. 5.

As shown in Fig. 5, it is obvious that the response magnitude as well as the response rate decrease with decreasing concentration. These results might offer up some valuable information about quantitative analysis.

Selectivity of the sensor

The gas-sensitivity of the poly(aniline) composite film to a series of vapors (trimethylamine, triethylamine, ammonia, formaldehyde, alcohol, toluene, and n-hexane) was examined, and the blank comparison test was also carried out considering the effect of moisture on the sensitivity by H₂O injection instead of trimethylamine. The results are shown in Fig. 6.

Fig. 6 shows that distinct differences of the gas-sensitivity and response speed to similar vapors can be observed. The value of the gas-sensitivity and the response speed to trimethylamine were much higher than those of other similar vapors so that the composite film might be used to distinguish trimethylamine and some similar vapors with the aid of a sensor array and an artificial neural network system.

It is well known that trimethylamine, triethylamine and ammonia are materials with electron donors, and the ability of the electron donor of methyl and ethyl groups is different to lead to that of the interaction between film and adsorbed molecular gas, resulting in the variation of response current.

Regarding the effect of moisture on the gas-response, this influence was very small although the baseline shifts a little.

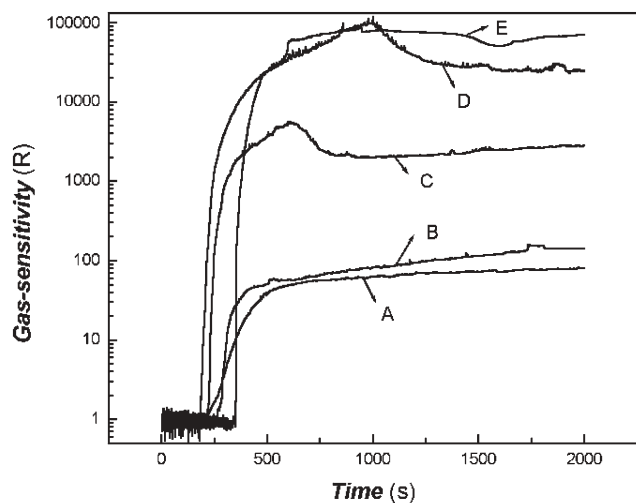


Fig. 5 Effects of trimethylamine concentration on the gas-response of the sensor to trimethylamine (A: 3.21×10^{-8} mol mL⁻¹; B: 6.41×10^{-8} mol mL⁻¹; C: 2.56×10^{-7} mol mL⁻¹; D: 5.13×10^{-7} mol mL⁻¹; E: 1.54×10^{-6} mol mL⁻¹).

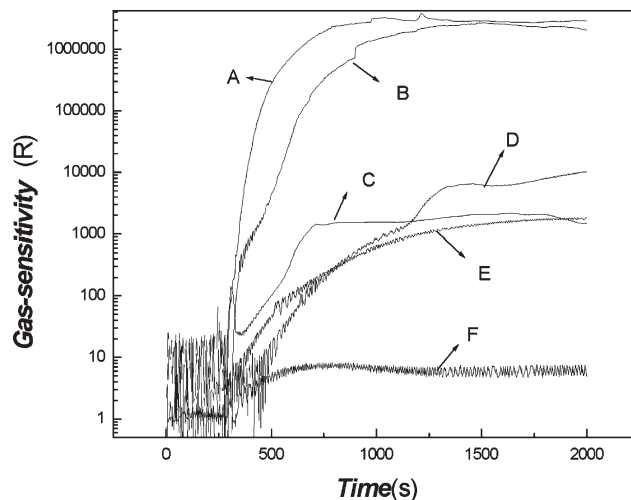


Fig. 6 The gas-response of the poly(aniline) composite film to a series of vapors (A: trimethylamine; B: triethylamine; C: ammonia; D: formaldehyde; E: alcohol; F: H₂O).

For other vapors, such as toluene and n-hexane, there were no responses at all.

Repeatability of the sensor

The repeated measurement curve of the sensor is depicted in Fig. 7, which shows that the composite film has good repeatability.

Fig. 7 also suggests that the present gas-sensing mechanism is possibly based on the physical adsorption/desorption process which induces the resistance change of the film.

Mechanism discussion

The preparation of poly(aniline) was generally carried out in acid media, so the product obtained was usually emeraldine salt, which had good conductivity. During the process of deprotonation, there will be several redox forms of poly(aniline), such as leucoemeraldine base (fully reduced form), emeraldine base (half-oxidized form), conducting emeraldine

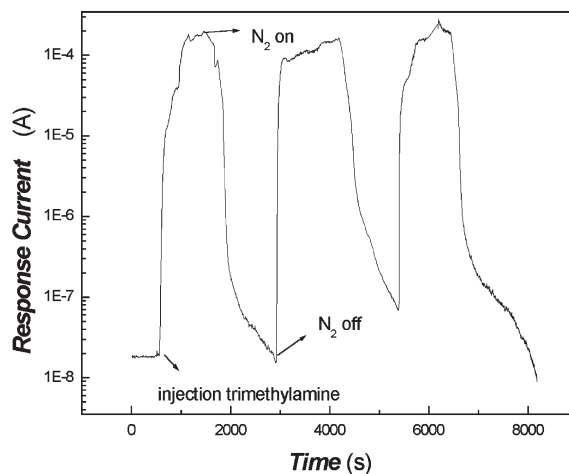


Fig. 7 The cycle test examination of the poly(aniline) composite film to trimethylamine (5.13×10^{-7} mol mL⁻¹).

salt (half-oxidized and protonated form), and pernigraniline base (fully oxidized form).⁴² Therefore, its mechanism of gas-sensitivity to vapors will be complex.³¹

The main reasons for gas-sensitivity should be attributed to the interaction between the sensing film and adsorbed molecular gas, including strong interactions (chemical bond) and weak interactions (such as hydrogen bonding, van der Waals force, and so on). For a strong interaction system, the recovery was generally very difficult, and for a weak interaction system, the recovery was easy at room temperature with highly pure N₂. For the sensor based on the reversible reaction of the acid/base of poly(aniline), the mechanism was a protonation and deprotonation process. The unusual electrical response of poly(aniline) pretreated in our studies should be attributed to the van der Waals interactions.

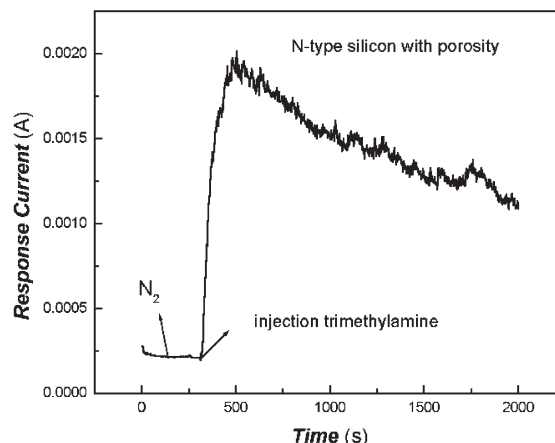
When the poly(aniline) film was exposed to basic atmosphere again (second, third, fourth time), because the surface of the poly(aniline) base still adsorbed the vapors and the resistance of the poly(aniline) base was very large, the resistance of the adsorbed gas film varies so that the response current increases. In addition, since the electronegativity of the nitrogen of the poly(aniline) base was very large, the radius of the nitrogen atom was small, and nitrogen atom had a lone electron, the interaction between the surface of the poly(aniline) base and polar vapors would contain hydrogen bonding and a strong van der Waals force. Moreover, poly(aniline) was a typical electroactive polymer. When a voltage was applied, the poly(aniline) film adsorbed many more polar vapors by the inducement effects of the electric field. All these were possible reasons resulting in the electrical response of the film.

In order to illustrate this problem, we carried out comparative tests under similar conditions through a series of polar vapors (such as alcohol, toluene, n-hexane, and so on). The results indicated that the increase of the poly(aniline) conductivity after pretreatment strongly depended on the polarity of adsorbed vapors. The bigger the polarity of vapor, the larger the conductivity increased. For the non-polar or weak polar vapors (such as n-hexane, toluene), there was a small response and for alcohol, it still had a good response although the sensitivity was lower than that of trimethylamine. These results agree well with the above discussions.

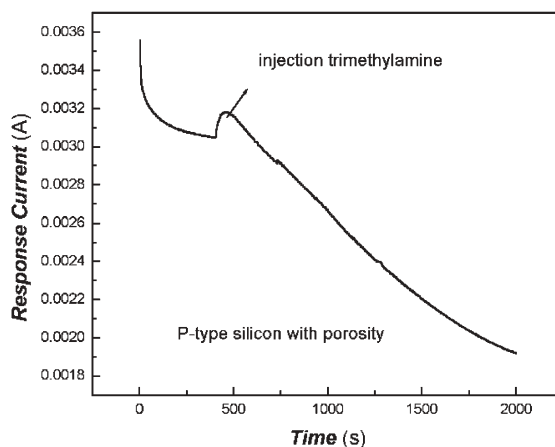
Trimethylamine was an electron donor and a typical biological base while the poly(aniline) salt usually belonged to a p-type semiconductor material. When the film of the poly(aniline) salt was first exposed to the atmosphere of trimethylamine vapor, the current of film decreased corresponding to the deprotonation process of poly(aniline). Afterwards, the proton was taken away by molecular trimethylamine along with desorption with highly pure N₂. When the deprotonated poly(aniline) film was exposed to the trimethylamine vapor atmosphere once again, the film current increases due to a strong interaction of the van der Waals force. The question was: did this cause changes (transition from P-type to N-type because of a doping effect in the gas phase) in the conductive type of poly(aniline) during the two time exposure cycle to the trimethylamine vapor atmosphere? This problem still needed to be investigated further.

To examine this hypothesis, considering the N-type and P-type silicon to be one kind of mature semiconductor material, we carried out comparative tests under similar conditions *via* N-type and P-type silicon with porosity as sensitive materials. It was found that the current of the N-type silicon with porosity was increased when exposed to the trimethylamine vapor atmosphere, while the current of P-type silicon with porosity decreased under the same conditions. The results for comparison are shown in Fig. 8. This also indirectly supported our deduction.

Further evidence of transition from P-type to N-type due to a doping effect in the gas phase was the result of the electric field-induced surface photovoltage spectrum (FISPS) on poly(aniline) composite films before and after pretreatment. It is well known that the FISPS is considered as one of the more common methods to examine different types of semiconductor. When the semiconductor films were applied with an electric field, their surface photovoltage signal varied. When it was applied with a reversed electric field, the surface photovoltage signal reversed. For P-type and N-type films, the surface photovoltage signal would be reversed. The scheme for



(A) The response of N-type silicon with porosity to trimethylamine.



(B) The response of P-type silicon with porosity to trimethylamine.

Fig. 8 The response of N-type and P-type silicon with porosity to trimethylamine (5.13×10^{-7} mol mL⁻¹). (A) The response of N-type silicon with porosity to trimethylamine. (B) The response of P-type silicon with porosity to trimethylamine.

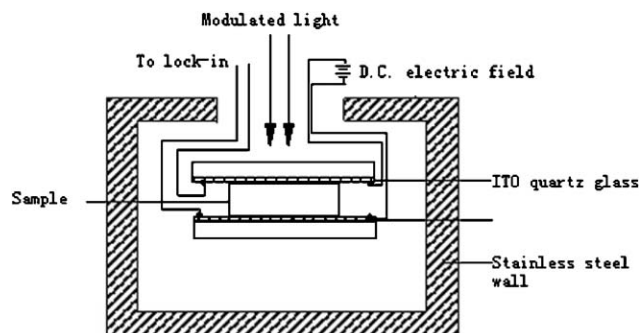


Fig. 9 Scheme for the electric field-induced surface photovoltage spectrum (FISPS) experiment.

the electric field-induced surface photovoltage spectrum (FISPS) experiment is shown in Fig. 9. The results are shown in Fig. 10.

Fig. 10 shows that the results of FISPS on poly(aniline) before and after pretreatment agreed well with the hypothesis mentioned above. This also strongly supported the above discussion.

We had also carried out comparative experiments using nitrogen-based dopants such as ammonia and hydrazine for pre-treatment poly(aniline) film, the effects obtained were very similar. Of course, some details, such as the different oxidation states, need more discussions. Because the toxicity of hydrazine is very high, we usually did not use hydrazine as a pretreatment.

The results of FISPS on poly(aniline) before and after pretreatment with hydrazine are shown in Fig. 11.

Fig. 11 also shows that the results of FISPS on poly(aniline) before and after pretreatment agreed well with the hypothesis mentioned above. Consequently, the sensing mechanism was mainly the result of grain boundary effects.

Conclusion

In summary, we examined an unusual electrical response of a poly(aniline) composite film exposed to a basic atmosphere.

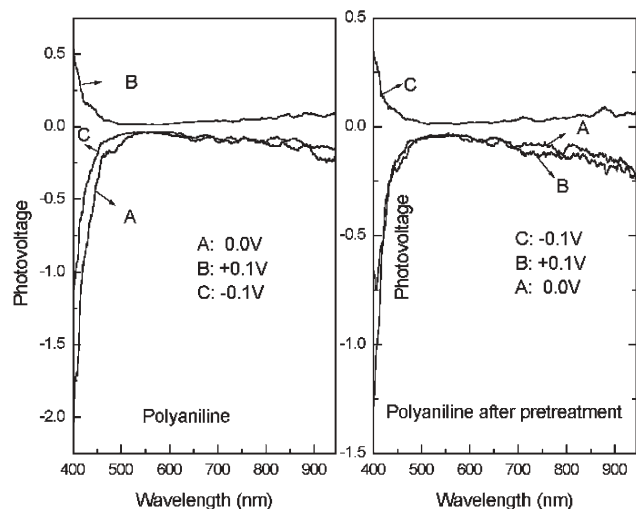


Fig. 10 FISPS of poly(aniline) composite film before and after pretreatment.

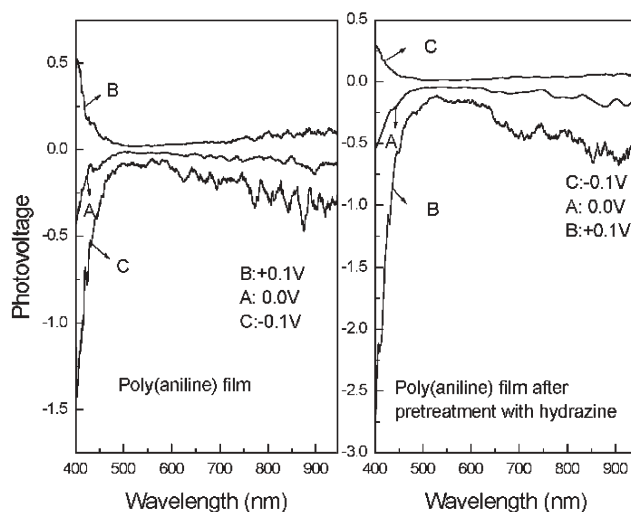


Fig. 11 FISPS of poly(aniline) composite film before and after pretreatment with hydrazine.

The results indicated that this kind of response strongly depended on the polarity of adsorbed vapors, and it was very easy to be recovered with N_2 , avoiding contaminating the surface of the sensing film *via* the reversible reaction of the acid/base in the gas phase. Consequently, it was possible to develop a new kind of sensor exhibiting high sensitivity and rapid response, which would have a good potential for application as an electronic nose or other sensor systems.

Some evidence showed that the transition from P-type to N-type of a poly(aniline) composite film might exist because of doping effects in the gas phase.

Acknowledgements

The work was supported by the key project (No. 50433020) and the main international cooperation project from the NSFC.

References

- 1 S. Chopra and A. Pham, *Appl. Phys. Lett.*, 2002, **80**, 4632.
- 2 J. W. Gardrer, H. W. Shim and E. L. Hines, *Sens. Actuators, B*, 2000, **70**, 19.
- 3 M. A. Aronova, K. S. Chang and I. Takeuchi, *Appl. Phys. Lett.*, 2003, **83**, 1255.
- 4 E. Comini, G. Faglia and G. Sberveglieri, *Appl. Phys. Lett.*, 2002, **81**, 1869.
- 5 A. Khanna, R. Kumar and S. S. Bhatti, *Appl. Phys. Lett.*, 2003, **82**, 4388.
- 6 D. Lee, Y. T. Kim, J. Huh and D. Lee, *Thin Solid Films*, 2002, **416**, 271.
- 7 V. Guidi, M. A. Butturi, M. C. Carotta, B. Cavicchi, M. Ferroni, C. Malagù, G. Martinelli, D. Vincenzi, M. Sacerdoti and M. Zen, *Sens. Actuators, B*, 2002, **84**, 72.
- 8 A. Modi, N. Koratkar, E. Lass, B. Wei and P. M. Ajayan, *Nature*, 2003, **424**, 171.
- 9 J. Kong, N. R. Franklin, C. Zhou, M. G. Chapline, S. Peng, K. Cho and H. Dai, *Science*, 2000, **287**, 622.
- 10 L. Valentini, I. Armentano and J. M. Kenny, *Appl. Phys. Lett.*, 2003, **82**, 961.
- 11 S. Chopra, K. McGuire, N. Gothard, A. M. Rao and A. Pham, *Appl. Phys. Lett.*, 2003, **83**, 2280.
- 12 M. M. Ayad, N. Salahuddin and M. A. Sheneshin, *Synth. Met.*, 2003, **132**, 185.

- 13 A. Göka, B. Sarý b and M. Talu, *Synth. Met.*, 2004, **142**, 41.
- 14 O. A. Raitman, E. Katz, A. F. Bückmann and I. Willner, *J. Am. Chem. Soc.*, 2002, **124**, 6487–6496.
- 15 J. K. Avlyanov, J. Y. Josefowicz and A. G. MaceDiarmid, *Synth. Met.*, 1995, **73**, 205.
- 16 I. Sapurina, A. Riede and J. Stejskal, *Synth. Met.*, 2001, **123**, 503.
- 17 M. Matsuguchi, J. Io, G. Sugiyama and Y. Sakai, *Synth. Met.*, 2002, **128**, 15.
- 18 A. Riul Jr., A. M. G. Soto, S. V. Mello, S. Bone, D. M. Taylor and L. H. C. Mattoso, *Synth. Met.*, 2003, **132**, 109.
- 19 V. V. Chabukswar, S. Pethkar and A. A. Athawale, *Sens. Actuators, B*, 2001, **77**, 657.
- 20 V. R. Albertini, A. Generosi, B. Paci, P. Perfetti, G. Rossi, A. Capobianchi, A. M. Paoletti and R. Caminiti, *Appl. Phys. Lett.*, 2003, **82**, 3868.
- 21 T. Miyata, S. Kawaguchi, M. Ishii and T. Minami, *Thin Solid Films*, 2003, **425**, 255.
- 22 E. van Faassen and H. Kerp, *Sens. Actuators, B*, 2003, **88**, 329.
- 23 N. A. Rakow and K. S. Suslick, *Nature*, 2000, **406**, 710.
- 24 J. Huang and R. B. Kaner, *J. Am. Chem. Soc.*, 2004, **126**, 851.
- 25 X. Zhang, W. J. Goux and S. K. Manohar, *J. Am. Chem. Soc.*, 2004, **126**, 4502.
- 26 J. Huang and R. B. Kaner, *Angew. Chem., Int. Ed.*, 2004, **43**, 5817.
- 27 Y. Ma, J. Zhang, G. Zhang and H. He, *J. Am. Chem. Soc.*, 2004, **126**, 7097.
- 28 L. Zhang, Y. Long, Z. Chen and M. Wan, *Adv. Funct. Mater.*, 2004, **14**, 693.
- 29 A. D. W. Carswell, E. A. O'Rear and B. P. Grady, *J. Am. Chem. Soc.*, 2003, **125**, 14793.
- 30 J. Huang, S. Virji, B. H. Weiller and R. B. Kaner, *J. Am. Chem. Soc.*, 2003, **125**, 314.
- 31 S. Virji, J. Huang, R. B. Kaner and B. H. Weiller, *Nano Lett.*, 2004, **4**, 491.
- 32 J. Huang, S. Virji, B. H. Weiller and R. B. Kaner, *Chem.–Eur. J.*, 2004, **10**, 1314.
- 33 X. Ma, M. Wang, H. Chen, G. Li, J. Sun and R. Bai, *Green Chem.*, 2005, **7**, 507.
- 34 S. Gupta and T. N. Misra, *Sens. Actuators, B*, 1997, **41**, 199.
- 35 J. Hong, J. Cao, J. Sun, H. Li, H. Chen and M. Wang, *Chem. Phys. Lett.*, 2003, **380**, 366.
- 36 Y. Lin, D. Wang, Q. Zhao, M. Yang and Q. Zhang, *J. Phys. Chem. B*, 2004, **108**, 3202.
- 37 S. G. Chen, J. W. Hu, M. Q. Zhang, M. W. Li and M. Z. Rong, *Carbon*, 2004, **42**, 645.
- 38 X. M. Dong, R. W. Fu, M. Q. Zhang, B. Zhang, J. R. Li and M. Z. Rong, *Carbon*, 2003, **41**, 369.
- 39 J. R. Li, J. R. Xu, M. Q. Zhang and M. Z. Rong, *Carbon*, 2003, **41**, 2353.
- 40 X. M. Dong, R. W. Fu, M. Q. Zhang, B. Zhang and M. Z. Rong, *Carbon*, 2004, **42**, 255.
- 41 G. Gordon and A. Leon, *Adv. Mater.*, 2002, **14**, 953.
- 42 V. K. Milind, K. V. Annamraju, R. Marimuthu and S. Tanay, *J. Polym. Sci., Part A: Polym. Chem.*, 2004, **42**, 2043.

Distribution of sulfur-containing aromatics between [hmim][Tf₂N] and supercritical CO₂: a case study for deep desulfurization of oil refinery streams by extraction with ionic liquids

Josef Planeta, Pavel Karásek and Michal Roth*

Received 18th August 2005, Accepted 19th October 2005

First published as an Advance Article on the web 9th November 2005

DOI: 10.1039/b511778j

Stringent regulations of the maximum content of sulfur in transportation fuels have prompted an intense search for new processes of deep desulfurization to complement common catalytic hydrodesulfurization. One of the alternative processes under development involves extraction of sulfur-containing aromatic compounds (SAs) from diesel fuel and gasoline with ionic liquids (ILs). In these applications, recycling of ILs will be highly important, and reextraction of SAs from ILs with supercritical carbon dioxide (scCO₂) appears to be a possible method to regenerate ILs. The design and feasibility assessment of supercritical reextraction requires the partition coefficients of SAs between ILs and scCO₂. We used open tubular capillary-column chromatography to measure the partition coefficients of several SAs between 1-hexyl-3-methylimidazolium bis(trifluoromethylsulfonyl)imide ([hmim][Tf₂N]) and scCO₂, with [hmim][Tf₂N] serving as the stationary liquid and scCO₂ as the mobile phase (carrier fluid). The results confirm that the partition coefficients of SAs can be tuned within wide limits (over a decadic order of magnitude) by relatively modest changes in temperature (40–80 °C) and pressure (8.7–17.6 MPa). However, even the most favourable values of the partition coefficients of SAs between [hmim][Tf₂N] and scCO₂ suggest that feasibility of a large-scale supercritical reextraction process is questionable at best.

Introduction

In order to decrease SO_x emissions, a number of countries have recently adopted stringent regulations of the maximum content of sulfur in transportation fuels. In the USA, the Environmental Protection Agency promulgated regulations stating that, effective September 1, 2006, the upper limit of sulfur content in the diesel fuel for use in highway vehicles will be 15 ppm (1 ppm = 1 mg kg⁻¹).¹ The European Commission proposed to reduce the sulfur content in the diesel fuel for use in highway vehicles to 10 ppm in every member state by January 2009.² Currently, the prevailing technology for removing organic sulfur compounds from oil refinery streams is hydrodesulfurization (HDS), *i.e.*, catalytic hydrogenation conducted at around 350 °C and at hydrogen pressure 3–10 MPa.³ The purpose of HDS is to convert the sulfur compounds to hydrogen sulfide and hydrocarbons. While the process is efficient with aliphatic sulfur structures, some sulfur-containing aromatic compounds (SAs), notably 4,6-dimethyldibenzothiophene (4,6-DMDBT) and other multiple alkylated derivatives of dibenzothiophene (DBT), are highly resistant to hydrotreatment and difficult to remove by HDS. Therefore, although efforts to improve the efficiency of HDS are under way,⁴ it is not clear whether HDS alone can secure conformity of the resultant fuels to the proposed limits of sulfur content. Consequently, the search has recently intensified for

alternative, efficient, less-energy-demanding processes of deep desulfurization of oil-derived fuels.^{5,6}

The search for alternative methods of deep desulfurization currently involves diverse techniques including reactive distillation,⁷ oxidative desulfurization in liquid–liquid systems,^{8–10} complexation in liquid–liquid systems¹¹ or on an adsorbent,^{12,13} biodesulfurization by action of bacteria,^{14,15} and extraction with ionic liquids (ILs).^{16–20} The latter method makes use of the solubility differential between polarizable aromatic compounds and nonpolar aliphatic hydrocarbons in most imidazolium-containing ILs, and a variety of ILs have been tested for the purpose. Although the ILs containing the chloroaluminate anion were shown to be very effective in removing SAs,^{16,18} their sensitivity to moisture makes large-scale application difficult. Currently, therefore, attention is focused on hydrolysis-resistant ILs.¹⁹

In the process extraction of a refinery stream with ILs, regeneration and recycling of the SA-loaded IL will be essential, and several suggestions for separation of SAs from ILs have appeared in the literature. Zhang and Zhang¹⁷ suggested two ways to separate SAs (and the co-extracted hydrocarbons) depending on the properties of the IL employed. A hydrophilic, moisture-insensitive IL can be dissolved in water, with SAs separating or precipitating. As most ILs have no effective vapour pressure, water can be removed by evaporation under a stream of nitrogen at 110 °C. This procedure requires a large amount of heat, and would be difficult to integrate in a continuous process on a multi-ton scale. From a hydrophobic or moisture-sensitive IL, SAs can

Institute of Analytical Chemistry, Academy of Sciences of the Czech Republic, Veveří 97, 61142 Brno, Czech Republic. E-mail: roth@iach.cz

be removed by distillation. The distillation again requires heat, and it is only feasible with low-boiling SAs (*e.g.*, thiophene) that are not likely to occur in hydrotreated diesel fuel. With high-boiling SAs such as DBT or 4,6-DMDBT, distillation is not effective. Esser *et al.*¹⁹ showed that DBT could not be removed from 1-butyl-3-methylimidazolium octylsulfate even after a 3-day stripping with air at 120 °C, and they suggested reextraction with low-boiling hydrocarbons such as pentane or hexane as a promising method to separate SAs from ILs. They also mentioned the possibility of using reextraction with supercritical CO₂ (scCO₂) but expressed doubts about the applicability of the process on a multi-ton scale because of energy expenses.

Supercritical fluid extraction of organic nonelectrolytes from ILs with scCO₂ was originally suggested by Blanchard *et al.*^{21,22} Although the solvating power of scCO₂ is generally lower as compared with organic solvents, extraction with scCO₂ has a specific feature with potential importance to separation of SAs from ILs. On decompression of the fluid solution in scCO₂, the solvating power of the expanding CO₂ decreases rapidly, and the dissolved SAs and co-extracted hydrocarbons nucleate and can be separated from CO₂. The Joule–Thomson cooling of the expanding mixture assists the solidification of the precipitating material. Consequently, SAs and co-extracted hydrocarbons can be expected to come out of the process in a concentrated form rather than being diluted in a liquid solvent. In our judgement, this particular feature makes the reextraction of SAs from ILs with scCO₂ worthy of closer inspection. It is possible to consider a continuous, bicyclic extraction process shown schematically in Fig. 1. In the first (left) counter-current extraction column operated at ambient temperature and pressure, the fuel stream is contacted with IL to extract SAs as discussed by others before.^{16–20} In the second counter-current extraction column operated at a temperature and pressure above the respective critical data of pure CO₂ ($t_c = 30.98$ °C, $P_c = 7.377$ MPa), scCO₂ is used to reextract the dissolved compounds from IL. On expansion of the fluid solution, the dissolved compounds nucleate, aggregate and can be removed for further processing/disposal while CO₂ is recompressed and recycled. On decompression

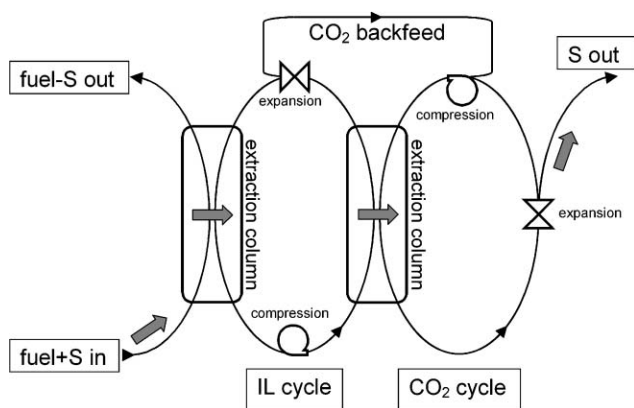


Fig. 1 Continuous bicyclic process of fuel desulfurization with IL and scCO₂. Grey arrows mark the desirable route of sulfur-containing aromatic compounds.

of the regenerated IL, CO₂ dissolved in the IL during the high-pressure reextraction is released and returned to the CO₂ cycle, and the IL returns to the first extraction column.

The most important data needed for feasibility assessment of the reextraction step in Fig. 1 are the partition coefficients of SAs between IL and scCO₂. The purpose of this study is to provide the partition coefficient data measured in a model system.

Determination of the partition coefficients

At present, the available data on partitioning of low-volatility solutes between both phases in IL–scCO₂ systems come mostly from retention measurements by open tubular capillary-column supercritical fluid chromatography (SFC),^{23,24} with the recent exception of the IR-spectroscopic study by Sakellarios and Kazarian.²⁵ SFC yields the limiting partition coefficients at an effective infinite dilution of the solute in both phases, and we also used SFC in the present study, with the IL employed as the stationary liquid and scCO₂ as the mobile phase (carrier fluid).

Selection of IL and SAs for the case study

We used 1-hexyl-3-methylimidazolium bis(trifluoromethylsulfonyl)imide ([hmim][Tf₂N]) as a model IL. From the perspective of deep desulfurization of oil refinery streams, this choice may seem surprising as the ILs containing Tf₂N anion have not been investigated for the purpose,^{16–20} probably because they were not readily accessible from cheap starting materials. Our study, however, was focused on the distribution of SAs between IL and scCO₂ rather than on the distribution of SAs between a fuel stream and IL. To evaluate the process feasibility of the reextraction step in Fig. 1, it is expedient to select an IL–scCO₂ system in which the reextraction of SAs can be expected to be relatively easy, *i.e.*, a system where the distribution of SAs will be shifted to the scCO₂ phase to the maximum possible extent. A simple consideration based on the regular solution theory suggests that an IL with low cohesive energy density (c) should be selected. In a series of 1-butyl-3-methylimidazolium ILs, [bmim][BF₄], [bmim][PF₆], [bmim][Tf₂N] and [bmim][TfO], c values are 998, 912, 650 and 620 J cm⁻³, respectively, at 25 °C.²⁶ Because of the longer alkyl chain on the imidazolium ring, c of [hmim][Tf₂N] can be expected to be even lower than c of [bmim][Tf₂N]. This was recently confirmed experimentally.²⁷ Besides, [hmim][Tf₂N] has been included in a recent study²⁸ of high-pressure phase equilibria in IL–CO₂ systems, and shown to be one of the best solvents for scCO₂ among the ILs studied. This finding also reflects the low c value of [hmim][Tf₂N]. As [hmim][Tf₂N] has a relatively low viscosity,^{29–31} it is also useful for the secondary purpose of the present work, namely, for a feasibility test of SFC measurements in an open tubular column with a low-viscosity IL.

Fig. 2 shows the structures of the SAs included in this study, namely, benzo[*b*]thiophene = thianaphthene (1), benzothiazole (2), DBT (3), 4,6-DMDBT (4), phenoxathiin (5) and thianthrene (6).

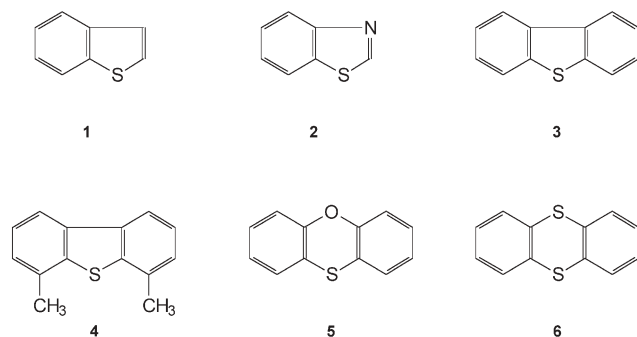


Fig. 2 Sulfur-containing aromatic compounds included in this study.

Results and discussion

Data reduction

The quantities pertaining to the solute, IL and scCO_2 will be denoted by subscripts 1, 2 and 3, respectively. In column chromatography, the retention factor of the solute, k_1 , is given by

$$k_1 = (t_R - t_0)/t_0 \quad (1)$$

where t_0 is the column hold-up time and t_R is the retention time of the solute. The retention factor reflects the distribution of a trace amount of the solute (= SA compound) between the gas and the liquid phases in the column. To consider the efficiency of reextraction of the SA compound from [hmim][Tf₂N] with scCO_2 , it is expedient to define a “practical” partition coefficient of SA by

$$K_N = (m_{1G}/m_{1L})(m_{2L}/m_{3G}) \quad (2)$$

where m_{1G} and m_{1L} are the equilibrium masses of the solute in the gas and the liquid phases, respectively, m_{2L} is the mass of IL in the liquid phase, and m_{3G} is the mass of CO_2 in the gas phase. Under conditions of linear chromatography (= independence of both k_1 and K_N on the solute concentration in either phase), K_N is related to k_1 by

$$K_N = m_{2L}/(k_1 m_{3G}) \quad (3)$$

Being defined on a CO_2 -free-IL basis, the values of K_N are not thermodynamically rigorous partitioning characteristics because alkyimidazolium ILs typically absorb large amounts of scCO_2 .^{21,28,32–35} However, the K_N data are useful for evaluation of attainable extraction factors and for feasibility assessment of the counter-current reextraction of SAs from [hmim][Tf₂N] with scCO_2 . The pertinent value of m_{2L} to be used in eqn (3) can be obtained from the initial amount of [hmim][Tf₂N] in the column and from the time dependence of k_1 for a reference solute (see below). The value of m_{3G} can be calculated from the temperature, pressure and void volume of the column using the equation of state for CO_2 developed by Span and Wagner.³⁶

Partition coefficients of SAs

In contrast with our previous SFC studies on [bmim][PF₆]²³ and [bmim][BF₄],²⁴ we observed a gradual decrease of the

amount of [hmim][Tf₂N] in the column during the retention measurements, with the rate of decrease depending on the column preparation method (see Experimental section). The probable reason for the decrease was a higher solubility of [hmim][Tf₂N] in scCO_2 as compared with both [bmim][PF₆] and [bmim][BF₄]. This view is supported by the cohesive energy density considerations mentioned above. On the basis of the regular solution theory and the literature values of c ,^{26,27} therefore, an estimated order of IL solubility in scCO_2 at a particular temperature and pressure would be [bmim][BF₄] < [bmim][PF₆] << [bmim][Tf₂N] < [hmim][Tf₂N].

At higher densities of scCO_2 , we even observed a mechanical washout of a small amount of CO_2 -expanded [hmim][Tf₂N] from the column. This was indicated by spikes in the flame ionization detector response suggesting that microdroplets of IL were washed out from the column to the detector by the flow of scCO_2 . Such an explanation has been supported by the relatively low viscosity of Tf₂N-containing ILs.^{29–31} Moreover, the viscosity of CO_2 -saturated [hmim][Tf₂N] is likely to be significantly lower than the viscosity of pure [hmim][Tf₂N] at the same temperature. This can be expected because of several previous studies^{37–39} reporting a marked reduction of viscosity of [bmim][PF₆] on CO_2 dissolution at elevated pressures.

To correct for the gradual decrease in the amount of [hmim][Tf₂N] in the column, the retention factors were recalculated to the initial amount of IL in the column using the ratio between the current value and the initial value of the retention factor, k_{naph} , of naphthalene at 60 °C and 12 MPa. The initial value of k_{naph} was measured immediately after the preparation of the column. The current value of k_{naph} relevant to the retention factors of SAs at a particular temperature and pressure was interpolated between the k_{naph} values measured immediately before and after the measurement of the retention factors of SAs at the particular temperature and pressure.

The retention factors corrected as described above displayed the usual appearance of the logarithmic plots of k_1 versus density of CO_2 . A sample plot at 60 °C is shown in Fig. 3. It is interesting to note the reversal in elution order between DBT and 4,6-DMDBT with increasing density of CO_2 . The reversal was observed at 40 °C and 80 °C as well. The corrected values

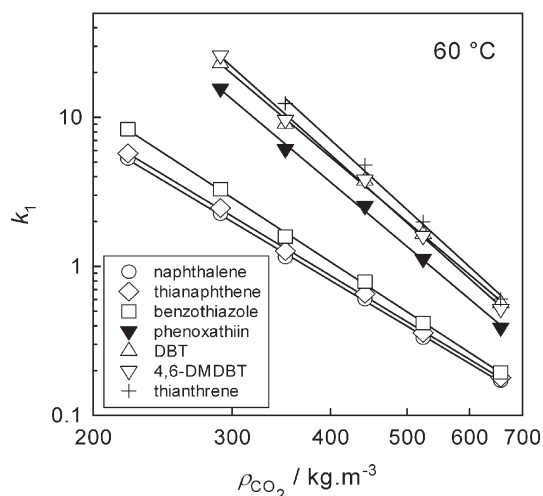


Fig. 3 Retention factors vs. CO_2 density at 60 °C.

Table 1 Mean values of partition coefficients

$t/^\circ\text{C}$	P/MPa	$\rho_{\text{CO}_2}/\text{kg m}^{-3}$	$100 \times K_N$							
			Naphthalene	Thianaphthene	Benzothiazole	Phenoxathiin	DBT	4,6-DMDBT	Thianthrene	
40	8.8	429	1.99	1.94	1.74	0.419				
40	9.2	532	3.91	3.60	3.26	0.947	0.624	0.590		0.763
40	10.5	660	6.89	6.54	5.92	2.15	1.44	1.43		1.46
40	13.2	747	8.99	8.59	8.40	4.02	2.63	2.80		2.50
60	8.7	221	0.876	0.808	0.556					
60	10	290	1.57	1.44	1.07	0.226	0.153	0.136		
60	10.9	350	2.54	2.31	1.85	0.478	0.323	0.304		0.236
60	12.1	442	3.85	3.54	2.94	0.913	0.618	0.607		0.484
60	13.3	524	5.90	5.48	4.70	1.75	1.19	1.23		0.984
60	16.7	657	9.13	8.73	8.06	4.02	2.77	3.02		2.60
80	10	222	1.63	1.49	1.03	0.187				
80	11.8	289	2.45	2.25	1.65	0.380				
80	13.3	352	3.59	3.33	2.55	0.726	0.512	0.471		0.376
80	15.3	440	5.78	5.31	4.35	1.57	1.10	1.09		0.891
80	17.6	526	7.90			2.79	1.93	2.03		1.68

of k_1 were used to calculate the partition coefficients K_N from eqn (3), and the results are listed in Table 1. Within the region of temperature and pressure covered by the measurements, solute partition coefficients vary widely, with the ratio between the maximum and the minimum value in any individual solute being 10 or more. The primary factor determining the accuracy of the data in Table 1 is the uncertainty in the initial amount of [hmim][Tf₂N] in the column. The accuracy of the K_N values in Table 1 can be estimated to be $\pm 13\%$ of the mean value. The relative values for the individual solutes at a particular temperature and pressure are more robust, and their accuracy can be estimated to be within 4% of the mean value.

Implications for counter-current reextraction of SAs from IL with scCO₂

If a SA compound is extracted from IL with scCO₂ in a counter-current extraction process with n stages, the relative decrease in the concentration of SA in the IL can be obtained from⁴⁰

$$w_{1R}/w_{1F} = (E - 1)/(E^{n+1} - 1) \quad (4)$$

where w_{1F} is the mass fraction of SA in the feed IL and w_{1R} is the mass fraction of SA in the raffinate IL (on a CO₂-free-IL basis). It follows from eqn (4) that, for counter-current extraction to be feasible, the extraction factor E has to be greater than 1. The extraction factor is given by

$$E = (F_{3G}/F_{2L})K_N \quad (5)$$

where F_{3G} is the mass flow rate of scCO₂ in the gaseous phase and F_{2L} is the mass flow rate of IL in the liquid phase. It should be noted that the value of F_{3G} does not include the portion of CO₂ that will dissolve in the IL at the operating temperature and pressure of extraction.

The data listed in Table 1 indicate that, for a particular SA at a particular pressure of scCO₂, K_N increases with decreasing temperature. Therefore, in order to base further considerations on the maximum attainable partition coefficients of SAs between [hmim][Tf₂N] and scCO₂ while keeping pressure

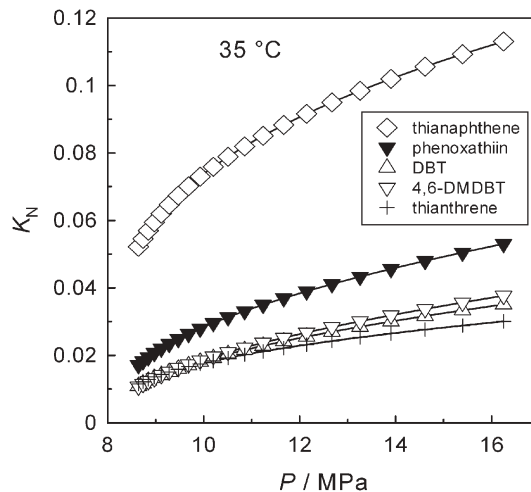
within reasonable limits, we extrapolated the data in Table 1 to 35 °C. We did not attempt an extrapolation to a lower temperature because of proximity to the critical temperature of CO₂. In large-scale applications, the enhanced compressibility in the near-critical region makes near-critical CO₂ difficult to work with. In an analogy with variations of k_1 with temperature (T , in kelvins) and density of CO₂ (ρ_{CO_2}) known from SFC,^{41–43} the extrapolations were accomplished assuming validity of the linear relationships

$$\ln K_N = a \ln \rho_{\text{CO}_2} + b [T = \text{const.}] \quad (6)$$

and

$$\ln K_N = d/T + e [\rho_{\text{CO}_2} = \text{const.}] \quad (7)$$

The coefficients a and b in eqn (6) were obtained by regression of the data in Table 1 at the three temperatures, and used to obtain interpolated values of K_N at a set of fixed densities of CO₂. At the individual densities, the interpolated data were used to fit d and e in eqn (7) and to estimate K_N at 35 °C and at the respective density of CO₂. Fig. 4 shows the

**Fig. 4** Partition coefficients K_N at 35 °C (extrapolated data).

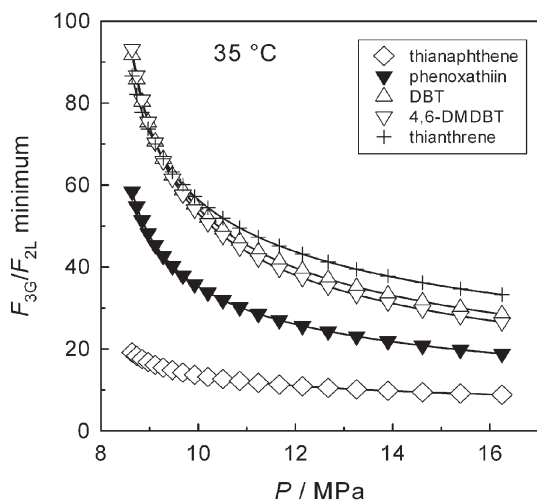


Fig. 5 Minimum values of the scCO₂/IL relative mass flow rate needed to make supercritical reextraction of SAs feasible ($E > 1$).

resultant partition coefficients at 35 °C, with the pressure values obtained from T and ρ_{CO_2} using the equation of state.³⁶

From the K_N values at 35 °C (Fig. 4), the minimum values of F_{3G}/F_{2L} needed to make $E > 1$ in the individual SAs are readily obtained using eqn (5), and the results are plotted in Fig. 5. Even at the highest pressure shown in Fig. 5, the relative flow rates F_{3G}/F_{2L} needed to make $E > 1$ appear too high for a feasible reextraction, with the possible exception of thianaphthene. Moreover, the quantities F_{3G} and F_{2L} are mass flow rates. As the density of CO₂-saturated [hmim][Tf₂N]²⁸ is invariably higher than that of scCO₂ at the respective

temperature and pressure, the corresponding ratio of volumetric flow rates will be even more prohibitive to a feasible reextraction.

Thermal effects associated with reextraction with scCO₂

Because of the very large flow rate of scCO₂ needed to make the reextraction possible, a brief consideration is given here to the thermal effects associated with keeping a steady state (thermal balance) in the CO₂ cycle shown in Fig. 1. The expansion and compression of CO₂ in the reextraction cycle are accompanied by changes in the temperature of the gas. As the thermodynamic path of expansion is not known and depends on the particular process arrangement, the isenthalpic and isentropic paths are considered here as models. The quantity governing the temperature change on isenthalpic expansion of a fluid is the derivative $(\partial T/\partial P)_H$ called the Joule–Thomson coefficient or the isenthalpic throttling coefficient. For CO₂, the Joule–Thomson coefficient at a particular temperature and density can be calculated from the equation of state for CO₂.³⁶ The quantity governing the temperature change on isentropic expansion of a fluid is $(\partial T/\partial P)_S$, the isentropic temperature–pressure coefficient. The two coefficients are related through the thermodynamic identity

$$(\partial T/\partial P)_S = (\partial T/\partial P)_H + 1/(\rho C_P) \quad (8)$$

where ρ is the density and C_P is the isobaric heat capacity of the fluid. In CO₂, these properties can also be obtained from the Span–Wagner equation of state.³⁶ Fig. 6 shows the calculated values of $(\partial T/\partial P)_H$ and $(\partial T/\partial P)_S$ of CO₂ within the relevant region of temperature and pressure. As both

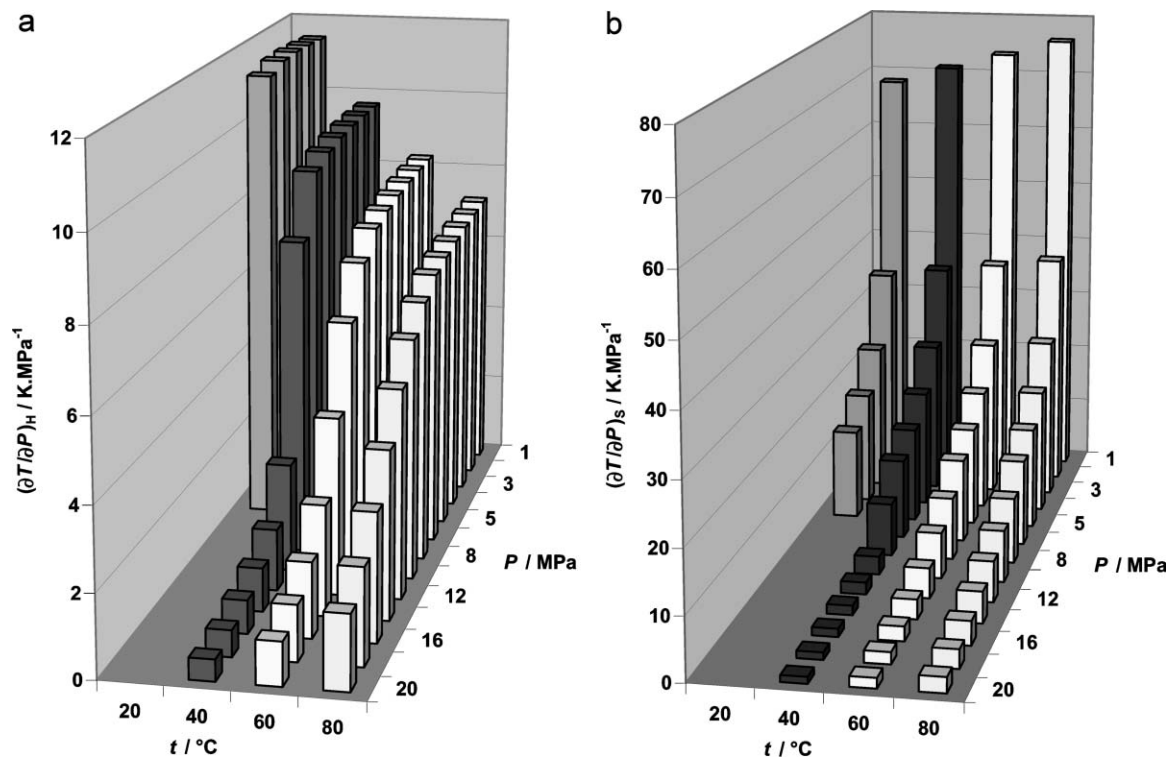


Fig. 6 Joule–Thomson coefficient (a) and isentropic temperature–pressure coefficient (b) of CO₂ as functions of temperature and pressure.

coefficients are positive and relatively large, especially at lower pressures, they indicate a significant cooling of CO₂ on expansion along either isentropic or isenthalpic paths. The decrease in temperature alone would be beneficial for solidification of the material nucleating from the expanding fluid. However, Fig. 5 shows that very large CO₂/IL relative flow rates will be needed in the reextraction step. At the temperature and pressure conditions shown in Fig. 6, C_P values of CO₂ range within 0.9–5.7 kJ kg⁻¹ K⁻¹. Consequently, to keep the reextraction process in thermal balance (steady state), large amounts of heat will have to be transferred between the expanding and the compressed CO₂, and the heat transfer effects can be difficult to accommodate within the multi-ton scale process typical of oil refinery operations.

Conclusion

SFC retention measurements were employed here to obtain the partition coefficients of several SAs between [hmim][Tf₂N] and scCO₂, and the K_N values were used to derive other properties relevant to counter-current reextraction of the SAs from [hmim][Tf₂N] with scCO₂. The results indicate that, for the reextraction of SAs from IL with scCO₂ to be feasible, competitive in a large-scale process and efficient even with heavier SAs not included in this study (e.g., benzonaphthothio-phenes), an IL would have to be found with significantly (~10 times) higher values of K_N as compared with the present data for [hmim][Tf₂N]. Simple considerations based on the regular solution theory suggest that the IL would have to display a very low value of cohesive energy density. Therefore, if found, the IL would most likely be soluble in scCO₂ (and in the fuel stream) to the extent precluding it from being used for deep desulfurization of oil refinery streams. Thermal effects associated with expansion and compression of CO₂ can present another hindrance to a large-scale reextraction of SAs from ILs with scCO₂.

Experimental

Materials

Benzo[*b*]thiophene (thianaphthene) (99%), benzothiazole (96%), DBT (>99%), 4,6-DMDBT (97%), thianthrene (97%), phenoxathiin (97%), naphthalene (>99%), ammonium hydrogen difluoride (>95%), hexane (>99.9%), methanol (>99.9%) and methylene chloride (99.9%) were purchased from Sigma-Aldrich s. r. o. (Prague, Czech Republic) and used as received. Ionic liquid [hmim][Tf₂N] was obtained from Merck s. r. o. (Prague, Czech Republic). To remove moisture from [hmim][Tf₂N] prior to the column preparation, 1 cm³ of [hmim][Tf₂N] was purged with a gentle stream of nitrogen in a gas chromatographic oven at a programmed temperature, with the final period of 12 hours at 120 °C. Carbon dioxide (purity grade 4.5, mole fraction of residual water <5 × 10⁻⁶) was obtained from Messer Griesheim GmbH (Krefeld, Germany). Fused-silica capillary tubing for preparation of the column and of the outlet restrictor was purchased from CACO s. r. o. (Bratislava, Slovak Republic).

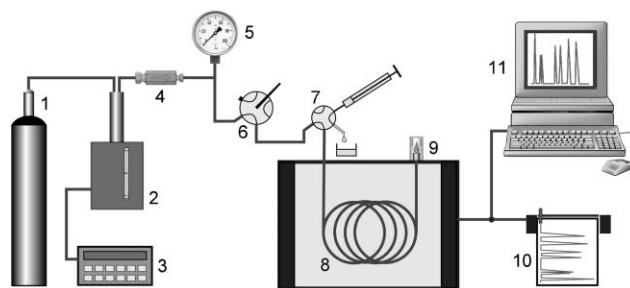


Fig. 7 Overall layout of the chromatographic apparatus. 1 CO₂ supply tank, 2 HPLC pump modified for isobaric operation, 3 pressure controller, 4 stainless-steel filters, 5 pressure gauge, 6 main control valve, 7 injection valve, 8 open tubular capillary column, 9 flow restrictor + detector, 10 line recorder, 11 data acquisition system.

Apparatus

A schematic diagram of the experimental arrangement is shown in Fig. 7. Chromatographic retention measurements were carried out using a modified Varian 3700 gas chromatograph employed before.^{23,24} High-pressure CO₂ was delivered by a HPP 5001 syringe pump (Laboratorní přístroje, Prague, Czech Republic) equipped with an in-house-developed pressure control system. Injections were performed with a helium-actuated high-pressure injection valve (model AC14W, Valco Instrument Co., Schenkon, Switzerland) fitted with a 60 nL sampling rotor. The detector response data were collected and processed with a CSW32 chromatography station (DataApex s. r. o., Prague, Czech Republic).

Column preparation

Compared with our previous SFC experiments employing [bmim][PF₆]²³ and [bmim][BF₄],²⁴ it was considerably more difficult in the present study to prepare a [hmim][Tf₂N] column with at least sufficient stability. The open tubular columns with [bmim][PF₆] and [bmim][BF₄] in our previous studies were sufficiently stable, and we did not observe a measurable loss of either [bmim][PF₆] or [bmim][BF₄] from the column during the set of chromatographic measurements. When applying to [hmim][Tf₂N] the same column preparation method as that used for [bmim][PF₆] and [bmim][BF₄], we observed a rapid washout of [hmim][Tf₂N] from the column by the flowing CO₂. The probable causes of this behaviour are discussed in the Results and Discussion section.

To promote adhesion of [hmim][Tf₂N] to the inner wall of the column, we etched the inner surface of the fused-silica capillary prior to applying the surface modification procedure employed before.^{23,24} It should be noted that etching of the capillary is a rather delicate operation. If etching is too intense, it can produce a brittle capillary that breaks easily, especially if exposed to a high-pressure fluid such as in the present application. Initially, we used etching with either aqueous hydrofluoric acid (40 wt%) or with vapour of aqueous hydrofluoric acid. However, both these methods failed to produce a uniformly etched surface. Satisfactory results were only obtained from etching the inner surface with saturated solution of ammonium hydrogen difluoride in methanol at 25 °C for 48 hours. This technique produced a uniformly

etched surface, and the capillary retained excellent flexibility for easy coiling. After etching the inner wall of the capillary, we applied the surface modification procedure used in our previous studies, and only then was the pre-treated capillary coated with [hmim][Tf₂N]. The coating procedure consisted of filling the capillary with a solution of [hmim][Tf₂N] in methylene chloride, sealing one end of the capillary, and careful evaporation of methylene chloride by applying vacuum to the open end. The resultant column (2745 mm long × 95 μm i.d.) initially contained 4.4×10^{-7} mol [hmim][Tf₂N], with an equivalent film thickness of IL equal to 0.18 μm (at 25 °C). The rate of decrease of the amount of [hmim][Tf₂N] in the column was sufficiently low to provide credible values of retention factors. During the whole sequence of measurements needed to produce the data listed in Table 1, 23% of the initial amount of [hmim][Tf₂N] was removed from the column by scCO₂.

Measurement procedure

At a particular temperature and density, triplicate measurements of the solute retention factors were carried out. The injection solutions were prepared so as to secure sufficient resolution of the solute peaks. Hexane was used as the injection solvent and each solution contained naphthalene as a reference, with the concentrations of individual solutes ranging within 1.5–3 mg cm⁻³. The column hold-up time was marked by injecting a small amount of methane simultaneously with every injection of solutes as described before.^{23,24} The retention factors of SAs were measured along three isotherms (40, 60 and 80 °C) with the mean pressure in the column within 8.7–17.6 MPa. The pressure drop along the column was calculated from the Hagen–Poiseuille equation using the correlation for CO₂ viscosity developed by Vesovic *et al.*,⁴⁴ and it did not exceed 0.015 MPa. To minimize the uncertainty induced by the decreasing amount of [hmim][Tf₂N] in the column, the data were measured in the sequence of increasing density of scCO₂. At a particular stage of measurement, the current amount of [hmim][Tf₂N] in the column was obtained from the current value of the retention factor of naphthalene as described in the Results and Discussion section.

Acknowledgements

We thank Prof. Dr.-Ing. Wolfgang Wagner (Institute of Thermo- and Fluid Dynamics, Faculty of Mechanical Engineering, University of Bochum, Germany) and Prof. Dr.-Ing. Roland Span (Chair of Thermodynamics and Energy Technology, Institute for Energy and Process Technology, University of Paderborn, Germany) for the software package based on the wide-range thermodynamic formulation for CO₂ (ref. 36). We acknowledge the Grant Agency of the Academy of Sciences of the Czech Republic for financial support of this work through Project No. A4031301.

References

- 1 Regulatory Announcement: Heavy-Duty Engine and Vehicle Standards and Highway Diesel Fuel Sulfur Control Requirements, United States Environmental Protection Agency, Air and Radiation, EPA420-F-00-057, Washington (DC), December 2000, available from <http://www.epa.gov/otaq/regs/hd2007/frm/f00057.pdf>.
- 2 EU-Directives: 1998/70/EC, OJ L 350, 28.12.1998, p. 58 (Directive as amended by Commission Directive 2000/71/EC OJ L 287, 14.11.2000, p. 46), and 2003/17/EC OJ L 76, 22.3.2003, p. 10.
- 3 M. J. Girgis and B. C. Gates, *Ind. Eng. Chem. Res.*, 1991, **30**, 2021–2058.
- 4 S. K. Bej, S. K. Maity and U. T. Turaga, *Energy Fuels*, 2004, **18**, 1227–1237.
- 5 I. V. Babich and J. A. Moulijn, *Fuel*, 2003, **82**, 607–631.
- 6 C. Song, *Catal. Today*, 2003, **86**, 211–263.
- 7 T. Viveros-García, J. A. Ochoa-Tapia, R. Lobo-Oehmichen, J. A. de los Reyes-Heredia and E. S. Pérez-Cisneros, *Chem. Eng. J.*, 2005, **106**, 119–131.
- 8 K. Yazu, Y. Yamamoto, T. Furuya, K. Miki and K. Ukegawa, *Energy Fuels*, 2001, **15**, 1535–1536.
- 9 J. M. Campos-Martin, M. C. Capel-Sanchez and J. L. G. Fierro, *Green Chem.*, 2004, **6**, 557–562.
- 10 A. Deshpande, A. Bassi and A. Prakash, *Energy Fuels*, 2005, **19**, 28–34.
- 11 S. G. McKinley and R. J. Angelici, *Energy Fuels*, 2003, **17**, 1480–1486.
- 12 A. J. Hernández-Maldonado and R. T. Yang, *Ind. Eng. Chem. Res.*, 2003, **42**, 3103–3110.
- 13 M. Sévignon, M. Macaud, A. Favre-Régouillon, J. Schulz, M. Rocault, R. Faure, M. Vrinat and M. Lemaire, *Green Chem.*, 2005, **7**, 413–420.
- 14 K. Kirimura, T. Furuya, Y. Nishii, Y. Ishii, K. Kino and S. Usami, *J. Biosci. Bioeng.*, 2001, **91**, 262–266.
- 15 A. B. Martin, A. Alcon, V. E. Santos and F. Garcia-Ochoa, *Energy Fuels*, 2005, **19**, 775–782.
- 16 A. Bösmann, L. Datsevich, A. Jess, A. Lauter, C. Schmitz and P. Wasserscheid, *Chem. Commun.*, 2001, 2494–2495.
- 17 S. Zhang and Z. C. Zhang, *Green Chem.*, 2002, **4**, 376–379.
- 18 S. Zhang, Q. Zhang and Z. C. Zhang, *Ind. Eng. Chem. Res.*, 2004, **43**, 614–622.
- 19 J. Esser, P. Wasserscheid and A. Jess, *Green Chem.*, 2004, **6**, 316–322.
- 20 C. Huang, B. Chen, J. Zhang, Z. Liu and Y. Li, *Energy Fuels*, 2004, **18**, 1862–1864.
- 21 L. A. Blanchard, D. Hancu, E. J. Beckman and J. F. Brennecke, *Nature*, 1999, **399**, 28–29.
- 22 L. A. Blanchard and J. F. Brennecke, *Ind. Eng. Chem. Res.*, 2001, **40**, 287–292.
- 23 J. Planeta and M. Roth, *J. Phys. Chem. B*, 2004, **108**, 11244–11249.
- 24 J. Planeta and M. Roth, *J. Phys. Chem. B*, 2005, **109**, 15165–15171.
- 25 N. I. Sakellarios and S. G. Kazarian, *J. Chem. Thermodyn.*, 2005, **37**, 621–626.
- 26 K. Swiderski, A. McLean, C. M. Gordon and D. H. Vaughan, *Chem. Commun.*, 2004, 2178–2179.
- 27 S. H. Lee and S. B. Lee, *Chem. Commun.*, 2005, 3469–3471.
- 28 S. N. V. K. Aki, B. R. Mellein, E. M. Saurer and J. F. Brennecke, *J. Phys. Chem. B*, 2004, **108**, 20355–20365.
- 29 J. M. Crosthwaite, M. J. Muldoon, J. K. Dixon, J. L. Anderson and J. F. Brennecke, *J. Chem. Thermodyn.*, 2005, **37**, 559–568.
- 30 H. Tokuda, K. Hayamizu, K. Ishii, M. Abu Bin Hasan Susan and M. Watanabe, *J. Phys. Chem. B*, 2004, **108**, 16593–16600.
- 31 H. Tokuda, K. Hayamizu, K. Ishii, M. Abu Bin Hasan Susan and M. Watanabe, *J. Phys. Chem. B*, 2005, **109**, 6103–6110.
- 32 L. A. Blanchard, Z. Gu and J. F. Brennecke, *J. Phys. Chem. B*, 2001, **105**, 2437–2444.
- 33 A. P.-S. Kamps, D. Tuma, J. Xia and G. Maurer, *J. Chem. Eng. Data*, 2003, **48**, 746–749.
- 34 A. Shariati and C. J. Peters, *J. Supercrit. Fluids*, 2004, **29**, 43–48.
- 35 A. Shariati, K. Gutkowski and C. J. Peters, *AIChE J.*, 2005, **51**, 1532–1540.
- 36 R. Span and W. Wagner, *J. Phys. Chem. Ref. Data*, 1996, **25**, 1509–1596.
- 37 S. N. Baker, G. A. Baker, M. A. Kane and F. V. Bright, *J. Phys. Chem. B*, 2001, **105**, 9663–9668.
- 38 J. Lu, C. L. Liotta and C. A. Eckert, *J. Phys. Chem. A*, 2003, **107**, 3995–4000.

- 39 Z. Liu, W. Wu, B. Han, Z. Dong, G. Zhao, J. Wang, T. Jiang and G. Yang, *Chem.—Eur. J.*, 2003, **9**, 3897–3903.
- 40 <http://www.cheresources.com/extraction.shtml>, The Chemical Engineers' Resource Page, Midlothian (VA), USA, 2004.
- 41 U. van Wasen, I. Swaid and G. M. Schneider, *Angew. Chem., Int. Ed. Engl.*, 1980, **19**, 575–587.
- 42 H. H. Lauer, D. McManigill and R. D. Board, *Anal. Chem.*, 1983, **55**, 1370–1375.
- 43 J.-J. Shim and K. P. Johnston, *J. Phys. Chem.*, 1991, **95**, 353–360.
- 44 V. Vesovic, W. A. Wakeham, G. A. Olchoway, J. V. Sengers, J. T. R. Watson and J. Millat, *J. Phys. Chem. Ref. Data*, 1990, **19**, 763–808.

Chemical Technology

A well-received news supplement showcasing the latest developments in applied and technological aspects of the chemical sciences



Free online and in print issues of selected RSC journals!*

- **Application Highlights** – newsworthy articles and significant technological advances
- **Essential Elements** – latest developments from RSC publications
- **Free access** to the original research paper from every online article

*A separately issued print subscription is also available

RSC Publishing

www.rsc.org/chemicaltechnology

03005020

Highly efficient and clean synthesis of 3,4-epoxytetrahydrofuran over a novel titanosilicate catalyst, Ti-MWW

Haihong Wu, Lingling Wang, Haijiao Zhang, Yueming Liu, Peng Wu* and Mingyuan He

Received 15th August 2005, Accepted 13th October 2005

First published as an Advance Article on the web 1st November 2005

DOI: 10.1039/b511594a

A much greener synthesis method is discovered for the synthesis of 3,4-epoxytetrahydrofuran (ETHF), an important synthetic intermediate for stereo-controllable synthesis of complex organic compounds. 3,4-ETHF is synthesized with a conversion >95% and a selectivity >99% through a heterogeneous epoxidation of 2,5-dihydrofuran (DHF) with hydrogen peroxide in the liquid phase over a novel titanosilicate catalyst, Ti-MWW.

Introduction

3,4-Epoxytetrahydrofuran (ETHF) is becoming an increasingly important intermediate in chemical syntheses. The polymerization of 3,4-ETHF gives linear polymers having intrinsic viscosity and good hydrophilicity.¹ It also serves as an important class of substrate for new desymmetrisation methodologies,^{2,3} and also provides a useful building block of the tetrahydrofuran ring in combinatorial chemistry for pharmaceutical applications.^{4,5} For example, it is a key synthesis component for the HIV-protease inhibitor nelfinavir⁶ and the cysteine protease cathepsin K which has been postulated as a target for the treatment of osteoporosis.⁷ Thus, 3,4-ETHF tends to be versatile in the stereo-controllable synthesis of complex organic compounds and is receiving considerable research interest because of the promising applications.

3,4-ETHF is usually prepared by oxidizing 2,5-dihydrofuran (DHF) with peracids such as *m*-chloroperbenzoic acid (CPBA)⁸ and trifluoroperacetic acid,⁹ and also using urea hydrogen peroxide together with phthalic anhydride.⁴ These stoichiometric oxidations suffer major disadvantages such as production of a large quantity of toxic by-products, slow reaction rates, low product selectivity, and difficulty in product separation. The chlorohydrin method, widely used for various epoxides, has also been applied to the synthesis of 3,4-ETHF via ring-closing of *trans*-4-chloro-tetrahydrofuran-3-ol.^{9,10} On the other hand, an improved method has been proposed to obtain the corresponding halohydrin first through the reaction of 2,5-DHF with 1,3-dibromo-5,5-dimethylhydantoin, and then 3,4-ETHF via dehalogenation.¹¹ However, the product yield is still not as high as expected, and more importantly, the procedure is not environmentally benign because poisonous and corrosive halogens are involved in both reactants and by-products.

The discovery of titanosilicate (with TS-1 as a representative), which is capable of catalyzing a variety of reactions under mild conditions using aqueous H₂O₂ as an oxidant and

co-producing essentially water as the only by-product, opens up the possibility of developing environmentally friendly chemical processes.¹² Concerning the epoxidation of alkenes, the medium pore system (10-membered ring, MR) of TS-1 produces steric hindrance particularly for cyclic substrates with relatively bulky molecular dimensions. Furthermore, the fact that TS-1 favors the protic solvent methanol makes the solvolysis of epoxide unavoidable, which results in useless by-products and then lowers the epoxide selectivity significantly.¹³ In fact, catalyst of TS-1 monoliths have been used in the attempted epoxidation of 2,5-DHF in methanol.¹⁴ By prolonging the reaction time and using an excess of H₂O₂, 2,5-DHF is converted almost completely in methanol solvent but the selectivity for 3,4-ETHF, initially not high enough (<80%), drops continuously to *ca.* 70%. Therefore, to synthesize 3,4-ETHF more efficiently and cleanly using an aqueous H₂O₂-involving system, it is crucial to design and prepare a new titanosilicate catalyst superior to TS-1 in both the pore system and the nature of the crystalline framework.

Recently, we developed a novel titanosilicate with the MWW structure, Ti-MWW.¹⁵ Since it contains large pores of 12 MR side pockets and supercages both of which serve as open reaction spaces for cyclic molecules, and its unique hydrophilic/hydrophobic nature preserves its high catalytic performance in aprotic solvents or even water,¹⁶ Ti-MWW is thus considered to be a suitable candidate for the epoxidation of cyclic alkenes of 2,5-DHF. We communicate in this paper an efficient and environmentally friendly way for the selective synthesis of 3,4-ETHF by using the Ti-MWW-H₂O₂ system.

Experimental

Ti-MWW (Si/Ti = 55) was prepared following a post-synthesis method reported previously.¹⁷ For control experiments, TS-1 (Si/Ti = 51) was synthesized by the method widely adopted.¹⁸

The structures of the titanosilicates were checked with X-ray diffraction patterns recorded on a Bruker D8 AVANCE diffractometer (Cu-K_α). The chemical analyses were carried out by inductively coupled plasma (ICP) on a Thermo IRIS Intrepid II XSP atomic emission spectrometer. UV-visible spectra were collected on a Shimadzu UV-2550

Shanghai Key Laboratory of Green Chemistry and Chemical Processes, Department of Chemistry, East China Normal University, North Zhongshan Rd. 3663, Shanghai, 200062, P. R. China.
E-mail: pwwu@chem.ecnu.edu.cn

spectrophotometer using Spectralon[®] as a reference to characterize the coordination states of Ti species.

The oxidation of 2,5-DHF (>98%, TCI, Japan) with H₂O₂ was carried out batchwise in a 25 mL flask connected to a cooling condenser. In a typical run, 5 mmol of 2,5-DHF, 5 mL of solvent and 0.07 g catalyst were charged into the flask. H₂O₂ (30 wt%, 5 mmol) was then added to the mixture to begin the reaction at 333 K under vigorous agitation. After the catalyst solid was removed, the liquid phase was analyzed on a gas chromatograph (Shimadzu GC-14B) equipped with a DB-1 capillary column. The absolute amount was quantified using cyclohexanone as an internal standard. The amount of unconverted H₂O₂ was determined by the standard titration method using a 0.1 M Ce(SO₄)₂ solution. The products were verified using authentic chemicals commercially available or determined on a gas chromatograph-mass spectrometer (Agilent HP6890/5973N).

Results and discussion

Fig. 1 shows the XRD patterns and UV-visible spectra of Ti-MWW and TS-1. Both samples had high crystallinity and contained essentially isolated tetrahedral Ti species in the framework as indicated by the single UV-visible band at 220 nm. Thus, the two samples were qualified as liquid-phase oxidation catalysts with H₂O₂.

The products from the epoxidation of 2,5-DHF greatly depend on the reaction conditions such as the kind of catalyst and solvent employed. After analyzing the products with GC-MS carefully together with using authentic samples, a clear diagram of product distribution was obtained (Fig. 2). The two solvolysis products were determined by synthesizing the corresponding chemicals from 3,4-ETHF in water or MeOH using H-ZSM-5 zeolite as a solid catalyst (333 K, 5 h). The other products particularly those produced from the allylic reactions were deduced based on the fact that the final products of allylic reactions, 5H-furan-2-one and maleic

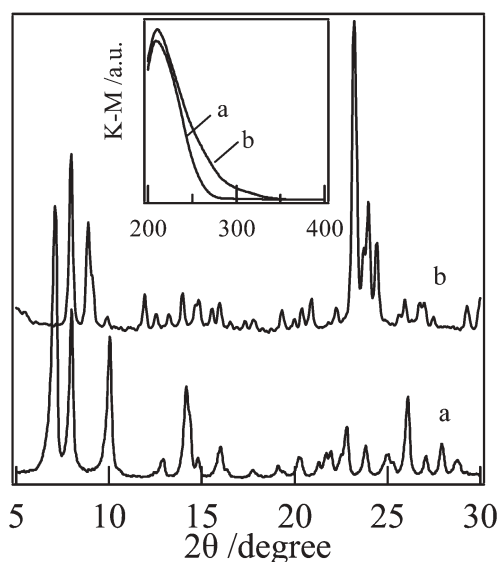


Fig. 1 Representative XRD patterns and UV-visible spectra (inset) of Ti-MWW (a) and TS-1 (b).

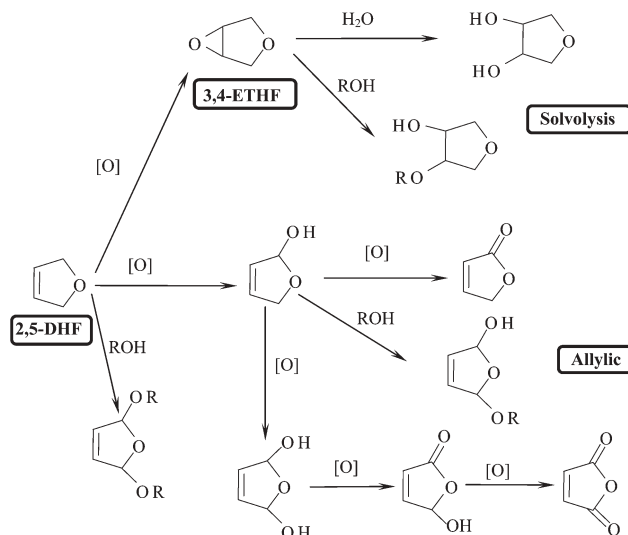


Fig. 2 Reaction paths in the epoxidation of 2,5-DHF (R = Me, Et etc.).

anhydride, were actually obtained as confirmed by authentic samples, and that chemicals with the same mass numbers were detected on GC-MS. The main product was 3,4-ETHF as a result of the oxidation of the C=C bond. The acid sites contained within the titanasilicate catalysed the reaction of 3,4-ETHF with water or alcohols to give solvolysis products. The oxidation occurred also on allylic positions to give the corresponding products which underwent successive oxidation by H₂O₂ and/or solvolysis by protic solvents. A product resulting from the direct addition reaction of alcohol on the allylic positions of 2,5-DHF was also observed. To evaluate the catalytic results simply among the catalysts and solvents, the products have been sorted into three groups, *i.e.* 3,4-ETHF, allylic reaction products and solvolysis products of 3,4-ETHF.

Table 1 compares the results from the catalytic epoxidation of 2,5-DHF in various solvents. The same reaction conditions other than the solvent were adopted for Ti-MWW and TS-1.

Table 1 A comparison of epoxidation of 2,5-DHF in various solvents^a

No.	Cat.	Solvent	Conv. (mol%)	Prod. sel. (mol%)			H ₂ O ₂ (mol%)	
				Oxide	Allyl ^b	Others ^c	Conv.	Eff. ^d
1	Ti-MWW	MeCN	97.2	99.8	0.2	0.0	99.8	98
2	Ti-MWW	Water	95.6	99.7	0.3	0.0	98.1	97
3	Ti-MWW	MeOH	60.1	62.3	18.3	19.4	69.4	80
4	Ti-MWW	EtOH	55.2	83.4	16.6	0.0	64.3	71
5	TS-1	MeCN	62.7	80.8	19.2	0.0	94.0	60
6	TS-1	Water	58.0	77.4	1.0	21.6	94.4	57
7	TS-1	MeOH	71.3	74.0	14.8	11.2	99.3	72
8	<i>m</i> -CPBA ^e	CH ₂ Cl ₂	69.0	97.4	2.6	0.0		

^a Reaction conditions: cat., 0.07 g; 2,5-DHF, 5 mmol; H₂O₂ (30 wt%), 5 mmol; solvent, 5 mL; temp., 333 K; time, 2 h. ^b Allylic reaction products. ^c Solvolysis products of 3,4-ETHF. ^d H₂O₂ efficiency was calculated by relating all the oxidation products to the amount of H₂O₂ converted. The consumption of more H₂O₂ for the products formed involving second and third oxidations has been taken into account. ^e The molar ratio of 2,5-DHF to *m*-CPBA was 1 : 1.9, and the procedures followed the literature.⁸

The characters of the solvents had a great influence not only on the intrinsic activity of Ti species but also on the product distribution. Both Ti-MWW and TS-1 showed a clear but different solvent effect. The most favorable solvents for Ti-MWW were water and aprotic MeCN in which high conversion of 2,5-DHF (>95%), 3,4-ETHF selectivity (>99%) and efficiency for H₂O₂ utilization (>97%) were obtained (Table 1, no. 1 and 2). In protic solvents MeOH and EtOH, the catalytic activity of Ti-MWW retarded greatly (no. 3 and 4). Moreover, the selectivity to 3,4-ETHF was lowered greatly due to simultaneous allylic oxidation and solvolysis of 3,4-ETHF particularly in MeOH. The result that Ti-MWW favored MeCN with weak basicity in the present oxidation of 2,5-DHF is similar to the solvent effect previously observed on the epoxidation of simple alkenes, allyl alcohol and diallyl ether,^{15,16} which has been associated with the unique hydrophilic/hydrophobic nature of the Ti-MWW framework.

In comparison to Ti-MWW, TS-1 showed a lower catalytic activity, product selectivity and H₂O₂ efficiency whichever solvents were used. MeOH was obviously the most effective for TS-1 among the solvents examined from the viewpoint of 2,5-DHF conversion (no. 5–7). Nevertheless, MeOH promoted the solvolysis of 3,4-ETHF to a relatively high level. MeCN suppressed the solvolysis of 3,4-ETHF effectively but allowed the allylic reactions. On the other hand, the water solvent exhibited a reversal reaction phenomenon, making the selectivity to 3,4-ETHF also low. It should be noted that all these results obtained with TS-1 are very similar to those reported on a TS-1 monolith catalyst.¹⁴

The reason for the distinct solvent effects between Ti-MWW and TS-1 would lie in the different hydrophilic/hydrophobic nature of their frameworks. Ti-MWW prepared from a layered precursor contains many defect sites such as silanol groups as a result of incomplete dehydroxylation between the layers,¹⁵ while TS-1 with a highly crystalline structure has fewer silanol groups and is characteristic of higher hydrophobicity. Thus, TS-1 preferentially adsorbs MeOH and H₂O₂ molecules into hydrophobic channels where they interact with Ti active sites to form a five-membered ring Ti hydroperoxo species.¹² These intermediate species then catalyze actively the oxidation of alkenes. In contrast, in the case of Ti-MWW, MeOH molecules and H₂O₂ presumably prefer to adsorb on its surface silanol groups rather than on the Ti sites, which leads to lower activity. Nevertheless, the aprotic solvent MeCN with weak basicity would neutralize partially the surface acidity. This then makes H₂O₂ and H₂O avoid being adsorbed on the surface but diffuse easily into the channels to reach the Ti sites to accelerate the oxidation.

The above results prove that Ti-MWW is obviously superior to TS-1 in catalytic activity, epoxide selectivity, and H₂O₂ efficiency when choosing MeCN or water as a solvent. In the case of TS-1, the medium pores of 10-MR are assumed to produce more steric hindrance to 2,5-DHF with a relative bulky molecular size, which then lowers the catalytic activity. The higher intrinsic activity of Ti active species of Ti-MWW should be due to its more open pore system such as 12-MR side cups and supercages which serve as open reaction spaces and are favorable for inside channel diffusion and access to Ti active sites of bulky molecules of cyclic alkenes.

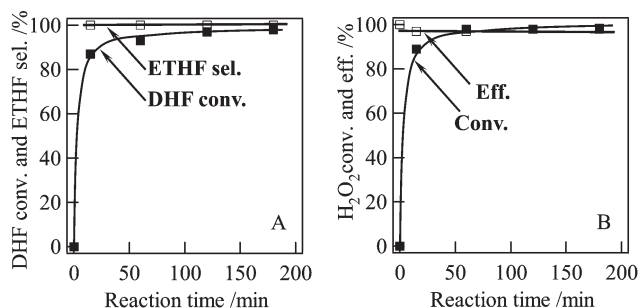


Fig. 3 Changes of 2,5-DHF conversion and 3,4-ETHF selectivity (A), and H₂O₂ conversion and efficiency (B) with the reaction time. Reaction conditions: Ti-MWW, 0.07 g; 2,5-DHF, 5 mmol; H₂O₂ (30 wt%), 5 mmol; water, 5 mL; temp., 333 K.

For control experiment, the homogeneous oxidation of 2,5-DHF with *m*-CPBA has been carried out following the same procedures reported in the literature.⁸ The stoichiometric reaction gave a conversion for 2,5-DHF and a selectivity to 3,4-ETHF of 69.0 and 97.4%, respectively (Table 1, no. 8), which obviously is much lower than those obtained in the Ti-MWW–H₂O₂ system.

Our research interest was attracted by the fact that the water solvent shows comparably high efficiency to MeCN in the epoxidation of 2,5-DHF over Ti-MWW catalyst since this would lead to a more environmentally benign process for the synthesis of 3,4-ETHF. Fig. 3 shows the time course for the 2,5-DHF epoxidation in the presence of water. The 2,5-DHF conversion increased rapidly with the reaction time, reached 85% at 15 min and finally 99% at 180 min. The selectivity for 3,4-ETHF and the H₂O₂ efficiency were always over 99% and 95%, respectively.

The recycling of the Ti-MWW catalyst in the epoxidation of 2,5-DHF has been investigated (Fig. 4). After the used catalyst was gathered and regenerated by washing with acetone and subsequent drying at 393 K, it was reused in the reaction under the same conditions. After being reused three times, Ti-MWW showed a conversion of 2,5-DHF of 87% which was slightly lower than that of the fresh catalyst (97%). However, the

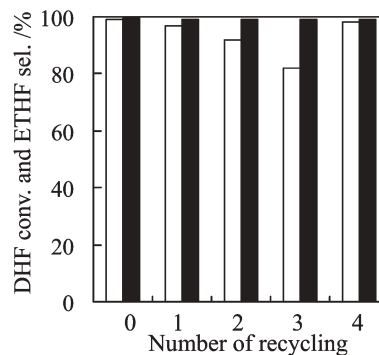


Fig. 4 The 2,5-DHF conversion (blank) and 3,4-ETHF (black) when Ti-MWW was reused in the epoxidation of 2,5-DHF. Reaction conditions: cat., 0.07 g; 2,5-DHF, 5 mmol; H₂O₂ (30 wt%), 5 mmol; MeCN, 5 mL; temp., 333 K; time, 2 h. Regeneration: used catalyst was washed with acetone and dried at 393 K up to the third recycling, and was further calcined at 773 K in air for the fourth recycling.

conversion was totally restored after burning off the organic species of high boiling points deposited inside the zeolite pores by a further calcination at 773 K in air. During the examination of the catalyst recycling, a high selectivity for 3,4-ETHF was always maintained. The used Ti-MWW showed nearly the same XRD and UV-visible spectra as those of the fresh one, indicating an unchanged nature of Ti active species and crystalline structure. These results prove the stability and reusability of Ti-MWW for the present reaction.

Conclusions

Ti-MWW with open reaction spaces and suitable hydrophilic/hydrophobic characters is a superior catalyst for the selective oxidation of 2,5-DHF with H₂O₂ to 3,4-ETHF. Ti-MWW shows extremely high efficiency and reusability in the presence of MeCN or water solvent. Especially, by using water as a solvent, the Ti-MWW–H₂O₂ catalytic system provides an effective, economic and environmentally friendly methodology for the synthesis of 3,4-ETHF. This would solve the problems of corrosion, toxicity and waste formation that the conventional methods are encountering.

Acknowledgements

P.W. thanks the Program for New Century Excellent Talents in University (NCET). Financial support by the National Natural Science Foundation of China (Grants No. 20473027 and 20233030), 973 projects (2003CB615801) and Science and Technology Commission of Shanghai Municipality (05DJ1402, 05JC14069, 03DJ14005) is appreciated.

References

- 1 S. Imura and M. Ohtsuru, *Jpn. Pat.*, 52 147 699, 1977.
- 2 D. M. Hodgson, M. A. H. Stent and F. X. Wilson, *Org. Lett.*, 2001, **3**, 3401.
- 3 D. M. Hodgson, M. A. H. Stent, B. Stefane and F. X. Wilson, *Org. Biomol. Chem.*, 2003, **1**, 1139.
- 4 G. F. Lai, *Synth. Commun.*, 2004, **34**, 1981.
- 5 S. E. Schaus, J. F. Larrow and E. N. Jacobsen, *J. Org. Chem.*, 1997, **62**, 4197; L. E. Martinez, J. L. Leighton, D. H. Carsten and E. N. Jacobsen, *J. Am. Chem. Soc.*, 1995, **117**, 5897.
- 6 S. E. Zook, J. K. Busse and B. C. Borer, *Tetrahedron Lett.*, 2000, **41**, 7017.
- 7 R. W. Marquis, Y. Ru, J. Zeng, R. E. L. Trout, S. M. LoCastro, A. D. Gribble, J. Witherington, A. E. Fenwick, B. Garnier, T. Tomaszek, D. Tew, M. E. Hemling, C. J. Quinn, W. W. Smith, B. G. Zhao, M. S. McQueney, C. A. Janson, K. D'Alessio and D. F. Veber, *J. Med. Chem.*, 2001, **44**, 725.
- 8 W. K. Anderson and R. H. Dewey, *J. Med. Chem.*, 1977, **20**, 306; P. L. Barili, G. Berti and E. Mastroilli, *Tetrahedron*, 1993, **49**, 6263; K. Ogasawara and O. Yamada, *Jpn. Pat.*, 09 110 849, 1997; B. Schmidt and H. Wildemann, *Eur. J. Org. Chem.*, 2000, **18**, 3145.
- 9 E. G. E. Hawkins, *J. Chem. Soc.*, 1959, 248.
- 10 W. Reppe, *Justus Liebigs Ann. Chem.*, 1955, **596**, 99.
- 11 N. W. Boaz, *US Pat.*, 6 162 924, 2000.
- 12 G. Bellussi and M. S. Rigguto, *Stud. Surf. Sci. Catal.*, 2001, **137**, 911.
- 13 A. Corma, P. A. Esteve, A. Martinez and S. Valencia, *J. Catal.*, 1995, **152**, 18.
- 14 W. J. Kim, T. J. Kim, W. S. Ahn, Y. J. Lee and K. B. Yoon, *Catal. Lett.*, 2003, **91**, 123.
- 15 P. Wu, T. Tatsumi, T. Komatsu and T. Yashima, *J. Phys. Chem. B*, 2001, **105**, 2897; P. Wu, T. Tatsumi, T. Komatsu and T. Yashima, *J. Catal.*, 2001, **202**, 245.
- 16 P. Wu and T. Tatsumi, *J. Catal.*, 2003, **214**, 317; P. Wu, Y. Liu, M. He and T. Tatsumi, *J. Catal.*, 2004, **228**, 183.
- 17 P. Wu and T. Tatsumi, *Chem. Commun.*, 2001, 897.
- 18 T. Taramasso, G. Perego and B. Notari, *US Pat.*, 441 050, 1983.

Assessing the factors responsible for ionic liquid toxicity to aquatic organisms *via* quantitative structure–property relationship modeling

David J. Couling,^a Randall J. Bernot,^b Kathryn M. Docherty,^b JaNeille K. Dixon^a and Edward J. Maginn^{*a}

Received 8th August 2005, Accepted 1st November 2005

First published as an Advance Article on the web 30th November 2005

DOI: 10.1039/b511333d

Using previously published toxicity data as well as a small set of heretofore-unpublished results, quantitative structure–property relationship models are developed to assess the factors that govern the toxicity of a range of different ionic liquids to two aquatic organisms (*Vibrio fischeri* and *Daphnia magna*). With at most four molecular descriptors, \log_{10} EC50 and \log_{10} LC50 data are reproduced with an R^2 of 0.78–0.88. Besides the well-established link between toxicity and alkyl chain length on imidazolium, pyridinium and quaternary ammonium-based ionic liquids, the models predict that toxicity increases slightly with the number of nitrogen atoms in an aromatic cation ring. All other things being equal, toxicity is expected to show the trend with cation type of ammonium < pyridinium < imidazolium < triazolium < tetrazolium. In addition, toxicity is expected to decrease with ring methylation as well as with an increase in the number of negatively charged atoms on the cation. The anion plays a secondary role in toxicity for the compounds studied here, although the presence of positively charged atoms on the anion are predicted to slightly increase toxicity.

Introduction

Ionic liquids (ILs), defined as pure ionic compounds with melting points below 100 °C, have drawn a great deal of interest due to their unique properties. Such properties include excellent solvation ability for a wide range of compounds, high thermal stability and immeasurably low vapour pressure. This last property has sparked interest in the potential environmental benefits of these compounds over conventional volatile organic solvents.¹ While ILs cannot volatilise and lead to air pollution, they have at least some miscibility with water.^{2,3} Many ILs are minimally retained by geologic adsorption in non-interlayer clay systems,⁴ suggesting that their release into the environment could lead to their unimpeded transport through subsurface groundwater. Thus, ILs may pose environmental risks to aquatic ecosystems, but the potential impact of ILs on aquatic organisms is largely unknown. Knowledge of IL toxicity to aquatic organisms is necessary before an accurate assessment of their true environmental influence can be made. For this reason, ILs based on the pyridinium, imidazolium and pyrrolidinium cation have been nominated to the United States National Toxicology Program (NTP) for toxicological testing, based upon their widespread interest as possible alternatives to organic solvents.⁵

Several recent toxicity studies have documented IL effects on organisms. Li *et al.*⁶ showed that polymeric materials with pyridinium functionality can exhibit significant toxicity to bacteria. Pernak *et al.* observed that antimicrobial activity increased as the alkyl chain length increased on pyridinium,

imidazolium, and quaternary ammonium salts.^{7–11} This trend was also observed with the marine bacterium *Vibrio fischeri* for alkylimidazolium cations paired with BF_4^- , PF_6^- and Cl^- anions¹² as well as for various alkylimidazolium and alkylpyridinium cations.¹³ A similar trend of increasing toxicity with increasing alkyl chain length was observed for mammalian cell cultures¹² and higher organisms, including the soil nematode *Caenorhabditis elegans*¹⁴ and the freshwater snail *Physa acuta*¹⁵ and was consistent among different cation and anion combinations.¹⁶ This result is perhaps not surprising, given that cetylpyridinium chloride is a well-known anti-microbial agent.¹⁷ Other studies include the effects of ionic liquids on enzyme activity,¹⁸ survivorship and life history of the freshwater crustacean *Daphnia magna*,¹⁹ and behavior of *Physa acuta*.¹⁵

Varying the anion has a minimal effect on the toxicity of pyridinium and imidazolium salts, which suggests that toxicity is largely driven by the cation,^{7,12–14} although recent studies indicate that the anion can play a role in toxicity.¹⁶

Experimental studies have been helpful in establishing general guidelines for the selection of ILs with low potential for toxicity. However, relatively little is still known about the toxicity of these materials as a class, especially when compared to conventional organic solvents. The general lack of knowledge and uncertainty surrounding the environmental impact of ILs is a major impediment to the adoption of these compounds by industry. In addition to generating data for *existing* ILs, there is a pressing need to be able to *understand and predict* the toxicity of compounds that could be made into ILs. Since IL research and development efforts are in their infancy, only a small fraction of the compounds that could be made into ILs have actually been synthesized. By being able to predict the factors that are responsible for increased or decreased toxicity, it should be possible to direct synthesis efforts along paths that

^aDepartment of Chemical and Biomolecular Engineering, University of Notre Dame, Notre Dame, IN, USA. E-mail: ed@nd.edu; Fax: +1 574 631 5687; Tel: +1 574 631 5687

^bDepartment of Biological Sciences, University of Notre Dame, Notre Dame, IN, USA. Tel: +1 574 631 6522

will result in the development of IL classes that are safe both from an air and water pollution standpoint.

In this paper, we report experimental data on the aquatic toxicity of a range of ILs on two aquatic organisms. First, microbial toxicity was estimated using a standard Microtox Acute Toxicity test system to determine the effective concentration at 50% (or EC50) to the marine bacterium *Vibrio fischeri*. Second, toxicity to a freshwater crustacean (*Daphnia magna*) was determined using 48 h acute toxicity bioassays. These data were then used to build a predictive toxicity model based upon quantitative structure–property relationship modeling (QSPR) methods. The model was used to elucidate the chemical and structural factors that govern the toxicity of these compounds to *V. fischeri* and *D. magna*. This information can be used as the basis for “design rules” in synthesizing ILs with minimal toxicity to aquatic organisms.

Background

The Microtox Acute Toxicity test is an ASTM standard test method²⁰ that provides a rapid means of determining the acute toxicity of aqueous compounds by measuring decreases in light output from the luminescent bacterium *Vibrio fischeri* NRRL B-11177. A decrease in luminescence is linked to a decrease in respiration, and serves as an indirect measure of the toxicity of the test compound. The Microtox Acute Toxicity test is used widely for determining the toxicity of single compounds, for monitoring industrial effluents in environmental water quality surveys, and in sediment contamination studies.²¹ An extensive database of individual chemicals tested using the Microtox method is readily available.²¹

Daphnia magna are freshwater crustaceans often used as standard toxicity test organisms because they are easily cultured in the laboratory and are sensitive to a variety of pollutants.²² *Daphnia* are used as model organisms in standard toxicity bioassays used by regulatory agencies (e.g., United States Environmental Protection Agency) to compare the relative toxicities of different compounds. In natural freshwater ecosystems, *Daphnia* are an important link between microbial and higher trophic levels,²³ and have been the focus of hundreds of physiological, evolutionary, and ecological studies.²⁴

Quantitative structure–property relationship (QSPR) modeling is based on the idea that chemical structure completely determines the physical properties of a given compound. Given a reasonable set of experimental data for the property of interest (a “training set”), QSPR relates these properties to the chemical structure of the compounds. QSPR modeling requires that the “structure” of the compounds be quantified through various molecular-based descriptors. Numerous descriptors have been proposed to capture the many different aspects of structure.^{25,26} In past studies, we have successfully applied the QSPR method to predict the melting point of IL compounds²⁷ as well as the infinite dilution activity coefficients of various organic compounds in three different ILs.²⁸ In this work, we show that the QSPR method can be used to effectively correlate and predict the toxicity of ionic liquids.

Experimental

Synthesis of ionic liquids

The materials used in this study, including source, grade, and purification method (if any), are as follows: sodium bromide (Aldrich $\geq 99.0\%$, used as received), 1-chlorobutane (Aldrich 99.5%, redistilled), 1-bromohexane (Aldrich $\geq 98.0\%$, redistilled), sodium dicyanoamide (Aldrich 96%, used as received), pyridine (Aldrich $\geq 99.0\%$, redistilled over KOH), 3,5-dimethylpyridine (Aldrich $\geq 99.0\%$, redistilled over KOH), 4-dimethylaminopyridine (Reilly 99%, used as received), 1-methylimidazole (Aldrich 99%, redistilled over KOH), and lithium bis(trifluoromethanesulfonyl)imide (3 M 97%, used as received).

All the pyridinium and imidazolium ILs except 1-*n*-butyl-3-methylimidazolium bis(trifluoromethanesulfonyl)imide ([bmim][Tf₂N]) were synthesized in our laboratory using standard procedures.^{29–31} A typical synthesis involved mixing equal molar amounts of a nitrogen base and alkyl halide in a flask then stirring the mixture overnight. Acetonitrile was frequently used as a solvent for reactions, but some of the reactions were done neat. The solvent was removed from the IL under vacuum. If the IL was a solid at room temperature, it was recrystallised from acetonitrile/ethylacetate. ILs that are liquids at room temperature were dissolved in methylene chloride and stirred over activated charcoal to remove any coloured impurities. The solutions were then filtered and the solvent removed *in vacuo*. The dicyanoamide ILs were made by reacting freshly prepared silver dicyanoamide and the appropriate pyridinium or imidazolium halide. The silver halide was then filtered and the IL dried on a vacuum line. The identity of all ILs was confirmed by ¹H and ¹³C NMR. Impurity levels of halide ions in the ILs synthesized in-house were measured using an Oakton Ion 510 meter with Cole-Parmer Ion Specific Probes. All values were less than 10 ppm for halogen. NMR results indicate that amine impurities were below the detection limit, but the NMR detection limit is roughly 5 wt%. Based on previous experience, the actual value is likely significantly less than this.

[bmim][Tf₂N] was provided by Covalent Associates, with purity $\geq 99\%$, and was used as received. The quaternary ammonium ILs were purchased from Aldrich with the following purities: tetramethylammonium bromide ($\geq 99\%$), tetraethylammonium bromide ($\geq 99\%$), tetrabutylammonium bromide ($\geq 99\%$), hexyltriethylammonium bromide (99%), and choline chloride ($\geq 99\%$). Choline bis(trifluoromethanesulfonyl)imide was synthesized in-house by a metathesis reaction between choline chloride and lithium bis(trifluoromethanesulfonyl)imide. Purity was determined as described above. Trihexyl(tetradecyl)phosphonium bromide and tributylethylphosphonium diethyl phosphate were obtained from CYTEC and used as received.

Microtox experiments—methodology

Pure ILs were diluted to 10 000 mg L⁻¹ in sterile distilled water. Three replicated EC50 (effective IL concentration at which *V. fischeri* respiration was reduced by 50%) values at 15 min were determined for each IL. EC50 values were

determined using the Microtox M500 Rapid Toxicity Testing System (Azur Environmental, Strategic Diagnostics, Newark, DE) and the ASTM standard toxicity protocol.²⁰

Daphnia magna bioassays—methodology

Daphnia magna IL exposure bioassays were conducted as 48 h static acute tests according to standard procedures.³² Each IL exposure used *D. magna* neonates (age, <24 h) born from parthenogenic females grown in batch cultures. Eight neonates were placed in each of 30 glass beakers (250 mL), with five replicates for each of six treatment concentrations (control plus five IL concentrations). The number of living and dead neonates was noted at 24 and 48 h after the initiation of each trial. Neonates observed as motionless and without a discernable heartbeat were considered to be dead. Each trial was conducted at 20 ± 1 °C in the laboratory with a 16 : 8 h light : dark photoperiod. Ionic liquid test concentrations were based on preliminary range-finding tests of acute toxicity using concentrations from 0.001 to 100 mmol L⁻¹. The median lethal concentration (LC50) and associated 95% confidence intervals were obtained by fitting dose–response curves to a normal model using the maximum likelihood method.³³ The LC50 is the concentration of a chemical that causes death to 50% of the test organisms. Statistical analyses were performed using SAS Version 8.02 statistical software (SAS, Cary, NC, USA).

Modeling details

The compounds used in the initial training set for *Vibrio fischeri* toxicity are listed in Table 1 with a superscript *a*, while those for *Daphnia magna* are listed with a superscript *a* in Table 2. The toxicity of compounds whose log EC50 values

were greater than 2.0 could not be reliably determined; for the model, these compounds were assigned a log EC50 value between 2.16 and 2.19. A second QSPR equation was developed for *V. fischeri* using all the compounds in Table 1. Each compound was registered into the QSPR software (Accelrys, San Diego, CA, USA) by entering the cation and anion as separate entities. The geometries of both the cation and the anion were optimized separately and partial charges were calculated using MOPAC with the AM1 semi-empirical method.^{34–36}

The descriptor pool included electronic, spatial, structural, thermodynamic, and topological descriptors. Descriptors were calculated for both the cation and anion separately. The same symbols were used for each descriptor, but those for the anion were designated with an asterisk. Values of the descriptors varied widely in magnitude. To enable the relative importance of a given descriptor to be easily determined from the magnitude of its coefficient, each descriptor set was scaled to the range [0,1] according to the following equation

$$D' = \frac{D - D_{\min}}{D_{\max} - D_{\min}} \quad (1)$$

where D' is the scaled descriptor, D is the unscaled value of the descriptor, and D_{\max} and D_{\min} are the maximum and minimum value of the particular descriptor for all training set compounds. All descriptors in this work were positive numbers, so the sign and magnitude of the associated coefficient was directly related to the importance of that descriptor on toxicity. That is, negative coefficients indicated that the property characterized by the descriptor lowers either EC50 or LC50, thus increasing toxicity. The larger the magnitude of a coefficient, the more important the associated descriptor was in governing toxicity.

Table 1 Experimental and predicted toxicity results for *V. fischeri*

Compound	CAS #	log EC50 expt.	Ref.	log EC50 pred.
1- <i>n</i> -Butylpyridinium chloride ^a	1124-64-7	0.41 ± 0.08	13	0.13
1- <i>n</i> -Butylpyridinium dicyanoamide ^a	827033-71-6	0.31 ± 0.10	13	0.13
1- <i>n</i> -Butyl-3-methylpyridinium dicyanoamide ^a	712355-12-9	-0.34 ± 0.05	13	-0.43
1- <i>n</i> -Butyl-3,5-dimethylpyridinium dicyanoamide ^a	—	-0.62 ± 0.18	13	-0.12
1- <i>n</i> -Butylpyridinium bromide ^a	874-80-6	0.40 ± 0.01	13	0.13
1- <i>n</i> -Butyl-3-methylpyridinium bromide ^a	26576-85-2	-0.25 ± 0.13	13	-0.43
1- <i>n</i> -Butyl-3,5-dimethylpyridinium bromide ^a	26576-98-7	-0.31 ± 0.09	13	-0.12
1- <i>n</i> -Hexyl-3-methylpyridinium bromide ^a	67021-56-1	-0.94 ± 0.16	13	-0.81
1- <i>n</i> -Octyl-3-methylpyridinium bromide ^a	—	-2.21 ± 0.05	13	-2.56
1- <i>n</i> -Butyl-4-dimethylaminopyridinium bromide	395677-61-9	-0.68 ± 0.05	pw	-0.89
1- <i>n</i> -Butyl-3-methylimidazolium dicyanoamide ^a	44824-52-1	0.67 ± 0.10	13	0.47
1- <i>n</i> -Butyl-3-methylimidazolium chloride ^a	79917-90-1	0.71 ± 0.14	13	0.47
1- <i>n</i> -Butyl-3-methylimidazolium bromide ^a	85100-77-2	1.01 ± 0.05	13	0.47
1- <i>n</i> -Butyl-3-methylimidazolium bis(trifluoromethanesulfonyl)imide ^a	174899-83-3	0.39 ± 0.08	pw	-0.25
1- <i>n</i> -Hexyl-3-methylimidazolium bromide ^a	85100-78-3	-1.58 ± 0.12	13	-0.46
1- <i>n</i> -Octyl-3-methylimidazolium bromide ^a	61545-99-1	-2.37 ± 0.07	13	-1.05
Tetramethylammonium bromide	64-20-0	>2.0	pw	2.37
Tetraethylammonium bromide	71-91-0	>2.0	pw	1.23
Tetrabutylammonium bromide ^a	1643-19-2	0.27 ± 0.07	pw	-0.08
Hexyltriethylammonium bromide	13028-71-2	-0.54 ± 0.16	pw	-0.62
Tetrabutylphosphonium bromide	3115-68-2	-0.29 ± 0.00	pw	0.76
Tributylethylphosphonium diethylphosphate	20445-94-7	0.07 ± 0.09	pw	0.21
Trihexyl(tetradecyl)phosphonium bromide	654057-97-3	0.41 ± 0.02	pw	-0.21
Choline chloride	67-48-1	>2.0	pw	2.29
Choline bis(trifluoromethanesulfonyl)imide	475998-66-4	1.15 ± 0.03	pw	1.57

^a Indicates members of initial training set; pw means present work. Predictions obtained with eqn (14).

Table 2 Experimental and predicted toxicity results for *D. magna*

Compound	CAS #	log LC50 expt.	UCL	LCL	Ref.	log LC50 pred.
1- <i>n</i> -Octyl-3-methylpyridinium bromide ^a	—	-2.60	0.07	0.07	pw	-3.22
1- <i>n</i> -Hexyl-3-methylpyridinium bromide ^a	67021-56-1	-2.41	0.59	0.43	pw	-2.06
1- <i>n</i> -Butyl-3-methylpyridinium bromide ^a	26576-85-2	-1.24	0.11	0.08	pw	-0.92
1- <i>n</i> -Octyl-3-methylimidazolium bromide ^a	61545-99-1	-4.33	0.33	0.25	pw	-3.65
1- <i>n</i> -Hexyl-3-methylimidazolium bromide ^a	85100-78-3	-2.22	0.48	0.43	pw	-2.52
1- <i>n</i> -Butyl-3,5-dimethylpyridinium bromide ^a	26576-98-7	-1.01	0.05	0.06	pw	-1.07
1- <i>n</i> -Hexyl-4-piperidinopyridinium bromide	—	-3.66	0.38	0.23	pw	-5.59
1- <i>n</i> -Hexyl-4-dimethylaminopyridinium bromide	—	-3.28	0.40	0.23	pw	-2.98
1- <i>n</i> -Hexyl-3-methyl-4-dimethylaminopyridinium bromide	—	-2.79	0.17	0.15	pw	-2.65
1- <i>n</i> -Hexylpyridinium bromide	74440-81-6	-1.93	0.25	0.15	pw	-2.13
1- <i>n</i> -Hexyl-2,3-dimethylimidazolium bromide	—	-2.19	0.48	0.27	pw	-2.41
1- <i>n</i> -Butyl-3-methylimidazolium chloride ^a	79917-90-1	-1.07	0.07	0.06	19	-1.34
1- <i>n</i> -Butyl-3-methylimidazolium bromide ^a	85100-77-2	-1.43	0.07	0.07	19	-1.34
1- <i>n</i> -Butyl-3-methylimidazolium tetrafluoroborate ^a	174501-65-6	-1.32	0.16	0.08	19	-1.34
1- <i>n</i> -Butyl-3-methylimidazolium hexafluorophosphate ^a	174501-64-5	-1.15	0.14	0.08	19	-1.34
Tetrabutylammonium bromide ^a	1643-19-2	-1.53	0.16	0.11	pw	-1.33
Tetrabutylphosphonium bromide ^a	3115-68-2	-2.05	0.37	0.36	pw	-2.25

^a Indicates members of training set; pw means present work. Predictions obtained with eqn (15).

Correlations were generated using the scaled descriptors and a genetic function approximation (GFA) statistical method. Since the GFA generates many different correlations, correlations with higher R^2 values were more favored. In addition, care was taken to ensure that the descriptors selected by the GFA were independent by using a correlation matrix and discarding descriptors that were highly correlated with other descriptors (*i.e.* had R^2 values > 0.8). When such close correlations were observed, the descriptor deemed to have the most “physical” significance was retained.

The initial equation for the *V. fischeri* correlations was generated using sixteen training set compounds (Table 1). This equation was then applied to predict the toxicity of nine additional (“predicted”) compounds. A second equation was generated using all the *V. fischeri* data. A similar procedure was followed to generate the toxicity equation for *D. magna*. An initial equation was generated using twelve training set compounds (Table 2). This equation was used to predict the toxicity of five additional compounds. Since the initial equation accurately predicted the toxicity of these five additional compounds, only one equation was generated for *D. magna*.

Descriptor definitions

The following descriptor types and classes were used to generate toxicity correlations.

E-state indices

The electrotopological state (E-state) accounts for both electrostatic and steric influences of individual atoms in a molecule. To determine an E-state index, an intrinsic value I is assigned based on the valences

$$I = \frac{\left(\frac{2}{N}\right)^2 \delta^v + 1}{\delta} \quad (2)$$

in which $\delta^v = \sigma + \pi + n - h$, $\delta = \sigma - h$, and N is the principal quantum number of the atom in question. In these definitions, σ and π are the numbers of σ and π electrons, respectively, on a particular atom. n is defined as the number of electrons in lone

pair orbitals, and h is defined as the number of bonded hydrogen atoms.

To this intrinsic value I a perturbation term ΔI_{ij} is added, in which

$$\Delta I_{ij} = \frac{I_i - I_j}{(d_{ij} + 1)^2} \quad (3)$$

where d_{ij} is defined as the number of atoms separating atoms i and j . The E-state index, therefore, is the sum of the intrinsic value and all its perturbation terms

$$S_i = I_i + \sum_j \Delta I_{ij} \quad (4)$$

E-state sum descriptors were formed by summing E-state indices for the atoms of a given type. For example, $[S_{\text{aasN}}]$ is the sum of the E-state indices for all nitrogen atoms (N) with two aromatic (a) bonds and one single (s) bond.

Surface area descriptors

Solvent-accessible surface area (SASA) was calculated using a sphere of radius 0.15 nm to approximate the contact surface formed when a water molecule interacts with the IL.

[PPSA₂] is the total charge weighted positive surface area, and is computed by multiplying the partial positive solvent-accessible surface area by the total positive charge Q^+ :

$$\text{PPSA}_2 = Q^+ \sum_{a^+} \text{SA}_{a^+} \quad (5)$$

where SA_{a^+} is the surface area contribution of the a^{th} positively charged atom on the molecule. The sum is thus restricted to positively charged atoms a^+ .

Likewise, [PNSA₂] is the partial negative solvent-accessible surface area multiplied by the total negative charge Q^- :

$$\text{PNSA}_2 = Q^- \sum_{a^-} \text{SA}_{a^-} \quad (6)$$

where SA_{a^-} is the surface area contribution of the a^{th} negatively charged atom on the molecule, with the sum restricted to negatively charged atoms a^- .

[DPSA₂] is the total charge weighted partial positive solvent-accessible surface area minus the total charge weighted partial

negative solvent-accessible surface area, given by

$$DPSA_2 = PPSA_2 - PNSA_2 = Q^+ \sum_{a^+} SA_{a^+} - Q^- \sum_{a^-} SA_{a^-} \quad (7)$$

[PPSA₃] is the atomic charge weighted positive surface area, given by

$$PPSA_3 = \sum_{a^+} q_a^+ SA_{a^+} \quad (8)$$

where q_a^+ is the positive partial charge on atom a. Likewise, [PNSA₃] is the atomic charge weighted negative surface area, given by

$$PNSA_3 = \sum_{a^-} q_a^- SA_{a^-} \quad (9)$$

where q_a^- is the negative partial charge on atom a.

[DPSA₃] is simply the difference between the atomic charge weighted positive and negative solvent-accessible surface areas:

$$DPSA_3 = PPSA_3 - PNSA_3 = \sum_{a^+} q_a^+ SA_{a^+} - \sum_{a^-} q_a^- SA_{a^-} \quad (10)$$

[RPCG] is the partial charge of the most positive atom divided by the total positive charge:

$$RPCG = \frac{Q_{\max}^+}{Q^+} \quad (11)$$

[RNCG] is the partial charge of the most negative atom divided by the total negative charge:

$$RNCG = \frac{Q_{\max}^-}{Q^-} \quad (12)$$

Shadow parameter

[Shadow-v] is the ratio of the longest to the shortest side of the rectangle that envelops a molecular structure and at the same time maximizes the aspect ratio, assuming van der Waals radii for atoms and standard bond lengths.

Results and discussion

Toxicity for *Vibrio fischeri*—experimental results

The trend of increasing toxicity with increasing alkyl chain length of a substituted alkyl chain was observed in both pyridinium- and imidazolium-based ILs.¹³ Ionic liquid toxicity to *V. fischeri* has been linked with the cation structure and branching,^{8,12,13} and was reflected in the EC50 values of the starting compounds for IL synthesis (Table 3). Salts used for anion substitution, such as sodium bromide and sodium dicyanoamide, were less toxic to *V. fischeri* than the compounds used for synthesis of the cation. The addition of a butyl chain to the C-1 carbon of the pyridinium or imidazolium cation slightly increased IL toxicity to *V. fischeri* relative to starting compounds such as 3-methyl pyridine and 1-methylimidazole. The addition of a hexyl or octyl chain further increased the toxicity of both pyridinium and imidazolium cation compounds from their respective initial starting compounds.

A similar trend of increased toxicity with increasing alkyl chain length was observed for a series of quaternary ammonium ILs (Table 1). These results reflect previous experimental and theoretical findings that quaternary ammonium chloride antimicrobial effects are related to the

Table 3 *Vibrio fischeri* toxicity values for common organic solvents and some compounds used to synthesize ionic liquids; pw means present work

Compound	CAS #	log ₁₀ EC50	Ref.
Methanol	67-56-1	3.50	21
Acetonitrile	75-05-8	2.77	21
Acetone	67-64-1	2.52	21
Benzene	71-43-2	0.14	21
Phenol	108-95-2	-0.49	21
Methyl tertiary butyl ether	1634-04-4	-0.89	21
Sodium bromide	7647-15-6	2.29	pw
1-Chlorobutane	109-69-3	1.92	pw
1-Bromobutane	111-25-1	0.95	pw
Sodium dicyanoamide	1934-75-4	1.72	pw
Pyridine	110-86-1	0.87	pw
3-Methylpyridine	108-99-6	0.07	13
3,5-Dimethylpyridine	591-22-0	-0.36	pw
4-Dimethylaminopyridine	1122-58-3	-0.41	pw
1-Methylimidazole	616-47-7	1.17	13

lipophilicity of the cation.⁹ The quaternary ammonium compounds examined in this study were also less toxic to *V. fischeri* than the pyridinium and imidazolium compounds tested. Choline chloride and choline dicyanoamide were significantly less toxic than pyridinium and imidazolium ILs with the same anions.

Many of the ILs tested, excluding those substituted with long alkyl chains, were less toxic to *V. fischeri* than some traditional industrial solvents such as methyl tertiary butyl ether, phenol and benzene (Table 3). However, our results also indicate that many of the imidazolium and pyridinium compounds were more toxic to *V. fischeri* than common high-volume solvents such as acetonitrile, acetone and methanol. Some exceptions include low alkyl chain length quaternary ammonium ILs and those ILs containing choline as the cation, which were relatively nontoxic to *V. fischeri*. The data suggest that choline or quaternary ammonium solvents may be more environmentally friendly alternatives than both aromatic ILs and some traditional industrial solvents. We note, however, that single species acute toxicity is not the only measure of the environmental impact of a chemical. Other factors not investigated here, including biodegradation and bioaccumulation, are also important and need to be studied before firm conclusions can be drawn.

Toxicity for *Vibrio fischeri*—QSPR results

The following 4-parameter equation was obtained for EC50 values of *V. fischeri* using the training set data

$$\log_{10} \text{EC50}/\text{mmol L}^{-1} = 6.82837 - 4.80633[S_{\text{aaCH}}] - 3.2043[S_{\text{aaN}}] - 6.55084[DPSA_2] - 1.38266[S_{\text{aaC}}] \quad (13)$$

There are four descriptors in the correlation: [DPSA₂], [S_{aaN}], [S_{aaCH}], and [S_{aaC}]. [S_{aaN}], [S_{aaCH}], and [S_{aaC}] are all sums of E-state indices for atoms of a given type. [S_{aaN}] is the sum of the E-state indices for all nitrogen atoms (N) with two aromatic (a) bonds and one single (s) bond. Similarly, [S_{aaCH}] is the sum of the E-state indices for all carbon atoms with two aromatic bonds and one hydrogen (CH) bond, and [S_{aaC}] is the E-state sum for all carbon atoms with two aromatic bonds and one single bond.

Each descriptor is preceded by a negative coefficient, indicating that each structural aspect encoded in the descriptors leads to higher toxicity at higher incidence. $[DPSA_2]$ is highly correlated with the length of the alkyl chain on the aromatic cations, since the partial positive surface area increases as the length of the alkyl chain increases, while the partial negative surface area remains essentially constant with alkyl chain length. Therefore, this descriptor is consistent with the experimental observation that aromatic cations with longer alkyl chains were more toxic (*i.e.* 1-*n*-hexyl-3-methylimidazolium bromide was more toxic than 1-*n*-butyl-3-methylimidazolium bromide). Since $[S_{\text{aasN}}]$ describes compounds with nitrogen atoms having two aromatic (a) bonds and one single (s) bond, it indicates that toxicity increased as the number of nitrogen atoms of this form increased. Imidazolium cations, with two nitrogen atoms of this form, are predicted by this equation to be more toxic than pyridinium cations, which only have one nitrogen atom of this form. For example, 1-*n*-hexyl-3-methylpyridinium bromide was less toxic than 1-*n*-hexyl-3-methylimidazolium bromide. Following this reasoning, triazolium-based ionic liquids should be more toxic than those with imidazolium cations, although there are no experimental toxicity data that we know of for triazolium-based ionic liquids. In addition, the correlation predicts that quaternary ammonium cations are less toxic than those with cations consisting of nitrogen-bearing rings.

$[S_{\text{aaCH}}]$ and $[S_{\text{aasC}}]$ both describe carbon atoms with two aromatic bonds. Because the coefficient in front of $[S_{\text{aaCH}}]$ is larger in magnitude than that of $[S_{\text{aasC}}]$, carbon atoms with two aromatic bonds and one bonded hydrogen atom are predicted to be more toxic than carbon atoms with two aromatic bonds and a single bond to an alkyl group. This suggests that adding methyl groups to the aromatic rings may help decrease the toxicity. However, one must be careful drawing too many qualitative conclusions with such correlations, since the partial positive surface area would also tend to increase with an additional methyl group. Notably, all descriptors in Equation 25 are cation descriptors. This is in accord with the experimental finding that IL toxicity to *V. fischeri* is mainly cation-dependent.

Eqn (13) fits the training set data very well ($R^2 = 0.887$) but the toxicity of the additional (“predicted”) compounds not used in the correlation is not modeled with similar high accuracy (Fig. 1). These “predicted” compounds were not used in the training set because their experimental values were not known at the start of the modeling work. The inadequacy of eqn (13) for these compounds is not surprising, since the majority of the training set ILs have aromatic cations (imidazolium or pyridinium) while the majority of the new “predicted” compounds have ammonium or phosphonium cations. The correlation only yields accurate toxicity predictions for compounds of the same class as the training set, as indicated by the fact that the “predicted” compound most accurately modeled with eqn (13) was 1-*n*-butyl-4-dimethylaminopyridinium bromide, which contains an aromatic pyridinium cation. Interestingly, however, this particular predicted compound also contains an amino group, unlike any of the training set compounds.

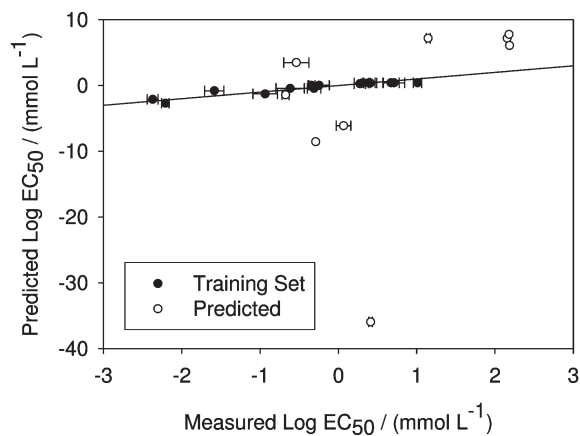


Fig. 1 Predicted versus measured \log_{10} EC₅₀ values of different ionic liquids for *Vibrio fischeri* using eqn (13). While the training set data is reproduced well ($R^2 = 0.887$), the model fails to capture the toxicity of predicted compounds. Note the scale for predicted EC₅₀.

Given the diversity of the compounds available from the experimental data, a new correlation was developed using all of the data

$$\log_{10} \text{EC}_{50}/\text{mmol L}^{-1} = 0.885055 + 1.90609[\text{RNCG}] - 3.81771[\text{Shadow-v}] - 1.13277[\text{RPCG}^*] \quad (14)$$

Eqn (14) fits the training set data very well ($R^2 = 0.782$; Fig. 2) and contains additional information which can help shed light on important features responsible for toxicity. The three new descriptors are [RNCG], [Shadow-v], and [RPCG*]. Although [Shadow-v] is related to the size of the cation, it is more an indicator of whether the molecule is spherical or cylindrical in shape. The negative [Shadow-v] coefficient indicates that IL toxicity to *V. fischeri* is more likely to be higher in long, asymmetric cations.

[RNCG] is a charged partial surface area descriptor that increases with highly concentrated or localized negative charge. Because it is a cation descriptor, and because of its positive coefficient, eqn (14) indicates that IL toxicity should

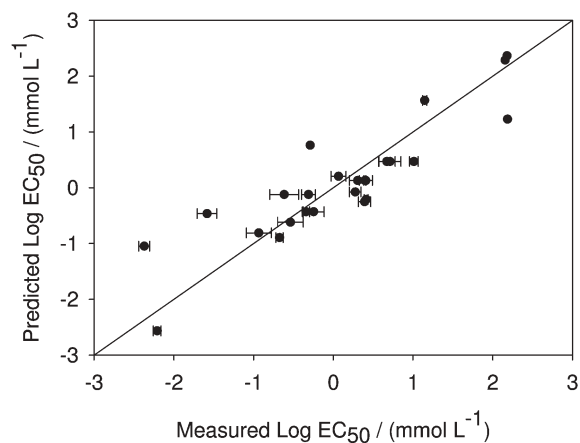


Fig. 2 Predicted versus measured \log_{10} EC₅₀ of different ionic liquids for *Vibrio fischeri* using eqn (14). All the experimental data were used to generate this correlation, and an acceptable result is achieved for a diverse set of compounds ($R^2 = 0.782$).

decrease with an increase in the localization of negatively charged atoms in the cation (such as the oxygen atom in [choline]). [RPCG*], while similar to [RNCG], is different in two key ways. First, it increases with highly localized positive charge, not negative charge. Second and more importantly, it is an anion descriptor. Unlike the [RNCG] descriptor, which indicated that a localization of negative charge in the cations tends to decrease the toxicity of the compound, the negative coefficient for [RPCG*] indicates that localization of positive charge on anions tends to increase the toxicity of the compound. Therefore, monatomic anions such as bromide and chloride are predicted to be less toxic than very large anions containing regions of positive charge, such as bis(trifluoromethanesulfonyl)imide.

Toxicity for *Daphnia magna*—experimental results

Ionic liquid toxicity to *D. magna* ranged from the highly toxic 1-*n*-octyl-3-methyl imidazolium bromide ($LC_{50} = 0.00004 \text{ mmol L}^{-1}$) to the less toxic 1-*n*-butyl-3,5-dimethyl pyridinium bromide ($LC_{50} = 0.097 \text{ mmol L}^{-1}$; Table 2). In general, ionic liquids with longer alkyl chain substituents had toxicities comparable to phenol, while those with shorter substituents (e.g., 1-*n*-butyl-3-methylimidazolium bromide) were more toxic to *D. magna* than benzene and methanol.¹⁹

Toxicity for *Daphnia magna*—QSPR results

The following equation was developed using training set compounds to model ionic liquid toxicity to *Daphnia magna*

$$\log_{10} LC_{50}/\text{mmol L}^{-1} = 1.37806 - 3.62486[DPSA_3] - 1.50205[S_{\text{aaN}}] - 1.54858[S_{\text{aaCH}}] \quad (15)$$

Eqn (15) fits the training data set very well ($R^2 = 0.862$; Fig. 3). Like the training set correlation generated for *V. fischeri*, this expression both verifies previously observed indicators of toxicity and presents previously unknown indicators. The descriptors are similar to those given for *V. fischeri*, which suggests that there may be similar indicators of toxicity found in many different species. Like $[DPSA_2]$ in *V. fischeri*, $[DPSA_3]$ in *D. magna* is highly correlated with the length of the alkyl chain on the aromatic cations. Due to its negative coefficient, increasing $[DPSA_3]$ will increase IL toxicity to *D. magna*. Therefore, the correlation given in eqn (15) verifies the experimental observation that increased alkyl chain length is highly correlated with increased toxicity.

Both E-state sums $[S_{\text{aaCH}}]$ and $[S_{\text{aaN}}]$ are found in the *D. magna* correlation as well. Because of their negative coefficients, the E-state sums indicate the same behaviors as the *V. fischeri* data. The negative $[S_{\text{aaN}}]$ coefficient indicates that imidazolium cations tend to be more toxic than pyridinium cations, which are more toxic than quaternary ammonium cations. The negative $[S_{\text{aaCH}}]$ coefficient indicates that methylating the aromatic carbon atoms may reduce the toxicity of the compounds. Noticeably absent from this correlation is $[S_{\text{aaC}}]$, suggesting that methylating the aromatic carbons may be more effective in reducing IL toxicity to *D. magna* than to *V. fischeri*.

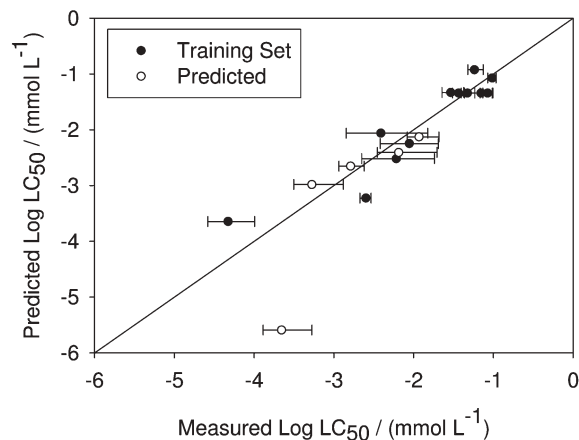


Fig. 3 Predicted versus measured values of $\log_{10} LC_{50}$ of different ionic liquids for *Daphnia magna*. The model is based on eqn (15) using only the training set compounds ($R^2 = 0.862$).

Eqn (15) not only models the training set data well, it also can be used to predict the toxicity of compounds left out of the training set ($R^2 = 0.775$; Fig. 3). This is contrary to the case with *Vibrio fischeri*, where the toxicity predictions for left out data were poor. While this may be due to intrinsic differences between the two species, a more likely explanation is simply that the compounds left out of the *Daphnia magna* training set are more similar to the training set compounds than was the case with *Vibrio fischeri*.

The only compound not used in the training set whose toxicity was not predicted within error is 1-*n*-hexyl-4-piperidinopyridinium bromide ([hmpy][Br]). This is reasonable, since the additional ring on the cation of [hmpy][Br] make it the least similar compound with regard to the training set compounds. Nevertheless, the correlation does correctly place it as the most toxic of all the left out compounds. Moreover, if the [hmpy][Br] data point is ignored, the fit of the remaining data points improves slightly over that of just the training set data, with an $R^2 = 0.875$.

It is also worthwhile to note that the inference that methylating the aromatic carbons could be effective in reducing toxicity to *D. magna* is consistent with the data. 1-*n*-butylpyridinium bromide is more toxic than 1-*n*-butyl-3-methylpyridinium bromide, which is more toxic than 1-*n*-butyl-3,5-dimethylpyridinium bromide. This applies to the left out compounds set as well—1-*n*-hexyl-4-dimethylaminopyridinium bromide is more toxic than 1-*n*-hexyl-3-methyl-4-dimethylaminopyridinium bromide. Given the accuracy with which eqn (15) represented all the data, a separate correlation using all the experimental data was not generated.

Conclusions

Toxicity data for a range of different ILs on *V. fischeri* and *D. magna* have been presented. Using these data, correlative and predictive equations were generated using quantitative structure-property relationship modeling. The models performed well, with R^2 values ranging from 0.78 to 0.88, using at most four molecular descriptors. In accordance with experimental trends, the models predict that increasing alkyl chain

length increases the IL toxicity for both *V. fischeri* and *D. magna*, and that cation properties have a larger effect on toxicity than anion properties. Many ILs are similar to cationic surfactants,³⁷ which are known to induce polar narcosis³⁸ due to their ability to be incorporated into biological membranes.³⁹ Therefore, longer alkyl chains may be incorporated into the polar headgroups of the phospholipid bilayer, which are the major structural components of membranes.⁴⁰ Narcosis then results because membrane-bound proteins are disrupted by the toxicant. Many of the imidazolium and pyridinium compounds were more toxic to *V. fischeri* than common high-volume solvents such as acetonitrile, acetone and methanol. Some exceptions include low alkyl chain length quaternary ammonium ILs and those ILs containing choline as the cation, which were relatively nontoxic to *V. fischeri*. The data suggest that choline or quaternary ammonium solvents may be more environmentally friendly alternatives than both aromatic ILs and some traditional industrial solvents.

Additional insight into other less obvious factors influencing toxicity was also obtained. For both organisms, toxicity was predicted to increase slightly with the number of nitrogen atoms having two aromatic bonds and one single bond. Thus, the model correctly indicates that ammonium cations are less toxic than pyridinium cations, which are slightly less toxic than imidazolium cations. If true, this would mean that triazolium-based ILs would be even more toxic than imidazolium-based compounds, although we are unaware of any data to support this. The model predicts that IL toxicity to *V. fischeri* should decrease as the number of negatively charged atoms on the cation increases. This result is consistent with the experimental finding that the choline cation (with a negatively charged oxygen atom) is relatively non-toxic. Although anions play a secondary role in determining toxicity, the models indicate that the presence of positively charged atoms in the anion leads to higher toxicity than those systems with a single negative anion atom. The correlations also indicate that methylating the aromatic ring of the cation should reduce toxicity, and that this effect will be larger for *D. magna* than *V. fischeri*. The predictions from the present study suggest several additional ionic liquid classes that should be evaluated for aquatic toxicity.

Acknowledgements

Funding for this work was provided by the Indiana 21st Century Research and Technology Fund and the U. S. National Oceanic and Atmospheric Administration. Dr Mark Muldoon is acknowledged for having synthesized many of the compounds examined in this study. David Eike and Profs. Joan Brennecke, Charles Kulpa Jr. and Gary Lambertini are acknowledged for their many helpful discussions and comments. Mike Brueseke assisted with *Daphnia* bioassays.

References

- 1 *Ionic Liquids: Industrial Applications to Green Chemistry*, ed. R. D. Rogers and K. R. Seddon, American Chemical Society Symposium Series 818, 2002.
- 2 J. L. Anthony, E. J. Maginn and J. F. Brennecke, *J. Phys. Chem. B*, 2001, **105**, 10942.
- 3 J. McFarlane, W. B. Ridenour, H. Luo, R. D. Hunt, D. W. DePaoli and R. X. Ren, *Sep. Sci. Technol.*, 2005, **40**, 1245.
- 4 D. J. Gorman-Lewis and J. B. Fein, *Environ. Sci. Technol.*, 2004, **38**, 2491.
- 5 National Toxicology Program (NTP) and National Institute of Environmental Health Sciences (NIEHS), *Review of Toxicological Literature for Ionic Liquids*, prepared by Integrated Laboratory Systems Inc., Research Triangle Park, NC, May 2004.
- 6 G. Li, J. Shen and Y. Zhu, *J. Appl. Polym. Sci.*, 1998, **67**, 1761.
- 7 J. Pernak, J. Kalewska, H. Ksycinska and J. Cybulski, *Eur. J. Med. Chem.*, 2001, **36**, 899.
- 8 J. Pernak, J. Rogoza and I. Mirska, *Eur. J. Med. Chem.*, 2001, **36**, 313.
- 9 J. Pernak and P. Chwala, *Eur. J. Med. Chem.*, 2003, **38**, 1035.
- 10 J. Pernak, I. Goc and I. Mirska, *Green Chem.*, 2004, **6**, 323.
- 11 J. Pernak, K. Sobaszekiewicz and I. Mirska, *Green Chem.*, 2003, **5**, 52.
- 12 J. Ranke, K. Molter, F. Stock, U. Bottin-Weber, J. Poczobutt, J. Hoffman, B. Ondruschka, J. Filser and B. Jastorff, *Ecotoxicol. Environ. Saf.*, 2004, **58**, 396.
- 13 K. M. Docherty and C. F. Kulpa, Jr., *Green Chem.*, 2005, **7**, 185.
- 14 R. P. Swatloski, J. D. Holbrey, S. B. Memon, G. A. Caldwell, K. A. Caldwell and R. D. Rogers, *Chem. Commun.*, 2004, 668.
- 15 R. J. Bernot, E. E. Kennedy and G. A. Lamberti, *Environ. Toxicol. Chem.*, 2005, **24**, 1759.
- 16 B. Jastorff, K. Molter, P. Behrend, U. Bottin-Weber, J. Filser, A. Heimers, B. Ondruschka, J. Ranke, M. Schaefer, H. Schroder, A. Stark, P. Stepnowski, F. Stock, R. Stormann, S. Stolte, U. Welz-Biermann, S. Ziegert and J. Thoming, *Green Chem.*, 2005, **7**, 362.
- 17 M. P. Edlind, W. L. Smith and T. D. Edlind, *Antimicrob. Agents Chemother.*, 2005, **49**, 843.
- 18 F. Stock, J. Hoffman, J. Ranke, R. Störmann, B. Ondruschka and B. Jastorff, *Green Chem.*, 2004, **6**, 286.
- 19 R. J. Bernot, M. A. Brueseke, M. A. Evans-White and G. A. Lamberti, *Environ. Toxicol. Chem.*, 2005, **24**, 87.
- 20 Standard Test Method for Assessing the Microbial Detoxification of Chemically Contaminated Water and Soil Using a Toxicity Test with a Luminescent Marine Bacterium, ASTM Designation: D 5660-96, 1996.
- 21 K. L. E. Kaiser and V. S. Palabrica, *Water Pollut. Res. J. Can.*, 1991, **26**, 361.
- 22 D. M. M. Adema, *Hydrobiologia*, 1978, **69**, 125.
- 23 D. J. McQueen, J. R. Post and E. L. Mills, *Can. J. Fish. Aquat. Sci.*, 1986, **43**, 1571.
- 24 D. G. Smith, Pennak's Freshwater Invertebrates of the United States: Porifera to Crustacea, Wiley, New York, 4th edn, 2001.
- 25 *Topological Indices and Related Descriptors in QSAR and QSPR*, ed. J. Devillers and A. T. Balaban, Gordon and Breach Science Publishers, Amsterdam, 1999.
- 26 R. Todeschini and V. Consonni, Handbook of Molecular Descriptors, in *Methods and Principles in Medicinal Chemistry*, ed. R. Mannhold, H. Kubinyi and H. Timmerman, Wiley-VCH: Weinheim, 2000, vol. 11.
- 27 D. M. Eike, J. F. Brennecke and E. J. Maginn, *Green Chem.*, 2003, **5**, 323.
- 28 D. M. Eike, J. F. Brennecke and E. J. Maginn, *Ind. Eng. Chem. Res.*, 2004, **43**, 1039.
- 29 P. Bonhote, A. P. Dias, N. Papageorgiou, K. Kalyanasundaram and M. Gratzel, *Inorg. Chem.*, 1996, **35**, 1168.
- 30 L. Cammarata, S. G. Kazarian, P. A. Salter and T. Welton, *Phys. Chem. Chem. Phys.*, 2001, **3**, 5192.
- 31 C. P. Fredlake, J. M. Crosthwaite, D. G. Hert, S. N. V. K. Aki and J. F. Brennecke, *J. Chem. Eng. Data*, 2004, **49**, 954.
- 32 United States Environmental Protection Agency, *Methods for measuring the acute toxicity of effluents and receiving waters to freshwater and marine organisms*, EPA 600/4-90/027F, 1993.
- 33 M. C. Newman, *Quantitative Methods in Aquatic Ecotoxicology*, Lewis Publishers, Boca Raton, FL, 1995.
- 34 J. J. P. Stewart, *MOPAC, version 6.0 for UNIX; Quantum Chemistry Exchange Program*, Indiana University, Bloomington, IN, USA.
- 35 J. J. P. Stewart, *J. Comput. Chem.*, 1989, **10**, 209.
- 36 J. J. P. Stewart, *J. Comput. Chem.*, 1989, **10**, 221.

- 37 J. Cross, Introduction to Cationic Surfactants, in *Cationic Surfactants: Analytical and Biological Evaluation*, ed. J. Cross and E. J. Singer, Marcel Dekker, New York, 1994, pp. 3–28.
- 38 D. W. Roberts and J. Costello, *QSAR Comb. Sci.*, 2003, **22**, 220.
- 39 M. J. Rosen, F. Li, S. W. Morrall and D. J. Versteeg, *Environ. Sci. Technol.*, 2001, **35**, 954.
- 40 D. W. Roberts and J. Costello, *QSAR Comb. Sci.*, 2003, **22**, 226.

Find a SOLUTION

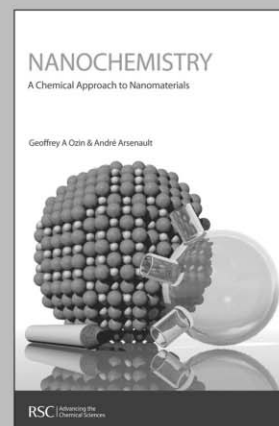
... with books from the RSC

Choose from exciting textbooks, research level books or reference books in a wide range of subject areas, including:

- Biological science
- Food and nutrition
- Materials and nanoscience
- Analytical and environmental sciences
- Organic, inorganic and physical chemistry

Look out for 3 new series coming soon ...

- RSC Nanoscience & Nanotechnology Series
- Issues in Toxicology
- RSC Biomolecular Sciences Series



28040542

RSC Publishing

www.rsc.org/books

Cerium (IV) ammonium nitrate (CAN) as a catalyst in tap water: A simple, proficient and green approach for the synthesis of quinoxalines

Shivaji V. More, M. N. V. Sastry and Ching-Fa Yao*

Received 27th July 2005, Accepted 18th October 2005

First published as an Advance Article on the web 9th November 2005

DOI: 10.1039/b510677j

Various biologically important quinoxaline derivatives have been efficiently synthesized in excellent yields using catalytic amounts of cerium (IV) ammonium nitrate (CAN) in water. This inexpensive, nontoxic, and readily available catalytic system (5 mol%) in water efficiently catalyzes the condensation reaction of various 1,2-diketones and 1,2-diamines. Several aromatic as well as aliphatic 1,2-diketones and aromatic 1,2-diamines such as substituted phenylene diamines, and tetra amines were further subjected to condensation using catalytic amounts of CAN to yield the products in excellent yield. Besides this, ambient conditions, excellent product yields and water as a universal solvent display both economic and environmental advantages.

Introduction

The chemical industry is a major contributor to environmental pollution due to the ubiquitous use of several hazardous organic solvents, flammables, explosives, carcinogens, *etc.* The development of nonhazardous alternatives is not only due to the increased regulatory pressure focusing on organic solvents, but also of great importance with respect to green chemistry. However, performing organic reactions in water is one of the fundamental challenges to organic chemists. Water emerged as a useful alternative solvent for several organic reactions¹ owing to many of its potential advantages such as safety, economy and environmental concern. Reactions in water have been very useful to the synthetic chemist for many years and their utility is reflected by the many studies to discover new processes with which they can be performed catalytically and stereoselectively.

Among lanthanide reagents, cerium (IV) ammonium nitrate (CAN) is the most notable one electron oxidant and has been utilized extensively for a broad variety of oxidative transformations in organic chemistry.² Additionally, many advantages such as excellent solubility in water, inexpensiveness, eco-friendly nature, uncomplicated handling and high reactivity makes CAN a potent catalyst in organic syntheses. Recently, studies have also revealed protocols for mild conditions, fast conversions and convenient work-up procedures using CAN, to make it a powerful tool in chemistry under green and safer approaches. Besides this, CAN is able to catalyze various organic transformations not only based on the Lewis acidic property, but also with electron transfer capability. Quinoxaline derivatives are important components of several pharmacologically active compounds³ and a number of antibiotics such as Echinomycin, Leromycin and Actinomycin, which are known to inhibit the growth of Gram-positive bacteria and are also active against various transplantable tumors.⁴ Besides

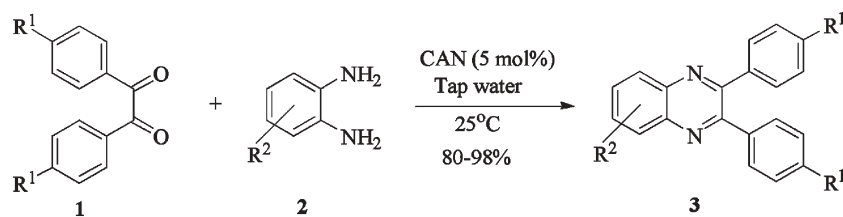
this, they are well known for their application in dyes,⁵ efficient electroluminescent materials,⁶ organic semiconductors,⁷ building blocks for the synthesis of anion receptors,⁸ cavitands,⁹ dehydroannulenes¹⁰ and DNA cleaving agents.¹¹ A number of methods have been developed for the synthesis of substituted quinoxalines and the most common method is the condensation of an aryl 1,2-diamine with 1,2-dicarbonyl compounds in refluxing ethanol or acetic acid.¹² In addition to the above catalytic methods, reports are also known using zeolites,¹³ microwave¹⁴ and solid phase synthesis.¹⁵ Nevertheless, most of these methods suffer from unsatisfactory product yields, critical product isolation procedures, expensive and detrimental metal precursors and harsh reaction conditions, which limit their use. As part of our ongoing program to develop more efficient and environmentally benign methods for organic syntheses using economic and ecofriendly materials as catalysts, we have looked into the synthesis of quinoxalines using catalytic amounts of CAN in tap water.

Results and discussion

In the beginning, efforts were directed towards the catalytic evaluation of CAN towards the synthesis of quinoxalines. Initially, a blank reaction was carried out using benzil and *o*-phenylenediamine in boiling ethanol, resulting in the formation of a condensation product after 45 min (50% Y). With similar substrates, using catalytic amounts of CAN either in CH₃CN or in any protic solvent, afforded the products in quantitative yield during 20 min. Thus, in the absence of CAN, the reaction was slow and also requires harsh refluxing conditions with unsatisfactory yields. While screening different solvents, following the report by Xi *et al.*,^{2b} we attempted the condensation of benzil and *o*-phenylenediamine using CAN in water at room temperature for the synthesis of quinoxalines. To our surprise, the reaction proceeded smoothly during 10 min and resulted in the formation of products in quantitative yield (Scheme 1).

The method of CAN catalyzed synthesis of quinoxalines is very simple, efficient, clean, and without any other side

Department of Chemistry, National Taiwan Normal University, 88, Sec. 4, Tingchow Road, Taipei, Taiwan 116 R. O. C.
E-mail: cheyaocf@scc.ntnu.edu.tw; Fax: 011-886-2-29324249;
Tel: 011-886-2-29309092



Scheme 1

products. It was also observed during the reaction that the substrates were insoluble and do not react in the absence of CAN. By adding catalytic amounts of CAN, the reaction mixture turns into a clear reddish brown colored solution and the product precipitates out as a solid in most cases. In order to evaluate the amount of CAN required for this transformation, a couple of experiments were carried out using varying amounts of CAN. As less as 3 mol% of CAN is sufficient to catalyze the reaction to the same extent, but needs prolonged reaction times (>50 min). Conducting the reaction either by using 5 mol% or 10 mol% of CAN results in almost the same yield, without even affecting the reaction rate. Thus, under an optimized reaction condition, 1,2-diketone (**1** mmol) and 1,2-diamine (1.2 mmol) in water (1.0 mL) were mixed with CAN (0.05 mmol) and stirred at room temperature for 10–50 min. After completion of the reaction, a simple filtration affords the products in good to excellent yield. In order to demonstrate the versatility of the CAN promoted synthesis of quinoxalines, a series of 1,2-diketones and 1,2-diamines were subjected to condensation using catalytic amounts of CAN (Table 1). With symmetrical aromatic diamines the reaction showed good product yields. In the case of diamines, such as naphthalene-2,3-diamine, steric factors played a key role in affecting the rate of reaction and the reaction requires a longer time. With electron donating substituents in the amine part, increased yields of products were obtained and the effect is the reverse with electron withdrawing substituents. On the other hand, electron donating substituents associated with aromatic 1,2-diketone decreased the product yields and with electron withdrawing groups the effect is opposite. However, the variations in the yields were very small and both substituted aromatic diamines such as 4-chloro and 3-methyl gave the condensed products in excellent yields with different substituted 1,2-diketones. To check the versatility of this method, we have also studied compounds other than symmetrical 1,2-diketones, such as furil and 1-phenyl-1,2-propanedione, and obtained the products in excellent yields. In the case of unsymmetrical 1,2-diketones such as 1-phenyl-1,2-propanedione, different aromatic diamines delivered a 1 : 1 ratio of regioisomers in almost quantitative yield (**3r** and **3s**). In another variation, tetra amines such as 3,3',4,4'-tetraamino-1,1'-biphenyl **4** underwent condensation with diketone (benzil) in the presence of catalytic amounts of CAN (5 mol%) affording the product **5** in 80% yield (Scheme 2). This methodology is very useful for the synthesis of a sterically hindered amines such as 2,3,2',3'-tetra phenyl [6,6'] biquinoxaliny **5**. Though the intimate mechanistic details of this condensation reaction are not yet fully understood, a feasible pathway might involve the complexation of cerium with the

diketone by acting as a Lewis acid and also playing a complex role in promoting the dehydration steps.

Conclusion

In summary, we describe a simple, efficient, and ecofriendly method for the synthesis of quinoxalines from various 1,2-diketones and 1,2-diamines using cheap and readily available CAN as a catalyst. The ambient conditions, high reaction rates, excellent product yields and simple filtration, not only make this methodology an alternative platform to the conventional acid/base catalyzed thermal processes, but it also becomes significant under the umbrella of environmentally greener and safer processes. Moreover, water as a universal solvent used with CAN has both economic and environmental advantages, and the ability to further explore this efficient catalytic system to various organic syntheses.

Experimental

General

All chemicals were of research grade and were used as obtained from Aldrich or Acros. The reactions were carried out in a round-bottomed flask of 10 ml capacity at room temperature. Analytical thin layer chromatography was performed with E. Merck silica gel 60F glass plates and flash chromatography by use of E. Merck silica gel 60 (230–400 mesh). All melting points were determined on a MEL-TEMP II melting point apparatus and were uncorrected. ¹H and ¹³C NMR spectra were recorded with a Bruker EX 400 FT NMR. All NMR data were obtained in CDCl₃ solution and chemical shifts (δ) were given in ppm relative to TMS and are compared with the reported literature values. Elemental analyses were analyzed by HERAEUS VarioEL-III (for CHN).

General procedure for the synthesis of quinoxalines

A mixture containing 1,2-diketone **1** (1 mmol), 1,2-diamine **2** (1.2 mmol) and cerium (IV) ammonium nitrate (5 mol%) in water (1 mL) were stirred at room temperature for 10 min (monitored by TLC). After completion of the reaction, the crude product was filtered, washed with water (3 × 10 mL) and dried to obtain quinoxaline **3a** in almost pure form (98% Y). In the case of liquid compounds, the crude reaction mixture was diluted with EtOAc (15 mL) and washed with water (3 × 10 mL). The organic layer was dried over anhydrous MgSO₄, followed by the evaporation of the solvent to obtain the crude product, which was passed through a small plug of silica to obtain pure product.

Table 1 Synthesis of quinoxalines using different aromatic and heterocyclic 1,2-diketones

Entry ^a	Product ^b	Time/min	Yield (%) ^c	
1		3a	10	98
2		3b	30	92
3		3c	10	90
4		3d	25	90
5		3e	10	94
6		3f	20	92
7		3g	30	90
8		3h	40	90
9		3i	10	88
10		3j	20	85
11		3k	30	82
12		3l	10	95
13		3m	15	93

2,3-Diphenyl-quinoxaline (3a)

White solid, (0.276 g, 98%); mp 126–127 °C; ¹H NMR (CDCl₃, 400 MHz): δ 8.20 (m, 2H), 7.76 (m, 2H), 7.56 (m, 4H), 7.35 (m, 6H); ¹³C NMR (CDCl₃, 100 MHz): δ 153.50, 141.29, 139.15, 130.01, 129.93, 129.27, 128.87, 128.33; Anal. Calcd. for C₂₀H₁₄N₂: C, 85.08; H, 5.00; N, 9.92. Found: C, 84.97; H, 4.94; N, 10.00.

2,3-Diphenyl-[g]quinoxaline (3b)

Yellow solid, mp 187–188 °C, ¹H NMR (CDCl₃, 400 MHz): δ 8.68 (s, 2H), 8.07 (m, 2H), 7.51 (m, 6H), 7.32 (m, 6H); ¹³C NMR (CDCl₃, 100 MHz): δ 154.10, 138.98, 137.78, 133.92, 129.73, 128.90, 128.41, 128.14, 127.40, 126.61. Anal. Calcd. for C₂₄H₁₆N₂: C, 86.72; H, 4.85; N, 8.43. Found: C, 86.60; H, 4.74; N, 8.30.

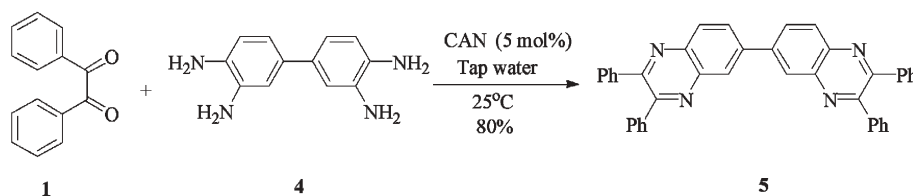
6-Methyl-2,3-di-*p*-tolyl-quinoxaline (3f)

Pale yellow solid, mp 137 °C, ¹H NMR (CDCl₃, 400 MHz): δ 8.06 (d, *J* = 8.5 Hz, 1H), 7.94 (s, 1H), 7.55 (dd, *J* = 8.5, 1.4 Hz, 1H), 7.46 (dd, *J* = 8.1, 1.9 Hz, 4H), 7.14 (d, *J* = 7.9 Hz, 4H), 2.58 (s, 3H), 2.36 (s, 6H); ¹³C NMR (CDCl₃, 100 MHz): δ

Table 1 Synthesis of quinoxalines using different aromatic and heterocyclic 1,2-diketones (*Continued*)

Entry ^a	Product ^b	Time/min	Yield (%) ^c	
14		3n	25	89
15		3o	50	87
16		3p	10	91
17		3q	50	80
18		3r	10	86 ^d
19		3s	30	83 ^d

^a All reactions were performed on a 1 mmol scale using 5 mol% of CAN in 1 mL of water. ^b All products were well characterized using ¹H-NMR, ¹³C-NMR and elemental analysis. ^c Isolated yields of pure products after passing through a small bed of silica. ^d The yield belongs to the overall yield of two regio isomers which are formed in 1 : 1 ratio.



Scheme 2

153.34, 152.61, 141.27, 140.11, 139.69, 138.60, 138.53, 136.64, 132.01, 129.85, 129.82, 128.98, 128.70, 128.03, 21.93, 21.40. Anal. Calcd. for $C_{23}H_{20}N_2$: C, 85.15; H, 6.21; N, 8.63. Found: C, 84.97; H, 5.94; N, 8.52.

2,3-Di-*p*-tolyl-benzo[*g*]quinoxaline (3h)

Yellow solid, mp 198 °C, 1H NMR ($CDCl_3$, 400 MHz): δ 8.71 (s, 2H), 8.09 (m, 2H), 7.53 (m, 6H), 7.18 (d, $J = 8$ Hz, 4H), 2.39 (s, 6H); ^{13}C NMR ($CDCl_3$, 100 MHz): δ 154.25, 139.04, 138.03, 136.55, 133.97, 129.84, 129.01, 128.54, 127.42, 126.57, 21.45. Anal. Calcd. for $C_{26}H_{20}N_2$: C, 86.64; H, 5.59; N, 7.77. Found: C, 85.95; H, 5.44; N, 8.01.

6-Chloro-2,3-bis-(4-methoxyphenyl)-quinoxaline (3k)

Pale yellow solid, mp 151 °C, 1H NMR ($CDCl_3$, 400 MHz): δ 8.10 (d, $J = 2.3$ Hz, 1H), 8.04 (d, $J = 8.9$ Hz, 1H), 7.64 (dd, $J = 8.9, 2.2$ Hz, 1H), 7.5 (m, 4H), 6.88 (d, $J = 8.7$ Hz, 4H), 3.82 (s, 6H); ^{13}C NMR ($CDCl_3$, 100 MHz): δ 160.45, 160.37, 153.82, 153.17, 141.33, 139.55, 135.14, 131.38, 131.33, 131.26, 130.47, 130.23, 127.89, 113.85, 55.34. Anal. Calcd. for $C_{22}H_{17}ClN_2O_2$: C, 70.12; H, 4.55; N, 7.43. Found: C, 69.62; H, 4.14; N, 7.10.

2,3-difuran-2-yl-quinoxaline(3l)

Pale brown solid, mp 131 °C, 1H NMR ($CDCl_3$, 400 MHz): δ 8.07 (m, 2H), 7.66 (m, 2H), 7.56 (d, $J = 1.6$ Hz, 2H), 6.6 (d, $J = 3.4$ Hz, 2H), 6.48 (m, 2H); ^{13}C NMR ($CDCl_3$, 100 MHz): δ 150.81, 144.19, 142.57, 140.57, 130.35, 129.07, 113.01, 111.92. Anal. Calcd. for $C_{16}H_{10}N_2O_2$: C, 73.27; H, 3.84; N, 10.68. Found: C, 72.97; H, 3.24; N, 10.23.

2,3-difuran-2-yl-benzo[*g*]quinoxaline (3o)

Dark brown solid, mp 157 °C, 1H NMR ($CDCl_3$, 400 MHz): δ 8.59 (s, 2H), 7.98 (m, 2H), 7.60 (s, 2H), 7.45 (m, 2H), 6.67 (d, $J = 3.3$ Hz, 2H), 6.52 (m, 2H); ^{13}C NMR ($CDCl_3$, 100 MHz): δ 151.00, 144.43, 143.07, 137.05, 134.20, 128.50, 127.46, 126.90, 113.54, 112.00. Anal. Calcd. for $C_{20}H_{12}N_2O_2$: C, 76.91; H, 3.87; N, 8.97. Found: C, 76.47; H, 3.34; N, 8.25.

2-Methyl-3-phenyl-quinoxaline (3p)

Orange solid, mp 56 °C, 1H NMR ($CDCl_3$, 400 MHz): δ 8.13–8.02 (m, 2H), 7.75–7.60 (m, 4H), 7.57–7.47 (m, 3H), 2.77 (s, 3H); ^{13}C NMR ($CDCl_3$, 100 MHz): δ 154.40, 152.35, 140.75, 141.07, 138.85, 129.59, 129.08, 128.85, 128.79, 128.42, 128.14, 24.31. Anal. Calcd. for $C_{15}H_{12}N_2$: C, 81.79; H, 5.49; N, 12.72. Found: C, 81.37; H, 5.24; N, 12.31.

2-Methyl-3-phenyl-benzo[*g*]quinoxaline (3q)

Yellow solid, mp 134 °C, 1H NMR ($CDCl_3$, 400 MHz): δ 8.66 (d, 2H), 8.10 (m, 2H), 7.71 (m, 2H), 7.56 (m, 5H), 2.80 (s, 3H); ^{13}C NMR ($CDCl_3$, 100 MHz): δ 155.73, 153.47, 139.07, 137.95, 137.92, 133.88, 133.58, 129.21, 128.94, 128.62, 128.53, 128.46, 127.68, 126.70, 126.47, 126.38, 25.01. Anal. Calcd. for $C_{19}H_{14}N_2$: C, 84.42; H, 5.22; N, 10.36. Found: C, 84.07; H, 5.02; N, 10.13.

2,6-Dimethyl-3-phenyl-quinoxaline (3r)

Yellow viscous oil, 1H NMR ($CDCl_3$, 400 MHz): δ 7.96–7.79 (m, 4H), 7.67–7.55 (m, 4H), 7.54–7.43 (m, 8H), 2.70 (s, 6H), 2.52 (d, 6H); ^{13}C NMR ($CDCl_3$, 100 MHz): δ 154.52, 153.84, 152.00, 151.16, 141.12, 140.91, 139.93, 139.42, 139.33, 139.25, 138.86, 131.70, 131.20, 128.68, 128.59, 128.55, 128.42, 128.21, 127.77, 127.51, 126.89, 24.11, 24.03, 21.67, 21.57. Anal. Calcd. for $C_{16}H_{14}N_2$: C, 82.02; H, 6.02; N, 11.96. Found: C, 81.95; H, 5.94; N, 11.85.

6-Chloro-3-methyl-2-phenyl-quinoxaline (3s)

Orange solid, mp 80 °C, 1H NMR ($CDCl_3$, 400 MHz): δ 8.10–7.95 (m, 4H), 7.75–7.58 (m, 6H), 7.57–7.47 (m, 6H), 2.75 (s, 6H); ^{13}C NMR ($CDCl_3$, 100 MHz): δ 155.52, 154.84, 153.47, 152.66, 141.32, 141.11, 139.53, 139.32, 138.48, 138.43, 135.22, 134.69, 130.52, 130.30, 130.07, 129.45, 129.12, 129.05, 128.79, 128.47, 127.96, 127.19, 24.39, 24.35. Anal. Calcd. for $C_{15}H_{11}ClN_2$: C, 70.73; H, 4.35; N, 11.00. Found: C, 69.97; H, 4.04; N, 10.83.

2,3,2',3'-Tetraphenyl-[6,6'] biquinoxalinyne (5)

Pale yellow solid, mp > 295 °C, 1H NMR ($CDCl_3$, 400 MHz): δ 8.6 (s, 2H), 8.33 (d, $J = 8.6$ Hz, 2H), 8.20 (dd, $J = 8.7, 1.7$ Hz, 2H), 7.58 (m, 8H), 7.41 (m, 12H); ^{13}C NMR ($CDCl_3$, 100 MHz): δ 154.19, 153.75, 141.48, 141.28, 140.98, 139.00, 129.98, 129.92, 129.55, 129.01, 128.35, 127.50. Anal. Calcd. for $C_{40}H_{26}N_4$: C, 85.38; H, 4.66; N, 9.96. Found: C, 84.91; H, 4.54; N, 9.50.

Acknowledgements

Financial support of this work by the National Science Council of the Republic of China and National Taiwan Normal University (ORD93-C) is gratefully acknowledged.

References

- (a) C. J. Li and T. H. Chan, *Organic Reactions in Aqueous Medium*, John Wiley & Sons, New York, 1997; (b) P. T. Anastas and

- J. C. Warner, *Green Chemistry: Theory and Practice*, Oxford University Press, Oxford, 1998; (c) U. M. Lindstrom, *Chem. Rev.*, 2002, **102**, 2751; (d) C. J. Li, *Chem. Rev.*, 2005, **105**, 3095; (e) A. Lubineau and J. Auge, in *Topics in Current Chemistry*, Springer, Berlin, Heidelberg, 1999, vol. 206, p. 1.
- 2 (a) V. Nair, T. D. Suja and M. Kishor, *Tetrahedron Lett.*, 2005, **46**, 3217; (b) C. Xi, Y. Jing and X. Yang, *Tetrahedron Lett.*, 2005, **46**, 3909; (c) V. Nair, L. balagopal, R. Rajan and J. Mathew, *Acc. Chem. Res.*, 2004, **37**, 21; (d) V. Nair, J. Mathew and Prabhakaran, *J. Chem. Soc. Rev.*, 1997, 127; (e) J. R. Hwu and K. Y. King, *Curr. Sci.*, 2001, **8**, 1043; (f) T. L. Ho, *Synthesis*, 1973, 354; (g) T. L. Ho, *Organic Synthesis by Oxidation with Metal Compounds*, Plenum, New York, 1986; (h) T. Imamoto, *Lanthanide Reagents in Organic synthesis*, Academic, London, 1994, p. 119.
- 3 (a) M. M. Ali, M. M. F. Ismail, M. S. A. El-Gabby, M. A. Zahran and T. A. Ammar, *Molecules*, 2000, **5**, 864; (b) R. Sarges, H. R. Howard, R. C. Browne, L. A. Label and P. A. Seymour, *J. Med. Chem.*, 1990, **33**, 2240; (c) G. Sakata, K. Makino and Y. Kurasawa, *Heterocycles*, 1998, **27**, 2481; (d) G. Arthur, K. B. Elor, G. S. Robert, Z. Z. Guo, J. P. Richard, D. Stanley, R. K. John and T. Sean, *J. Med. Chem.*, 2005, **48**, 744; (e) E. S. Laine, J. S. William and C. R. Robert, *J. Med. Chem.*, 2002, **45**, 5604; (f) J. Andres, Z. Belen, A. Ibnacio and M. Antonio, *J. Med. Chem.*, 2005, **48**, 2019.
- 4 (a) A. Dell, D. H. William, H. R. Morris, G. A. Smith, J. Feeney and G. C. K. Roberts, *J. Am. Chem. Soc.*, 1975, **97**, 2497; (b) C. Bailly, S. Echeperre, F. Gago and M. Waring, *Anti-Cancer Drug Des.*, 1999, **15**, 291; (c) S. Sato, O. Shiratori and K. Katagiri, *J. Antibiot.*, 1967, **20**, 270.
- 5 E. D. Brock, D. M. Lewis, T. I. Yousaf and H. H. Harper, (*The Procter and Gamble Company, USA*) WO 9951688, 1999.
- 6 K. R. Justin Thomas, V. Marappan, T. L. Jiann, C. Chang-Hao and T. Yu-ai, *Chem. Mater.*, 2005, **17**, 1860.
- 7 (a) S. Dailey, J. W. Feast, R. J. Peace, R. C. Saga, S. Till and E. L. Wood, *J. Mater. Chem.*, 2001, **11**, 2238; (b) D. O'Brien, M. S. Weaver, D. G. Lidzey and D. D. C. Bradley, *Appl. Phys. Lett.*, 1996, **69**, 881.
- 8 L. S. Jonathan, M. Hiromitsu, M. Toshihisa, M. L. Vincent and F. Hiroyuki, *Chem. Commun.*, 2002, 862.
- 9 (a) L. S. Jonathan, M. Hiromitsu, M. Toshihisa, M. L. Vincent and F. Hiroyuki, *J. Am. Chem. Soc.*, 2002, **124**, 13474; (b) P. C. Peter, Z. Gang, A. M. Grace, H. Carlos and M. G. T. Linda, *Org. Lett.*, 2004, **6**, 333.
- 10 O. Sascha and F. Rudiger, *Synlett*, 2004, 1509.
- 11 (a) T. Kazunobu, T. Ryusuke, O. Tomohiro and M. Shuichi, *Chem. Commun.*, 2002, 212; (b) L. S. Hegedus, M. G. Marc, J. W. Jory and P. B. Joseph, *J. Org. Chem.*, 2003, **68**, 4179.
- 12 (a) *VOGEL's Textbook of Practical Organic Chemistry*, 5th edn, 1989, p. 1190; (b) D. J. Brown, Quinoxalines: supplements II, in *The Chemistry of Heterocyclic Compounds*, ed. E. C. Taylor and P. Wipf, John Wiley and Sons, New Jersey, 2004.
- 13 (a) A. Sylvain and D. Elisabet, *Tetrahedron Lett.*, 2002, **43**, 3971; (b) B. Jose, A. Fernando, L. Ramon and C. Maria-Paz, *Synthesis*, 1985, 313; (c) A. R. Steven, D. W. Cecilia and J. K. T. Richard, *Chem. Commun.*, 2003, 2286; (d) G. Shyamaprosad and K. A. Avijit, *Tetrahedron Lett.*, 2005, **46**, 221; (e) C. Yoram, Y. M. Amatzya and R. Mordecai, *J. Am. Chem. Soc.*, 1986, **108**, 7044; (f) N. P. Xekoukoulotakis, M. Hadjiantoniou and A.J. Maroulis, *Tetrahedron Lett.*, 2000, **41**, 10299; (g) D. Venugopal and M. Subrahmanmyam, *Catal. Commun.*, 2001, **2**, 219.
- 14 (a) G. Shyamaprosad and K. A. Avijit, *Tetrahedron Lett.*, 2002, **43**, 8371; (b) Z. Zhijian, D. W. David, E. W. Scoot, H. L. William and W. L. Craig, *Tetrahedron Lett.*, 2004, **45**, 4873.
- 15 (a) W. Zemin and J. E. Nicholas, *Tetrahedron Lett.*, 2001, **42**, 8115; (b) A. A. Orazio, D. C. Lucia, F. Paolino, M. Fabio and S. Stefania, *Synlett*, 2003, **8**, 1183; (c) K. S. Sanjay, G. Priya, D. Srinavas and K. Bijoy, *Synlett*, 2003, **14**, 2147.

Novel quaternary ammonium ionic liquids and their use as dual solvent-catalysts in the hydrolytic reaction

Jiayang Weng, Congmin Wang, Haoran Li* and Yong Wang

Received 13th June 2005, Accepted 25th October 2005

First published as an Advance Article on the web 14th November 2005

DOI: 10.1039/b508325g

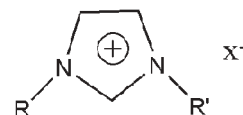
Ionic liquids (ILs) are no longer just a class of esoteric compounds, but are proving to be valuable and useful in a multitude of different applications. Herein, novel quaternary ammonium ionic liquids have been synthesized and characterised. These ionic liquids are Brønsted acidic, available from cheap raw materials and easy to prepare. They have been used both as a catalyst and environmentally benign solvent for the hydrolytic reaction of 1,1,1,3-tetrachloro-3-phenylpropane, eliminating the need for a volatile organic solvent and additional catalyst. The results clearly demonstrate that these ILs can be easily separated and reused without losing their activity and quality. Also, the yields obtained with this methodology are significantly increased in comparison with those reported in organic solvents to date.

Introduction

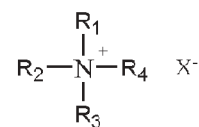
Ionic liquids (ILs) are very attractive and environmentally acceptable solvents because they have very low vapor pressure and are stable in a wide temperature range.^{1–3} Therefore, they can be used as environmentally benign solvents for a number of chemical processes, such as separations,⁴ reactions,⁵ homogeneous two-phase catalysis⁶ and extractions.⁷ The current emphasis on novel reaction media is motivated by the need for efficient methods for replacing of toxic or hazardous solvents and catalysts. The use of ionic liquids as novel reaction media may offer a convenient solution to both the solvent emission and the catalyst recycling problem.⁸

Seddon *et al.*⁹ cooperated with many chemistry companies, such as BP, and manufactured the linear alkyl benzene based on ionic liquids as reaction media. Furthermore, after the announcement of the first industrial process involving ionic liquids by BASF (BASIL¹⁰ process) in 2003 the potential of ionic liquids for new chemical processes and technologies is beginning to be recognized. However, currently the industry application of ionic liquids is limited because of the high cost of ionic liquids, the difficulty in separations or recycling, and so on. In this paper, novel quaternary ammonium ionic liquids, which are Brønsted acidic and easy to prepare from cheap amines, have been synthesized and used both as catalysts and environmentally benign solvents for the hydrolytic reaction of 1,1,1,3-tetrachloro-3-phenylpropane to prepare cinnamic acid, Fig. 1.

Cinnamic acid is a highly valuable class of fine chemicals with applications in polymer formulations, medication, pesticide, sensitive resin and plastics as well as general organic synthesis. It is a key intermediate in the synthesis of Segontin, Cinnarizine, chlorobenzene ammonic butyric acid and so on. Several methods are reported to prepare cinnamic acid: the Perkin reaction,^{11–15} halo-benzene with acrylic acid,^{16,17}



R=H,CH₃; R'=H,C₂H₅,C₄H₉; X=HSO₄,H₂PO₄,PF₆,BF₄,AcO



R_{1,2,3}=Me,Et,Pro,But; X=HSO₄

Fig. 1 Structures of two sorts of ionic liquids.

benzaldehyde with acetone,¹⁸ benzaldehyde with ketene or acetic acid,¹⁹ the preparation from cinnamic aldehyde by air-oxidation,²⁰ using microwave irradiation for the Knoevenagel–Doebner synthesis of cinnamic acid,²¹ styrene with carbon monoxide or carbon dioxide,²² the hydrolyzation of 1,1,1,3-tetrachloro-3-phenylpropane from styrene and CCl₄,²³ and a new direct synthesis from aromatic aldehydes and aliphatic carboxylic acid in the presence of sodium borohydride.²⁴ Today, the hydrolyzation of 1,1,1,3-tetrachloro-3-phenylpropane is the one of the main routes for industrial production of cinnamic acid because the yield is high and CCl₄ can be used up. CCl₄ can not be used as solvent any longer and another product must be used because CCl₄ may destroy the ozone-sphere, and it is harmful to the human body. In the hydrolyzation of 1,1,1,3-tetrachloro-3-phenylpropane, solvents such as acetic acid and a strong acid catalyst such as sulfuric acid are needed. The yield of the hydrolytic reaction is low due to the use of the strong acid. Despite numerous attempts to overcome these drawbacks, no benign methods have been used for the synthesis of cinnamic acid.

Department of Chemistry, Zhejiang University, Hangzhou, 310027, P. R. China. E-mail: lihr@zju.edu.cn; Fax: +86-571-8795-1895; Tel: +86-571-8795-2424

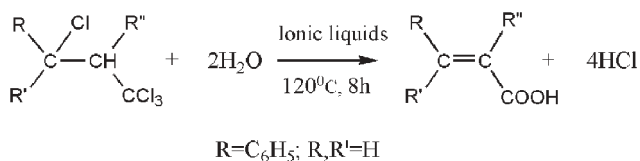


Fig. 2 Hydrolytic reaction in ionic liquids.

We describe here the hydrolyzation of 1,1,1,3-tetrachloro-3-phenylpropane to synthesize cinnamic acid in different ionic liquids, Fig. 2. The process of hydrolyzation can be carried out without additional catalyst and solvent and the ionic liquids can be easily separated and reused. In particular, the effect of the ionic liquid, temperature, dosage and recycling on the yield is discussed.

Experimental

Chemicals

Styrene, copper(I) chloride, carbon tetrachloride, acetic acid, sulfuric acid, acetone, n-butyl bromide, bromoethane, 1-chlorobutane, potassium hexafluorophosphate, sodium tetrafluoroborate, imidazole, 1-methylimidazole, ethyl acetate, trimethylamine, diethylamine, triethylamine, n-triisopropylamine, iso-propylamine, tri-n-butylamine, n-butylamine, and chloroform were all used as received unless otherwise stated.

Instruments

NMR spectra were recorded on a 500 MHz Bruker spectrometer in DMSO, CDCl₃ and calibrated with tetramethylsilane (TMS) as the internal reference. The purity was analyzed using a high pressure liquid chromatogram (HPLC-10 ATVP SHIMADZU). The column was Kromasil C18 (4.6 mm × 250 mm). An acetonitrile–water–acetic acid (100 : 99 : 1) mixture was used as solvent. IR measurements were performed on an FT-IR 470 Nicolet using KBr optics. The melting point was recorded on a digital melting point apparatus (WRS-1A).

Synthesis of ionic liquids

The ionic liquids of general type [amine][HSO₄] were synthesized in the following way.

Trimethylamine sulfate [Me₃NH][HSO₄]. Into a 250 ml three-necked flask under vigorous stirring, was placed 0.5 mol trimethylamine water solution, then sulfuric acid was dropped in. The temperature was kept at 0 °C. After the reaction, the water was separated. The white crystalline powder was dried by evaporation in high vacuum at 50 °C overnight (>99% yield). δ_H (DMSO) 2.55 (s, 1H), 2.76 (s, 1H).

Diethylamine sulfate [Et₂NH₂][HSO₄]. Under vigorous stirring, 0.5 mol sulfuric acid was dropped into the solution of the diethylamine (0.5 mol diethylamine and 150 ml chloroform) under ice. After the reaction, the chloroform was filtered on a rotatory evaporator. Upon cooling the ionic liquid, a white solid was obtained. The white crystalline powder was dried by evaporation in high vacuum at 50 °C

overnight (>99% yield). δ_H (DMSO) 1.16 (t, 3H), 2.92 (m, 2H), 8.18 (s, 1H).

The following four kinds of ionic liquids were synthesized as [Et₂NH₂][HSO₄].

Triethylamine sulfate [Et₃NH][HSO₄]. δ_H (DMSO) 1.18 (t, 3H), 3.10 (m, 2H), 8.89 (s, 1H).

n-Tripropylamine sulfate [n-Pr₃NH][HSO₄]. δ_H (DMSO) 0.90 (t, 3H), 1.63 (m, 2H), 2.99 (m, 3H), 9.15 (s, 1H).

iso-Propylamine sulfate [iso-PrNH₂][HSO₄]. δ_H (DMSO) 1.17 (d, 3H), 3.28 (t, 2H), 7.69 (s, 3H).

Tri-n-butylamine sulfate [tri-n-Bu₃NH][HSO₄]. δ_H (DMSO) 0.91 (t, 3H), 1.31 (m, 2H), 1.58 (m, 2H), 3.00 (m, 2H), 8.32 (s, 1H).

Other ionic liquids used in this paper were synthesized using standard literature methods.²⁵

The hydrolyzation of 1,1,1,3-tetrachloro-3-phenylpropane in ionic liquids

The hydrolyzation of 1,1,1,3-tetrachloro-3-phenylpropane was investigated in several ionic liquids. The choice of ionic liquids were motivated by their being the most widely used, and therefore the most widely available (Fig. 2). These reactions were carried out in a 250 ml volumetric flask set in a recirculating heated bath and stirred with a magnetic stir bar. In a typical reaction 1,1,1,3-tetrachloro-3-phenylpropane (0.5 mol) was added to quaternary ammonium ionic liquids (trimethylamine sulfate [Me₃NH][HSO₄], 0.5 mol), and water (1.0 mol) was dropped into the flask, then the mixture was stirred at 120 °C for several hours. During the reaction, cinnamic acid and ionic liquid were mixed together, giving out hydrochloric acid from the liquid system, which was absorbed by water. At the end of the reaction, the mixture was treated with water. The products were separated by filtration as the ionic liquids could be dissolved in water while the cinnamic acid could not.

The characterisation of cinnamic acid: ¹H NMR (ppm, δ_H CDCl₃): 6.46 (s, 1H), 7.40 (s, 1H), 7.41 (s, 1H), 7.55 (s, 1H), 7.80 (s, 1H), 11.19 (s, 1H); ¹³C NMR (ppm, δ_CCDCl₃): 117.57; 128.91; 132.63; 147.37; 172.92. IR (cm⁻¹): 3448.22, 3024.46, 2922.08, 2830.52, 1685.07, 1631.09, 1560.06, 1449.75, 1134.05, 762.08, 705.41. melting point: 132.5–134.5 °C.

Results and discussion

Table 1 summaries the results of the hydrolytic reaction in the ionic liquids. It can be seen that the conversion and yield were better achieved in ionic liquids than in acetic acid as solvent. Not only the cation of ionic liquids but also the anion of ionic liquids affects the conversion and the yield of the hydrolytic reaction. In the case of sulfate acid ionic liquids only, the conversion and yield in the quaternary ammonium ionic liquids are better than those in the other ionic liquids from entries 1, 2, 3, 4, 5 and 6. The reaction appeared to be largely dependent on the anion of the ionic liquids. The yield and the conversion are better for [Bmim][HSO₄] than for

Table 1 Hydrolyzation of 1,1,1,3-tetrachloro-3-phenylpropane in ionic liquids^a

Entry	Solvent	<i>T</i> /°C	Conversion ^b (%)	Yield (%)
1	[Me ₃ NH][HSO ₄]	120	100	87
2	[Et ₂ NH ₂][HSO ₄]	120	100	88
3	[Bmim][HSO ₄]	120	100	89
4	[Emim][HSO ₄]	120	100	88
5	[Hmim][HSO ₄]	120	100	89
6	[ImI][HSO ₄]	120	100	88
7	[Bmim][PF ₆]	120	87	84
8	[Emim][BF ₄]	120	89	83
9	[Hmim][OAc]	120	90	82
10	[Bmim][H ₂ PO ₄]	120	90	85
11 ^c	Acetic acid	120	98	85

^a Reactions were performed at 120 °C. ^b Conversions after 8 h. ^c The reaction was in acetic acid as solvent and sulfuric acid as catalyst; conversion after 15 h.

[Bmim][H₂PO₄] and [Bmim][PF₆] from entries 3, 7 and 10. Similar results are obtained from entries 4 and 8, and entries 5 and 9. It was surprising that the hydrolyzation of 1,1,1,3-tetrachloro-3-phenylpropane could be carried out in neutral ionic liquids, which is different from the method according to the patent²⁶ that it should be carried out under acid conditions. Above all, the yield of cinnamic acid was greater in sulfate acid ionic liquids.

An important feature of these reactions in ionic liquids is that there is no evidence for significant formation of a side reaction. There was good conversion in the sulfate acid ionic liquids.

In order to obtain a higher yield, different quaternary ammonium ionic liquids were used in the hydrolytic reaction. Table 2 shows the effect of the ionic liquid on the conversion and the yield. We found that [Et₃NH][HSO₄] might be best for the hydrolyzation of 1,1,1,3-tetrachloro-3-phenylpropane in all the quaternary ammonium ionic liquids.

The effort required to find the influence of dosage and temperature for [Et₃NH][HSO₄] was great. Firstly, we investigated the influence of dosage of ionic liquids, which was recorded from 0.25 mol to 2.00 mol; see Table 3 entries 1 to 6. The higher dosage of [Et₃NH][HSO₄], the better conversion and yield of 1,1,1,3-tetrachloro-3-phenylpropane and the higher yield of cinnamic acid obtained. However, the result did not continue improving when the dosage reached 1.00 mol or greater. Entries 3, 7, 8, 9 and 10 in Table 3 show that the temperature appears to affect the reaction. Low temperature (<100 °C) led to poor conversion levels. When the temperature was so high that 1,1,1,3-tetrachloro-3-phenylpropane and cinnamic acid decomposed by themselves, the yield

Table 2 Hydrolyzation of 1,1,1,3-tetrachloro-3-phenylpropane in amine ionic liquids^a

Entry	Solvent ^b	<i>T</i> /°C	Conversion ^c (%)	Yield (%)
1	[Me ₃ NH][HSO ₄]	120	100	87
2	[Et ₂ NH ₂][HSO ₄]	120	100	88
3	[Et ₃ NH][HSO ₄]	120	100	90
4	[n-Pr ₃ NH][HSO ₄]	120	96	87
5	[iso-PrNH ₃][HSO ₄]	120	96	88
6	[Bu ₃ NH][HSO ₄]	120	90	86

^a Reactions were performed at 120 °C. ^b Type of ionic liquid. ^c Conversions after 8 h.

Table 3 Effect of the temperature and the dosage of [Et₃NH][HSO₄] ionic liquid to the conversion of the cinnamic acid^a

Entry	Dosage/mol	<i>T</i> /°C	conversion ^b (%)	Yield (%)
1	0.25	120	85	54
2	0.50	120	95	82
3	1.00	120	100	90
4	1.25	120	100	90
5	1.50	120	100	90
6	2.00	120	100	90
7	1.00	140	100	86
8	1.00	160	100	60
9	1.00	100	60	37
10	1.00	80	36	12

^a Reactions were performed at 120 °C, the dosage of 1,1,1,3-tetrachloro-3-phenylpropane was 1.00 mol. ^b Conversions after 8 h.

decreased significantly. In contrast, the desired cinnamic acid was obtained with good results at 120 °C.

The product of the reaction resulted in a one phase system after reaction. Water was added into this system once the reaction was completed. Filtration was sufficient to remove products from the solution because the ionic liquids could dissolve in water while the cinnamic acid could not. The ionic liquids could be recycled after separating away most of the water under vacuum which was left in the liquid. Also, it did not affect the recycling of the ionic liquid with a small amount of water in the ionic liquid. The hydrolyzation of 1,1,1,3-tetrachloro-3-phenylpropane to produce cinnamic acid was repeated ten times. It can be seen (Table 4) that the conversions and the yield were not reduced after being reused ten times and [Et₃NH][HSO₄] could have the potential to be used more than ten times.

Conclusion

For the application in industry, many ionic liquids are expensive. In this paper, some quaternary ammonium ionic liquids were synthesized, which were relatively cheap and easy to prepare. These ionic liquids were used in the hydrolytic reaction of 1,1,1,3-tetrachloro-3-phenylpropane to cinnamic acid without the use of tradition volatile organic compounds (VOCs) such as acetic acid and additional catalyst. The reactions proceeded well in sulfate ionic liquids and cinnamic acid is obtained with high conversion and yield, especially in the quaternary ammonium ionic liquids. The effect of the ionic

Table 4 Effect of reused [Et₃NH][HSO₄] ionic liquid on the hydrolyzation^a

Entry	Recycling	<i>T</i> /°C	conversion ^b (%)	Yield (%)
1	0	120	100	90
2	1	120	99	86
3	2	120	100	90
4	3	120	100	88
5	4	120	98	87
6	5	120	100	89
7	6	120	100	90
8	7	120	99	87
9	8	120	100	90
10	9	120	99	90

^a Reactions were performed at 120 °C. ^b Conversions after 8 h.

liquids, temperature, dosage and recycling on the yield was discussed. Good conversion and high yield of cinnamic acid could be obtained with a 1 : 1 mole ratio under 120 °C for 8 h with [Et₃NH][HSO₄]. These ionic liquids provide a good alternative for the industrial synthesis of cinnamic acid and this method has been applied by Juhua Group Corporation Lanxi Agricultural Chemistry Factory.

Acknowledgements

We gratefully acknowledge financial support from the Natural Science Foundation of China (NO.20434020).

References

- 1 P. Wasserscheid and W. Keim, *Angew. Chem.*, 2000, **112**, 3926; P. Wasserscheid and W. Keim, *Angew. Chem., Int. Ed.*, 2000, **39**, 3772; P. Wasserscheid and W. Keim, *Angew. Chem., Int. Ed.*, 2000, **39**, 3773; P. Wasserscheid and T. Welton, *Ionic liquids in synthesis*, Wiley-VCH, Weinheim, 2003, p. 364.
- 2 J. S. Wilkes, J. A. Levisky, R. A. Wilson and C. L. Hussey, *Inorg. Chem.*, 1982, **21**, 1263; J. S. Wikes and M. J. Zaworotko, *Chem. Commun.*, 1992, 965.
- 3 *Ionic liquids as green solvent: progress and prospects*, ed. R. D. Rogers and K. R. Seddon, ACS Symposium Series 856, American Chemical Society, Washington, DC, 2003, p. 599.
- 4 J. G. Huddleston, H. D. Williams, R. P. Swatloski, A. E. Visser and R. D. Rogers, *Chem. Commun.*, 1998, 1765.
- 5 R. Sheldon, *Chem. Commun.*, 2001, 2399; C. J. Adams, M. J. Earle, G. Roberts and K. R. Seddon, *Chem. Commun.*, 1998, 2097; C. M. Gordon and A. McCluskey, *Chem. Commun.*, 1999, 1431.
- 6 J. D. Holbrey and K. R. Seddon, *Clean Prod. Process.*, 1999, **1**, 223.
- 7 S. Zhang, Q. Zhang and Z. C. Zhang, *Ind. Eng. Chem. Res.*, 2004, **43**, 614; J. Esser, P. Wasserscheid and A. Jess, *Green Chem.*, 2004, **6**, 316.
- 8 T. Welton, *Chem. Rev.*, 1999, **99**, 2071; F. Liu, M. B. Abrams, R. T. Baker and W. Tumas, *Chem. Commun.*, 2001, **5**, 433; E. D. Bates, R. D. Mayton, I. Ntai and J. H. Davis, *J. Am. Chem. Soc.*, 2002, **124**, 926; S. K. Ritter, *Chem. Eng. News*, 2001, **79**, 27; Y. Wang, H. R. Li, C. M. Wang and J. Hui, *Chem. Commun.*, 2004, 1938; S. Gmouh, H. Yang and M. Vaultier, *Org. Lett.*, 2003, **5**, 3365.
- 9 M. J. Earle, P. B. McCormac and K. R. Seddon, *Chem. Commun.*, 1998, 2245.
- 10 M. Volland, V. Seitz, M. Maase, M. Flores, R. Papp, K. Massonne, V. Stegmann, K. Halaritter, R. Noe, M. Bartsch, W. Siegel, M. Becker and O. Huttenloch, *Method for the separation of acids from chemical reaction mixtures by means of ionic liquids*, *PCT Int. Appl., WO 03/06225*, 31. 7. 2003, BASF AG; M. Huttenloch, *Chem. Eng. News*, 2003, **81**, 9.
- 11 J. R. Johnson, *Org. React.*, 1942, **1**, 210; J. R. Johnson, *Org. Syn. Coll.*, 1955, **3**, 426; R. E. Ruckles, *J. Chem. Educ.*, 1950, **27**, 210.
- 12 E. Koepp and V. Fritz, *Synthesis*, 1987, **2**, 177.
- 13 R. Kern, *DE Pat.*, DE 3 139 994, 1983.
- 14 M. G. Mihaiescu, N. Vasile and T. Sachelarie, *RO Pat.*, RO 90 224, 1986.
- 15 W. R. Peterson, *US Pat.*, US 2 401 099, 1986.
- 16 W. J. Houlihan and J. Nadelson, *US Pat.*, US 3 870 751, 1975; J. E. Telschow, *US Pat.*, US 4 571 432, 1986.
- 17 N. A. Bumagin, N. P. Andryukhova and I. P. Beletskaya, *Metalloorg. Khim.*, 1989, **2**, 911.
- 18 J. H. Teles, N. Rieber, K. Breuer, D. Demuth, H. Hibst, H. Etzrodt and U. Rheude, *US Pat.*, US 6 211 416, 1999.
- 19 K. Karl, K. Thomas and S. Heinrich, *DE Pat.*, DE 3 437 624, 1986; G. Ihl, G. Roscher and N. Mayer, *DE Pat.*, DE 3 743 616, 1988.
- 20 B. Ramesh Babu and K. K. Balasubramaniam, *Org. Prep. Proced. Int.*, 1994, **26**, 123; E. Dalacanalé, G. Bottaccio, S. Compolmi and F. Montamari, *EP Pat.*, 0 146 373, 1985; H. Harada, *EP Pat.*, EP 0 170 520, 1986.
- 21 K. H. M. Sampath, R. B. V. Subba and R. P. Thirupathi, *Org. Prep. Proced. Int.*, 2000, **32**, 81.
- 22 H. Heinz, Y. Peres and A. Milchereit, *J. Organomet. Chem.*, 1986, **307**, c38.
- 23 I. Gerdlin, *Pollena: Thuszce, Srodki, Piorace Kosnet*, 1987, **31**, 13; M. Hajek, J. Malek and P. Silhavy, *CS Pat.*, 217 518, 1983; M. Hajek and P. Silhavy, *DE Pat.*, DE 3 524 475, 1986; M. Hajek, J. Malek and P. Silhavy, *CS Pat.*, CS 209 347, 1981.
- 24 I. C. Constantin, T. Fulga and O. Marioara, *Tetrahedron Lett.*, 2003, **44**, 3579.
- 25 G. Y. Zhao, T. Jiang, H. X. Gao, B. X. Han, J. Huang and D. H. Sun, *Green Chem.*, 2004, **6**, 75; Lauric Ropel, S. B. Lionel, N. V. K. A. Sudhir, A. S. Mark and J. F. Brennecke, *Green Chem.*, 2005, **7**, 83; J. F. Dubreuil, K. Bourahla, M. Rahmouni, J. P. Bazureau and J. Hamelin, *Catal. Commun.*, 2002, **3**, 185.
- 26 M. Hajek and P. Šilhav, *US Pat.*, US 4 806 681, 1998; CA, 104; 186139w.

Conversion of scallop viscera wastes to valuable compounds using sub-critical water

Omid Tavakoli and Hiroyuki Yoshida*

Received 25th May 2005, Accepted 21st October 2005

First published as an Advance Article on the web 15th November 2005

DOI: 10.1039/b507441j

The large amount of seafood wastes discharged from related industries has become a serious problem. Since these wastes contain high concentrations of organic variables such as proteins and fat, a method for recovery of these useful materials would be a highly desirable process. In this work, sub- and supercritical water hydrolysis of scallop viscera wastes has been studied in a batch-type reactor. Experiments were performed at a temperature range of 443–673 K with the reaction time between 1–50 min. Through the hydrolysis reaction, this method produced valuable materials such as amino acids, organic acids, fat and oil phases, soluble proteins and peptides. At 513 K and 50 min, maximum amino acids (0.15 kg per kg dry scallop waste) were obtained, while maximum organic acids were found at 553 K and 40 min (0.08 kg per kg dry scallop waste). The optimum temperature for amino and organic acids was close to the temperature at which the ion product of water is maximum. Among amino acids, glycine was the most abundant while in organic acids pyroglutamic acid was most plentiful. Experimental results demonstrated that this technique has great potential for practical application because it was not only energy saving, environmentally friendly and cost effective but also produced many useful materials with zero emission.

Introduction

As a new green conversion method, reactions in sub-critical water have been gaining more attention of late. Sub-critical water can provide a new reaction medium and/or act as a catalyst in many chemical reactions. Changes in physical and chemical properties of water under sub-critical conditions, especially in hydrogen bond, ion product and dielectric constant, could facilitate reactions with a wide range of organic compounds resulting in many useful materials.^{1–4}

One of the great challenges in the treatment of organic wastes is related to seafood wastes from seafood and fishery industries world wide. Prevention of marine pollution from dumping of organic wastes provided by the London treaty^{5,6} of 1996 and other new environmental legislation restricted the disposal of these wastes. Immediately after 1996, incineration became an alternative procedure to process seafood wastes. In addition to its very expensive cost, incineration showed two major disadvantages. First, because seafood wastes contain a high level of protein, incineration destroyed these potentially useful materials. Second and also more importantly, some seafood wastes such as those of scallop and squid contain high concentrations of toxic metals and incineration could cause additional environmental problems. Another alternative methods to deal with such wastes is the supercritical water oxidation which decomposes almost all organic compounds mainly to carbon dioxide, water and nitrogen. Furthermore it suffers some major disadvantages including corrosion

problems, expensive materials and lack of recycling and resource recovery.^{7–9} Therefore, a better, cheaper and cleaner process for the conversion of seafood wastes to useful materials would be highly beneficial.

Yoshida *et al.* have first showed that hydrolysis in sub-critical water could be an ideal new chemical process to treat seafood wastes.^{10–13} Using sub-critical water hydrolysis, some useful materials such as amino acids, organic acids, fatty acids, oil phase, and other materials could be produced from fish and squid wastes.^{10–16}

Other research has demonstrated the possibility of using sub-critical water technology to convert organic wastes to useful substances and resources. Some recent studies have been reported on the treatment of organic wastes,^{17–19} sewage sludge,^{20–21} decomposition of glucose, fructose and cellobiose,²² hydrolysis of cellulose,^{23–24} amino acid decomposition,²⁵ and hydrolysis of methyl *t*-butyl ether.²⁶

In Japan alone, the production of scallops in the year 1998 reached 550 000 tonnes. With a conversion factor of waste as 40% of meat and internal organs, this large scale production resulted in large amounts of waste containing proteins on an annual basis. Therefore, a green and/or clean conversion method of those wastes to useful materials is extremely urgent for this country.

It is expected that sub-critical water as a powerful reactant and medium can be used for effective treatment of these scallop wastes. With regard to the proteins contained in scallop, some research is available in the literature, which deals with the major protein bands, protein–mineral interactions, and analysis of the proteins.^{27–29}

The aim of this work is to investigate the feasibility of treatment of the valueless scallop viscera wastes in sub-critical

Department of Chemical Engineering, College of Engineering, Osaka Prefecture University, 1-1 Gakuen-Cho, Sakai, Osaka, 599-8531, Japan.
E-mail: yoshida@chemeng.osakafu-u.ac.jp; Fax: +81-72-254-9298;
Tel: +81-72-254-9298

water to produce valuable materials. From the results of our experiments, we propose an optimum procedure for hydrolysis conversion.

Materials and methods

Materials, reagents, and equipment

The waste of scallop internal organs (*Patinopecten yessoensis*) was supplied from Aomori prefecture (Japan). Before the experiments, the waste was homogenized with a Waring blender (Model 31 BL 92, Dynamic Corporation of America) for 10 min. The resulting homogenous wastes were stored in a freezer at 255 K. Water content of the sample was approximately 83.8%. All reagents were laboratory grade and water was Milli-Q which is deionized distilled double pure water (18.2 M Ω cm purity grade at 25 °C). A stainless tube (SUS 316, id 0.0075 m \times 0.15 m) with Swagelok caps was used as a reactor (reactor volume 9.0 cm³).^{10–12}

Reaction and analytical methods

The reactions were conducted in the temperature range of 443–673 K and pressure range of 0.792–30 MPa. In each run, about 2.5×10^{-3} kg sample of scallop viscera wastes was used. The sample and Milli-Q water were put into the reactor and then the oxygen dissolved in the sample and the water was removed by purging argon gas to avoid the oxidation process. The reactor was then sealed and immersed in a preheated molten salt bath (Thomas Kagaku Co. Ltd., Tokyo, Japan) containing a mixture of potassium nitrate and sodium nitrate. Soaking the reactor into a water bath after the desired reaction time terminated the reaction.

After the reaction, the aqueous phase was diluted to 50 cm³ with distilled pure water and was filtered through Millipore membranes (0.22 μ m) to remove fat and oil droplets as well as water insoluble residues.

The amino acids content in the reaction products was measured using an amino acid HPLC (LC-10A, ISC-07/S 1504 column incorporated with a post-column labeling method, Shimadzu Corp.). The quantity of 17 amino acids was analyzed using a fluorescence detector (Shimadzu, RF-10A) at 350 nm of excitation wavelength and 450 nm of emission wavelength. Data acquisition and analysis software were provided by the instrument manufacturer. A mixture of sodium citrate, ethanol and perchloric acid (60%) at pH 3.31 was employed as the mobile phase. The HPLC was operated at an oven temperature of 333 K and a 0.6 ml min⁻¹ flow rate of mobile phase with 45 min run times.

Organic acid HPLC (SCL-10A, Shimadzu Corp.) was used to determine the quantities of 7 organic acids with two serial ion-exclusion chromatography columns (Shim-pack SCR-102H, id 0.008 m \times 0.3 m) equipped with a guard column (SCR-102H, id 0.006 m \times 0.05 m) and a post-column pH-buffered electroconductivity detection (Shimadzu, CDD-6A). The mobile phase was 5 mM of *p*-toluenesulfonic acid solution at a flow rate of 0.8 ml min⁻¹. A mixture of 5 mM *p*-toluenesulfonic acid, 20 mM of bis-tris and 100 mM of EDTA was used as post column reagent at a flow rate of 0.8 ml min⁻¹. The column temperature was kept at 318 K.

To obtain total organic carbon (TOC) of the products, total carbon (TC), and inorganic carbon (IC) in aqueous samples were measured with a TOC analyzer (TOC-500, Shimadzu Corp.). Air was used as both a sparging and carrier gas at 150 ml min⁻¹. The aqueous phase (0.01 cm³) was injected into the high temperature combustion tubes (953 K) prior to entering the infrared detector.

Carbon, hydrogen, nitrogen, and sulfur content in the raw scallop wastes and solid residual was measured with a CHNS coder (Perkin Elmer 2400). The samples were dried in an oven (348 K) for 2 days prior to the CHNS analysis.

Results and discussion

Total yields of products as a function of reaction temperature and time

The temperature–time profiles of scallop waste inside the reactor demonstrated that after immersing the reactor into the salt bath, about 30 s is required to reach the expected reaction temperature. After the reaction, three phases of aqueous, oil, and fat were produced. Some parts of the wastes remained as a solid residual. The total amount of gases (such as CO₂, H₂O, N₂ and O₂) produced during sub-critical water reaction was very small and negligible. Fig. 1 shows photographs of the reaction products of scallop wastes at 553 K for different reaction times in the range of 1–40 min, respectively, compared to the one before the reaction. The changing of the color in the aqueous phase from dark to light brown with increasing reaction time means that the amount of soluble proteins and other organic compounds has gradually decreased in the aqueous phase. On the other hand, the amount of oil phase has increased with time. Fig. 2 illustrates the time course of the solid residual and the yields of fat and oil. The solid has decreased in volume due to the decomposition of the solid-proteins and the extraction of fat and oil. The yield of the fat phase has also decreased along with increasing of the oil phase. Fig. 3 demonstrates the effect of temperature on the solid residual and the yields of fat and oil. An increase in the temperature caused a dramatic decrease in the fat yield and the solid residual whereas the oil yield increased. As shown in these figures, the fat phase exhibited the largest yield among the three phases at 443 K, and through rising temperature this phase decomposed and some of its parts were converted to the oil-phase. Since oil and fat contain fatty acids, such as DHA and EPA, those phases could be considered as important

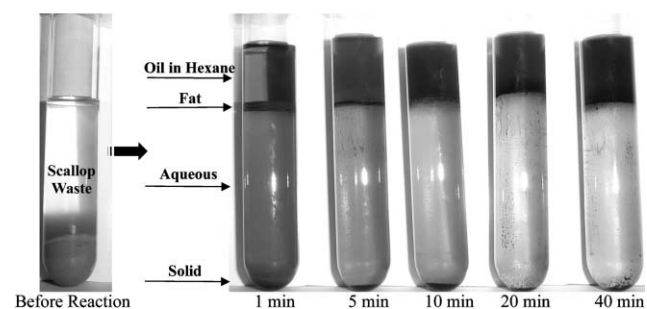


Fig. 1 Photographs of the reaction products of the scallop wastes reacted at 553 K for different reaction times.

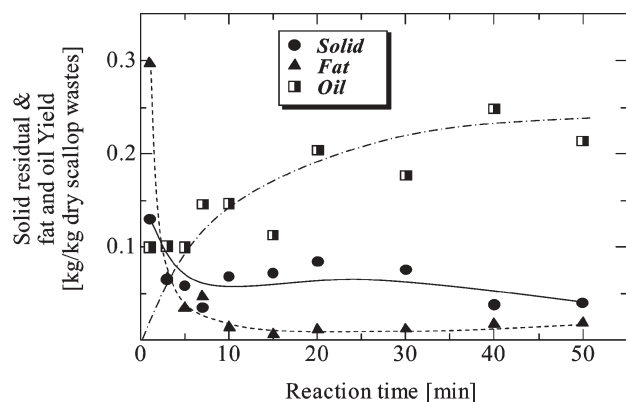


Fig. 2 Time course of solid residual and yield of fat, and oil phases at 553 K.

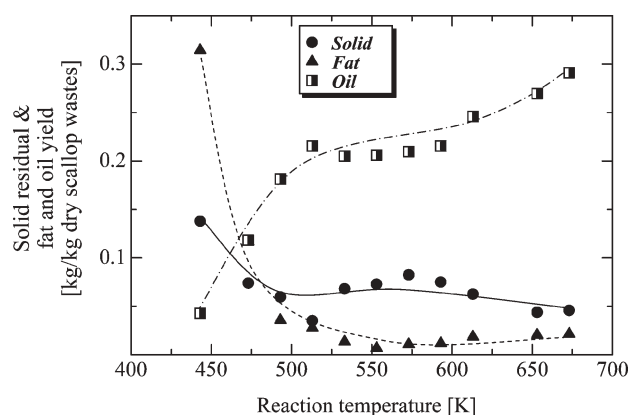


Fig. 3 Effect of reaction temperature on solid residual and yield of fat, and oil phases for a reaction time of 5 min.

sources to produce not only energy but also variable materials. The amount of solid residual, which were unreacted wastes, reached a plateau around 500 K.

The contents of carbon, hydrogen, nitrogen, sulfur, oxygen, and ash in the dry raw scallop wastes were found to be 48.55%, 7.56%, 9.94%, 3.18%, 20.8%, and 10% respectively. These values provide information on scallop waste structure and describe the many organic molecules inside the waste, which contains carboxylic groups, amino groups, sulfur bonds and so on. Table 1 illustrates the effect of reaction temperature on the CHNS ratios (number of atoms to carbon) in the solid residual and the fat phase at 5 min as ratios of H/C, N/C and S/C. The values of H/C in both solid and fat phases are largest at 443 K. This value in the solid residual at 443 K and the one before reaction is close to 2. This means that they are almost single bond solid proteins. The values of H/C in the solid and the fat phase have gradually decreased with rising temperature. Decreasing this ratio could be helpful to find the structure of solid residual at different reaction points. This may suggest that carbon components of the solid during the sub-critical water hydrolysis reaction have gradually moved to aqueous, fat and oil phases in the form of organic substances. The nitrogen ratio also decreased and the ratio of sulfur is almost constant.

Table 1 Effect of temperature on CHNS ratios in solid residual and fat phase for a reaction time of 5 min

Reaction temperature/K	Solid/kg per kg carbon			Fat phase/kg per kg carbon		
	Ratio of no. of atoms to carbon			Ratio of no. of atoms to carbon		
	H/C	N/C	S/C	H/C	N/C	S/C
443	1.94	0.23	0.029	1.76	0.17	0.022
473	1.69	0.23	0.026	1.73	0.17	0.022
493	1.64	0.21	0.025	1.68	0.16	0.023
513	1.71	0.19	0.024	1.68	0.17	0.025
553	1.57	0.12	0.025	—	—	—
573	1.52	0.11	0.024	1.69	0.11	0.024
593	1.55	0.1	0.022	1.73	0.064	0.025
613	1.61	0.11	0.023	1.65	0.059	0.02
653	1.35	0.093	0.022	1.55	0.06	0.022
673	1.22	0.09	0.021	1.41	0.054	0.025

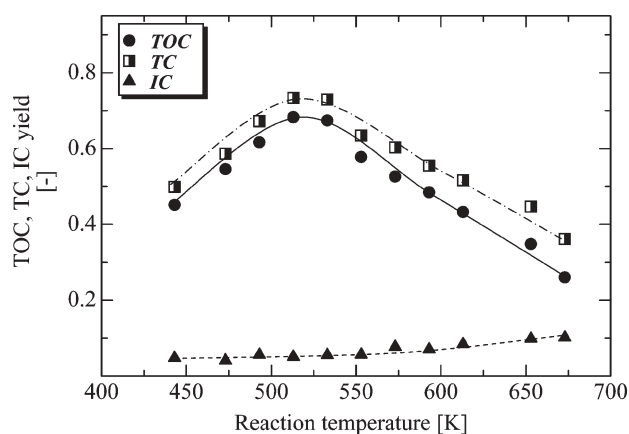


Fig. 4 Effect of temperature on total organic carbon (TOC), total carbon (TC) and inorganic carbon (IC) at a reaction time of 5 min in the aqueous phase.

Fig. 4 illustrates the temperature course of the yields of TOC, TC, and IC at a reaction time of 5 min in the aqueous phase. The course of TOC and TC are very similar to the course of ion product of water (K_w) versus temperature. The TC and TOC course showed the peaks of 0.73 and 0.68 kg C per kg C respectively around 513–533 K, where the ion product of water gives a maximum value. This means that the organic wastes were mainly decomposed by the hydrolysis reaction. In addition to the ion product of water which supplies the ability for water to act as an acid catalyst and enhancing the reaction rate, the dielectric constant of water provides a wide range of polarity to extract organic compounds. In other words, since in the supercritical area the above-mentioned properties became very small, the yield of TOC decreased to its lowest amount due to the thermal destruction of the organic compounds to some refractory acids and gasses. The increase in IC (such as carbonic acid) with rising temperature indicates that the effect of thermal decomposition increases with an increase in temperature.

Fig. 5 shows the total yield of produced organic compounds, ammonia, and phosphoric acid in the aqueous phase against reaction temperature at 5 min. The production of organic compounds is evident from the total yield of amino acids and

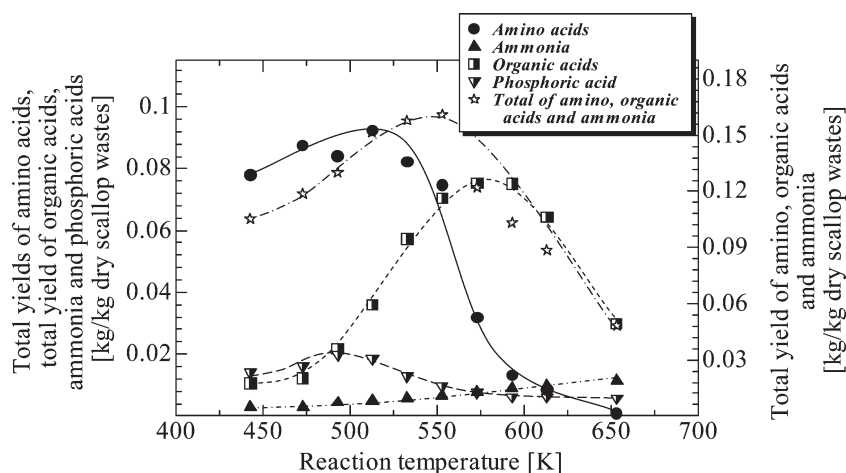


Fig. 5 Effect of temperature on total yield of amino acids, total yield of organic acids, yield of ammonia, yield of phosphoric acid and total yield of amino, organic acids and ammonia at a reaction time of 5 min in the aqueous phase.

the total yield of organic acids, which as illustrated peaks at around 513 K (0.093 kg per kg dry wastes) and 573 K (0.076 kg per kg dry wastes) respectively. The total yield of amino, organic acids and ammonia in the aqueous phase showed a peak at around 513 K. Since the ion product of water shows a similar peak at around 513–533 K under saturated vapor pressure, these results suggest that 513 K is the most favorable temperature for hydrolysis of proteins leading to the production of amino acids. In temperatures above 513 K, the yields of amino acids decreased due to the decrease of the ion product of water. Some of them may decompose to organic acids. Because of these reactions, the total yield of organic acids showed a peak at around 573 K, which was higher than the peak of the total yield of amino acids. Phosphoric acid showed a peak at about 493 K. The yield of ammonia in the aqueous phase gradually increased to 653 K (0.0115 kg per kg dry wastes) as a result of amino acid decomposition.

The total yield of major compounds in the aqueous phase as a function of reaction time for the two reaction temperatures of 513 and 553 K are summarized in Table 2. At 513 K with an increase in time the total yields of amino and organic acids continually increased up to 50 min. That the yield of TOC reached a plateau after 3 min may be due to the equal appearance of compounds containing carbon in the aqueous phase, which were produced by the decomposition of solid proteins. At 553 K, the total yield of amino acids and TOC decreased after peaks at 5 min (0.085 kg per kg dry wastes and 0.69 kg C per kg C, respectively). The total yield of organic acids increased and reached a plateau above 10 min (0.077 kg per kg dry wastes). The total yield of amino, organic and phosphoric acids showed a similar curve to TOC. This means that at high reaction temperatures, the decomposition rate of soluble proteins to amino acids in the aqueous phase, which were produced by the decomposition of solid protein, was very fast. There may be little soluble proteins in the

Table 2 Total yield of major compounds in aqueous phase during scallop waste sub-critical water treatment

Reaction temperature/K	Time/min	Total yield/kg per kg dry scallop wastes				
		Amino acids	Organic acids	Phosphoric acid	Amino, organic, phosphoric acids	TOC
513 (3.35 MPa)	1	0.108	0.018	0.017	0.143	0.545
	3	0.101	0.029	0.020	0.151	0.693
	5	0.093	0.037	0.019	0.149	0.686
	7	0.094	0.041	0.018	0.153	0.693
	10	0.097	0.046	0.017	0.161	0.684
	15	0.110	0.052	0.016	0.179	0.710
	20	0.115	0.054	0.016	0.186	0.690
	30	0.137	0.064	0.015	0.216	0.748
	40	0.141	0.065	0.014	0.219	0.681
	50	0.144	0.070	0.014	0.228	0.665
553 (6.42 MPa)	1	0.081	0.032	0.020	0.134	0.549
	3	0.077	0.049	0.015	0.141	0.685
	5	0.085	0.059	0.015	0.159	0.687
	7	0.081	0.064	0.014	0.159	0.585
	10	0.076	0.067	0.013	0.156	0.546
	15	0.063	0.070	0.014	0.146	0.598
	20	0.058	0.073	0.011	0.141	0.527
	30	0.046	0.071	0.0094	0.126	0.539
	40	0.044	0.079	0.0097	0.133	0.534
	50	0.040	0.075	0.009	0.125	0.468

aqueous phase at high temperatures such as 553 K. The yield of phosphoric acid for both temperatures gradually decreased with time.

The soluble protein composition in the aqueous phase was analyzed using sodium dodecyl sulfate polyacrylamide gel electrophoresis (SDS-PAGE). Many protein bands obtained include those at: 14, 29, 36, 45, and 66 kDa. Increasing both reaction temperature and time cause protein bands to decrease. The disappearance of these bands indicates that the protein molecules were decomposed to water-soluble low molecular weight organic compounds.

Organic acids and phosphoric acid productions in the aqueous phase

Fig. 6 shows the yields of the organic acids produced in the aqueous phase at a reaction time of 5 min, plotted against the reaction temperature. Pyroglutamic acid was predominant among organic acids and illustrated a peak at around 573 K (0.07 kg per kg dry wastes). This means that pyroglutamic acid is produced by the hydrolysis reaction of proteins. The yield of phosphoric acid showed a peak at around 493 K (0.02 kg per kg dry wastes) and then gradually decreased and reached a plateau above 573 K. On the other hand, acetic acid increased with an increase in temperature to 653 K (0.013 kg per kg dry wastes). The yield of formic and lactic acids was negligibly small.

Fig. 7 shows the time course of the yields of organic acids at 553 K. The yields of pyroglutamic, acetic and lactic acids increased and reached a plateau above 10–20 min of 0.068, 0.0054 and 0.0031 kg per kg dry wastes, respectively. This means that the hydrolysis reaction is fast. The yield of phosphoric acid gradually decreased with time.

Amino acids production in the aqueous phase

Fig. 8 shows the effect of temperature on amino acid yields at a reaction time of 5 min. Among amino acids, glycine was the most abundant, which dramatically decreased from 443 K (0.043 kg per kg dry wastes) with rising temperature. Fig. 8a illustrates amino acid yields which decreased with temperature from 443 K due to the decomposition to other organic

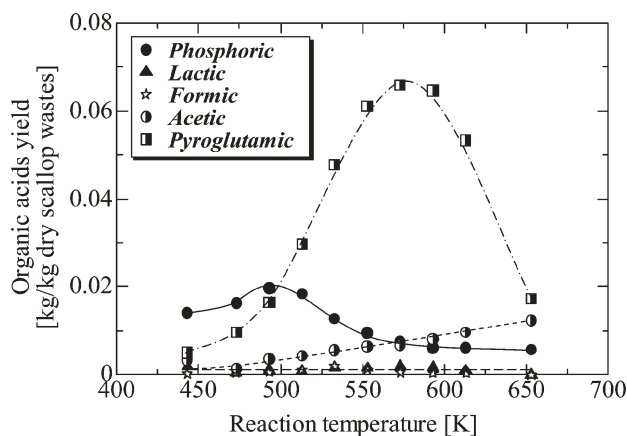


Fig. 6 Effect of temperature course on the yields of organic acids and phosphoric acid for a reaction time of 5 min in the aqueous phase.

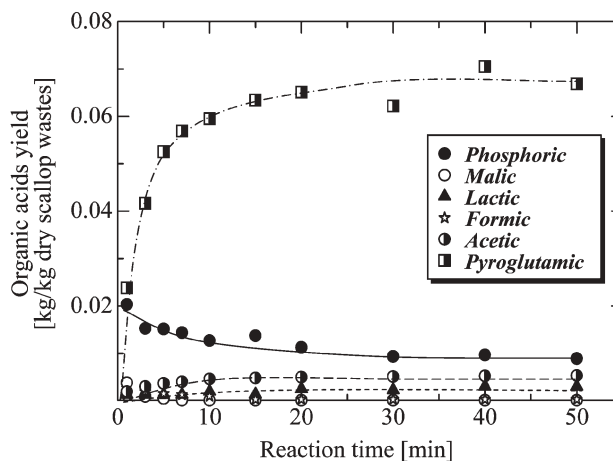


Fig. 7 Effect of reaction time course on the yields of organic acids and phosphoric acid for a reaction temperature of 553 K (6.42 MPa) in the aqueous phase.

compounds. As shown in Fig. 8b, the yield of amino acids exhibited a peak around 473–513 K, which suggests that those amino acids were produced from protein decomposition. The second largest yield among amino acids was alanine, which increased to a peak at around 513 K (0.013 kg per kg dry wastes) and then dramatically decreased. At 653 K almost no amino acids could be observed due to the complete destruction of organic compounds at this supercritical area.

The time course of amino acids at 513 K (the temperature of maximum total yield of amino acids in Fig. 5) was further studied and the results are represented in Table 3. With the exception of glycine, valine, glutamic and argentine, the other

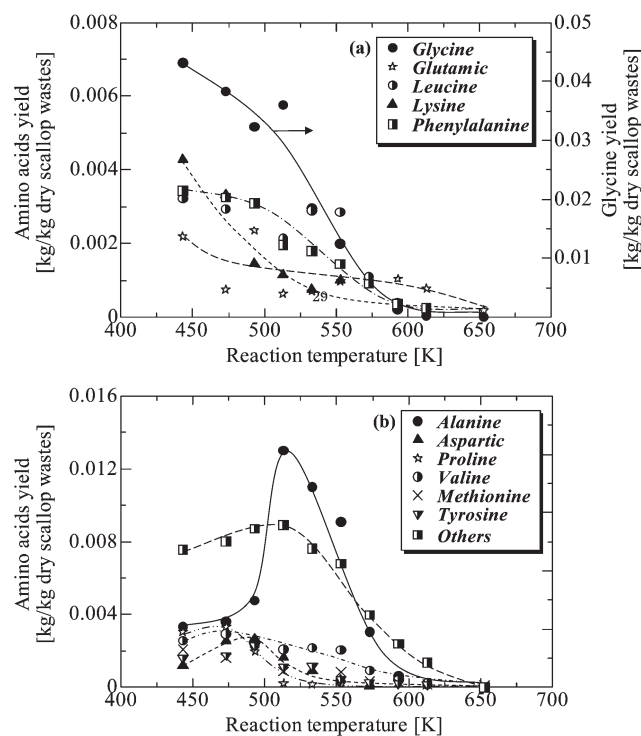


Fig. 8 Effect of temperature course on the yields of amino acids for a reaction time of 5 min in the aqueous phase.

Table 3 Yield of amino acids in the aqueous phase for a reaction temperature of 513 K (3.35 MPa)

Reaction time/min	Amino acid yield/kg per kg dry scallop wastes										
	Glycine	Alanine	Cystine	Valine	Leucine	Phenylalanine	Hystidine	Lysine	Glutamic	Argenine	Others
1	0.048	0.008	0.0013	0.0046	0.0038	0.0044	0.0046	0.0036	0.0044	0.0072	0.017
3	0.044	0.012	0.0021	0.0049	0.0041	0.0047	0.0048	0.0038	0.0019	0.0058	0.013
5	0.037	0.014	0.0034	0.0044	0.0042	0.0043	0.0048	0.0034	0.0010	0.0051	0.012
7	0.035	0.016	0.0043	0.0044	0.0052	0.0044	0.0051	0.0036	0.0007	0.0043	0.011
10	0.033	0.018	0.0059	0.0047	0.0062	0.0046	0.0054	0.0033	0.0005	0.0038	0.011
15	0.034	0.022	0.0085	0.0055	0.0083	0.0053	0.0061	0.0036	0.0004	0.0035	0.012
20	0.037	0.025	0.0099	0.0066	0.0093	0.0054	0.0058	0.0041	0.0003	0.0026	0.010
30	0.039	0.030	0.0133	0.0084	0.0123	0.0068	0.0069	0.0049	7.7 e-5	0.0017	0.012
40	0.040	0.030	0.0128	0.0085	0.0129	0.0069	0.0065	0.0056	7.6 e-5	0.0011	0.015
50	0.041	0.031	0.0133	0.0086	0.0135	0.0071	0.0065	0.0058	6.8 e-5	0.0004	0.016

amino acids gradually increased with time up to 50 min. Glycine with the highest yield among amino acids decreased from 1 min (0.048 kg per kg dry waste), and then started to increase after 10 min and reached a plateau (0.040 kg per kg dry waste) after 30 min. Valine also showed similar behavior in the first 10 min and then gradually increased to 50 min (0.009 kg per kg dry waste). The decrease of these two amino acids in the period of the first 10 min may be due to their hydrophobic property, which hinders them being released from the internal part of the protein during water hydrolysis. The yield of glutamic acid demonstrated a gradual fall from 1 min (0.0044 kg per kg dry waste) due to the dehydration to pyroglutamic acid. On the other hand, the yields of alanine, cystine and leucine showed values of 0.031, 0.013 and 0.014 kg per kg dry waste at a reaction time of 50 min, respectively.

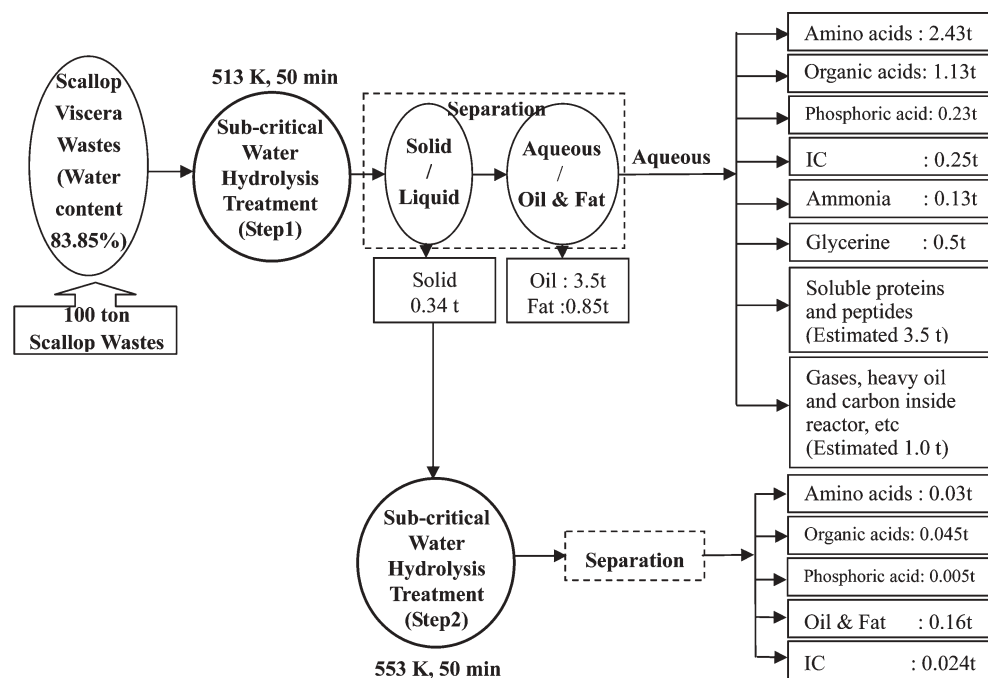
Material balance

Based on 100 tonnes of scallop wastes with water content of 83.8%, the overall mass balance is shown in Fig. 9. The major

concern is to find the optimum condition for protein hydrolysis, which mainly goes to amino and organic acid production.

For the first stage, 513 K and 50 min was selected due to the high yield of organic and amino acids. The solid residual was continuously processed at 553 K and 50 min until no more unreacted solid remained. A part of the scallop wastes may also be converted to some heavy compounds such as very heavy oils and carbon, which may adhere to the reactor wall. The estimated material balance showed that at least 88% of scallop wastes were converted to valuable materials under the optimum condition.

Besides hydrolysis reaction, separation and purification of the organic compounds in the aqueous phase reveals the central position of this study. The separating of amino and organic acids in single or binary systems has been already reported by one of the authors using adsorption/ion exchange technology.^{30–34} However, separation of multicomponent organic compounds will be reported in the subsequent stages of this research.

**Fig. 9** Material balance for sub-critical water treatment of scallop viscera wastes.

Conclusions

Hydrolysis in sub-critical water has been experimentally proven to be an effective way to convert scallop viscera wastes to valuable materials. Based on our experimental results, glycine was predominant among amino acids and pyroglutamic acid was the most abundant among organic acids. At 513 K and 50 min, the maximum yield of amino acids (0.15 kg per kg dry scallop waste) was obtained, while maximum organic acids were found at 553 K and 40 min (0.08 kg per kg dry scallop waste). Fat and oil produced by this method could be considered as valuable materials because they may be used as an energy source. The material balance based on the analytical results was estimated to be at least 88% of conversion from scallop wastes. This experimental finding leads to a new and greener method for the effective conversion of scallop wastes to useful compounds with significantly lower, and perhaps no, environmental emission. Applications of this technology in the fishery industry could have great potential economically and environmentally.

Acknowledgements

A part of this research funding was provided by the Ministry of Education, Culture, Sports, Science and Technology of Japan in the form of the 21st Century COE Program (E-1), entitled "Science and Engineering for Water-Assisted Evolution of Valuable Resources and Energy from Organic Wastes".

The authors would like to thank Mrs Yoshie Hirata, research assistant in the Department of Chemical Engineering, Osaka Prefecture University for her helpful support with some of the analytical work.

References

- N. Yoshii, S. Miura and S. Okazaki, *Chem. Phys. Lett.*, 2001, **345**, 1–2, 195.
- D. Laria, J. Marti and E. Guardia, *J. Am. Chem. Soc.*, 2004, **126**, 7, 2125.
- K. Tomita and Y. Oshima, *Ind. Eng. Chem. Res.*, 2004, **43**, 10, 2345.
- T. Yagasaki, K. Iwahashi, S. Saito and I. Ohmine, *J. Chem. Phys.*, 2005, **122**, 14, Art No. 144504.
- M. Dyoulgerov, *Ocean Coastal Manage.*, 1998, **39**, 3, 265.
- Protocol to the Convention on the Prevention of Marine Pollution by Dumping of Wastes and Other Matter, www.londonconvention.org/documents/meetings/consultative/26th/15.pdf, accessed on August 30, 2005.
- T. M. Hayward, I. M. Svishchev and R. C. Makhija, *J. Supercrit. Fluids*, 2003, **27**, 275.
- F. Vogel, K. A. Smith, J. W. Tester and W. A. Peters, *AIChE J.*, 2002, **48**, 8, 1827.
- M. Goto, T. Nada, A. Kodama and T. Hirose, *Ind. Eng. Chem. Res.*, 1999, **38**, 5, 1863.
- H. Yoshida, Y. Takahashi and M. Terashima, *Biotechnol. Prog.*, 1999, **15**, 6, 1090.
- H. Yoshida, Y. Takahashi and M. Terashima, *Jpn. Soc. Waste Manag. Experts*, 2001, **12**, 163.
- H. Yoshida, Y. Takahashi and M. Terashima, *J. Chem. Eng. Jpn.*, 2003, **36**, 4, 441.
- H. Yoshida and O. Tavakoli, *J. Chem. Eng. Jpn.*, 2004, **37**, 2, 253.
- O. Tavakoli and H. Yoshida, *Environ. Sci. Technol.*, 2005, **39**, 7, 2357.
- H. Yoshida and T. Nakahashi, *Proceedings of the 10th APCChE Congress*, November, 2004, 3P-03-026.
- H. Yoshida and Y. Katayama, *Proceedings of the 10th APCChE Congress*, November, 2004, 3P-03-025.
- H. Daimon, K. Kang, N. Sato and K. Fujie, *J. Chem. Eng. Jpn.*, 2001, **34**, 9, 1091.
- A. T. Quitain, M. Faisal, K. Kang, H. Daimon and K. Fujie, *J. Hazard. Mater.*, 2002, **93**, 2, 209.
- K. Y. Kang and B. S. Chun, *Korean J. Chem. Eng.*, 2004, **21**, 6, 1147.
- M. Goto, R. Obuchi, T. Hiroshi, T. Sakaki and M. Shibata, *Bioresour. Technol.*, 2004, **93**, 3, 279.
- A. Shanableh, *Water Res.*, 2000, **34**, 945.
- B. M. Kabyemela, T. Adschiri, R. M. Malalau and K. Arai, *Ind. Eng. Chem. Res.*, 1999, **38**, 2888.
- M. Sasaki, Z. Fang, Y. Fukushima, T. Adschiri and K. Arai, *Ind. Eng. Chem. Res.*, 2000, **39**, 2883.
- M. Sasaki, T. Adschiri and K. Arai, *AIChE J.*, 2004, **50**, 1, 192.
- N. Sato, A. T. Quitain, K. Kang, H. Daimon and K. Fujie, *Ind. Eng. Chem. Res.*, 2004, **43**, 13, 3217.
- J. D. Taylor, J. I. Steinfeld and J. W. Tester, *Ind. Eng. Chem. Res.*, 2001, **40**, 67.
- B. Myrnes and A. Johansen, *Prep. Biochem.*, 1994, **24**, 1, 69.
- I. Sarashina and K. Endo, *Am. Mineral.*, 1998, **83**, 1510.
- J. N. C. Whyte, N. Bourne and N. G. Ginther, *J. Exp. Mar. Biol. Ecol.*, 1991, **149**, 1, 67.
- H. Yoshida, O. Okamoto, H. Jitsukawa and T. Shigeta, *Fundam. Adsorpt.*, 2002, **7**, 520.
- H. Yoshida and W. A. Galinada, *AIChE J.*, 2002, **48**, 10, 2193.
- W. Takatsuji and H. Yoshida, *AIChE J.*, 1998, **44**, 5, 1216.
- W. Takatsuji and H. Yoshida, *AIChE J.*, 1998, **37**, 4, 1300.
- H. Yoshida, Y. Saiki and E. Kamio, *Proceedings of the 10th APCChE Congress*, November, 2004, 3P-12-056.

An environmentally benign process for the efficient synthesis of cyclohexanone and 2-methylfuran†

Hong-Yan Zheng,^{ab} Yu-Lei Zhu,^{*ab} Zong-Qing Bai,^{ab} Long Huang,^{ab} Hong-Wei Xiang^a and Yong-Wang Li^a

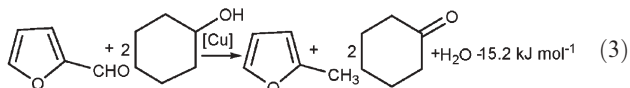
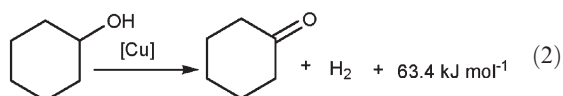
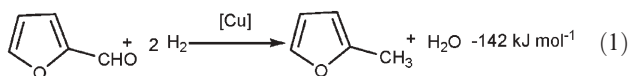
Received 26th September 2005, Accepted 28th October 2005

First published as an Advance Article on the web 17th November 2005

DOI: 10.1039/b513584b

A novel process involving the coupling of the dehydrogenation of cyclohexanol and the hydrogenation of furfural has been studied for the synthesis of cyclohexanone and 2-methylfuran over the same Cu–Zn–Al catalyst, realizing good energy efficiency, optimal hydrogen utilization, and environmentally benign process.

2-Methylfuran (2-MF) and cyclohexanone (CHN) are two important chemicals and versatile intermediates in fine chemical industrial practices. 2-MF is mainly used for the synthesis of crysanthemate pesticides, perfume intermediates and chloroquine lateral chains in medical intermediates.¹ CHN is mainly used for the production of caprolactum and adipic acid, and both of them are the major raw materials in producing polyamide fiber.² One of the important synthesis routes of 2-MF is the hydrogenation of furfural (FFA),^{1,3} and that of CHN is the dehydrogenation of cyclohexanol (CHL).⁴ However, there are many deficiencies existing in the conventional individual hydrogenation of FFA [eqn (1)] and dehydrogenation of CHL [eqn (2)], such as hardly controlled reaction temperature, conversion constrained by thermodynamic equilibrium, poor hydrogen utilization. So we have developed a new coupling route to synthesis 2-MF and CHN simultaneously [eqn (3)], in which the hydrogenation of FFA and the dehydrogenation of CHL are combined at the same reactor.



As shown in eqn (1), the vapor-phase hydrogenation of FFA to 2-MF is exothermic by 142 kJ mol⁻¹,¹ and this strongly exothermic nature makes it extremely difficult to control the temperature over this process, which results in apparent hot spots, typically in an industrial tubular fixed-bed reactor, thus seriously lowering the yield of desired product. The vapor-phase dehydrogenation of CHL to CHN [eqn (2)] is an

endothermic process (63.4 kJ mol⁻¹).⁵ Due to the endothermic properties of this reaction, the increase of the liquid hourly space velocity (LHSV) of CHL is relatively limited by low external heat supply in a practical reactor. In addition, the released hydrogen cannot be used effectively. Furthermore, the conventional dehydrogenation process is severely constrained by thermodynamic equilibrium, leading to lower conversion.⁶ The combined reaction in eqn (3) shows that producing 1 mol 2-MF and 2 mol CHN requires 1 mol FFA and 2 mol CHL, and is exothermic by 15.2 kJ mol⁻¹. The new catalytic process improves the selectivities of CHN and 2-MF, as well as leading to a better thermal balance and the effective use of hydrogen.

In industrial application of single FFA hydrogenation, Cr-containing catalysts are usually used, which are getting increasingly difficult due to their toxicity and pollution, while an environmentally friendly Cu–Zn–Al catalyst is used in this work. In addition, single FFA hydrogenation consumes a significant amount of hydrogen. Currently, hydrogen sources are dominantly manufactured with the carbonaceous substances, such as coal and natural gas. These processes result in many greenhouse gases and sulfur-compounds, such as CO₂, SO₂, H₂S, and cause serious environmental problems. The coupling process proposed in this work eliminates the separate hydrogen preparation procedures leading to a well arranged environmentally-friendly clean process.

Table 1 shows that almost complete conversion of FFA at 220–300 °C can be achieved over the Cu–Zn–Al catalyst. However, the selectivity of 2-MF varies substantially with operating temperature, with the best value of 87.0% at 250 °C.

Table 1 Influence of temperature on FFA hydrogenation to 2-MF^a

T/°C	Conv. (%)	Selectivity (%)	
		2-MF	Others ^b
220	99.1	70.9	29.1
250	99.3	87.0	13.0
270	99.2	85.3	14.7
280	99.9	82.8	17.2
300	99.3	81.2	18.8

^a Reaction conditions: 1 atm, LHSV = 0.3 h⁻¹, n(H₂) : n(FFA) = 10 : 1 (molar ratio). ^b Other products: mainly furfural alcohol, 2-pentanol, 2-pentanone, etc.

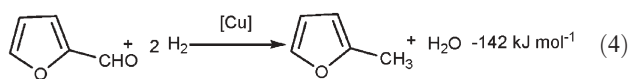
^aState Key Laboratory of Coal Conversion (SKLCC), Institute of Coal Chemistry, Chinese Academy of Sciences, P. O. Box 165, Taiyuan, 030001, P. R. China. E-mail: zhuyulei@sxicc.ac.cn;

Fax: +86 351-4124899; Tel: +86 351-4174341

^bGraduate School of the Chinese Academy of Sciences, Beijing, 10039, P. R. China

† Electronic supplementary information (ESI) available: Thermodynamic calculations. See DOI: 10.1039/b513584b

In this work, the equilibrium constant for the dehydrogenation of CHL to CHN is defined as eqn (4).



The equilibrium constant K^0 used in the present work is cited from reference.⁷ K_p represents the equilibrium constant based on partial pressure. The typical reaction condition in this work is at atmospheric pressure, so $P^0 = P$. Here χ_i is the mole fraction of component i , and ϕ_i is the fugacity coefficient. K_ϕ is the fugacity coefficient ratio. The values of ϕ_i and K_ϕ can be calculated on the basis of the Redlich–Kwong equation of state [eqn (5)].⁸

$$P = RT/(V - b) - a/T^{0.5}V(V + b) \quad (5)$$

The a and b are all constants in the Redlich–Kwong equation, which can be obtained from their critical properties.

Fig. 1 gives the influence of different ratios of hydrogen to CHL on the conversion of CHL dehydrogenation to CHN. There are no significant effects on the conversion of CHL in a wide range of 15 to 100, while the conversion rapidly decreases with the H_2/CHL ratio in the range of 0 to 15. The results of CHL dehydrogenation at different temperatures (Table 2) indicate that the conversion of the main reaction for CHL dehydrogenation to CHN (Conv2) is lower than the equilibrium conversion by thermodynamic calculation (Conv1) from 220 to 300 °C. In addition, side reactions become serious over 280 °C.

The coupling reaction results (Table 3) display that the conversion of CHL to CHN is improved from 220–300 °C. Furthermore, the conversion of the main reaction for CHL dehydrogenation to CHN (Conv2 in Table 3) from 220 to 280 °C is higher than the equilibrium conversion (Conv1 in Table 2), namely, the thermodynamic conversion of CHL dehydrogenation is broken by adding FFA (a hydrogen acceptor).⁹ The selectivities of CHN and 2-MF are also

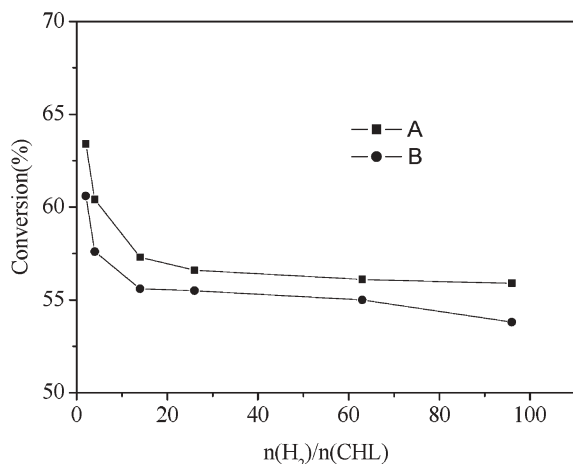


Fig. 1 Influence of $n(\text{H}_2)/n(\text{CHL})$ (molar ratio) on the dehydrogenation of CHL to CHN. Reaction conditions: 1 atm, $T = 270$ °C, $\text{LHSV}(\text{CHL}) = 0.6 \text{ h}^{-1}$. A = equilibrium conversion of CHL dehydrogenation to CHN by thermodynamic calculation. B = (moles of CHN produced by CHL)/100/(total moles of CHL).

Table 2 Influence of temperature on CHL dehydrogenation to CHN^a

$T/^\circ\text{C}$	Conv1 ^b (%)	Conv2 ^c (%)	Conv3 ^d (%)	Selectivity (%)	
				CHN	Others ^e
220	30.9	30.1	34.6	87.0	13.0
250	50.6	49.2	56.4	87.2	12.8
270	63.4	60.6	69.3	87.4	12.6
280	69.1	62.4	72.8	85.6	14.4
300	78.7	64.7	82.5	78.5	21.5

^a Reaction conditions: 1 atm, $\text{LHSV} = 0.6 \text{ h}^{-1}$, $n(\text{H}_2) : n(\text{CHL}) = 2 : 1$ (molar ratio). ^b Conv1 = equilibrium conversion of CHL to CHN by thermodynamic calculation. ^c Conv2 = (only moles of CHN produced by CHL) \times 100/(total moles of CHL). ^d Conv3 = (moles of all converted CHL) \times 100/(total moles of CHL). ^e Other products: mainly phenol, benzene, cyclohexene, etc.

Table 3 Influence of temperature on coupling of CHL and FFA to CHN and 2-MF^a

$T/^\circ\text{C}$	Conv2 ^b (%)	Conv3 (%)		Selectivity (%)	
		CHL ^c	FFA ^d	CHN ^e	2-MF ^f
220	40.7	42.5	99.0	95.8	77.5
250	58.2	61.0	99.6	96.0	89.5
270	67.2	70.0	99.6	96.1	92.8
280	70.6	76.7	99.4	94.4	89.4
300	76.9	81.5	99.8	92.1	83.8

^a Reaction conditions: 1 atm, $\text{LHSV}(\text{CHL} + \text{FFA}) = 0.9 \text{ h}^{-1}$, $n(\text{H}_2) : n(\text{CHL}) = 2 : 1$ (molar ratio), $n(\text{FFA}) : n(\text{CHL}) = 0.5 : 1$ (molar ratio). ^b Conv2 = (only moles of CHN produced by CHL) \times 100/(total moles of CHL). ^c Conv3(CHL) = (moles of all converted CHL) \times 100/(total moles of CHL). ^d Conv3(FFA) = (moles of all converted FFA) \times 100/(total moles of FFA). ^e Selectivity(CHN) = (moles of CHN produced by CHL) \times 100/(moles of converted CHL). ^f Selectivity(2-MF) = (moles of 2-MF produced by FFA) \times 100/(moles of converted FFA).

increased compared with those in the individual processes (Table 1 and Table 2). At 270 °C, for example, the selectivity of CHN is raised by 8.7%, and that of 2-MF is increased by 7.5%.

A 200 h stability test for the Cu–Zn–Al catalyst shows that the catalyst has relatively high activity and good stability (Fig. 2).

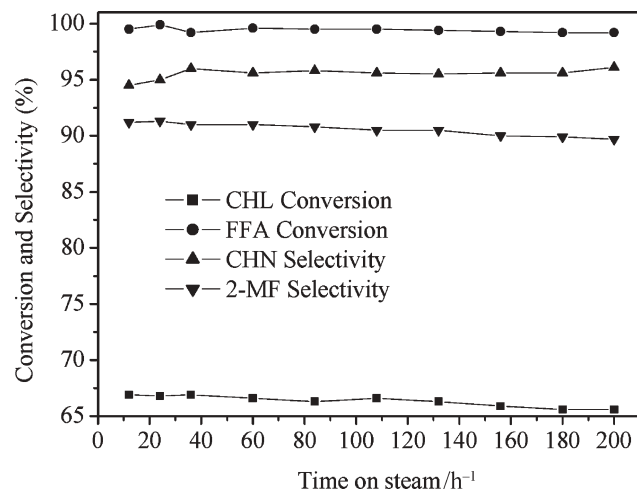


Fig. 2 Catalytic performance of Cu–Zn–Al in the coupling process of CHL dehydrogenation and FFA hydrogenation. Reaction conditions: 1 atm, $T = 270$ °C, $\text{LHSV}(\text{CHL} + \text{FFA}) = 0.7 \text{ h}^{-1}$, $n(\text{H}_2) : n(\text{CHL}) = 2 : 1$ (molar ratio), $n(\text{FFA}) : n(\text{CHL}) = 0.3 : 1$ (molar ratio).

The boiling point (at 101.3 kPa) of 2-MF is about 63 °C and that of CHN is about 155 °C, leading to easy separation of the product mixture, meaning less additional costs in the coupling process for industrial applications. These advantages may be of great interest for industrialization of the coupling process to produce these two important products, 2-MF and CHN.

In conclusion, the coupling process proposed in this work has several advantages over the two conventional single processes, such as enhanced conversion, good energy efficiency, optimal hydrogen utilization and environmentally benign process. In order to explain the enhancement in the catalyst performance observed in the coupling process, we propose that the activated hydrogen species on the catalyst surface due to CHL dehydrogenation probably plays an important role in improving the selectivity of 2-MF in the hydrogenation of FFA.⁹ Furthermore, the consuming of the activated hydrogen species breaks the thermodynamic equilibrium of CHL dehydrogenation and facilitates the dehydrogenation of CHL to CHN. In an industrial process, other factors like an improved temperature profile along the reactor may further enhance the effect, suggesting the potential for coupling reactions in practical applications. In addition, the simplified technical procedure due to a “no-hydrogen-supply” operation shows improved technology. Further exploration is of both practical and theoretical importance.

Experimental

The Cu–Zn–Al catalysts were prepared *via* the continuous precipitation method. In this preparation reaction, a solution of mixed Cu(NO₃)₂, Zn(NO₃)₂ and Al(NO₃)₃ (1 M of total metal ions) was used as metal precursors, with a 1 M Na₂CO₃ solution added as the precipitating agent. Precipitation was performed at 65 °C, and the flow rates of the two solutions were adjusted to give a constant pH of about 7.5. After precipitation, the suspension was washed and filtered. The precipitate was dried at 110–120 °C for 24 h in an air atmosphere. The dried catalyst was calcined at 350 °C for 4 h.

The reactions were carried out in a tubular fixed-bed reactor (length of 500 mm and diameter of 12 mm). Before the reaction, 5.0 g of catalyst with a particle size of 20–40 mesh packed in the reactor was activated *in situ* at atmospheric pressure in a flow of H₂/N₂ (5 : 95 v/v) stream, and the temperature was progressively increased from ambient temperature to 270 °C. After reduction, the gas flow was switched to a steam of reactant in hydrogen. The liquid products collected in the ice trap and gaseous products were all determined by a SP-2000 gas chromatograph (Ruihong Analyser Co., Shandong, P. R. China) with a flame ionization detector (FID).

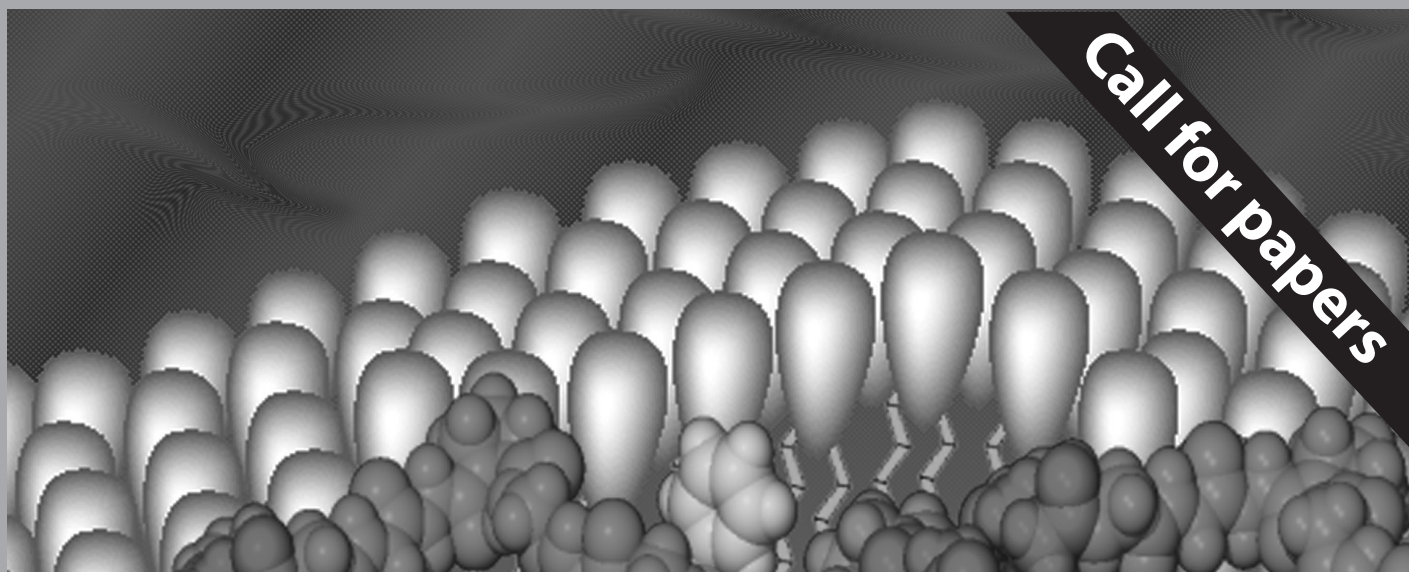
Acknowledgements

This work was financed by the Natural Science Foundation of China (No. 20276077). The authors would like to thank Dr Bo-Tao Teng for helpful discussions.

References

- 1 Y. L. Zhu, H. W. Xiang, Y. W. Li, H. J. Jiao, G. S. Wu, B. Zhong and G. Q. Guo, *New J. Chem.*, 2003, **27**, 208.
- 2 B. M. Nagaraja, V. Siva Kumar, V. Shashikala, A. H. Padmasri, S. Sreevardhan Reddy, B. David Raju and K. S. Rama Rao, *J. Mol. Catal. A: Chem.*, 2004, **223**, 339.
- 3 R. M. Lukes and C. L. Wilson, *J. Am. Chem. Soc.*, 1951, **73**, 4790.
- 4 (a) V. Z. Fridman, A. A. Davydov and K. Titievsky, *J. Catal.*, 2000, **195**, 20; (b) V. Z. Fridman, A. A. Davydov and K. Titievsky, *J. Catal.*, 2004, **222**, 545.
- 5 G. J. Kabo, Y. I. A. ursha, M. L. Frenkel, P. A. Poleshchuk, V. I. Fedoseenko and A. I. Ladutko, *J. Chem. Thermodyn.*, 1988, **20**, 429.
- 6 W. L. Yang, *Master's Thesis*, National Cheng Kung University, Taiwan, 1983, p. 8.
- 7 (a) A. H. Cubberley and M. B. Mueller, *J. Am. Chem. Soc.*, 1947, **69**, 1535; (b) *Manufacture and Application of Caprolactam*, ed. V. R. Yang, Hydrocarbon processing Press, Beijing, 1988, p.101.
- 8 O. Redlich and J. N. S. Kwong, *Chem. Rev.*, 1949, **44**, 233.
- 9 (a) R. A. W. Johnstone and A. H. Wilby, *Chem. Rev.*, 1985, **85**, 129; (b) G. Zassinovich and G. Mestroni, *Chem. Rev.*, 1992, **92**, 1051.

Call for papers



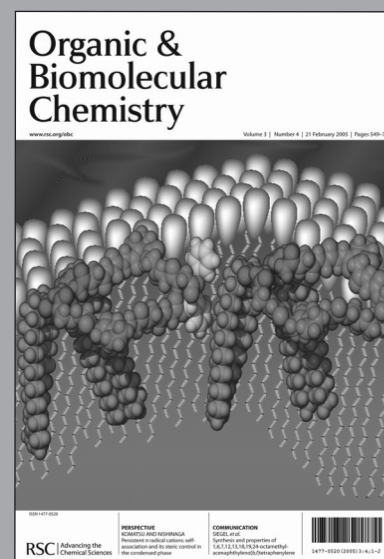
09030532

Organic & Biomolecular Chemistry

A major peer-reviewed international, high quality journal covering the full breadth of synthetic, physical and biomolecular organic chemistry.

Publish your review, article, or communication in OBC and benefit from:

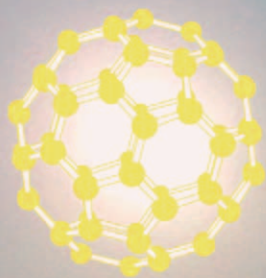
- The fastest times to publication (80 days for full papers, 40 days for communications)
- High visibility (OBC is indexed in MEDLINE)
- Free colour (where scientifically justified)
- Electronic submission and manuscript tracking via ReSource (www.rsc.org/ReSource)
- A first class professional service
- No page charges



Submit today!

RSC Publishing

www.rsc.org/obc



NJC

New Journal of Chemistry

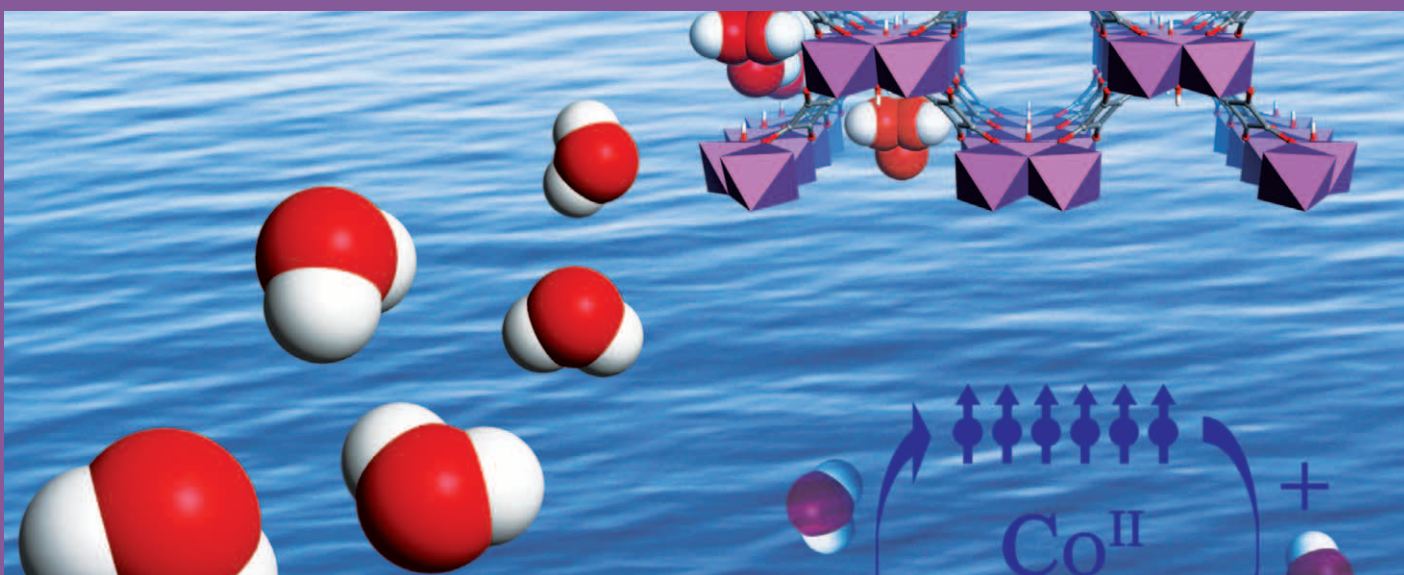
A prime source of international, cutting-edge research,
encompassing all areas of the chemical sciences

- Impact factor: 2.735
- Fast times to publication
- Multidisciplinary with broad appeal

Read it today!

RSC Publishing

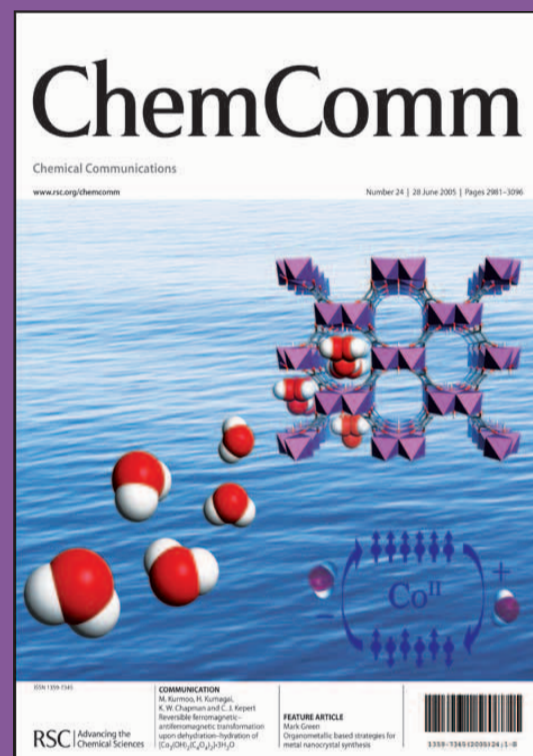
www.rsc.org/njc



ChemComm

The leading international journal for the publication of communications on important new developments in the chemical sciences.

- Weekly publication
- Impact factor: 3.997
- Rapid publication – typically 60 days
- 3 page communications – providing authors with the flexibility to develop their results and discussion
- 40 years publishing excellent research
- High visibility – indexed in MEDLINE
- Host of the RSC's new journal, *Molecular BioSystems*



RSC Publishing

www.rsc.org/chemcomm